DYNAMIC MODELING OF
PARALLEL MANIPULATORS

By

IVAN J. BAIGES-VALENTIN

A DISSERTATION PRESENTED TO THE GRADUATE SCHOOL
OF THE UNIVERSITY OF FLORIDA IN PARTIAL FULFILLMENT
OF THE REQUIREMENTS FOR THE DEGREE OF
DOCTOR OF PHILOSOPHY

UNIVERSITY OF FLORIDA

1996

The author would like to dedicate this work to his parents Salvador and Monsita Baiges and to his brothers and sisters who supported and encouraged him all the way. This work is also dedicated to Zita Sumaza whose friendship was a great source of inspiration during the most difficult moments. Finally and most important, this work is dedicated to the author's daughter Gianna Marie with all his love.

This work is dedicated to the memory of Prof. Richard H. Zimmerman.

ACKNOWLEDGEMENTS

TABLE OF CONTENTS

Abstract of Dissertation Presented to the Graduate School
of the University of Florida in Partial Fulfillment of the
Requirements for the Degree of Doctor of Philosophy

DYNAMIC MODELING OF
PARALLEL MANIPULATORS

By

IVAN J. BAIGES-VALENTIN

1996

Chairman: Dr. Joseph Duffy
Major Department: Mechanical Engineering

Parallel manipulators, which consist of two rigid bodies (a base and a platform) connected by six serial kinematic chains (connectors), offer distinct advantages when compared to their serial counterparts. The motion of the platform with respect to the base is controlled by the displacement of the six parallel connectors which generate a very stiff and accurate manipulator capable of handling high payloads with minimal positioning errors. These characteristics have generated great interest in the use of this type of manipulator in applications such as machining processes and automated assembly operations.

It is clearly desirable to develop a comprehensive dynamic model for effectively designing and controlling the parallel manipulators.

The major objective of this research is to derive explicit equations of motion for parallel manipulators. This will provide the means to understand their dynamic behavior and enable the design of more efficient devices capable of fast and accurate motions while handling heavy payloads. As far as the author is aware, this is the first time the explicit equations of motion have been derived (as opposed to numerical solutions). They were derived using Kane's Method which proved to be well suited to the intricate kinematics of parallel manipulators, and verified with the Newton-Euler formulation. Subsequently, the equations were used for a inverse dynamic simulation, which calculated the actuator forces

required for producing a desired motion of a given design whilst supporting a workpiece in a machining operation. Various geometric parameters, inertial properties and motion profiles were used for testing in order to understand some of the effects on the dynamic behavior.

The equations of motion indicate a high degree of coupling between the connectors caused by the gravitational, tangential, Coriolis and centrifugal accelerations acting upon the system. A most important result of the inverse dynamic simulations is that even for feed rates in excess of the limits of existing technology (1200 inches / min), the only significant coupling was due to gravity; the other coupling effects were negligible. This suggests the possibility of using mass balancing to reduce the coupling effects between the connectors and in the process creating faster and more accurate parallel manipulators.

CHAPTER 1
INTRODUCTION

Manipulators or robots can be classified according to the type of kinematic chain used for their implementation. Serial manipulators are based on open kinematic chains such as the 3 degree-of-freedom manipulator shown on the left hand side of figure 1.1. Parallel manipulators are based on closed kinematic chains such as the 3 degree-of-freedom system shown on the right hand side of Figure 1.1.

Serial manipulators generally have long reach, a great degree of dexterity, cover a large workspace and can enter small spaces among other advantages. However, serial manipulators have low stiffness and highly coupled nonlinear dynamic behavior, specially for high speed and high payload applications. The main reason for these limitations is the that the serial manipulator is a chain of cantilever type structures, where the compliance and positioning errors are accumulative effect of the individual joints.
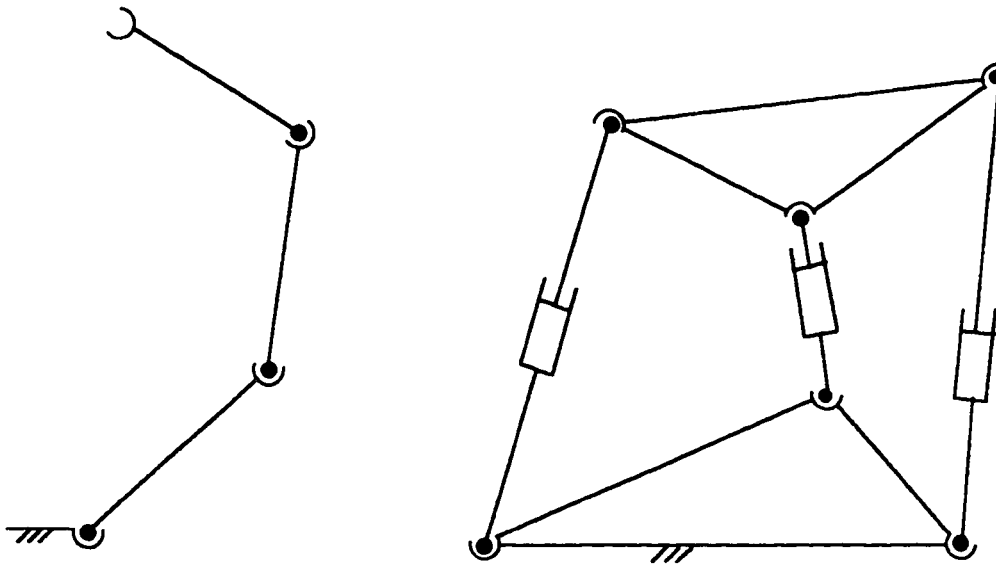
Figure 1.1 - Serial and Parallel Manipulators

1

Platform

link or
connector

Z

actuator

X   Y

Base
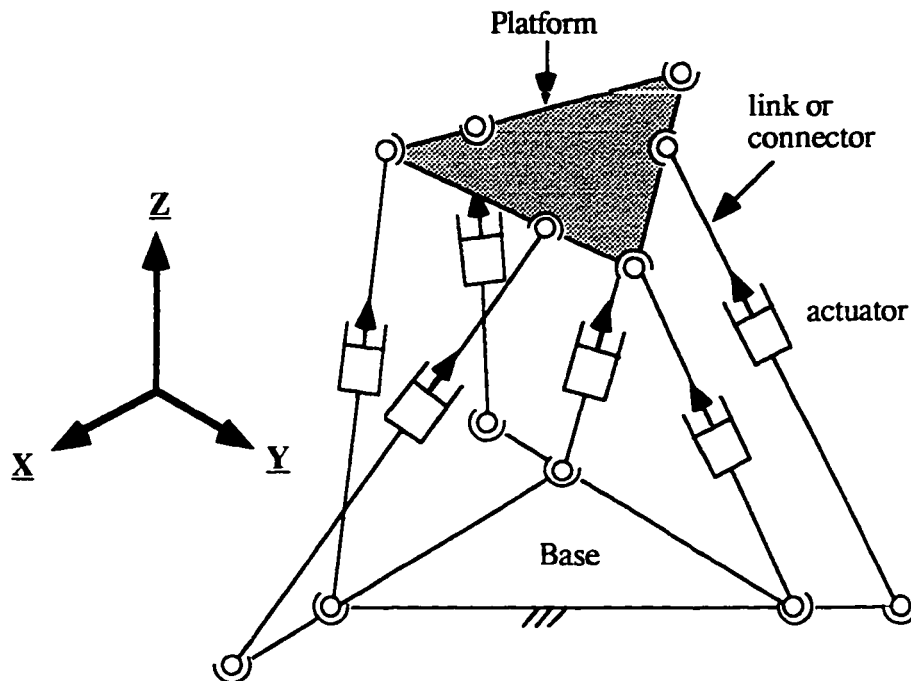
Figure 1.2 - Spatial Parallel Manipulator

In parallel manipulators (see Figure 1.2) the links act in parallel, generating a very stiff and accurate manipulator which can carry a high payload with minimal positioning errors. On the other hand, parallel manipulators cover smaller work spaces and are less dexterous than the serial manipulators. The particular nature of the parallel manipulator has generated great interest in robotic applications where high loads and precision are required such as in machining processes and automated assembly operations. The most typical parallel manipulator is the Stewart Platform [1] which consists of two rigid bodies connected by six linear parallel actuators. The motion of one of the rigid bodies (namely the platform) with respect to the other (the base) is controlled by the displacement of the six linear actuators.

1.1 Previous Work

The parallel manipulator presents a different set of problems than the serial manipulators. As an example the inverse kinematic analysis is simple to determine compared to the forward kinematic analysis problem, which is the opposite with serial

manipulators. The inverse and forward kinematics of this type of manipulators has been studied [2, 3, 4] in kinematics . Some general design guidelines have been developed by E.F. Fichter [5, 6]. The inverse dynamic analysis of the Stewart platform has been done using the Newton-Euler formulation [7, 8] and the Lagrange formulation [9, 10]. Although in all these cases the explicit equations of motion have not been derived, numerical solutions have been developed and used for the dynamic analysis.

Control systems have been developed and tested for Stewart platforms carrying out simple operations [9, 11, 12]. In these cases the dynamic behavior has been neglected, either by claiming that its not significant or that the error introduced by doing so can be corrected by the control system. These assumptions are valid for slow motions and small payloads. As the platform moves faster, the dynamic effects of the system will become more significant. For higher payloads, the links must be stiffer and the actuators stronger. This will increase the inertial parameters which can increase the dynamic effects on the system. Therefore designs and control systems based on the assumption that the dynamic behavior of the system is not relevant are going to be faulty and can not be used successfully in future applications.

The techniques developed up to now in the areas of dynamics and controls are adequate for analyzing existing manipulators but not adequate enough for designing platform based manipulators. In order to design platforms with good dynamic performance, the analytical equations of motion are required. These equations allow the designer to examine the effects of different factors upon the dynamic behavior of the system such as the geometry, link dimensions and inertial properties. This understanding of the dynamic behavior is difficult to obtain by just using numerical solutions. The explicit equations of motion also are required for designing control systems that will improve the dynamic performance of the parallel manipulator.

The idea of using the equations of motion of the manipulator for improving the design and developing high performance control systems has been done successfully in the area of serial manipulators by H. Asada et al.[13]. The result of this research has been the development of the high performance direct -drive serial manipulators [14].

1.2 Objectives

The designer interested in developing a platform based manipulator can usefully employ the research performed to analyze a given device. A set of manipulator parameters can be determined by a trial and error process using the actual level of knowledge. However, this process can be very time consuming and may produce a manipulator that is not optimal for the given application. The ultimate objective of this research is to develop an efficient computer-based design and analysis tool for parallel manipulators.

1.2.1 Dynamic Modeling

The primary main objectives of this project are to determine the analytical dynamic model for parallel manipulators and develop a dynamic simulation software. This simulation will be the basis for the computer base design / analysis tool for parallel manipulators. This model can be used for the forward dynamic analysis where the
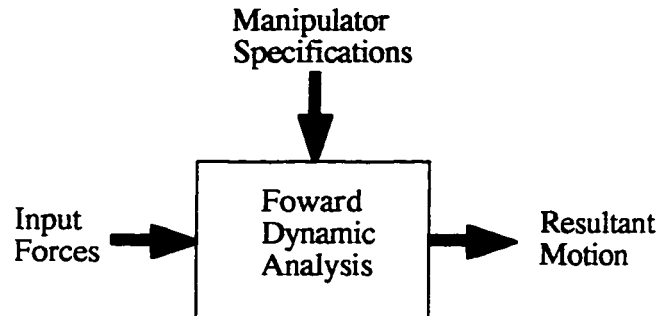
Figure 1.3 - Forward Dynamic Analysis
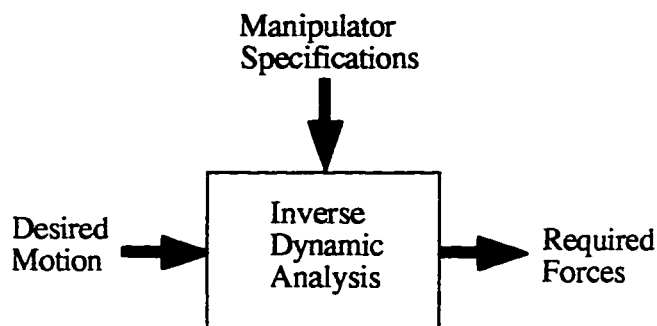
Figure 1.4 - Inverse Dynamic Analysis

loads are applied to the system and the resultant motion is determined as shown in Figure 1.3. The manipulator specifications consist of the dimensions, the geometry, the inertial parameters and other parameters used for describing the system. These will be discussed in detail in Chapter 2.

Most important is the use of the model for the inverse dynamic analysis of the parallel manipulator. In this case the desired motion is specified and the forces required to generate this motion are determined as shown in Figure 1.4. The inverse dynamic analysis is the tool that a designer would use to determine if a given manipulator or a proposed design is capable of generating a desired motion. This analysis can also be used to determine the effects of changing platform specifications on the required forces which is also useful for the design process.

1.2.2 Testing

The second objective of this work is to use the dynamic simulation for testing some manipulator designs. This will enable the designer to gain some basic insight of the dynamic behavior of the system and its relation to different system parameters such as geometry and inertia.

1.3 CAE Tool for Parallel Manipulators

Parallel manipulators have in the main been used as flight simulators for training pilots and for rides in theme parks such as Disney World. They have many other potential uses in different areas which have not been explored yet. The development a Computer Aided Engineering tool for parallel manipulators, such as that shown in Figure 1.5, will allow designers to determine the appropriate design of a platform based manipulator according to the desired application. The dynamic simulation, which is the immediate objective of this research, is one of the major building blocks for such a tool. The designer or user of this CAE tool provides the input through the description of the desired motion and task, and the workspace requirements. This information is used by the Manipulator Design Module, shown in Figure 1.6, to determine some possible geometries and manipulator parameters

user input   user input

motion & task   workspace
planning   specifications

Manipulator Design Module

modify

Actuator   Manipulator
Requirements   Design

Control System Design Module

meet
specifications
?

no

yes

Final Manipulator Design
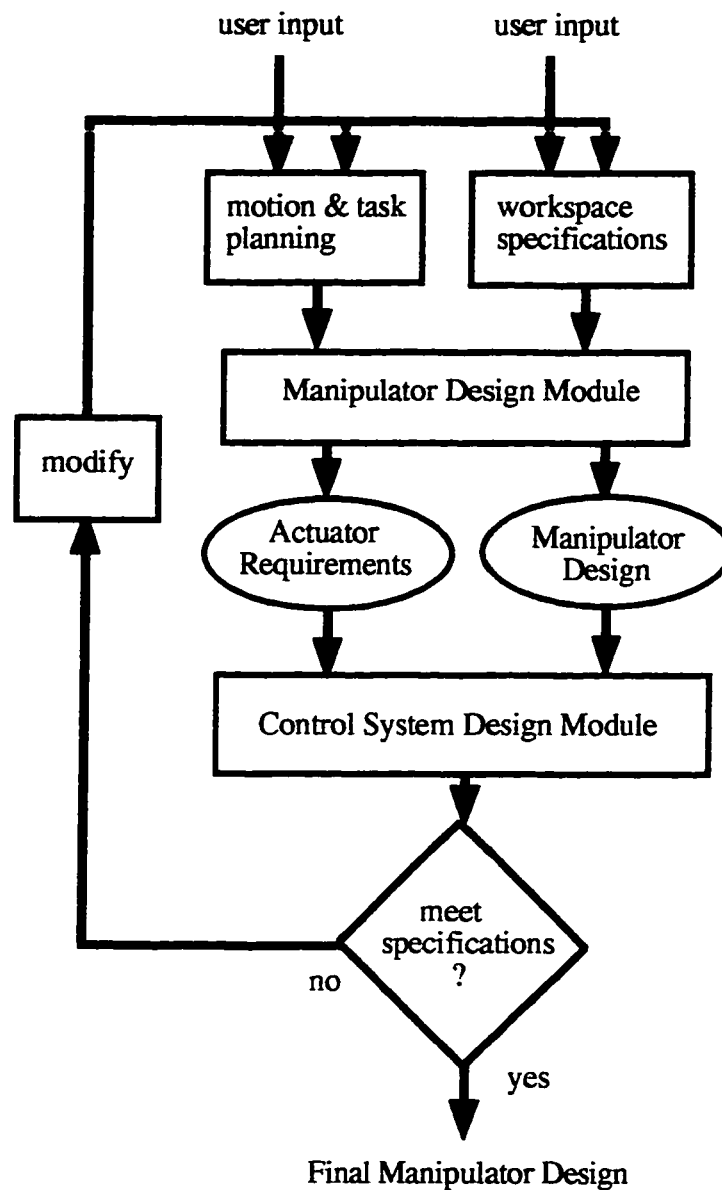
Figure 1.5 - CAE tool for Parallel Manipulators

by the Geometry Selection and Connector Design submodules. The applied loads are determined by the Load Analysis submodule using the motion planning information and the proposed geometry. Finally the Inverse Kinematic and Inverse Dynamic submodules are used to determine the actuator requirements.
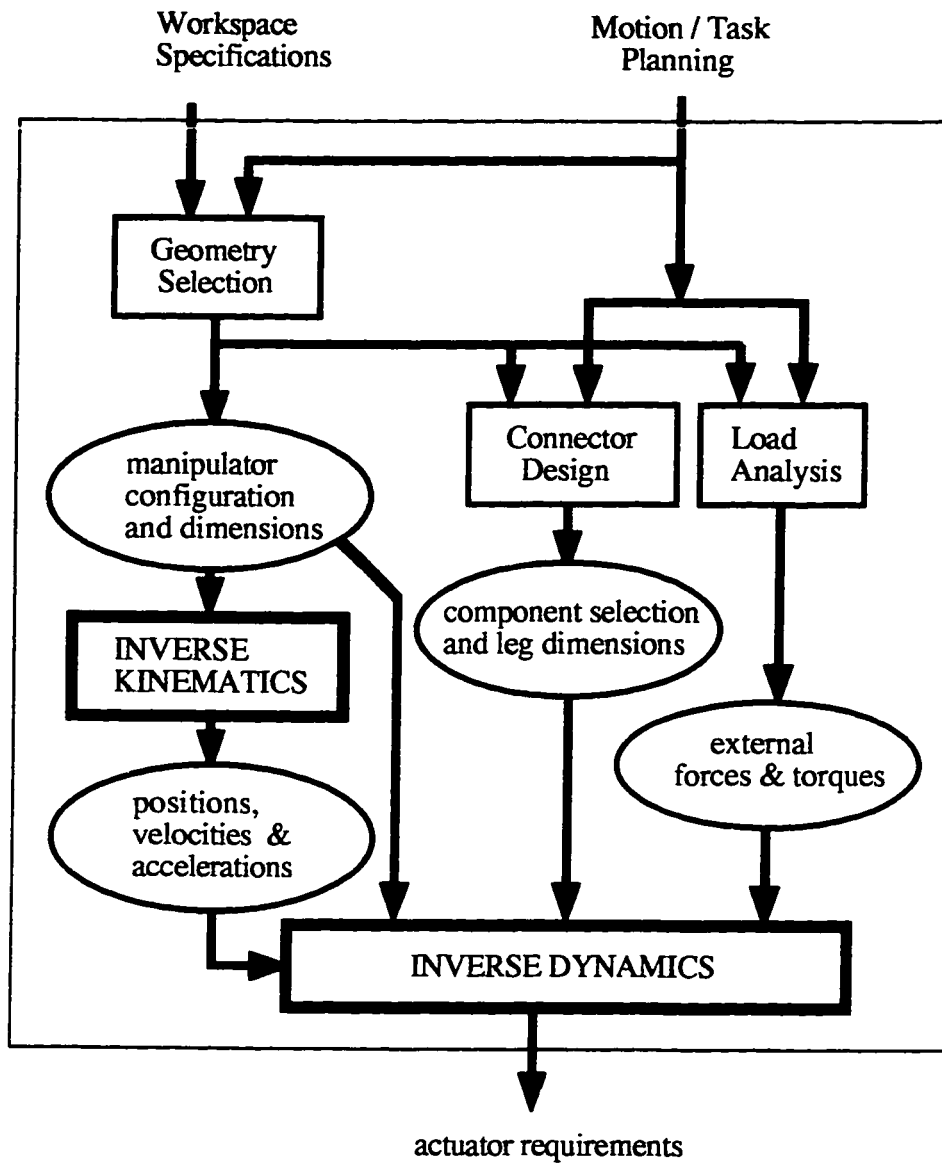
Figure 1.6 - Manipulator Design Module

If the actuator requirements meet the design specifications, the software invokes the Control System Design Module shown in Figure 1.7. This module uses the manipulator design generated in the Manipulator Design Module to determine the controller parameters using the Manipulator Control System submodule. Then the Forward Dynamics and Forward Kinematics submodules use the controller design and the actuator requirements to determine the resultant motion. This motion is then compared with the desired motion to
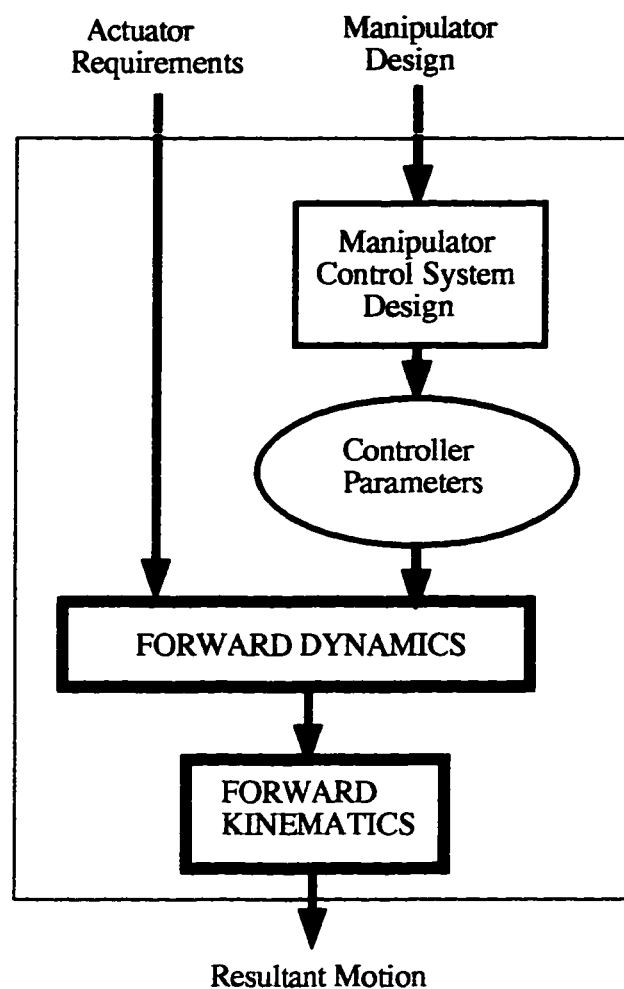
Figure 1.7 - Control System Design Module

determine whether the manipulator design is satisfactory or in the best case the optimum design.

1.4 Research Outline

As mentioned earlier, the development of the CAE tool for parallel manipulators is the ultimate objective of a research effort and this project is one of the initial phases. The objective of this research is to develop the equations to be used in the inverse and forward kinematics, and the equations of motion for the inverse and forward dynamic analysis.

The first step required for deriving the equations of motion is to develop a comprehensive lumped parameter model of the manipulator. In all the previous research into modeling [8, 9, 10, 11] simple connector models have been employed. Although adequate for a basic dynamic analysis, these models are not good enough for complex systems such as those required for implicit force control and for high frequency / disturbance rejection applications. The objective here is to develop a complete lumped parameter model which includes the effects of friction and compliance which can become significant factors in advanced applications. The lumped parameter model should be as comprehensive as possible in order to anticipate the needs of the designer and at the same time not overly complicated such that it would add unnecessary computational overhead.

The second step is to perform a complete inverse kinematic analysis. This analysis must generate analytical expressions that relate the motion of the platform to the motion of the connectors (position, velocity and acceleration). This analysis must also generate the equations for describing the motion of the platform.

The third step is to perform a complete force/torque analysis of the manipulator. This analysis determines the relationships between the externally applied loads, gravity, the actuator forces, the connector elements and the inertial motion of the platform.

At the outset the most important step is to determine the equations of motion for the system using the lumped parameter model, the kinematic analysis, and the force/torque analysis. One important issue is the selection of the formulation method [15] (Newton-Euler, Lagrange, ...). The formulation method will determine the difficulty of the deriving the equations of motion and the possibility of making mistakes in the derivation.

Once the equations of motion are derived, the dynamic simulation software can be developed and tested using different manipulator designs and desired motions. This will provide some useful insight of the dynamic behavior of the system and demonstrate that it is an important component of a future CAE tool for parallel manipulators.

CHAPTER 2
SYSTEM LUMPED PARAMETER MODEL

In most of the dynamic models for parallel spatial manipulators, the platform is assumed to be a rigid body with distributed mass; and the connectors are considered to be rigid massless bodies that apply forces to the platform as shown in figure 2.1. Although this approach can be considered a good first approximation, it does not provide a complete picture. Most of these models do not specify the minimum connector-to-platform inertia ratio at which the mass of the connector be considered neglible, nor the minimum connector stiffness values required to consider the connector infinitely rigid. In order to obtain proper results with such a simplistic model, the connectors would have to be carefully designed so that they are lightweight and extremely rigid. This causes the system to be complex and costly. Therefore the advantage of using a simplistic model may be outweighed by the increase of the design effort and costs.

An alternate approach is to assume that the connectors do have some inertia and compliance that can affect the system's dynamic performance. The use of a more complete lumped parameter model for the connector will increase the modeling complexity. The additional modeling effort will be compensated by decrease in the design effort and the increase in the system's actual performance. In this chapter more realistic connector models will be developed by including factors such as the actuator's inertial effects and friction; and the leg compliance. The goal of this chapter is to develop realistic lumped parameter models for the dynamic analysis of parallel manipulator. These models must describe the dynamic behavior of the system without being too complex.
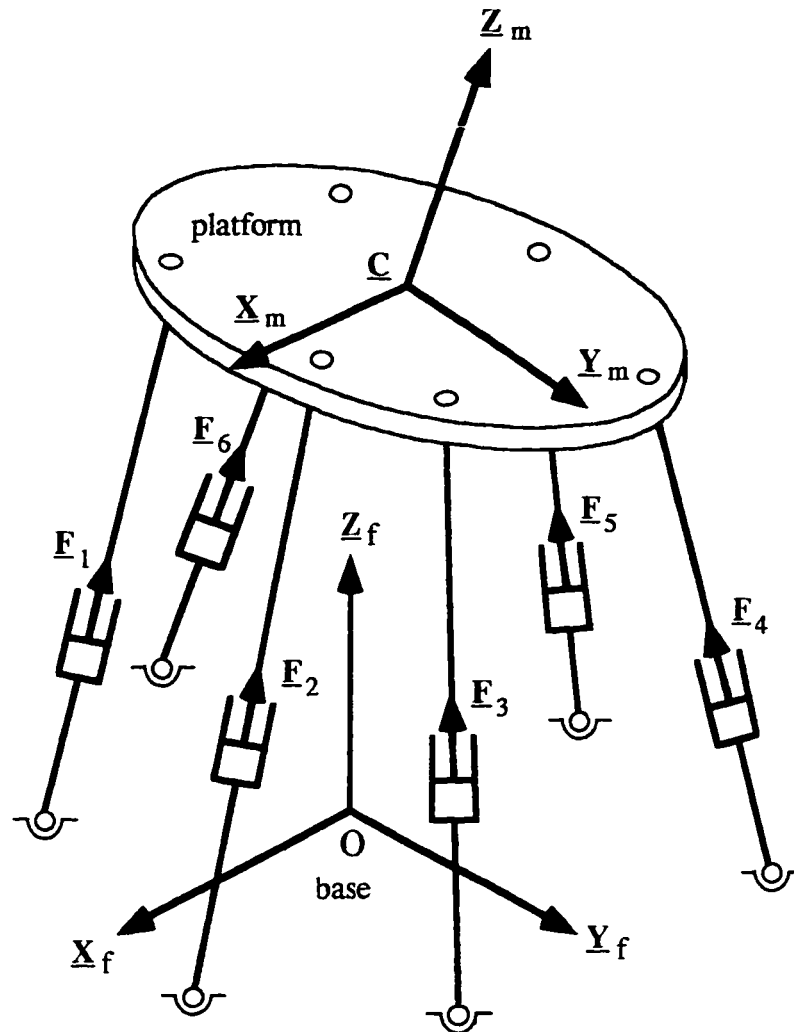
Figure 2.1 - Spatial Parallel Manipulator with rigid and massless connectors

$$\Delta \underline{F}_a = M_e \, \underline{\ddot{E}}$$

where $\underline{F}_a$ is the actuator's force, and E is the displacement of the mass of the connector as shown in Figure 2.2. The inertial effect is caused by this mass is compounded by the fact that it is also rotating. In this case the actuators will also have to generate the additional forces to cause the rotation of these connector masses. The rotation of this mass will require a normal acceleration term since the body is rotating; and a Coriolis acceleration
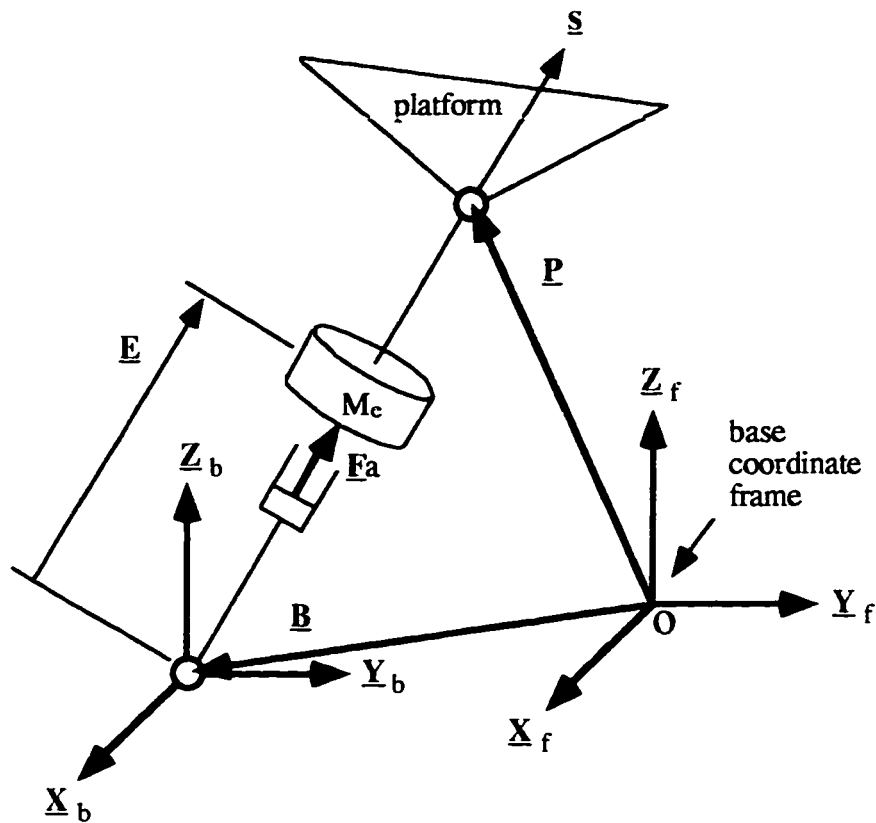
Figure 2.2 - Connector model with the actuator mass

term since the body is translating and rotating at the same time

$$\mathbf{A}_{normal} = \mathbf{E}\,(\underline{\omega})^2; \qquad \mathbf{A}_{coriolis} = 2\,\dot{\mathbf{E}} \times \underline{\omega}$$

where $\underline{\omega}$ is angular velocity vector of the connector. The manipulator will also store more

kinetic energy when the connector masses are included. The actuators will have to exert

more force to speed up/slow down the system since more energy must be added/removed

from the system.

In the parallel manipulator system, the actuators will increase (speed up) or decrease

(slow down) the energy content of the platform. The speed of response is a function of

how fast the actuators can transfer energy, stored in the form of kinetic energy, to or from

the moving platform as shown in Figure 2.3. The block diagram on the left illustrates the

Energy Input   Energy Output
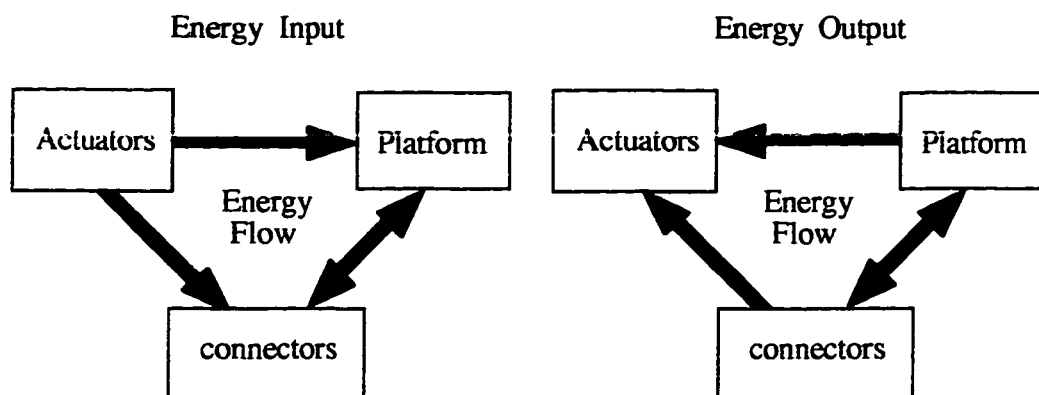
Figure 2.3 - Energy Flow in Parallel Manipulators

energy flow when the manipulator is sped up; the right block diagram illustrates the energy flow when the energy level of the manipulator is decreased (slowed down).

When the connectors are assumed to be rigid and massless, the actuators only have to transfer energy to or from the platform. When a more realistic connector model is used, the actuators have to transfer energy to or from the platform and the connector masses. For the same desired platform velocity, the energy level required is higher when the realistic connector model is used and the system's speed of response or reaction time is slower. In order to increase the velocity, the actuators have to add energy to the platform and the connectors . When the system has to be slowed down, the actuators have to remove energy from the platform and the connectors. The decrease of the speed of response can be detrimental to the performance of the platform if the connector masses was not taken into account when designing the system. The actuators have to more powerful if the original speed of response is desired. The use of more realistic connector models will help to quantify the decrease of the speed of response which will provide the designer with more accurate information when selecting the actuators.

2.2 Basic Connector Model

The simplest model for the connector of a spatial parallel manipulator is a rigid massless body. A more realistic but simple model for the connector is shown in Figure 2.4. The

mass M_e is the lumped mass of the connector and the moving part of the actuator; this includes the inertia of the actuator and the transmission used to convert rotational motion to linear motion when a rotational actuator is used. A transmission is not required if a linear actuator such as a hydraulic piston is used. The base mass of the actuator, M_b, is the fixed part of the actuator (this is in the direction of translational motion, the complete connector will rotate when the system is moving). In this model, the deformation of the connector and the friction of the actuator are also considered and are described by the lumped parameter elements K_L and C_t, respectively. The parameters and variables used in this basic connector model are (see Figure 2.4)

E, the displacement of the connector along the $\underline{s}$ direction;

K_L, the equivalent stiffness of the connector;

C_t, the actuator and transmission friction, modeled as a viscous damper; and

$\underline{F}_a$, the force produced by the actuator.

The equivalent force of the actuator is determined by using the torque and the transmission ratio of the actuator. This force (or torque) can be further related to the commands that the controller sends to the actuators. The force that the connector applies to the platform is a function of its displacement ε, and the connector stiffness K_L

$$F = K_L \varepsilon \qquad (1)$$

If the connector is very stiff ($K_l \Rightarrow \infty$), the actuator becomes rigidly coupled to the platform.

When the actuator is rigidly coupled to the platform, any damping or compliance required by the platform for vibration or force control must be provided by the active control of the actuator. In this case the dynamic behavior is mostly determined by the dynamic response of actuator and controller. The dynamic response can be tailored according to the desired performance criteria (within the dynamic response capabilities of the actuator). The main disadvantage is that the power efficiency of the system is reduced

Figure 2.4 - Basic Connector Model

when the actuators (active devices) are used to simulate springs and dampers (passive devices). An actuator can be made to behave as a damper and all the energy will be dissipated by the actuator. This can overheat the actuator, causing a degradation in performance and in the worse case lead to an actuator burnout. Furthermore, employing actuators as energy dissipators is costly. Better energy disspation can be achieved by incorporating a passive frictional element such as a viscous damper. Similar disadvantages will be encountered when the actuator is used as a spring. Another main disadvantage is that the dynamic response of the controller / actuator combination might not satisfy the desired system dynamic performance.

2.3 Implicit Force Control

One way to reduce or eliminate the complications associated with employing the actuator as a passive device is to include an actual spring/damper pair between the connector and the platform as shown in Figure 2.5. This is a model suitable for describe the behavior of the system when the implicit force control scheme is employed [16]. The additional components are as follows

K_c, is the stiffness element between the connector and the platform.

C_c, is the viscous damping element between the connector and the platform.

The Implicit Force Control scheme generates a force by controlling the displacement of an stiffness element [16]. The spring in the coupling stage between the connector and the platform can be used for such a control scheme, the damper can be used to limit the system's vibrations in the connector. The force $\underline{F}$ that the connector applies to the platform is a function of the displacement of the coupling stage Δ, and its first time derivative, the stiffness K_c and the damping coefficient C_c. It can be determined by using the following equation

$$\underline{F} = (K_c \Delta + C_c \frac{d\Delta}{dt}) \underline{s} \qquad (2)$$

where $\underline{s}$ is a unit vector parallel to the connector. It can now control a force by simply controlling a displacement variable Δ and its first time derivative and this process is called

Implicit Force Control. The actuator of the connector still has to generate a force in order to balance the force developed in the coupling spring and damper. The coupling spring is selected to be much more compliant than the connector, hence most of the deflection occurs in the coupling spring. This type of connector is well-suited for controlling the contact force between the platform and a rigid surface. Upon contact, the platform will yield to the shape of the rigid surface. An example would be the polishing of a mirror or glass with the platform. The contact force must be kept below some value to avoid damaging the surface.
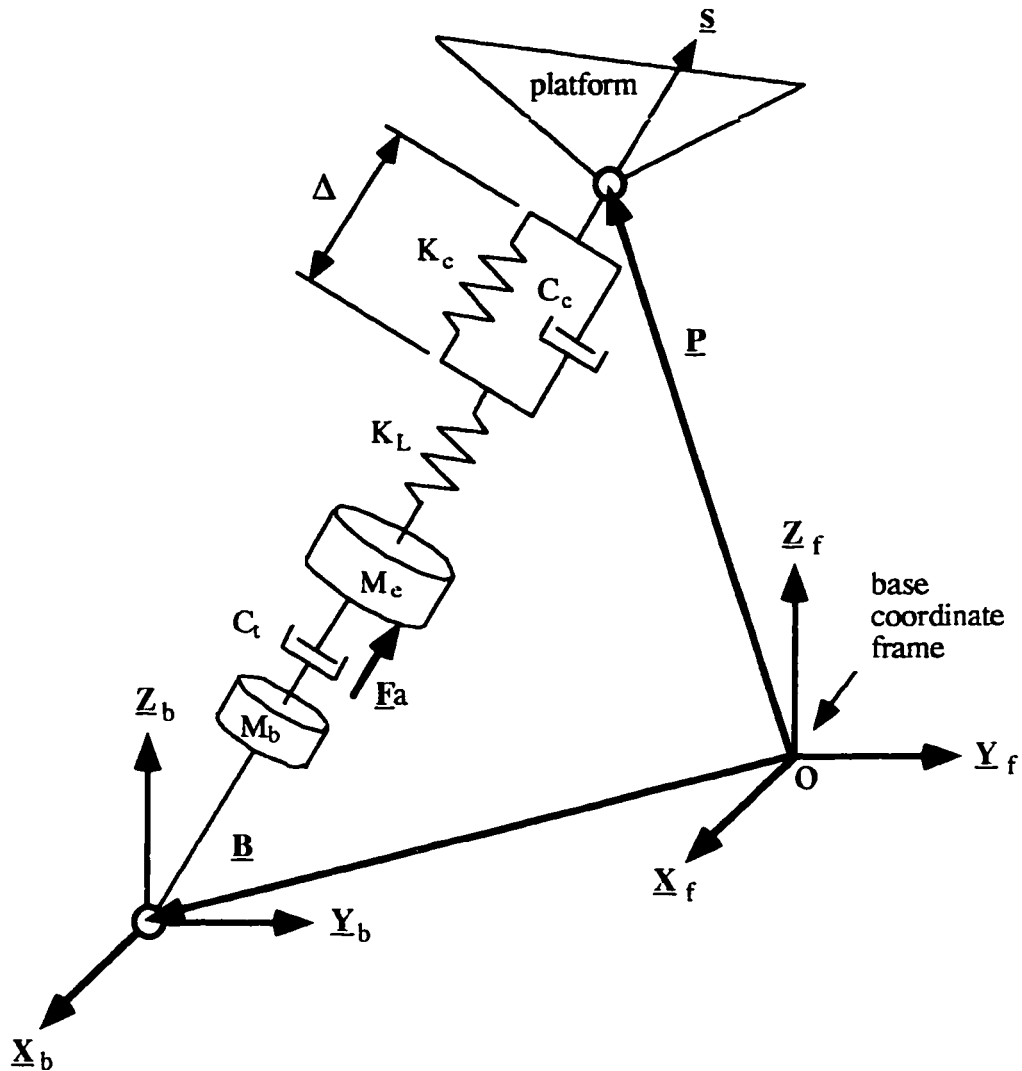
Figure 2.5 - Connector Model for the Implicit Force Control

One of the major disadvantages of employing this model is the relatively long time delay that the coupling stage introduces. When the actuator applies a force, the coupling stage has to deform before the force is transmitted to the platform. This reduces the speed at which the actuator force can be applied to the platform, and therefore the reaction time of the complete system is increased. This constitutes a major problem when high frequency disturbance forces are applied to the platform such as those generated when using the manipulator to support a workpiece that is being machined. The reaction time could be too slow in order to apply the required equilibrant forces to counteract these disturbances.

The damping element helps dissipate some of the energy the high frequency disturbances apply to the platform. The disadvantages of using the damping element in the model are that it also increases the reaction time of the system. Furthermore, some of the energy of the actuator is dissipated in this element instead of being transmitted to the platform.

2.4 Modified Implicit Force Control Mode

The use of a coupling damping element is not so effective in eliminating high frequency disturbances, since the vibrations will be transmitted to the actuator through the connector stiffness element. A possible solution to this problem is the use of a decoupling stage in parallel with the connector [17]. The model used for the implicit force control scheme can be modified as shown in Figure 2.6, the additional components are

K_d, is the decoupling stiffness element.

C_d, is the decoupling viscous damping element.

M_d, is the decoupling stage mass.

The decoupling stage damper C_d is used to reduce or eliminate the high frequency disturbances. This damper, unlike the coupling damping element C_c, will not transmit the vibrations to the actuator. Further more, it reduces the need to use the actuator as a passive energy dissipating element when high frequency disturbances are applied to the platform. The decoupling stage spring must be a very stiff component, as it models the support of the decoupling damper. If this spring is too compliant, the energy applied to the decoupling stage will deform the spring instead of being dissipated in the decoupling damping element. This energy will be returned to the platform increasing the vibrations instead of reducing them. At high frequencies, the decoupling damper generates a high reactive force that can be used to counteract the high frequency disturbances. The force F applied by the connector to the platform is a combination of the forces generated in the coupling and decoupling stages. The force generated in the coupling stage can be calculated by using equation (2). The force generated in the decoupling stage is a function of the first time

derivative of the its displacement λ, and the damping coefficient C_d. The force applied to

the platform can be calculated by using the following equation

$$\underline{F} = (K_c \delta + C_c \frac{d\delta}{dt} + C_d \frac{d\lambda}{dt}) \underline{s} \qquad (3)$$

The connector can now partially control a force by just controlling a displacement variable

Figure 2.6 - Connector model for the Modified Implicit Force Control

Δ_i and its first time derivative. This component of the force $\underline{F}$ is determined by the first

two terms of equation (3). The main drawback of using the decoupling stage is that it will always be dissipating energy. The decoupling stage can dissipate energy from either the disturbance force (which is the intended purpose) or from the actuator. In this latter case, part of the energy input from the connector actuator is being dissipated in the connector instead of being used to move the platform. Another disadvantage in using the decoupling stage is the increase of mass and moment of inertia caused by the element M_d. Some of the energy of the system will be used to move this additional inertia.

2.5 Combined High Frequency / Low Frequency Connector Model

It would be most desirable to have a connector capable of implementing the implicit force control scheme with minimum energy loss at low frequencies (such as the one shown in Figure 2.3, which has no decoupling stage), and a connector capable of effective disturbance rejection for high frequency applications. The coupling stage is undesirable for high frequency applications; the decoupling stage is not very useful for low frequency applications and reduces the power efficiency of the actuators.

A solution is to have a single connector with the capability of optimal performance at either low frequencies or high frequencies. This can be achieved provided that the decoupling and coupling stages employ viscous dampers with proportional control valves. The damping coefficient of a viscous damper can be regulated by opening or closing the valve. When the valve is fully closed, the viscous damper is locked (the viscous damping coefficient is extremely high, $C \Rightarrow \infty$) and will behave as an very rigid component with no damping. When the valve is completely open, the damper will act as a very low energy dissipating element (the damping coefficient $C \Rightarrow 0$). For the low frequency mode, the decoupling stage must be inactive (no energy will be dissipated in this stage). This can be achieved by completely opening the control valve of the decoupling damper. The decoupling stage would only dissipate a small amount of energy. In this case, the only noticeable effect of the decoupling stage would be its mass. This mass can be grouped
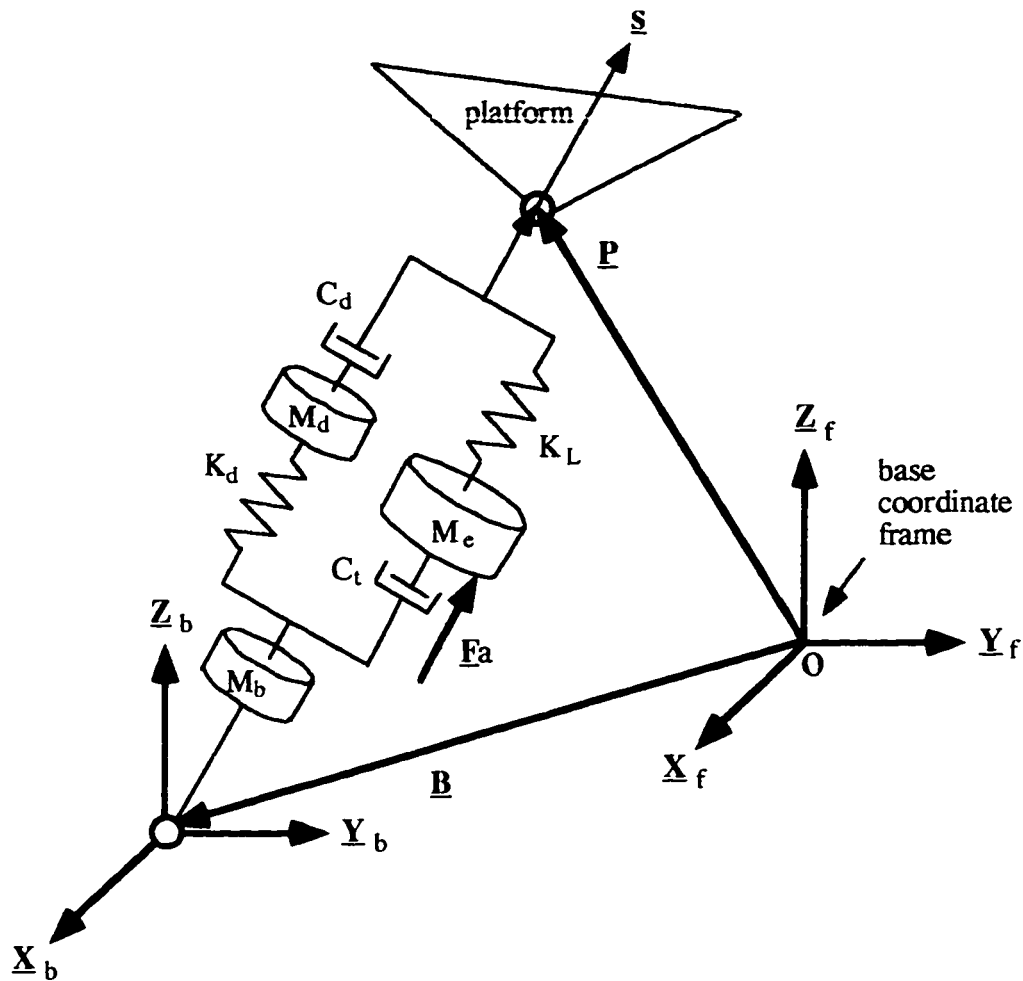
Figure 2.7 - Connector model for the High Frequency Mode

with the actuator base mass. The control valve of the coupling damper would be set to an opening that would provide the desired viscous damping for the coupling stage. The connector model would similar to the one shown in Figure 2.5, the difference being the higher base inertia $M'_b = M_b + M_d$.

For the high frequency mode, the coupling stage must be inactivated. This can be done by completely closing the control valve of the coupling damper. When the valve of the coupling damper is completely closed, it acts as an extremely rigid element. This means that there are no deflections in the coupling stage. The control valve of the decoupling damper would be set according to the desired damping coefficient for the decoupling stage.

The connector model for this case is the one shown in Figure 2.7.

Another possible mode of operation of this multi-purpose connector would be to inactivate the decoupling and coupling stages by completely opening the control valve of the decoupling damper and completely closing the control valve of the coupling damper. The connector model to be used in this case is the one shown in Figure 2.4. This allows the designer to tailor the dynamic response of the system by designing an appropriate controller.

2.6 Connector Model for Dynamic Modeling

The final connector model that will used for developing the system's complete dynamic model is shown in Figure 2.8. This has all the components described in the previous sections. The objective is to develop a model that can exhibit the system behavior in different operating modes. Each connector requires the following coordinates or variables to describe its complete configuration

$\underline{s}$, is a unit vector parallel to the connector.

E , is the location of M_i along the connector's direction.

H , is the actual length of the connector (the coupling stage is not included).

L , is the total length of the connector

D , is the location of the connection between the decoupling spring and damper.

bl , is the distance of the base mass, M_b, from the connector's base joint (this a fixed

distance).

$\underline{s}$ and L are dependent variables which can be described in terms of the platform's location and orientation. Each of the connectors has 3 degrees of freedom since the coordinates E, H, D are independent variables.
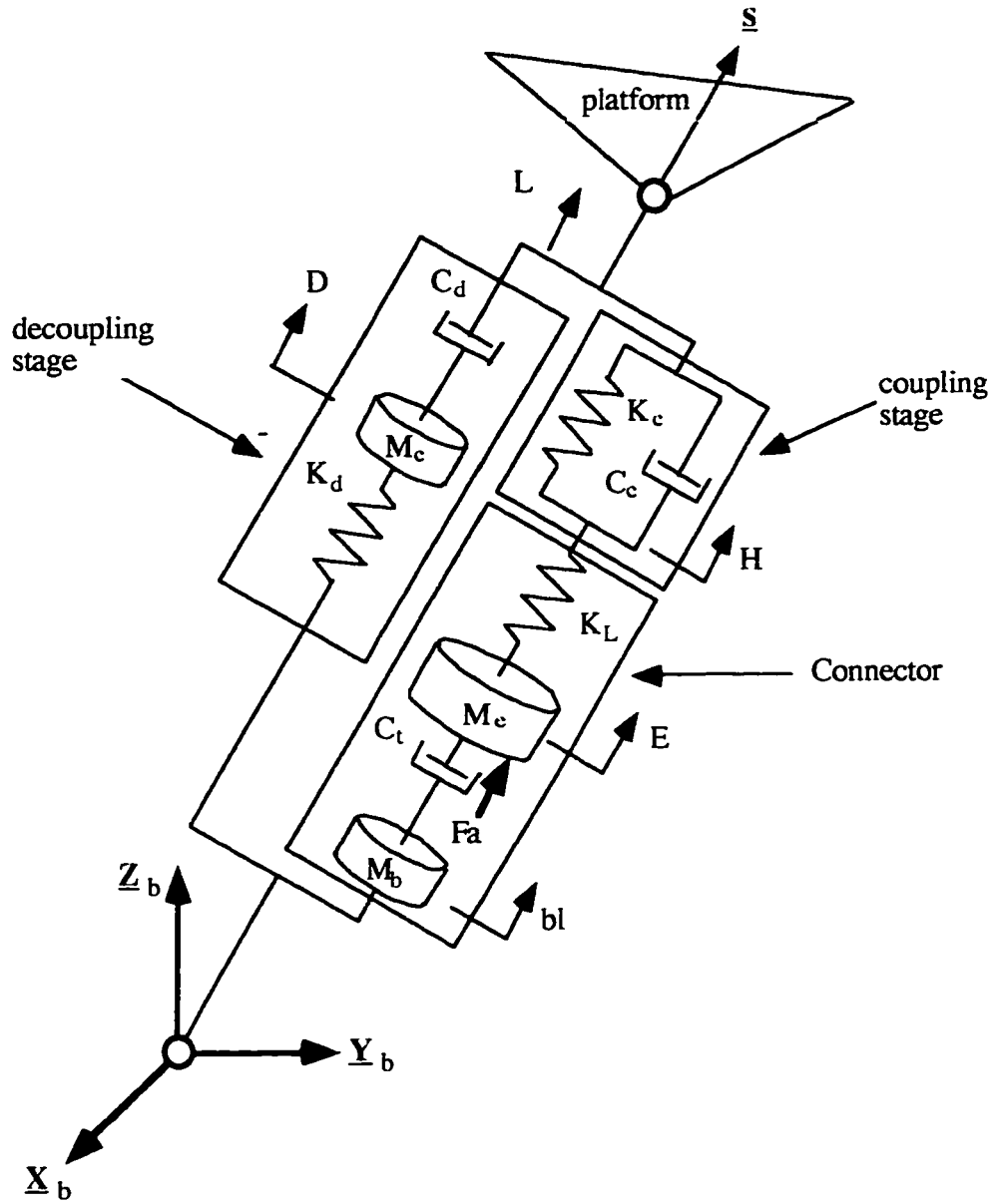
Figure 2.8 - Complete Connector Lumped Parameter Model

CHAPTER 3
PARALLEL MANIPULATOR KINEMATICS

The dynamic state of a multi-body system is a function of the position, velocity and acceleration of the multi-connected bodies. It is therefore neccessary to perform a complete kinematic analysis of the system.

The required input forces and torques can be determined for a specified kinematic state of a system (position, velocity and acceleration). This is known as the inverse dynamic formulation. It is also possible to compute the kinematic state of the system for a specified set of values of input forces and torques. This is known as the foward dynamic formulation. In the case of a spatial parallel manipulator, the kinematic state of the system (position, velocity and acceleration) will be specified according to a desired task; and then the forces and torques required to produce such kinematic state will be calculated.

3.1 Forward and Inverse Kinematics

The spatial parallel manipulator or platform is a 6-degree-of-freedom system. The location (position and orientation) of the platform is determined by the length of each of the six connectors. When the six connector lengths are specified, the location and orientation of the platform can be determined. This is known as the forward displacement analysis and it is extremely difficult because there are multiple solutions [2]. Fortunately, the foward displacement analysis of parallel manipulators is not required for the dynamic analysis of the system.

On the other hand, it is relatively simple to compute a unique set of connector lengths when the location of the platform is specified. This is known as the inverse displacement analysis and is useful in developing the dynamic model of the system. The location of the platform must be specified when it is used for example to present a workpiece to a machine tool or it is used as a flight simulator. The displacement and orientation of each of the

connectors that actuate the platform can be determined, once its motion time history has been specified. The inverse kinematics formulation will be used in describing the motion of the system because it is more application-oriented.

3.2 Kinematic Relationships

Prior to the kinematic analysis of the platform, some basic kinematic relationships required for such analysis will be derived.

3.2.1 Location Analysis of the Platform

The location of the platform will be specified firstly by defining a position vector $\underline{C}$ that locates the center point c of the platform (which is also its center of mass) together with its orientation as shown in Figure 3.1. This location is used to determine the length and
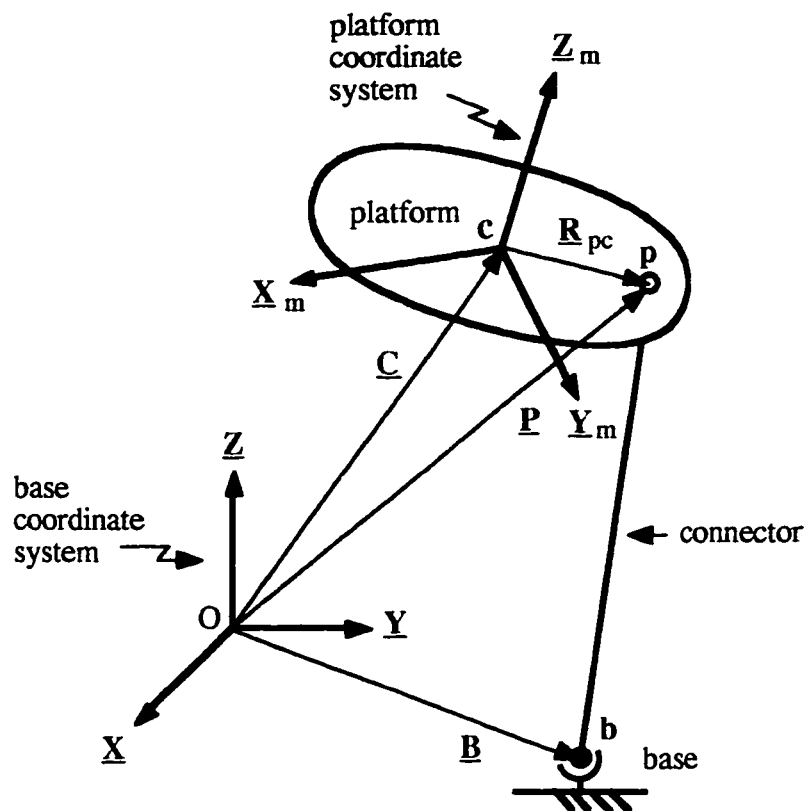

Figure 3.1 - Base, Platform and position vectors

orientation of each of the connectors. In Figure 3.1 a point O is chosen which is the origin of a set of fixed axes which is called the base frame. The ends of any connector are labeled p and b (see Figure 3.1) and the corresponding position vectors drawn from O are $\underline{P}$ and $\underline{B}$ respectively.

3.2.2 Description of the Orientation of the Platform

The orientation of the platform can be described by a set of three mutually perpendicular unit vectors attached to the platform : $\underline{X}_m$, $\underline{Y}_m$ & $\underline{Z}_m$. These vectors form a right handed set with an origin at point c and define the moving frame of the platform. Each of these vectors is described by three parameters (the directional cosines for each vector). Although nine parameters are required to define these three vectors, there really are only three independent parameters since the following six constraints that have to be satisfied

- For example, choosing unit vectors yields three constraints

$$|\underline{X}_m| = 1 \quad ; \quad |\underline{Y}_m| = 1 \quad \& \quad |\underline{Z}_m| = 1$$

- For mutually perpendicular vectors, their scalar products must be zero, which yields a further three constraints

$$\underline{X}_m \cdot \underline{Y}_m = 0 ; \quad \underline{X}_m \cdot \underline{Z}_m = 0 \quad \& \quad \underline{Z}_m \cdot \underline{Y}_m = 0$$

Therefore only three parameters have to be specified to completely describe the orientation of the platform with respect to the base (three degrees of freedom).

The specification of the frame of reference for the platform depends upon the desired system motion which is based on the motion and task planning. This will be discussed later in the Section 3.6.

3.3 Position Analysis

The location of the platform can be specified by the position of the center point c and the orientation of the platform itself. The position of any point on the platform can be determined by using the following equation

$$\underline{P} = \underline{C} \cdot \underline{R}_{pc} \qquad (1)$$

where $\underline{P}$ is the position of point p on the platform, defined in the base frame coordinate system; $\underline{C}$ is the position of the center point c ; $\underline{R}_{pc}$ is the relative position vector of point p with respect to the center point c as shown in Figure 3.2. These position vectors are defined with respect to the fixed or the base coordinate system.

The relative position vector $\underline{R}_{pc}$ is defined with respect to a coodinate system that is parallel to the base coordinate system, has its origin at c and is defined by the unit vectors
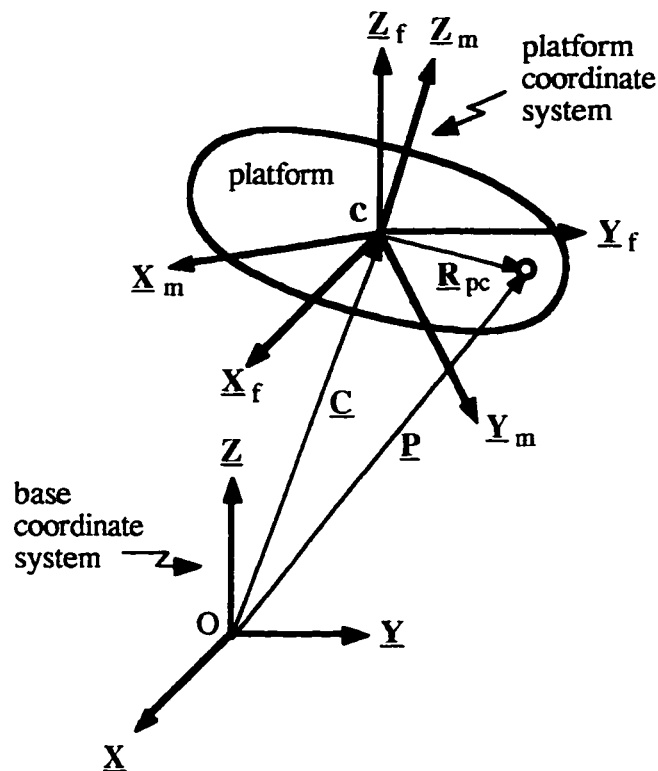
Figure 3.2 - Location Analysis

$\underline{X}_f, \underline{Y}_f$, and $\underline{Z}_f$ as shown in Figure 3.2. The vector $\underline{R}_{pc}$ can also be defined with respect to the moving coordinate system or the platform's coordinate system as

$$\underline{R}_{pc/m} = [\, x_{pc/m},\ y_{pc/m},\ z_{pc/m}\,]^T.$$

This vector is a constant when defined in the moving coordinate frame regardless of the orientation of the platform.

The unit vector $\underline{X}_m$ can be described in the fixed coordinate frame as (see Figure 3.3)

$$\underline{X}_m = a_{11}\underline{X}_f + a_{12}\underline{Y}_f + a_{13}\underline{Z}_f \qquad (2.a)$$

where a_{11}, a_{12} & a_{13} are the direction cosines of the unit vector $\underline{X}_m$ with respect to the fixed coordinate frame. In a similar fashion, the unit vectors $\underline{Y}_m$ and $\underline{Z}_m$ can also be defined in the fixed coordinate frame using their respective directional cosines

$$\underline{Y}_m = a_{21}\underline{X}_f + a_{22}\underline{Y}_f + a_{23}\underline{Z}_f \qquad (2.b)$$

$$\underline{Z}_m = a_{31}\underline{X}_f + a_{32}\underline{Y}_f + a_{33}\underline{Z}_f \qquad (2.c)$$

Figure 3.3 - Vector $\underline{X}_m$ described in the fixed coordinate frame

The relative position vector can be written as

$$\underline{R}_{pc/m} = x_{pc/m}\,\underline{X}_m + y_{pc/m}\,\underline{Y}_m + z_{pc/m}\,\underline{Z}_m$$

The relative position vector can be written with respect to the fixed coordinate frame by combing the above equation and equations (2.a), (2.b) and (2.c)

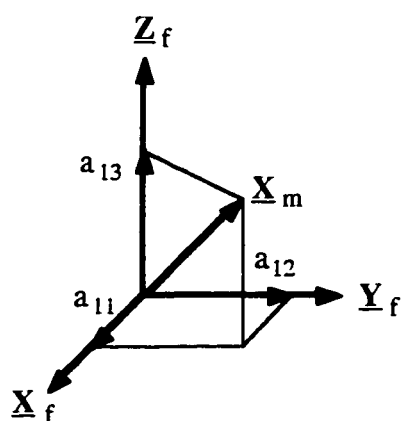$$\underline{R}_{pc} = x_{pc/m}\begin{bmatrix} a_{11}\underline{X}_f \\ a_{12}\underline{Y}_f \\ a_{13}\underline{Z}_f \end{bmatrix} + y_{pc/m}\begin{bmatrix} a_{21}\underline{X}_f \\ a_{22}\underline{Y}_f \\ a_{23}\underline{Z}_f \end{bmatrix} + z_{pc/m}\begin{bmatrix} a_{31}\underline{X}_f \\ a_{32}\underline{Y}_f \\ a_{33}\underline{Z}_f \end{bmatrix}$$

The vector $\underline{R}_{pc}$ can be also be written as

$$\underline{R}_{pc/f} = x_{pc/f}\,\underline{X}_f + y_{pc/f}\,\underline{Y}_f + z_{pc/m}\,\underline{Z}_f$$

where the components are given by

$$x_{pc/f} = x_{pc/m}\,a_{11} + y_{pc/m}\,a_{12} + z_{pc/m}\,a_{13} \qquad (3.a)$$

$$y_{pc/f} = x_{pc/m}\,a_{21} + y_{pc/m}\,a_{22} + z_{pc/m}\,a_{23} \qquad (3.b)$$

$$z_{pc/f} = x_{pc/m}\,a_{31} + y_{pc/m}\,a_{32} + z_{pc/m}\,a_{33} \qquad (3.c)$$

By using equations (3.a), (3.b) and (3.c) the relative position vector is transformed from the moving coordinate frame to the fixed coordinate frame. This relationship can be written in matrix form as

$$\underline{R}_{pc} = \begin{bmatrix} a_{11} & a_{12} & a_{13} \\ a_{21} & a_{22} & a_{23} \\ a_{31} & a_{32} & a_{33} \end{bmatrix} \underline{R}_{pc/m} \qquad (4)$$

The 3 x 3 matrix is generally known as the rotation matrix or the transformation matrix since it transforms a vector from one coordinate system to a second coordinate system [18].

The matrix elements are the directional cosines of the unit vectors of the first coordinate system with respect to the second coordinate system and are a function of the orientation of the platform with respect to the fixed coordinate frame. The specification of these directional cosines as a function of the desired motion of the platform will be discussed in detail in Section 3.6.

The center point position, given by the vector $\underline{C}$, is a user defined vector characterized by three variables: $\underline{C} = [\ X_c\ ,\ Y_c\ ,Z_c\ ]^T$. Each of these variables is a function of time. The position of the platform can be varied by changing the location of the center point and/or the orientation matrix of the platform. In order to completely locate the platform, three variables must be specified for the centerpoint's location and three variables for the platform's orientation. Therefore the platform has 6 degrees-of-freedom.

3.3.1 Connector Length and Orientation

The length and the orientation of each connector can be calculated once the position of the points **b** and **p** on each connector is known (see Figure 3.4). The position of point **p** can be calculated using equation (1). The location of point **b** is specified when defining the geometry of the manipulator. The Plücker line coordinates for each connector, $[\ \underline{s}, \underline{s}_o\ ]^T$, are calculated using

$$\hat{S} = [\underline{s}\ ;\ \underline{s}_o]\ ;\ \underline{s} = \text{Direction of the Line}\ ;\ \underline{s}_o = \text{Moment of the Line}$$

$$\underline{s} = \frac{[\ \underline{P} - \underline{B}\ ]}{|\ \underline{P} - \underline{B}\ |}\ ;\qquad \underline{s}_o = \frac{\underline{B}\ \text{x}\ [\ \underline{P} - \underline{B}\ ]}{|\ \underline{P} - \underline{B}|} \qquad (5)$$

The direction and the moment of the line are defined with respect to the base frame coordinate system as shown in Figure 3.4. A vector $\underline{L}$ along the connector can be defined as

$$\underline{L} = \underline{P} - \underline{B} = [\ L\ ]\ \underline{s} \quad \Rightarrow \quad \text{vector along the connector}$$

$$L = |\underline{P} - \underline{B}|\ \Rightarrow\ \text{length of the connector}\ ;\quad \underline{s} = \frac{\underline{P} - \underline{B}}{|\underline{P} - \underline{B}|}\ \Rightarrow\ \text{unit vector along the connector}$$
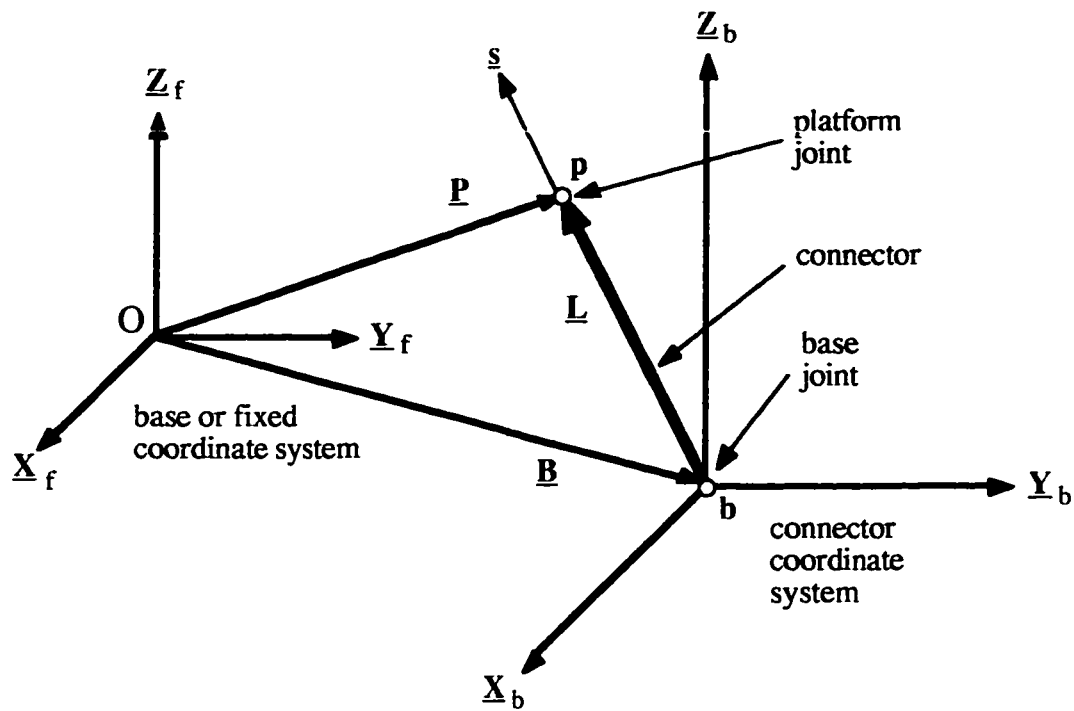
Figure 3.4 - Connector Location Analysis

3.4 Velocity Analysis

The velocity and angular velocity (also known as the velocity state) of a point on a rigid

body such as the platform can be described by a twist, $\hat{T}$

$$\hat{\underline{T}} = \begin{bmatrix} \underline{V}_o \\ \underline{\omega} \end{bmatrix}$$

where $\underline{\omega}$ is the angular velocity vector and $\underline{V}_o$ is the velocity of the point O on the rigid

body coincident with the point of reference [19, 20, 21, 22]. This twist or rotor can be

modeled as the resultant instantaneous motion generated by the rotation about a screw with

axis $\underline{s}$ and a pitch h

$$\hat{\underline{T}} = \omega \begin{bmatrix} [\underline{r}_o \times \underline{s}] + h\underline{s} \\ \underline{s} \end{bmatrix} \tag{6}$$

where $\underline{r}_o$ is vector from the point O to the axis of the screw as shown in Figure 3.5. The velocity of point O is given by

$$\underline{V}_o = \omega[(\underline{r}_o \times \underline{s}) + h\underline{s}]$$ (7)

The instantaneous motion or velocity of the centerpoint c can be described using the same notation by relocating the origin at point c. This can be done by substituting $\underline{r}_o$ for

$$\underline{r}_c = \underline{r}_o - \underline{C}$$

$$\underline{V}_c = \omega[(\underline{r}_c \times \underline{s}) + h\underline{s}]$$ (8)

Using equation (7), the velocity of point c can also be written as

$$\underline{V}_c = \underline{V}_o - \omega(\underline{C} \times \underline{s})$$ (9)

Figure 3.5 - Instantaneous Motion Analysis

The instantaneous motion or velocity of any point p on the platform can be described using the same notation by relocating the origin to that given point. The velocity of point p can be determined by relocating the origin at point p. This can be done by substituting $\underline{r}_o$ for

$$\underline{r}_p = \underline{r}_o - \underline{C} - \underline{R}_{pc}$$
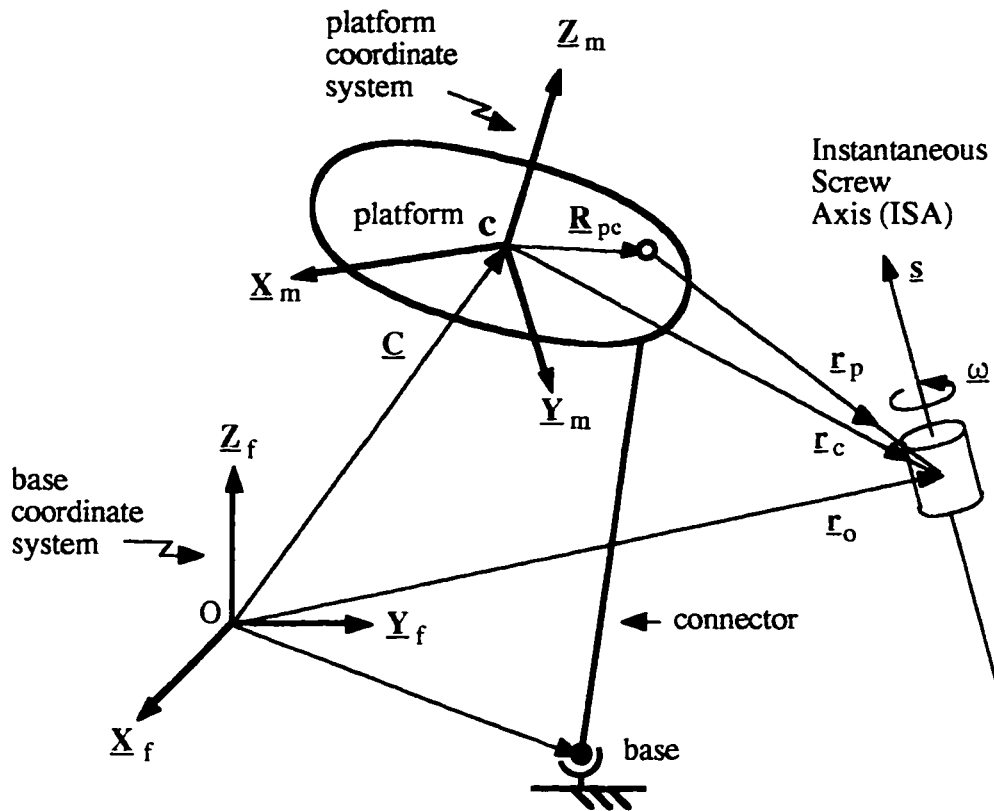
$$\underline{V}_p = \omega\left[\left(\left(\underline{r}_o - \underline{C} - \underline{R}_{pc}\right) \times \underline{s}\right) + h\underline{s}\right] \qquad (10)$$

By combining equations (8) and (10), the velocity $\underline{V}_p$ can be also be written as a function of the angular velocity vector $\underline{\omega}$ and the velocity of the centerpoint of the platform

$$\underline{V}_p = \underline{V}_c + \left(\underline{\omega} \times \underline{R}_{pc}\right) \qquad (11)$$

where $\underline{V}_p$ is the velocity of point p, $\underline{V}_c$ is the velocity of the centerpoint, $\underline{\omega}$ is the angular velocity vector of the platform ($\underline{\omega} = \omega_x \underline{i} + \omega_y \underline{j} + \omega_z \underline{k}$) and $\underline{R}_{pc}$ is the relative position vector of point p with respect to the centerpoint. The velocity vector $\underline{V}_p$ can then be written as in its expanded form as

$$\underline{V}_p = \begin{pmatrix} V_{cx} \\ V_{cy} \\ V_{cz} \end{pmatrix} + \begin{pmatrix} \omega_x \\ \omega_y \\ \omega_z \end{pmatrix} \times \begin{pmatrix} R_{pcx} \\ R_{pcy} \\ R_{pcz} \end{pmatrix} = \begin{pmatrix} V_{cx} + \omega_y \cdot R_{pcz} - \omega_z \cdot R_{pcy} \\ V_{cy} + \omega_z \cdot R_{pcx} - \omega_x \cdot R_{pcz} \\ V_{cz} + \omega_x \cdot R_{icy} - \omega_y \cdot R_{pcx} \end{pmatrix}$$

3.4.1 Connector Velocity Analysis

The parallel manipulator is made up of a platform joined to a fixed body or base through six connectors acting in parallel. Each connector consists of a serial HPS kinematic chain. The letters H, P and S denote respectively the Hooke joint and prismatic and spherical pairs and the order in which these pairs are connected. The Hooke joint is connected to ground, the prismatic joint which is the only actuated joint is the intermediate pair and the spherical joint connects to the platform as shown in Figure 3.6.

The coordinates for the twist or velocity state of the end effector or platform can be written as (see Figure 3.7)

$$\hat{\underline{T}} = \omega_1 \hat{\underline{S}}_1 + \omega_2 \hat{\underline{S}}_2 + V_3 \hat{\underline{S}}_3 + \omega_4 \hat{\underline{S}}_4 + \omega_5 \hat{\underline{S}}_5 + \omega_6 \hat{\underline{S}}_6 \qquad (12)$$

where $\hat{\underline{S}}_1$ and $\hat{\underline{S}}_2$ are the line coordinates of the pair of intersecting rotors modelling the Hooke joint of the HPS manipulator; $\hat{\underline{S}}_4$, $\hat{\underline{S}}_5$ and $\hat{\underline{S}}_6$ are the line coordinates of the three rotors modelling the spherical pair; and $\hat{\underline{S}}_3$ are the line coordinates of the prismatic pair

$$\hat{\underline{S}}_3 = \begin{bmatrix} \underline{s}_3 \\ 0 \end{bmatrix} \qquad (13)$$
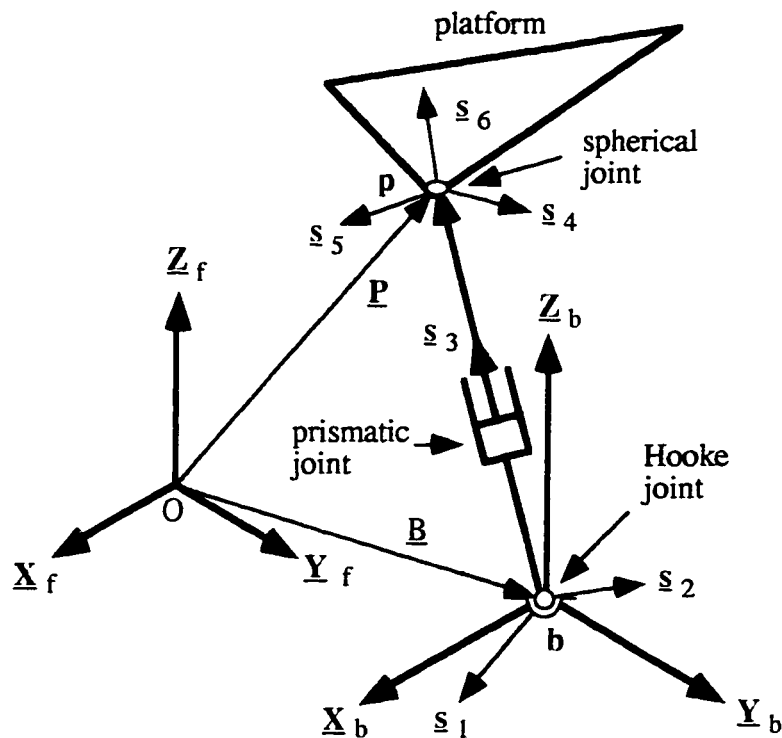
Figure 3.6 - The HPS serial manipulator

where $\underline{s}_3$ is a unit vector parallel to the connector. By selecting point p, the center of the spherical pair, as the origin of the coordinate system equation (12) can be written in the form

$$\begin{bmatrix} \underline{V}_p \\ \underline{\omega} \end{bmatrix} = \omega_1 \begin{bmatrix} \underline{S}_{o1} \\ \underline{S}_1 \end{bmatrix} + \omega_2 \begin{bmatrix} \underline{S}_{o2} \\ \underline{S}_2 \end{bmatrix} + V_3 \begin{bmatrix} \underline{S}_3 \\ 0 \end{bmatrix} + \omega_4 \begin{bmatrix} 0 \\ \underline{S}_4 \end{bmatrix} + \omega_5 \begin{bmatrix} 0 \\ \underline{S}_5 \end{bmatrix} + \omega_6 \begin{bmatrix} 0 \\ \underline{S}_6 \end{bmatrix} \qquad (14)$$

It can be seen that the velocity vector $\underline{V}_p$ is only a function of the first three rotors of the HPS chain

$$\underline{V}_p = \omega_1 \underline{S}_{o1} + \omega_2 \underline{S}_{o2} + V_3 \underline{S}_3 \qquad (15)$$

The direction vector of the angular velocity $\underline{\omega}_1$, $\underline{S}_1$, is a stationary or fixed vector that will be selected to be parallel to the fixed $\underline{X}_f$ axis. The direction vector of the angular velocity $\underline{\omega}_2$, $\underline{S}_2$, is perpendicular to the direction vectors $\underline{S}_1$ and $\underline{S}_3$, as shown in Figure 3.8,
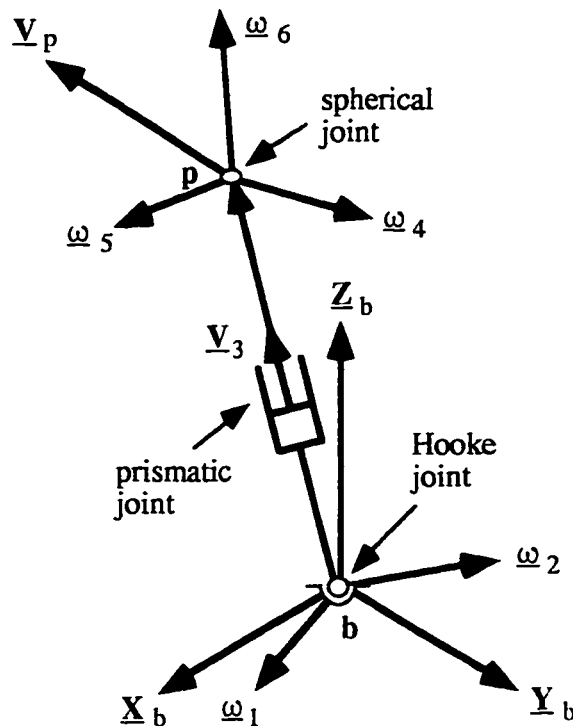
Figure 3.7 - Rotors of the HPS Manipulator
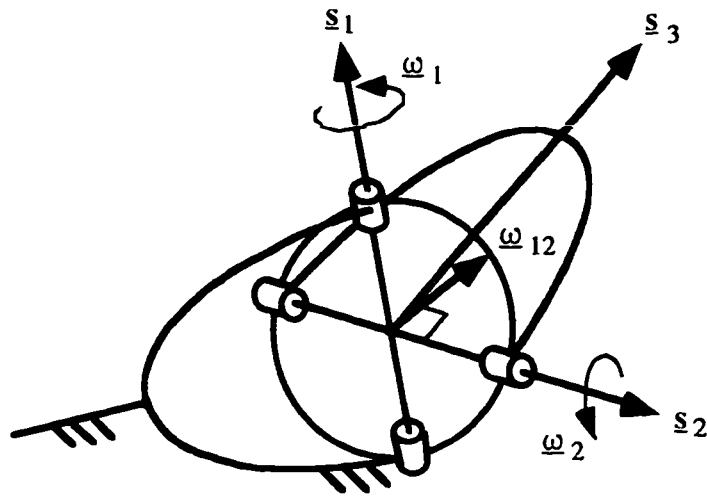
Figure 3. 8 - Hooke Joint at the connector's base

and can be determined by

$$\underline{S}_2 = \underline{S}_1 \times \underline{S}_3$$

Since the vector $\underline{s}_1$ is parallel to the fixed $\underline{X}_f$ axis, vector $\underline{s}_2$ is confined to the YZ plane. The required line coordinates for evaluating equation (15) are given by

$$S_{o1} = -L\underline{S}_3 \times \underline{S}_1; \quad S_{o2} = -L\underline{S}_3 \times \underline{S}_2; \quad \underline{S}_3 = \frac{[\underline{P} - \underline{B}]}{|\underline{P} - \underline{B}|} \quad (16)$$

where $\underline{P}$ is the position vector of point p, $\underline{B}$ is the position vector of point b and $\underline{L}$ is the vector along the connector from point b to point p. The line coordinates for rotors 1 and 2 can also be written as

$$S_{o1} = L\underline{S}_1 \times \underline{S}_3 = L\underline{S}_2; \quad S_{o2} = L\underline{S}_2 \times \underline{S}_3 = L\underline{S}_{23}$$

where the vector $\underline{s}_{23} = \underline{s}_2 \times \underline{s}_3$. Using the line coordinates for the three rotors and equation (15), the velocity vector $\underline{V}_p$ can be written as

$$\underline{V}_p = L\omega_1 \underline{S}_2 + L\omega_2 \underline{S}_{23} + V_3 \underline{S}_3 \quad (17)$$

3.4.2 Inverse Velocity Analysis

For the dynamic analysis it is most important to determine the velocity of the prismatic pair and the angular velocity of the Hooke joint of the HPS manipulator. A unit force vector acting along the connector itself has the following ray coordinates

$$\hat{\underline{S}}_3 = \begin{bmatrix} \underline{s}_3 \\ 0 \end{bmatrix}$$

This force is clearly reciprocal to the rotors 1, 2, 4, 5 and 6. Forming the reciprocal product of this unit force with equation (11) yields the following expression for the prismatic pair velocity V_3

$$V_3 = \underline{V}_p \cdot \underline{s}_3 \tag{18}$$

A unit force vector acting along unit vector $\underline{s}_2$ and going through point p has the following ray coordinates

$$\hat{\underline{S}}_2^* = \begin{bmatrix} \underline{s}_2 \\ 0 \end{bmatrix}$$

This force is clearly reciprocal to the rotors 2, 3, 4, 5 and 6. Forming the reciprocal product of this unit force with equation (11) and using the line coordinates derived previously yields the following expression for the angular velocity ω_1

$$\omega_1 = \frac{\underline{V}_p \cdot \underline{s}_2}{L} \tag{19}$$

A unit force vector acting along unit vector $\underline{s}_{23}$ and going through point p has the following ray coordinates

$$\hat{\underline{S}}_{23}^* = \begin{bmatrix} \underline{s}_{23} \\ 0 \end{bmatrix}$$

This force is clearly reciprocal to the rotors 1, 3, 4, 5 and 6. Forming the reciprocal product of this unit force with equation (11) and using the line coordinates derived previously yields the following expression for the angular velocity ω_2

$$\omega_2 = \frac{\mathbf{V}_p \cdot \mathbf{s}_{23}}{L} \qquad (20)$$

The connector angular velocity vector $\underline{\omega}_{12}$ is defined as the sum of the angular velocity vectors $\underline{\omega}_1$ and $\underline{\omega}_2$

$$\underline{\omega}_{12} = \frac{\left[\mathbf{V}_p \cdot \mathbf{s}_2\right]}{L}\,\mathbf{s}_1 + \frac{\left[\mathbf{V}_p \cdot \mathbf{s}_{23}\right]}{L}\,\mathbf{s}_2 \qquad (21)$$

This vector and can be written as a function of the platform's centerpoint velocity vector $\mathbf{V}_c$ and the platform's angular velocity vector $\underline{\omega}$

$$\underline{\omega}_{12} = \frac{\left[(\mathbf{V}_c \cdot \mathbf{s}_2) + \underline{\omega} \cdot (\mathbf{R}_{pc} \times \mathbf{s}_2)\right]}{L}\,\mathbf{s}_1 + \frac{\left[(\mathbf{V}_c \cdot \mathbf{s}_{23}) + \underline{\omega} \cdot (\mathbf{R}_{pc} \times \mathbf{s}_{23})\right]}{L}\,\mathbf{s}_2 \qquad (22)$$

3.4.3 Rigid Body Velocity Analysis

The velocity of point p, $\mathbf{V}_p$, can be determined by using equation (11) or (17). Expressions for the velocities and angular velocities of the rigid bodies in the connector model must also be found. As explained in Section 2.5, the connector can be modeled as the system shown in Figure 3.9. All the rigid bodies in the connector will have the same orientation and therefore the same angular velocity vector $\underline{\omega}_{12}$.

The velocity of mass M_b is only a function of the angular velocity of the Hooke joint $\underline{\omega}_{12}$ since its distance from the base, bl, is constant. The velocity of this rigid body can be written as

$$\mathbf{V}_b = bl\left[\underline{\omega}_{12} \times \mathbf{s}_3\right] \qquad (23)$$

Using the expression for the angular velocity vector $\underline{\omega}_{12}$ given in equation (22) and the definitions for the unit vector $\underline{s}_2$ and $\underline{s}_{23}$, the velocity of the base mass can be written as

$$\underline{V}_b = \frac{bl}{L}\left[(\underline{V}_c \cdot \underline{s}_2) + \underline{\omega} \cdot (\underline{R}_{pc} \times \underline{s}_2)\right]\underline{s}_2 +$$

$$\frac{bl}{L}\left[(\underline{V}_c \cdot \underline{s}_{23}) + \underline{\omega} \cdot (\underline{R}_{pc} \times \underline{s}_{23})\right]\underline{s}_{23} \qquad (24)$$

The velocity of mass M_d is function of the connector's rotation and the rate of change of the distance D

$$\underline{V}_d = \dot{D}\,\underline{s}_3 + D(\underline{\omega}_{12} \times \underline{s}_3) \qquad (25)$$

Using the expression for the angular velocity vector $\underline{\omega}_{12}$ given in equation (22) and the definitions for the unit vector $\underline{s}_2$ and $\underline{s}_{23}$, the velocity of the decoupling stage mass can be written as

$$\underline{V}_d = \dot{D}\underline{s}_3 + \frac{D}{L}\left[(\underline{V}_c \cdot \underline{s}_2) + \underline{\omega} \cdot (\underline{R}_{pc} \times \underline{s}_2)\right]\underline{s}_2 +$$

$$\frac{D}{L}\left[(\underline{V}_c \cdot \underline{s}_{23}) + \underline{\omega} \cdot (\underline{R}_{pc} \times \underline{s}_{23})\right]\underline{s}_{23} \qquad (26)$$

The velocity of the mass M_e is also a function of the connector's rotation and the rate of change of the distance E

$$\underline{V}_e = \dot{E}\,\underline{s}_3 + E(\underline{\omega}_{12} \times \underline{s}_3) \qquad (27)$$

Using the expression for the angular velocity vector $\underline{\omega}_{12}$ given in equation (22) and the definitions for the unit vector $\underline{s}_2$ and $\underline{s}_{23}$, the velocity of the connector equivalent mass can be written as

$$\underline{V}_e = \dot{E}\underline{s}_3 + \frac{E}{L}\left[(\underline{V}_c \cdot \underline{s}_2) + \underline{\omega} \cdot (\underline{R}_{pc} \times \underline{s}_2)\right]\underline{s}_2 +$$

$$\frac{E}{L}\left[(\underline{V}_c \cdot \underline{s}_{23}) + \underline{\omega} \cdot (\underline{R}_{pc} \times \underline{s}_{23})\right]\underline{s}_{23} \qquad (28)$$
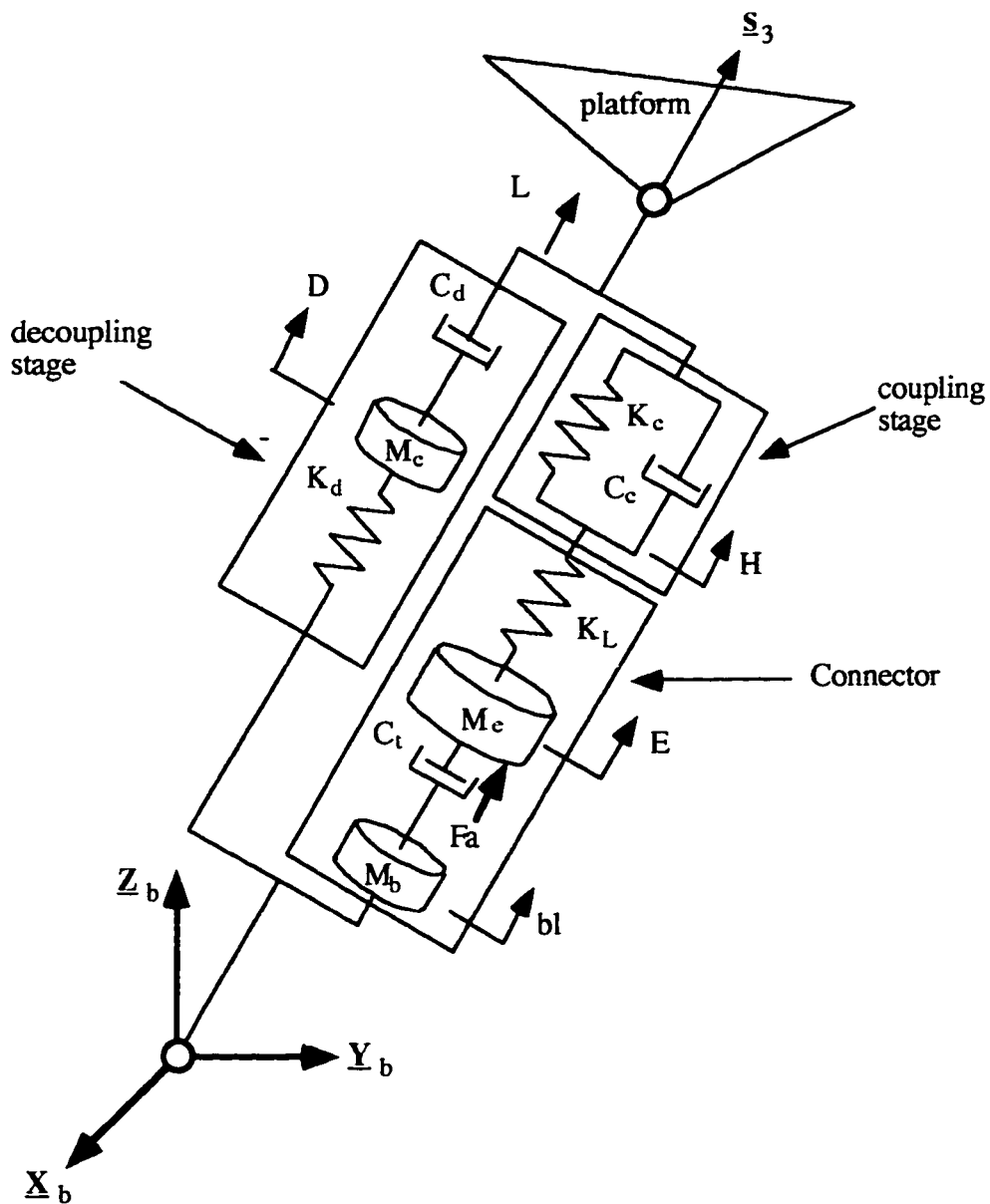
Figure 3.9 - Complete Connector Model

3.5 Acceleration Analysis

The acceleration and angular acceleration (also known as the acceleration state) of a rigid body such as the platform can be described by an accelerator $\hat{\underline{A}}$:

$$\hat{\underline{A}} = \begin{bmatrix} \underline{A}_o - \underline{\omega} \times \underline{V}_o \\ \underline{\alpha} \end{bmatrix}$$

where $\underline{\omega}$, $\underline{\alpha}$ are the angular velocity and acceleration vectors of the rigid body. The vectors $\underline{V}_o$ and $\underline{A}_o$ are the velocity and acceleration of the point O on the rigid body coincident with the point of reference. The accelerator is a motor [22] where the directional part $\underline{m}$, the angular acceleration vector $\underline{\alpha}$ in this case, is independent of the origin. The moment part of the motor $\underline{m}_o$, the acceleration vector term in this case
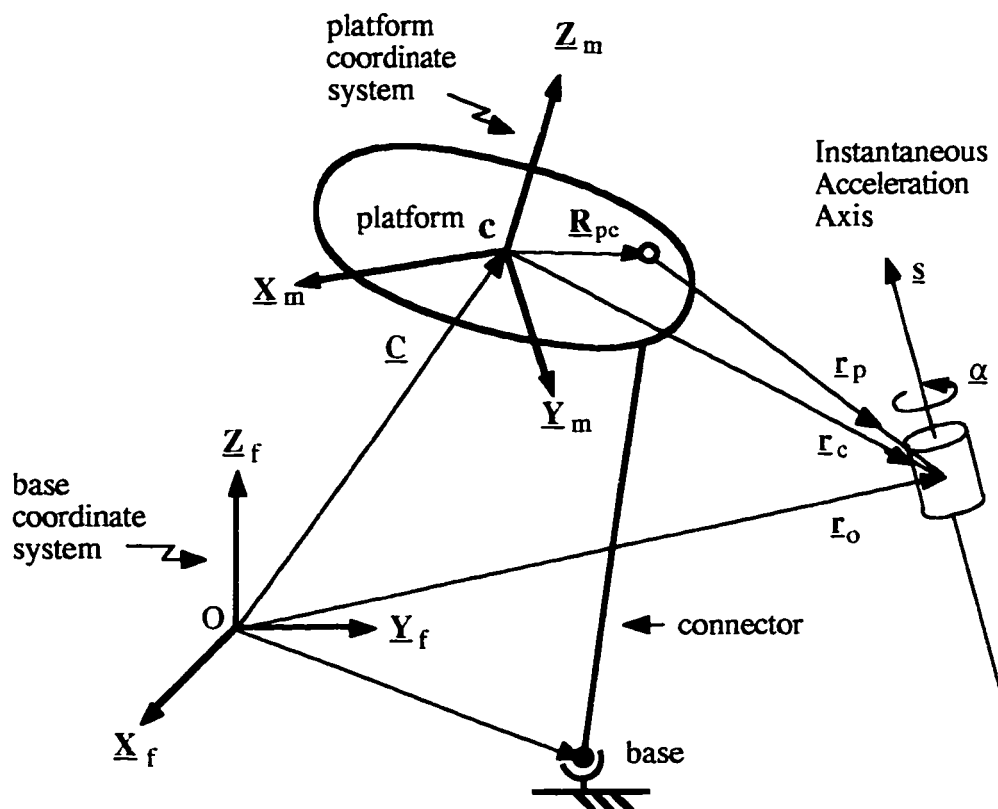
Figure 3.10 - Second Order Instantaneous Kinematics

$\underline{A}_o - \underline{\omega} \times \underline{V}_o$, changes to $\underline{m}_p = \underline{m}_o + \underline{PO} \times \underline{m}$ when the origin is moved from point O

to point p. The acceleration of the centerpoint of the platform c can be determined by

changing the origin from point O to point c as as shown in Figure 3.10. The velocity

vector $\underline{V}_o$ used in the accelerator's definition will also change with the relocation of origin

to point c

$$\underline{V}_c = \underline{V}_o - \underline{C} \times \underline{\omega}$$

The acceleration of the centerpoint can be determined by

$$\underline{A}_c - \underline{\omega} \times \underline{V}_c = \underline{A}_o - \underline{\omega} \times \underline{V}_o - \underline{C} \times \underline{\alpha}$$

Using the above equation for the velocity $\underline{V}_c$, the acceleration of point c can be written as

$$\underline{A}_c = \underline{A}_o - \underline{\omega} \times [\underline{C} \times \underline{\omega}] - \underline{C} \times \underline{\alpha} \tag{29}$$

The acceleration of the point where the connector and the platform are joined together, point

p, can be determined by relocating the origin from point c to point p

$$\underline{A}_p = \underline{A}_c + \underline{\omega} \times [\underline{\omega} \times \underline{R}_{pc}] + \underline{\alpha} \times \underline{R}_{pc} \tag{30}$$

3.5.1 Connector Acceleration Analysis

The acceleration of point p can be written as as a function of the velocities and

accelerations of the individual joints that make up the HPS manipulator (see Figure 3.7)

$$\underline{A}_p = \sum_{j=1}^{6} \dot{\omega}_j \underline{S}_{oj} + \sum_{j=1}^{6} \omega_j^2 (\underline{S}_j \times \underline{S}_{oj}) + 2\omega_1 \underline{S}_1 \times \sum_{j=2}^{6} \omega_j \underline{S}_{oj} +$$

$$2\omega_2 \underline{S}_2 \times \sum_{j=3}^{6} \omega_j \underline{S}_{oj} + 2\omega_3 \underline{S}_3 \times \sum_{j=4}^{6} \omega_j \underline{S}_{oj} + 2\omega_4 \underline{S}_4 \times \sum_{j=5}^{6} \omega_j \underline{S}_{oj} + 2\omega_5 \underline{S}_5 \times \omega_6 \underline{S}_{o6}$$

Using the line coordinates defined in section 3.4.1, the above equation can be simplified

considerably

$$\underline{A}_p = \dot{\omega}_1 \underline{S}_{o1} + \dot{\omega}_2 \underline{S}_{o2} + \dot{V}_3 \underline{S}_3 + \omega_1^2 (\underline{S}_1 \times \underline{S}_{o1}) + \omega_2^2 (\underline{S}_2 \times \underline{S}_{o2}) +$$

$$2\omega_1 \underline{S}_1 \times (\omega_2 \underline{S}_{o2} + V_3 \underline{S}_3) + 2\omega_2 \underline{S}_2 \times V_3 \underline{S}_3 \qquad (31)$$

3.5.2 Inverse Acceleration Analysis

The acceleration vector $\underline{A}_p$ can be calculated given the acceleration of the platform

center point c, $\underline{A}_c$, and the angular acceleration vector of the platform, $\underline{\alpha}$, as outlined in

equation (30). The joint velocities required in equation (31) were determined in section

3.4. Therefore, the only unknowns in equation (31) are the joint accelerations. All the

known terms in equation (31) will be grouped into

$$\underline{A}_p^* = \underline{A}_p - \omega_1^2 (\underline{S}_1 \times \underline{S}_{o1}) - \omega_2^2 (\underline{S}_2 \times \underline{S}_{o2}) -$$

$$2\omega_1 \underline{S}_1 \times (\omega_2 \underline{S}_{o2} + V_3 \underline{S}_3) - 2\omega_2 \underline{S}_2 \times V_3 \underline{S}_3 \qquad (32)$$

As in section 3.4.1, the line coordinates for rotors 1 and 2 can also be written as

$$\underline{S}_{o1} = L\underline{S}_1 \times \underline{S}_3 = L\underline{S}_2 ; \qquad \underline{S}_{o2} = L\underline{S}_2 \times \underline{S}_3 = L\underline{S}_{23}$$

Using these equations for the line coordinates, equations (31) and (32) can be combined to

obtain an expression for the unknown joint accelerations

$$\underline{A}_p^* = \dot{\omega}_1 L \underline{S}_2 + \dot{\omega}_2 L \underline{S}_{23} + \dot{V}_3 \underline{S}_3 \qquad (33)$$

A unit force vector acting along the connector itself has the following ray coordinates

$$\hat{\underline{S}}_3 = \begin{bmatrix} \underline{S}_3 \\ 0 \end{bmatrix}$$

This force is clearly reciprocal to the rotors 1, 2, 4, 5 and 6. Forming the reciprocal

product of this unit force with equation (33) yields the following expression for the acceleration of the prismatic pair A_3

$$A_3 = \dot{V}_3 = \underline{A}_p^* \cdot \underline{s}_3 \tag{34}$$

A unit force vector acting along unit vector $\underline{s}_2$ and going through point p has the following ray coordinates

$$\hat{\underline{S}}_2^* = \begin{bmatrix} \underline{s}_2 \\ 0 \end{bmatrix}$$

This force is clearly reciprocal to the rotors 2, 3, 4, 5 and 6. Forming the reciprocal product of this unit force with equation (33) and using the line coordinates derived previously yields the following expression for the angular acceleration α_1

$$\alpha_1 = \dot{\omega}_1 = \frac{\underline{A}_p^* \cdot \underline{S}_2}{L} \tag{35}$$

A unit force vector acting along unit vector $\underline{s}_{23}$ and going through point "p" has the following ray coordinates

$$\hat{\underline{S}}_{23}^* = \begin{bmatrix} \underline{s}_{23} \\ 0 \end{bmatrix}$$

This force is clearly reciprocal to the rotors 1, 3, 4, 5 and 6. Forming the reciprocal product of this unit force with equation (33) and using the line coordinates derived previously yields the following expression for the angular acceleration α_2

$$\alpha_2 = \dot{\omega}_2 = \frac{\underline{A}_p^* \cdot \underline{s}_n}{L} \tag{36}$$

The connector angular acceleration vector $\underline{\alpha}_{12}$ is defined as [19]

$$\underline{\alpha}_{12} = \alpha_1 \underline{s}_1 + \alpha_2 \underline{s}_2 + \omega_1 \omega_2 (\underline{s}_1 \times \underline{s}_2) \tag{37}$$

3.5.3 Rigid Body Acceleration Analysis

As explained in Section 2.6, the connector can be modeled as the system shown in Figure 3.7. All the rigid bodies in the connector will have the same orientation and therefore the same angular velocity vector $\underline{\omega}_{12}$ and angular acceleration vector $\underline{\alpha}_{12}$.

The acceleration of mass M_b is only a function of the angular velocity and acceleration of the Hooke joint, $\underline{\omega}_{12}$ and $\underline{\alpha}_{12}$, since its distance from the base, bl, is constant. The acceleration of this rigid body can be written as

$$\underline{A}_b = bl [\underline{\alpha}_{12} \times \underline{s}_3] + bl [\underline{\omega}_{12} \times (\underline{\omega}_{12} \times \underline{s}_3)] \tag{38}$$

Using the expressions for the angular velocity $\underline{\omega}_{12}$, angular acceleration $\underline{\alpha}_{12}$ and the definitions for $\underline{s}_2$ and $\underline{s}_{23}$, the acceleration $\underline{A}_b$ can also be written as

$$\underline{A}_b = bl (\alpha_1 \underline{s}_2 + \alpha_2 \underline{s}_{23}) +$$

$$bl [2\omega_1 \omega_2 (\underline{s}_1 \cdot \underline{s}_3) \underline{s}_2 + \omega_1^2 (\underline{s}_1 \cdot \underline{s}_3) \underline{s}_1 - (\omega_1^2 + \omega_2^2) \underline{s}_3] \tag{39}$$

The acceleration of mass M_d can be written as

$$\underline{A}_d = \ddot{D} \underline{s}_3 + 2\dot{D} (\underline{\omega}_{12} \times \underline{s}_3) + D [\underline{\alpha}_{12} \times \underline{s}_3] + D [\underline{\omega}_{12} \times (\underline{\omega}_{12} \times \underline{s}_3)] \tag{40}$$

Using the expressions for the angular velocity $\underline{\omega}_{12}$, angular acceleration $\underline{\alpha}_{12}$ and the definitions for $\underline{s}_2$ and $\underline{s}_{23}$, the acceleration $\underline{A}_d$ can also be written as

$$\underline{A}_d = \ddot{D}\,\underline{s}_3 + 2\dot{D}(\,\omega_1\underline{s}_2 + \omega_2\underline{s}_{23}) + D(\alpha_1\underline{s}_2 + \alpha_2\underline{s}_{23}) +$$

$$D\left[\,2\omega_1\omega_2(\underline{s}_1 \cdot \underline{s}_3)\underline{s}_2 + \omega_1^2(\underline{s}_1 \cdot \underline{s}_3)\underline{s}_1 - (\omega_1^2 + \omega_2^2)\underline{s}_3\right] \qquad (41)$$

The acceleration of mass M_e can be written as

$$\underline{A}_e = \ddot{E}\,\underline{s}_3 + 2\dot{E}(\,\underline{\omega}_{12} \times \underline{s}_3) + E[\underline{\alpha}_{12} \times \underline{s}_3] + E[\underline{\omega}_{12} \times (\underline{\omega}_{12} \times \underline{s}_3)] \qquad (42)$$

Using the expressions for the angular velocity $\underline{\omega}_{12}$, angular acceleration $\underline{\alpha}_{12}$ and the definitions for $\underline{s}_2$ and $\underline{s}_{23}$, the acceleration $\underline{A}_e$ can also be written as

$$\underline{A}_e = \ddot{E}\,\underline{s}_3 + 2\dot{E}(\,\omega_1\underline{s}_2 + \omega_2\underline{s}_{23}) + E(\alpha_1\underline{s}_2 + \alpha_2\underline{s}_{23}) +$$

$$E\left[\,2\omega_1\omega_2(\underline{s}_1 \cdot \underline{s}_3)\underline{s}_2 + \omega_1^2(\underline{s}_1 \cdot \underline{s}_3)\underline{s}_1 - (\omega_1^2 + \omega_2^2)\underline{s}_3\right] \qquad (43)$$

3.6 Motion Planning

Path planning consists of describing the motion of a given point of a manipulator. Motion planning describes the motion of a given point and the orientation of the end effector. Enough infomation should be provided in order to describe the desired motion for the system. Once this motion is determined, the position, velocity and acceleration of the connectors can be determined by an inverse kinematic analysis.

3.6.1 Motion Planning using Screw Theory

As outlined in Screw theory [20, 21, 22, 23] the instantaneous motion of a body can be described by the rotation about a screw as shown in Figure 3.11. The parameters required to describe this screw are the axis of rotation $\underline{s}$, the pitch h, and the location of the screw axis with respect to the base coordinate frame origin, $\underline{r}_o$. The displacement of a point p on the platform coincident with the point of reference can be determined using the screw

parameters and an angular displacement θ about the axis of rotation of the screw

$$\Delta \underline{P}_o = \theta \left[(\underline{r}_o \times \underline{s}) + h \underline{s} \right] \qquad (44)$$

The displacement of the centerpoint c can be written as

$$\Delta \underline{C} = \theta \left[(\underline{r}_c \times \underline{s}) + h \underline{s} \right] \qquad (45)$$

The new location of the centerpoint c after the rotation θ is given by

$$\underline{C}_{new} = \underline{C}_{old} + \theta \left[(\underline{r}_c \times \underline{s}) + h \underline{s} \right] \qquad (46)$$

platform coordinate system

$\underline{Z}_m$

Instantaneous Screw Axis (ISA)

platform c $\underline{R}_{pc}$

$\underline{X}_m$

$\underline{C}$

$\underline{s}$

$\underline{Y}_m$

$\underline{r}_c$ θ

$\underline{Z}_f$

$\underline{r}_o$

O $\underline{Y}_f$

base coordinate system

$\underline{X}_f$
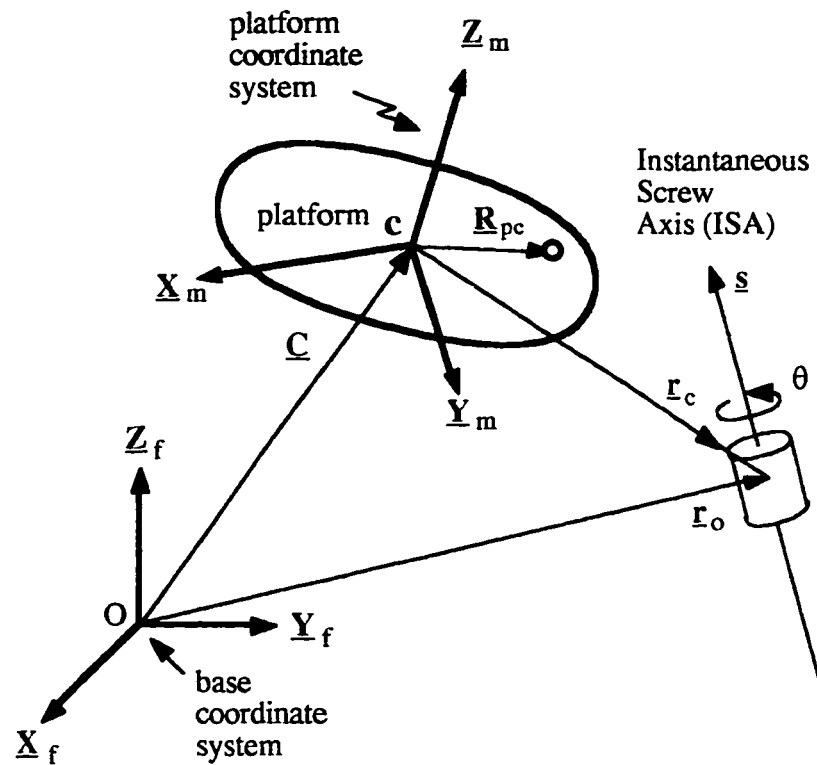
Figure 3.11 - Instantaneous Motion of the Platform

The displacement of any point on the platform can be determined by

$$\Delta \underline{P} = \theta \left[\left((\underline{r}_c - \underline{R}_{pc}) \times \underline{s} \right) + h \underline{s} \right] \tag{47}$$

The new location of a point p after the rotation θ is given by

$$\underline{P}_{new} = \underline{P}_{old} + \theta \left[\left((\underline{r}_c - \underline{R}_{pc}) \times \underline{s} \right) + h \underline{s} \right] \tag{48}$$

The location of any point on the platform can be also written in terms of the centerpoint position

$$\underline{P}_{new} = \underline{C}_{new} - \theta \left(\underline{R}_{pc} \times \underline{s} \right) \tag{49}$$

The vector $\underline{R}_{pc}$ is the relative position vector of any point p with respect to the centerpoint prior to the rotation θ and it is a function of the dimensions and orientation of the platform.

3.6.2. Describing the Orientation of the Platform

The relative position vector $\underline{R}_{pc}$ can be defined in terms of the vector $\underline{R}_{pc/m}$ which is the relative position vector described with respect to the moving coordinate frame attached to the platform as explained in section 3.3. As given by equation (4), $\underline{R}_{pc}$ can be written as

$$\underline{R}_{pc} = \begin{bmatrix} a_{11} & a_{12} & a_{13} \\ a_{21} & a_{22} & a_{23} \\ a_{31} & a_{32} & a_{33} \end{bmatrix} \underline{R}_{pc/m}$$

The columns of the 3 x 3 matrix in the above equation are the unit vectors that describe the orientation of the platform with respect to the a fixed coordinate frame. This matrix is known as the transformation or rotation matrix [R]. The elements of this matrix change as the platform moves. The change of the orientation caused by a rotation θ about the screw

axis $\underline{s}$ ($\underline{s} = s_x \; \underline{i} + s_y \; \underline{j} + s_x \; \underline{k}$) can be determined by

$$[\underline{X}_m, \underline{Y}_m, \underline{Z}_m]_{new} = [\underline{X}_m, \underline{Y}_m, \underline{Z}_m]_{old} [R] \qquad (50)$$

Where $[\underline{X}_m, \underline{Y}_m, \underline{Z}_m]_{old}$ is the orientation of the platform with respect to the fixed coordinate frame prior to the rotation, $[\underline{X}_m, \underline{Y}_m, \underline{Z}_m]_{new}$ is the orientation of the platform with respect to the fixed coordinate frame after the rotation, and [R] is a 3 x 3 rotation matrix given by

$$[R] = \begin{bmatrix} s_x{}^2 \, vsn \, \theta + cos \, \theta & s_x \, s_y \, vsn \, \theta - s_z \, sin \, \theta & s_x \, s_z \, vsn \, \theta + s_y \, sin \, \theta \\ s_x \, s_y \, vsn \, \theta + s_z \, sin \, \theta & s_y{}^2 \, vsn \, \theta + cos \, \theta & s_y \, s_z \, vsn \, \theta - s_x \, sin \, \theta \\ s_x \, s_z \, vsn \, \theta - s_y \, sin \, \theta & s_y \, s_z \, vsn \, \theta + s_x \, sin \, \theta & s_z{}^2 \, vsn \, \theta + cos \, \theta \end{bmatrix} \qquad (51)$$

where the versine function is $vsn \, \theta = 1 - cos \, \theta$. This rotation matrix [R] describes the change of orientation of a rigid body caused by a rotation θ about a unit vector $\underline{s}$ [18].

In the case of motion planning the initial orientation of the platform will be specified by the unit vectors $\underline{X}_m, \underline{Y}_m$ and $\underline{Z}_m$. These vectors must be specified according to the desired initial orientation of the platform. If the platform is being used in a machining operation, the initial orientation of the workpiece with respect to the machine tool will be the initial orientation of the platform. The orientation of the platform is subsequent locations will determined using equations (50) and (51).

The premultiplication of the relative position vector by the rotation matrix is equivalent to the second term of equation (49)

$$- \theta \, (\underline{R}_{pc} \times \underline{s}) = [R] \, \underline{R}_{pc/m}$$

The relative position vector $\underline{R}_{pc}$ used in the left hand of the equation is the vector before the rotation θ.

3.6.3 Motion Generation

The position of any point on the platform can be determined by using equation (48)

$$\underline{P}_{new} = \underline{P}_{old} + \theta \left[((\underline{r}_c - \underline{R}_{pc}) \times \underline{s}) + h\underline{s} \right] \qquad (48)$$

The velocity of any point can be determined using equations (8) and (11)

$$\underline{V}_p = \omega \left[((\underline{r}_c - \underline{R}_{pc}) \times \underline{s}) + h\underline{s} \right] \qquad (52)$$

The acceleration of any point on the platform can be determined by using equations (29) and (30)

$$\underline{A}_p = \underline{A}_o + \underline{\omega} \times \left[(\underline{r}_c - \underline{R}_{pc}) \times \underline{\omega} \right] + (\underline{r}_c - \underline{R}_{pc}) \times \underline{\alpha} \qquad (53)$$

where $\underline{\theta}$, $\underline{\omega}$ and $\underline{\alpha}$ are the angular displacement, velocity and acceleration vectors of the platform and are related by

$$\underline{\omega} = \frac{d\theta}{dt} \quad ; \quad \underline{\alpha} = \frac{d\omega}{dt} = \frac{d^2}{dt^2}\underline{\theta}$$

If the screw axis $\underline{s}$ remains fixed during the motion, which is the case in simple motions such as translation and rotation, the angular velocity and acceleration can be written as

$$\underline{\omega} = \frac{d\theta}{dt}\underline{s} \quad ; \quad \underline{\alpha} = \frac{d\omega}{dt}\underline{s} = \frac{d^2}{dt^2}\theta\,\underline{s}$$

A simple way to describe the motion of the platform is by using a continuous time function for the angular displacement such as a cycloidal motion curve used for designing cam displacement profiles [24]. This will assure that the angular velocity and acceleration vectors will also be continuous functions. The angular displacement function to be used is

$$\underline{\theta}(t) = \frac{\Delta\theta}{2}\left[1 - \cos\left(\frac{\pi t}{T}\right)\right]\underline{s} \tag{54}$$

where $\Delta\theta$ is the total angular displacement (in radians) and T is the total period or the time required to complete the desired motion. The angular velocity and acceleration vectors, $\underline{\omega}(t)$ and $\underline{\alpha}(t)$, are determined by the time derivatives of the angular displacement function

$$\underline{\omega}(t) = \frac{\Delta\theta\,\pi}{2\,T}\left[\sin\left(\frac{\pi t}{T}\right)\right]\underline{s} \tag{55}$$

$$\underline{\alpha}(t) = \frac{\Delta\theta\,\pi^2}{2\,T^2}\left[\cos\left(\frac{\pi t}{T}\right)\right]\underline{s} \tag{56}$$

3.6.4 Rectilinear Motion

Rectilinear motions of the platform can also be described using screw theory. The orientation of the platform is fixed which make the angular velocity and angular accelerations zero. For this type of motion it is said that the axis of rotation is located at infinity, which is specified by setting the angular rotation θ to 0, the radius of rotation $r_o \Rightarrow \infty$, and the pitch $h \Rightarrow \infty$. The product of the angular rotation and the pitch can be written as

$$h\,\theta = S$$

where S is the translational displacement of the platform. The axis of translation $\underline{w}$, which is parallel to the axis or rotation $\underline{s}$, is now used to describe the direction of translation of the platform. The displacement of any point on the platform can now be written as

$$\Delta\underline{P} = h\,\theta\,\underline{w} = S\,\underline{w} \tag{57}$$

The product of the rotational velocity and the pitch can be written as

$$h\omega = V_t$$

where V_t is the translational velocity along the vector $\underline{w}$. Using the above equation and equation (52), the velocity of any point on the platform can now be written as

$$\underline{V}_p = h\omega\underline{w} = V_t\underline{w} \qquad (58)$$

The acceleration of any point on the platform can now be written as

$$\underline{A}_p = \underline{A}_o = \frac{d}{dt}h\omega\underline{w} = A_t\underline{w} \qquad (59)$$

where A_t is the translational acceleration along the vector $\underline{w}$.

The translational displacement can be described by a time function similar to the one employed for the angular displacement

$$S(t) = \frac{\Delta S}{2}\left[1 - \cos\left(\frac{\pi t}{T}\right)\right] \qquad (60)$$

where ΔS is the total translational displacement, and T is the time period required to complete the motion. The translational velocity and acceleration can be determined by taking the time derivatives of the displacement function

$$V_t(t) = \frac{\Delta S}{2}\frac{\pi}{T}\sin\left(\frac{\pi t}{T}\right) \qquad (61)$$

$$A_t(t) = \frac{\Delta S}{2}\left(\frac{\pi}{T}\right)^2\cos\left(\frac{\pi t}{T}\right) \qquad (62)$$

3.6.5 Motion Planning for Machining and Mirror Polishing

Rectilinear motion is a typical motion used when machining a workpiece. In this case the motion can be determined by using equations (48) and (57) through (62). The
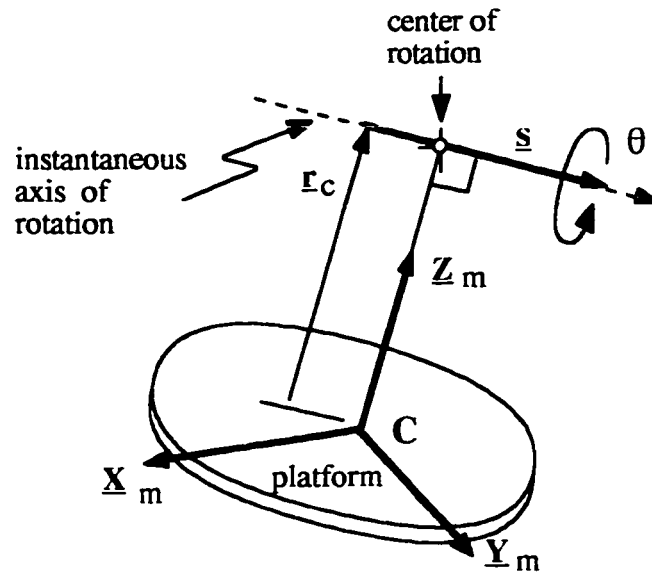
Figure 3.12 - Platform Rotation about a given axis $\underline{s}$

parameters that have to specified are the displacement ΔS, the period T and the axis of translation $\underline{w}$.

Another possible motion is when the platform has to follow a curve while remaining tangent to the curve at all times. Such a motion is used to polish a mirror or machine a cylindrical part. This type of motion can be described as a rotation of the platform about an axis of rotation $\underline{s}$ that is at a distance r_c from the platform's center point and perpendicular to the axis $\underline{Z}_m$ as shown in Figure 3.12. The platform's motion can be determined by using equations (48) and (54) through (66). The parameters required for planning this motion are the platform's initial location, the axis or rotation $\underline{r}$, distance r_c from the centerpoint, the total angular displacement $\Delta\theta$, and the period T. For this type of motion the position, velocity and acceleration of any point on the platform are given by

$$\underline{P} = \underline{P}_o + [\ R\ ]\ \underline{R}_{pc/m} \qquad (63)$$

$$\underline{V}_p = \omega [\ (\ \underline{r}_c - \underline{R}_{pc}\ ) \times \underline{s}\ ] \qquad (64)$$

$$\underline{A}_p = \underline{\omega} \times [\ (\ \underline{r}_c - \underline{R}_{pc}\ ) \times \underline{\omega}\ ] + (\ \underline{r}_c - \underline{R}_{pc}\ ) \times \underline{\alpha} \qquad (65)$$

CHAPTER 4
MANIPULATOR FORCE AND TORQUE ANALYSIS

In order to derive the equations of motion of the manipulator, it is necessary to perform a complete force and torque analysis. This analysis determines the resultant forces, $\underline{F}_j$, and the resultant torques, $\underline{T}_j$, acting on each body of the system. In addition, the force/torque analysis also determines the static capability. The issues of stability and actuator requirements are also examined.

A rigid body may experience forces and torques of the following types

- External : These are caused by external sources such as actuators and disturbances.
- Contact : These are generated by the contact with other rigid bodies or passive elements such as springs and dampers.
- Field: These are created by the action of a field such as a magnetic force or gravity.
- Inertial : These are the result of the rigid body's angular velocity, and the linear and angular acceleration.

The resultant force vector, $\underline{F}_j$, and the resultant torque vector, $\underline{T}_j$, acting on each body in the system produce a change of the dynamic state of the system which is described by the position, velocity and acceleration vectors. All the forces and torques acting on the platform are shown in Figure 4.1. This model does not include the connector model components (as outlined in Chapter 2) which will be considered later. The system shown in Figure 4.1 is a complete model when the connectors are modeled as rigid, massless bodies.

4.1 Platform External Forces and Torques

The external force, $\underline{F}_{ext}$, and torque, $\underline{T}_{ext}$, applied to the platform are determined by the use or application of the platform. One possible application is to use the platform as the
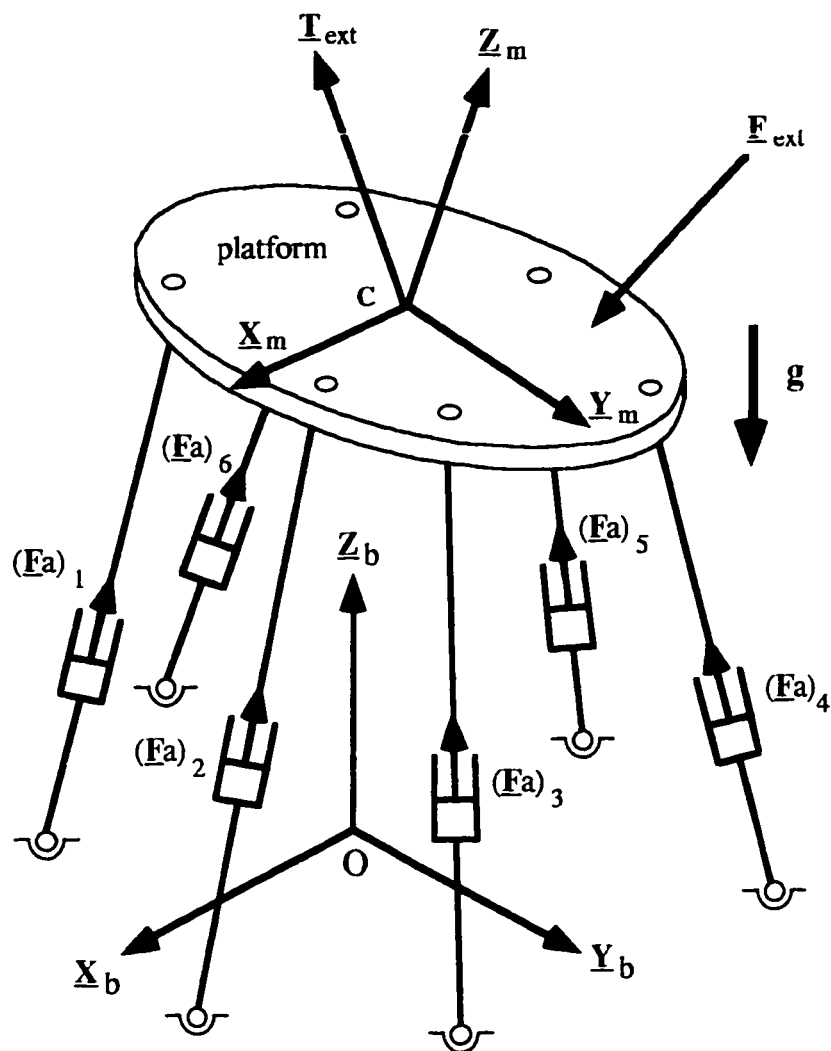
Figure 4.1 - Platform with Applied Forces and Torques

base for a work piece in a machining operation; another possibility is to use the platform to control the contact force with a surface such as when polishing a mirror. The equivalent force and torque generated by the external force and torque about the center point c, which is assumed to be coincident with the center of gravity, are given by the following equations

$$\mathbf{F}_c = \mathbf{F}_{ext} \quad ; \quad \mathbf{T}_c = \mathbf{T}_{ext} + (\mathbf{R}_{ec} \times \mathbf{F}_{ext}) \tag{1}$$

where $\mathbf{R}_{ec}$ is the relative position vector from the centerpoint of the platform to the line of action of force $\mathbf{F}_{ext}$, as shown in Figure 4.2. These equations can be expanded to

$$\begin{pmatrix} F_{cx} \\ F_{cy} \\ F_{cz} \end{pmatrix} = \begin{pmatrix} F_{ext,\,x} \\ F_{ext,\,y} \\ F_{ext,\,z} \end{pmatrix} \qquad \begin{pmatrix} T_{cx} \\ T_{cy} \\ T_{cz} \end{pmatrix} = \begin{pmatrix} T_{ext,\,x} \\ T_{ext,\,y} \\ T_{ext,\,z} \end{pmatrix} + \begin{pmatrix} R_{ecx} \\ R_{ecy} \\ R_{ecz} \end{pmatrix} \times \begin{pmatrix} F_{ext,\,x} \\ F_{ext,\,y} \\ F_{ext,\,z} \end{pmatrix} \qquad (2)$$

Any force / torque combination acting on a rigid body can be combined into a dual vector quantity called a wrench, $\widehat{W}$ and the external force and torque acting on the platform, with the center point c as the reference point, can be combined into an external wrench $\widehat{W}_{ext}$:

$$\widehat{W}_{ext} = \begin{bmatrix} F_{ext} \\ T_{ext} + (R_{ec} \times F_{ext}) \end{bmatrix} \qquad (3)$$

4.1.1 External Forces and Torques in Mirror Polishing

One possible use of the platform is to control the contact force between the end effector and a surface. An example of such application is polishing a mirror or glass. In this case the end effector will support some polishing material which will be moved about the surface using the manipulator while at the same time the contact force is kept below a safe limit to avoid any surface damages. The movable platform must be tangential to the surface at all times while applying a normal or contact force as shown Figure 4.3
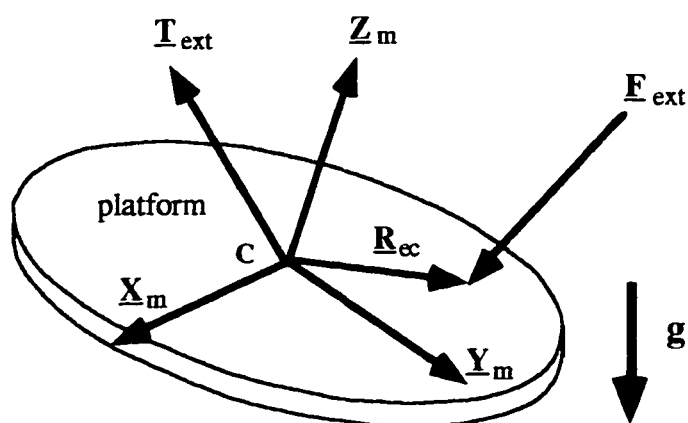
Figure 4.2 - External and Gravitational Forces &Torques acting on the platform

There are two forces applied to the platform, the first is the normal force $\mathbf{F}_n$ caused by the

contact between the polishing material and the mirror surface. This force vector is the

perpendicular to the platform and in the opposite direction of the unit vector $\mathbf{Z}_m$. Since the

normal force vector intersects the centerpoint it does not produce a torque. The second

force vector is a friction force $\mathbf{F}_{fr}$ and it is caused by the friction between the polishing

material and the mirror surface. This force is a function of the normal force $\mathbf{F}_n$ and the

coefficient of friction μ. Clearly it is tangent to the mirror surface and it is always opposite

to the direction of travel, which is described by the vector $\underline{t}$ as shown in Figure 4.4.
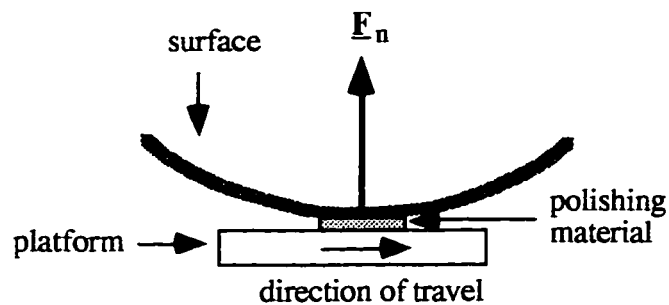
Figure 4.3 - Mirror polishing task
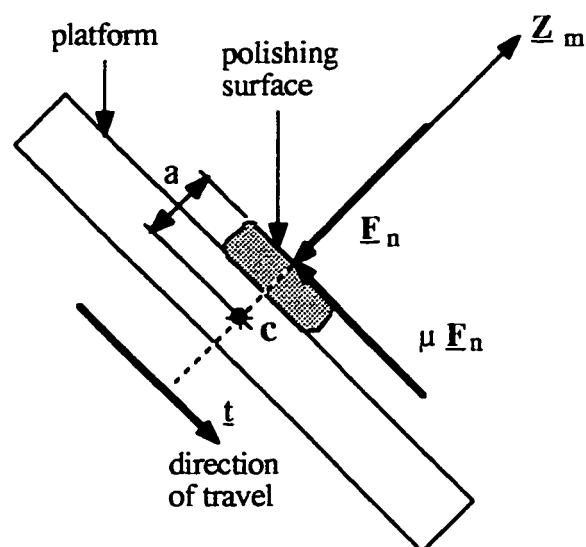
Figure 4.4 - Mirror polishing forces

When the platform is rotating about a given axis $\underline{s}$, the direction of travel is given by (see section 3.6)

$$\underline{t} = \underline{Z}_m \times \underline{s}$$

If the platform is following a pure translational motion, the direction of travel is given by the vector $\underline{w}$ (see Section 3.6). Since the line of action does not intersect the centerpoint c (see Figure 4.4) it produces a torque which is given by

$$\underline{T}_{fr} = a\underline{Z}_m \times \underline{F}_{fr}$$

The external wrench applied to the platform during the mirror polishing task is therefore

$$\widehat{\underline{W}}_{ext} = \begin{bmatrix} -F_n(\underline{Z}_m + \mu\underline{t}) \\ a\underline{Z}_m \times (-F_n\mu\underline{t}) \end{bmatrix} \tag{4}$$

4.1.2 External Forces and Torques in Machining

One of the most promising applications of the platform is in machining operations, where the workpiece is positioned and presented orientated by the moving platform to the cutter as shown in Figure 4.5. The advantage is that the system is stiffer when using a platform over a conventional machine tool . This offers the possibility of machining complex geometries with higher precision and greater material removal rates than what is possible with conventional multiaxis machine tools.

In general the forces developed in machining are somewhat complex to describe since it depends on many diverse factors such as the velocity of cutting, the thickness of the cut, the material being cut and the number of teeth of the cutter among other things [25]. For simplicity a full groove cut with a four tooth cutter, as shown in Figure 4.6, will be considered. Each tooth will be loaded with a cutting force when inside the cutting area which the arc between points e and d of Figure 4.6. The force applied to the platform is a combination of the individual loads on each tooth. As shown in Figure 4.7 the tooth cutting force can be divided into a component perpendicular to the cutting surface, the

normal force, and a component tangential to the cutting surface which is given by

$$F_t = K_s b \, Fr \sin \phi$$

where K_s is the specific stiffness, b is the depth of cut, Fr is the feed rate and ϕ is the angle shown in Figure 4.6. The tangential forces for the four teeth shown are given by

$$F_{t1} = K_s b \, Fr \sin \phi$$

$$F_{t2} = K_s b \, Fr \sin \left(\phi + 90° \right)$$

$$F_{t3} = K_s b \, Fr \sin \left(\phi + 180° \right)$$

$$F_{t4} = K_s b \, Fr \sin \left(\phi + 270° \right)$$

The cutting force of a tooth becomes zero when it is not touching the cutting surface. The resultant force applied to platform is the sum of all the cutting forces. In a full groove cut the force components perpendicular to the direction of travel cancel out and the resultant
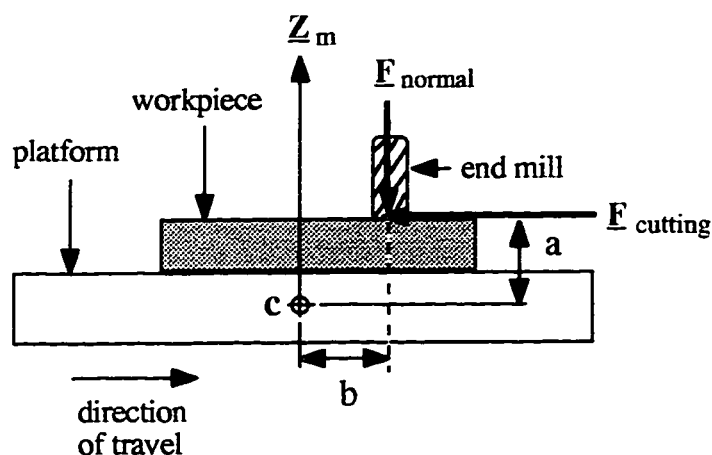
Figure 4.5 - Machining with a platform
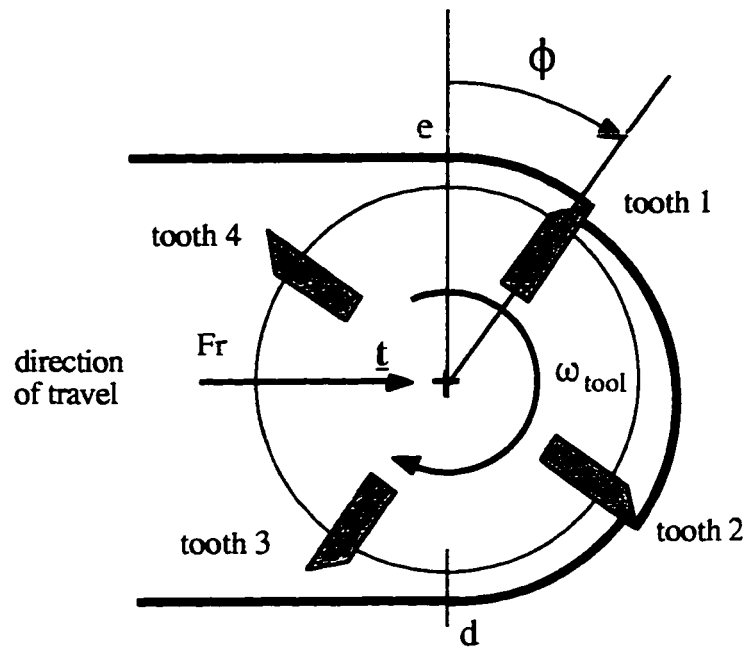
Figure 4.6 - Top view of a four tooth cutter in a full groove cut
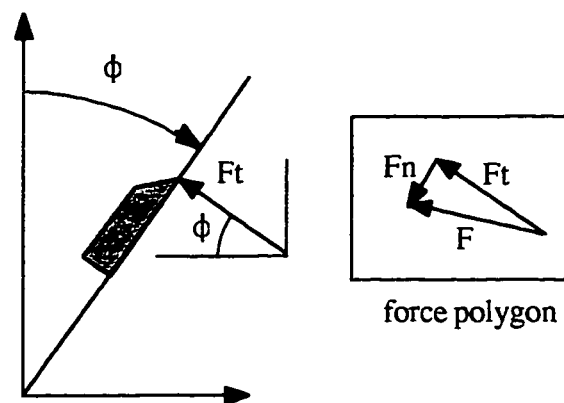
Figure 4.7 - Cutting forces

cutting force is a constant along the direction of travel

$$\underline{F}_{cutting} = K_s \, b \, Fr \, \underline{t}$$

where the direction of travel, $\underline{t}$, was determined in the previous section. This force acts in a

plane parallel to the platform at a distance a from the centerpoint of the platform as shown in Figure 4.5. The normal force shown in this figure is zero since the end mill or cutter is machining the workpiece with the sides of the cutter, therefore all the cutting forces are in a plane parallel to the platform.

The external wrench applied to the platform during the full groove cut is

$$\widehat{\mathbf{W}}_{ext} = \begin{bmatrix} -K_s b \, Fr \, \underline{t} \\ a \underline{Z}_m \times (-K_s b \, Fr \, \underline{t}) \end{bmatrix} \tag{5}$$

A more complex description of the machining external wrench is required for other type of cuts and also to include the effects of machine tool chatter [25].

4.2 Gravitational Forces and Torques

The gravitational force and torque vectors acting on the platform are given by (see Figure 4.2)

$$\mathbf{F}_g = - M_p \, \mathbf{g} \qquad \& \qquad \mathbf{T}_g = \mathbf{R}_{cg} \times \mathbf{F}_g$$

where $\mathbf{R}_{cg}$ is the relative position vector of the platform's center of gravity respect to the centerpoint of the platform. This equation can be also written as

$$\begin{pmatrix} F_{gx} \\ F_{gy} \\ F_{gz} \end{pmatrix} = \begin{pmatrix} 0 \\ 0 \\ -M_p \cdot g \end{pmatrix} \qquad \begin{pmatrix} T_{gx} \\ T_{gy} \\ T_{gz} \end{pmatrix} = \begin{pmatrix} R_{cgx} \\ R_{cgy} \\ R_{cgz} \end{pmatrix} \times \begin{pmatrix} 0 \\ 0 \\ -M_p \cdot g \end{pmatrix} \tag{6}$$

where M_p is the mass of the platform. The gravitational torque acting on the platform is zero since the reference point to be used on the platform, c, is coincident with the center of gravity of the platform. The location of the reference point c at the center of gravity makes the position vector $\mathbf{R}_{cg} = 0$. The gravitational effects on the platform will be described by a gravitational force

$$\widehat{\mathbf{W}}_g = \begin{bmatrix} \mathbf{F}_g \\ 0 \end{bmatrix} \tag{7}$$

4.3 Connector Forces and Torques

Each of the connectors applies an effective force $\underline{F}_L$ to the platform at its corresponding connection point with the platform as shown in Figure 4.8. This force is generated some of the connector components. How the connector exactly generates this force will be discussed later. When the connector is assumed to be a rigid massless body, the effective force $\underline{F}_L$ is the force generated by the linear actuator located on each connector. Each connector force has a magnitude of F_L and acts along the corresponding line $\underline{s}_3$ which is at a distance $\underline{R}_{pc}$ from the platform's center (as an example the distance $\underline{R}_{pc}$ for connector 2, $\underline{R}_{2c}$, is shown in Figure 4.3). The coordinates for each applied force are given by

$$\underline{F}_L = F_L \underline{s}_3 \quad \& \quad \underline{T}_L = F_L (\underline{R}_{pc} \times \underline{s}_3) \tag{8}$$

Which can also be combined into the dual vector form
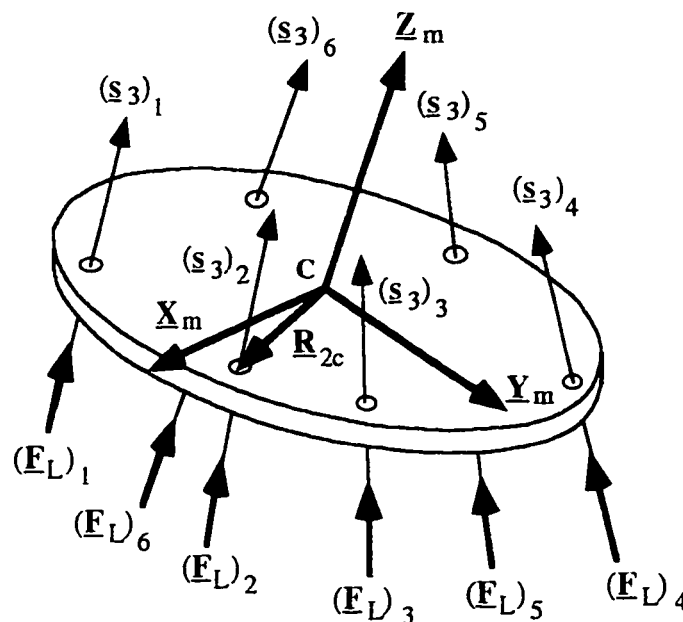
Figure 4.8 - Connector Forces acting on the Platform

$$\widehat{\underline{W}}_L = F_L \begin{bmatrix} \underline{s}_3 \\ \underline{R}_{pc} \times \underline{s}_3 \end{bmatrix} \qquad (9)$$

These applied forces can be combined into the resultant connector wrench given by

$$\widehat{\underline{W}}_{rL} = \left(\widehat{\underline{W}}_L\right)_1 + \left(\widehat{\underline{W}}_L\right)_2 + \left(\widehat{\underline{W}}_L\right)_3 + \left(\widehat{\underline{W}}_L\right)_4 + \left(\widehat{\underline{W}}_L\right)_5 + \left(\widehat{\underline{W}}_L\right)_6 \qquad (10)$$

which can also be written as

$$\widehat{\underline{W}}_{rl} = [J_m] \{F_L\} \qquad (11)$$

where $[J_m]$ is Manipulator Jacobian, and $\{F_L\}$ is the connector force column matrix

$$\{F_L\} = [(F_L)_1, (F_L)_2, (F_L)_3, (F_L)_4, (F_L)_5, (F_L)_6]^T.$$ The Jacobian $[J_m]$

can be written as

$$[J_m] = \left[\left(\widehat{\underline{S}}\right)_1 \left(\widehat{\underline{S}}\right)_2 \left(\widehat{\underline{S}}\right)_3 \left(\widehat{\underline{S}}\right)_4 \left(\widehat{\underline{S}}\right)_5 \left(\widehat{\underline{S}}\right)_6 \right] \qquad (12)$$

where each column of the Jacobian Matrix are the Plücker line coordinates of a connector (see Section 3.3.1)

$$\left(\widehat{\underline{S}}\right)_i = \left(\begin{matrix} \underline{s}_3 \\ \underline{R}_{pc} \times \underline{s}_3 \end{matrix} \right)_i$$

4.4 Platform Resultant Forces and Torques

The resultant wrench $\widehat{\underline{W}}_p$ acting upon the platform is the sum of the resultant connector wrench $\widehat{\underline{W}}_{rl}$, the external wrench $\widehat{\underline{W}}_{ext}$ and the gravitational force $\widehat{\underline{W}}_g$

$$\widehat{\underline{W}}_p = \widehat{\underline{W}}_{rL} + \widehat{\underline{W}}_{ext} + \widehat{\underline{W}}_g \qquad (13)$$

This resultant wrench produces the inertial force $\mathbf{F}^*_p$ and torque $\mathbf{T}^*_p$ acting upon the platform

$$\mathbf{F}^*_p = -M_p \mathbf{A}_c \;; \quad \mathbf{T}^*_p = -\left[\left(\underline{\alpha} \cdot \mathbf{Ip}^{\cdot}\right) + \left(\underline{\omega} \times \mathbf{Ip}^{\cdot} \cdot \underline{\omega}\right)\right] \quad (14)$$

where M_p is the mass of the platform; $\mathbf{A}_c$ is the acceleration of the center of gravity; $\underline{\alpha}$ is the angular acceleration of the platform; $\underline{\omega}$ is the angular velocity of the platform; and $\mathbf{Ip}^{\cdot}$ is the Inertia Dyadic of the platform about the center of gravity. The static solution for the platform can be obtained by using equation (13) and by setting the resultant wrench to zero

$$\widehat{\mathbf{W}}_{rL} + \widehat{\mathbf{W}}_{ext} + \widehat{\mathbf{W}}_g = 0 \quad (15)$$

4.5 System Singularities

The resultant wrench can be calculated given the inertial parameters of the platform M_p and $\mathbf{Ip}^{\cdot}$, the centerpoint acceleration vector $\mathbf{A}_c$, and the angular acceleration and velocity vectors $\underline{\alpha}$ and $\underline{\omega}$ which are determined by the motion planning process as outlined in Section 3.6. When the external and gravitational wrenches are known, equation (13) can be rearranged to determine the connector force matrix $\{\mathbf{F}_L\}$ required to generate the desired resultant platform wrench

$$[\mathbf{J}_m]\{\mathbf{F}_L\} = \widehat{\mathbf{W}}_p - \widehat{\mathbf{W}}_{ext} - \mathbf{W}_g \quad (16)$$

This is a system of 6 equations with the connector forces as the 6 unknowns: $(\mathbf{F}_L)_1$, $(\mathbf{F}_L)_2, (\mathbf{F}_L)_3, (\mathbf{F}_L)_4, (\mathbf{F}_L)_5, (\mathbf{F}_L)_6$. Premultiplying equation (16) by the inverse of the Manipulator's Jacobian, $[\mathbf{J}_m]^{-1}$, yields the following expression for the connector force matrix

$$\{\mathbf{F}_L\} = [\mathbf{J}_m]^{-1}\left(\widehat{\mathbf{W}}_p - \widehat{\mathbf{W}}_{ext} - \mathbf{W}_g\right) \quad (17)$$

If the above equation cannot be solved or the required connector forces calculated by the above equation exceed the physical limits of the system , the planned motion cannot be generated and the system is said to be degenerate or singular.

4.5.1 Geometric Singularities

When the det [J_m] = 0, it is not possible to obtain the inverse of the Jacobian matrix, and therefore the above equation cannot be solved. The rank of [J_m] is less than six and the system of equations formed by the product F_L [J_m] is not an independent set of equations. The columns of [J_m] have become linearly dependent which implies that the connector line coordinates have become linearly dependent. In practice the connector forces cannot equilibrate the applied wrench. The actuator magnitudes will have to be set to infinitely large values and the actuators will saturate in the process. When this situation arises the platform is said to be in a degenerate or singular configuration (position and orientation). This type of singularity will be defined here as a geometric singularity, since it is a function of the geometry of the connector lines.

It is important at the outset to determine the location of the geometric singularities, and to avoid them when planning a motion. It is desirable that the working volume of the workspace used for a proposed application does not include any geometric singularities.

It is clear that as the platform approaches a singularity, the connector forces will reach very high values (F_L)$_1$ = (F_L)$_2$ = (F_L)$_3$ = (F_L)$_4$ = (F_L)$_5$ = (F_L)$_6$ ⇒ ∞. Clearly this is physically impossible, and the actuators which generate the connector forces will saturate

$$\{F_a\} \Rightarrow \{F_{a\,max}\} = [\text{Fa}_{1max}, \text{Fa}_{2max}, \text{Fa}_{3max}, \text{Fa}_{4max}, \text{Fa}_{5max}, \text{Fa}_{6max}]^T$$

In this case, the desired resultant wrench will be different from the actual resultant wrench. This wrench $\widehat{W}_p^*$ is determined by setting F_L to F_{max} in equations (13):

$$\widehat{W}_p^* = [J_m] \{ F_{max} \} + \widehat{W}_{ext} + \widehat{W}_g \qquad (18)$$

Since the actual resultant wrench is not equal to the desired resultant wrench , the platform's actual acceleration and angular acceleration vectors will be different from those required by the planned motion. The platform will not be able to follow the planned motion and the system will be out of control or uncontrollable as it approaches a singularity.

The geometric singularities depend on the geometry and location of the platform. The geometry is determined by the dimensions and configuration of the manipulator. The location of the platform is specified by the center's position vector $\underline{C}$; and the orientation which is described by using the 3x3 rotation matrix [R] as explained in Section 3.3. Therefore the geometric singularities can be avoided by modifying the motion planning parameters (see Section 3.6).

4.5.2 Actuator Singularities

The platform can also become uncontrollable in a nonsingular location when one or more of the required connector forces exceed the allowed maximum connector forces, i.e. $\{\underline{F}_l\} > \{\underline{F}_{max}\}$. In this situation the saturating actuators will operate at their maximum force. The actual resultant wrench will of course be different from the desired or required wrench, and the motion of the platform will deviate from the desired motion profile.

The power required from each individual connector can be calculated by the following scalar product (power is a scalar quantity)

$$\text{Power} = [\ \underline{F}a \cdot \underline{V}_p\ ] \tag{19}$$

where $\underline{F}a$ is the actuator force and $\underline{V}_p$ is the connector's endpoint velocity. When the required power from any of the actuators exceeds its maximum capacity, the desired platform motion cannot be generated. A similar problem will arise whenever the required actuator speed of response or bandwidth exceeds the maximum bandwidth of the actuator. In general, whenever the required forces cannot be generated by the actuators and the system is in a nonsingular location, the system is said to be in a actuator singularity.

Actuator singularities create similar problems as the geometric singularities but are caused by the force, power and/or bandwidth limitations of the actuators.

Whenever the platform is in a singularity (either a geometric or an actuator singularity), the desired motion cannot be generated and its said that the system is out of control or uncontrollable. The platform's motion is altered or degraded. A consequence of a singularity is that the motion generated will be different from the planned one. A serious consequence of a singularity is that the change in motion might lead the platform to subsequent singular locations. In this case the system does not recover from the singularity and the platform will become unstable and totally out of control.

4.6 Connector Force Analysis

As mentioned before each connector applies a force to the platform. If the connector is modeled as a rigid massless body, the connector force will be generated by the linear actuator. When more complete models are considered, the connector force also depends on the system parameters (stiffness and damping), displacement and velocity. In order to generate the dynamic model, expressions for the connector forces, and the forces applied to each of the rigid bodies in each connector must be obtained. The complete connector model is discussed in Section 2.5. The first body on each connector is the equivalent mass M_e, the second body on each connector is the decoupling stage mass M_d, and the third is the actuator base mass M_b.

4.6.1 External Forces and Torques

The only external force acting on M_e is the actuator force Fa, as shown in Figure 4.9. The torque is zero since it is assumed that its line of action intersects the center of gravity . The external force acting upon M_e, $F_{(ext, e)}$, is given by

$$F_{(ext, e)} = Fa \qquad (20)$$

4.6.2 Contact Forces and Torques

There are two contact forces acting on M_e, F_{ct} and F_{kL} as shown in Figure 4.9. F_{kL} is produced by the deformation of K_L. F_{ct} is generated by the friction of the actuator and transmission which is modeled as a viscous damper with of damping coefficient C_t. The torque produced is zero since the line of action of all these forces intersects the center of gravity of the mass. The contact force acting upon M_e, $F_{(c, e)}$, is given by

$$F_{(c, e)} = -[F_{ct} + F_{kL}] \tag{21}$$

where the forces F_{ct} and F_{kL} are given by

$$F_{ct} = C_t \dot{E}; \quad F_{kL} = K_L \delta_L \tag{22}$$

where δ_L is the deformation of K_L and is given by

$$\delta_L = (E - H) - l_{Lo} \tag{23}$$

where l_{lo} is the free length of K_L.

There is are two contact forces acting on the decoupling stage mass M_d, F_{cd} and F_{kd} as shown in Figure 4.10. F_{kd} is produced by the deflection of K_d. F_{cd} is generated by the friction of viscous damper C_d. The torque is zero since all the forces go through the center of gravity. The contact force acting upon M_d, $F_{(c, d)}$, is given by

$$F_{(c, d)} = -[F_{cd} + F_{kd}] \tag{24}$$

where the forces F_{kd} and F_{cd} are given by

$$F_{cd} = C_d(\dot{D} - \dot{L}); \quad F_{kd} = K_d \delta_d \tag{25}$$
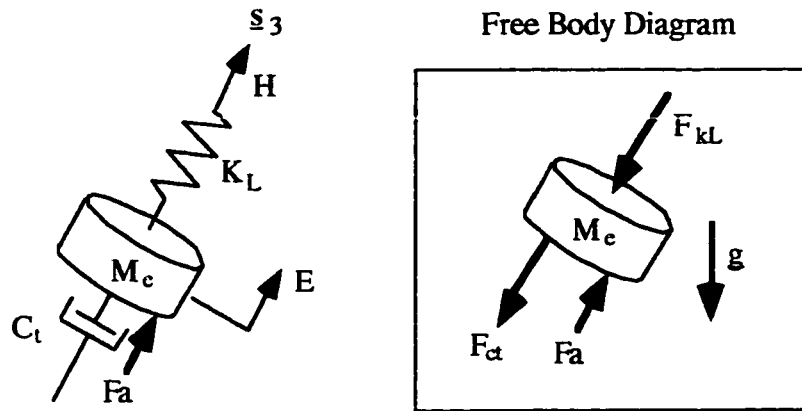
Figure 4.9 - Forces acting upon M_e
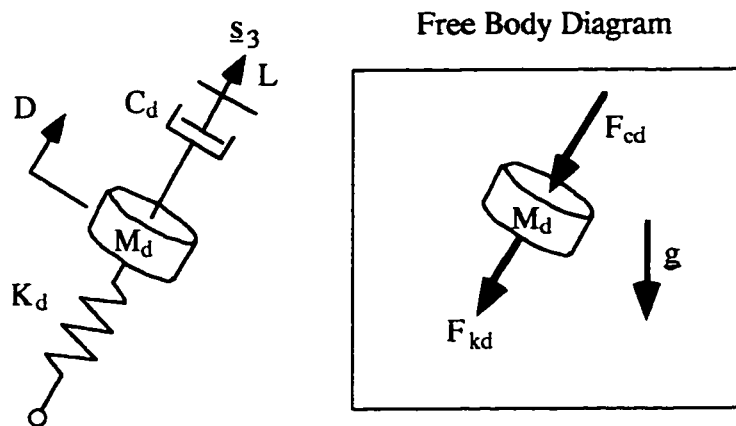
Figure 4.10 - Forces acting upon M_d

where δ_d is the deformation of the decoupling stage stiffness and is given by

$$\delta_d = D - l_{do} \qquad (26)$$

where l_{do} is the free length of the decoupling stage support.

There are two contact forces acting on the base inertia M_b, F_{ct} and F_r as shown in

Figure 4.10. F_r is a workless constraint caused by the rigid rod connection to the base.

F_{ct} is generated by the friction of the actuator and transmission which is modeled as a viscous damper with a damping coefficient C_t. The torque produced by these contact forces is zero since their line of action intersects the center of gravity. The contact force acting upon M_b, $F_{(c, b)}$, is given by

$$F_{(c, b)} = [F_{ct} - F_r]$$ (27)

4.6.3 Field Forces and Torques

The only field force acting on the rigid bodies of the connector is gravity as shown in Figures 4.9, 4.10 and 4.11. The gravitational torques are zero since the point selected for the sum of forces on each body is its center of gravity. The gravitational forces are

$$\underline{F}_{(g, e)} = -[M_e g] \underline{k}$$ (28)

$$\underline{F}_{(g, d)} = -[M_d g] \underline{k}$$ (29)

$$\underline{F}_{(g, b)} = -[M_b g] \underline{k}$$ (30)

Free Body Diagram
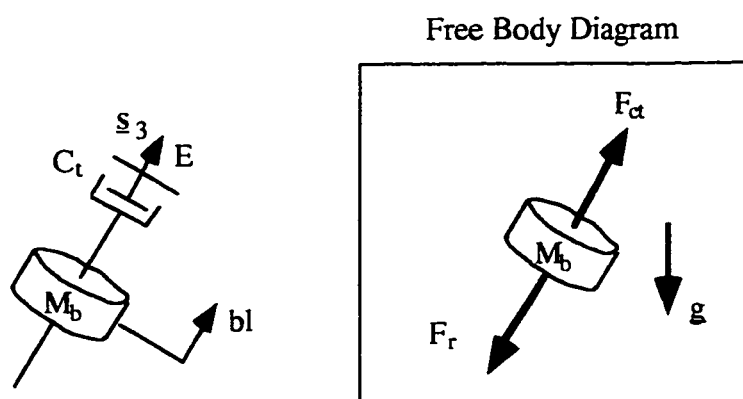
Figure 4.11 - Forces acting upon M_b

4.6.4 Resultant Forces and Torques

The resultant force and torque acting on each of the bodies of the connector is the combination of the external forces/torques, the contact forces/torques and the field forces/torques. The resultant torques is zero since the external, contact and field torques are zero. The resultant force vectors for the rigid bodies on each connector are given by

$$\mathbf{F}_e = \left[Fa - C_t \dot{E} - K_L \delta_L \right] \underline{s}_3 - \left[M_e g \right] \underline{k} \tag{31}$$

$$\mathbf{F}_d = \left[-C_{di} (\dot{D} - \dot{L}) - K_d \delta_d \right] \underline{s}_3 - \left[M_d g \right] \underline{k} \tag{32}$$

$$\mathbf{F}_b = \left[C_t \dot{E} - F_r \right] \underline{s}_3 - \left[M_b g \right] \underline{k} \tag{33}$$

4.6.5 Additional Equations

In order to completely describe the behavior of the connector, some additional force equations have to be derived. The platform is joined to the connector by the coupling stiffness and damper, and by the decoupling damper as shown in Figure 4.12. The connector force $\mathbf{F}_L$ is produced by the damping elements C_d, C_c and by the stiffness element K_c

$$\mathbf{F}_L = \left[F_{cd} + F_{cc} + F_{kc} \right] \underline{s}_3 \tag{34}$$

where F_{cd} is the frictional force of the decoupling stage damper C_d; F_{cc} is the frictional force of the coupling stage damper C_c; and F_{cc} is the spring force of the coupling stage spring K_c. These are given by

$$F_{cc} = C_c (\dot{H} - \dot{L}); \quad F_{kc} = K_c \delta_c \tag{35}$$

where δ_c is the deflection of the coupling stage stiffness and is given by
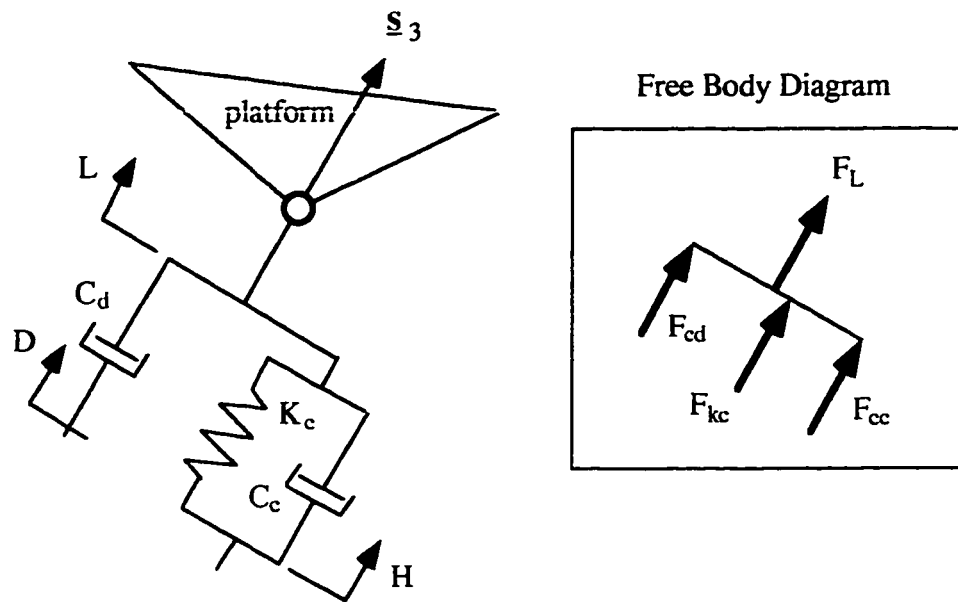
Figure 4.12 - Connector Force and Free Body Diagram
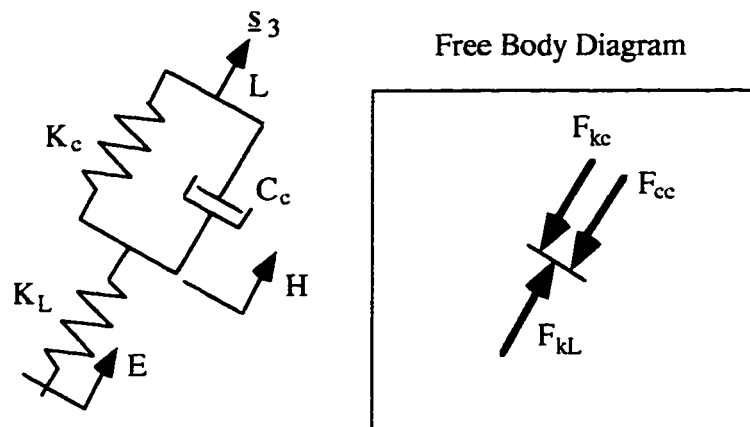
Figure 4.13 - Forces acting at the connection between the connector and coupling stage

$$\delta_c = (H - L) - l_{co} \qquad (36)$$

where l_{co} is the free length of the coupling stage spring. The forces acting at the

connection of the coupling stage and the connector itself are shown in Figure 4.13. The

balance of forces is given by

$$F_{kL}\underline{s}_3 = \lceil F_{cc} + F_{kc} \rceil \underline{s}_3 \tag{37}$$

An expression relating the connector force F_L and the force required to deform the connector can obtained by combining equations (23), (25), (34) and (37)

$$K_L \delta_L \underline{s}_3 = \underline{F}_L - C_d(\dot{D} - \dot{L})\underline{s}_3 \tag{38}$$

4.6.6 Force Analysis for the Simple Connector Model

As explained in Section 2.2, the connector can be modeled in different ways. For the complete leg model, the force analysis is given by equations (31), (32), (33) and (34).

The most simple model is obtained by assuming that the connector is a rigid and massless body. In this model the connector force is generated by the actuator. A more complete model is obtained by including the stiffness of the connector and the actuator's internal friction. In this connector model the decoupling stage is deactivated by setting the decoupling damping coefficient to a very low value ($C_d = 0$). The coupling stage is deactivated by setting the coupling damping coefficient to a very high value as discussed in Section 2.5 ($C_d \Rightarrow \infty$). This means that this displacement H is equal to the connector length L minus a fixed length which is the free length of the coupling stage spring K_c, l_{co}, and its first time derivative is zero. In this case the resultant forces acting upon masses M_e and M_b remain the same. The resultant force acting upon mass M_d, which is given by equation (32), is modified to

$$\underline{F}_d = \lfloor -K_d \delta_d \rfloor \underline{s}_3 - \lfloor M_d g \rfloor \underline{k} \tag{39}$$

The connector force vector, which is given by equation (38), can now be written as

$$\underline{F}_L = K_L \delta_L \underline{s}_3 \tag{40}$$

4.6.7 Force Analysis for the Low Frequency Model

Another model that can be used is the one that describes the connector's low frequency mode of operation (see Section 2.5). In this model, the coupling stage is active while the decoupling stage is deactivated by setting the decoupling damping coefficient to a very low value ($C_d \Rightarrow 0$). In this case the resultant forces of masses M_e and M_b remain the same.

The resultant force acting upon mass M_d, which is given by equation (32), is modified to

$$\mathbf{F}_d = \begin{bmatrix} -K_d \delta_d \end{bmatrix} \underline{s}_3 - [M_d g] \underline{k} \tag{39}$$

The connector force vector , which is given by equation (38), can now be written as

$$\mathbf{F}_L = \begin{bmatrix} C_c (\dot{H} - \dot{L}) + K_c \delta_c \end{bmatrix} \underline{s}_3 \tag{41}$$

This connector model is used when the system velocities are low and there are no disturbances applied to the platform as explained in Section 2.5.

4.6.8 Force Analysis for the High Frequency Model

The final model that can be used is the one that describes the connector's high frequency mode of operation where the coupling stage is inactivated by setting the coupling damping coefficient to a very high value as discussed in Section 2.5 ($C_c \Rightarrow \infty$). By using a high value for the coupling stage damping constant, this stage is made to behave as a rigid element. The force will be completely transmitted through the stage without being deflected ($H = L$). In this case the resultant forces acting upon masses M_e , M_d and M_b remain the same. The connector force vector, which is given by equation (38), can now be written as

$$\mathbf{F}_L = \begin{bmatrix} C_d (\dot{D} - \dot{L}) + K_L \delta_L \end{bmatrix} \underline{s}_3 \tag{42}$$

CHAPTER 5
PARALLEL MANIPULATOR DYNAMIC MODELING

As mentioned before, the dynamic model of the spatial parallel manipulator is needed in order to perform an inverse dynamic analysis. This analysis will determine the force, power and speed of response of the system actuators based on the desired task (based on the motion planning). This will help the designer to properly select the actuators, the dimensions of the manipulator, and to determine the values for system parameters such as the mass of the platform and the connector stiffness.

5.1 Selection of a Dynamic Formulation Method

The selection of the method for generating the system equations of motion is critical in the development of a dynamic model. Although the final set of equations of motion must be the same regardless of the method chosen, the difficulty of setting up the equations of motion depends on the method used. It is clearly desirable to choose a method which will generate the equations of motion in the simplest manner in order to reduce the amount of work and to avoid mistakes and.

5.1.1 Newton-Euler

The Newton-Euler method has been used for the dynamic analysis of the platform [5.1, 5.2]. One limitation of the Newton-Euler is that it becomes more cumbersome as more rigid bodies are included in system model. Another limitation is the workless constraints are included and have to be eliminated further on through some mathematical operations which can involve a considerable amount of work.

75

5.1.2 Lagrangian Dynamics

The basic concept behind this method is that the change of energy of a system is equal to the nonconservative forces applied to the system [26]. Nonconservative forces are basically external forces and frictional forces (such as viscous damping). These forces increase or decrease the energy level of the system. This method has been applied to a platform system to develop numerical simulations but not for deriving the explicit equations of motion [9, 10].

The energy of the system to be analyzed is described by the Lagrangian

$$L = KE - PE$$

where KE is the kinetic energy of the system and PE is the potential energy . The equations of motion are obtained by applying the following equation for each independent displacement variable of the system

$$\frac{d}{dt}\left(\frac{\partial L}{\partial \dot{q}_j}\right) - \frac{\partial L}{\partial q_j} = F_j$$

where q_j is the generalized or independent displacement variable j, and F_j is the generalized nonconservative force along the generalized displacement q_j. Since the potential energy is only a function of the displacement variables, the above equation can also be written as

$$\frac{d}{dt}\left(\frac{\partial KE}{\partial \dot{q}_j}\right) - \frac{\partial(KE - PE)}{\partial q_j} = F_j$$

The platform system has six independent displacement variables to describe the location of the platform and three for each connector. The system independent displacement variables are the location of the platform (position and orientation) and the displacements E, D and H as discussed in Sections 2.4, 2.5 and 3.3.

The kinetic energy for the platform system is given by

$$KE = \frac{M_p}{2} \left(\underline{V}_c \cdot \underline{V}_c \right) + \underline{\omega}^T \cdot \frac{[\,I_p\,]}{2} \cdot \underline{\omega} + \sum_i^6 \left[\underline{\omega}_{12}^T \cdot \frac{[\,I_e\,] + [\,I_d\,] + [\,I_b\,]}{2} \cdot \underline{\omega}_{12} \right]_i +$$

$$\sum_i^6 \left[\frac{M_e}{2} \left(\underline{V}_e \cdot \underline{V}_e \right) + \frac{M_d}{2} \left(\underline{V}_d \cdot \underline{V}_d \right) + \frac{M_b}{2} \left(\underline{V}_b \cdot \underline{V}_b \right) \right]_i$$

where M_p, M_e, M_d, M_b, [Ip], [Ie], [Id] and [Ib] are the masses and the inertia tensors of the platform and the connector rigid bodies respectively (see Section 2.5). The potential energy of the platform system is given by (see Section 2.5)

$$PE = \sum_i^6 \left[(M_e E + M_d D + M_b bl) g s_{3z} + \frac{K_c \delta_c^2 + K_d \delta_d^2 + K_l \delta_l^2}{2} \right]_i + M_p \underline{C} \cdot g \underline{k}$$

The partial derivatives required to determine the equations of motion using the Lagrange formulation can prove to be cumbersome to obtain for a parallel manipulator. As an example consider the fourth term of the kinetic energy expression

$$\sum_i^6 \left[\frac{M_e}{2} \left(\underline{V}_e \cdot \underline{V}_e \right) \right]_i = \sum_i^6 \left[\frac{M_e}{2} \left[\dot{E}^2 + E^2 \left(\omega_1^2 + \omega_2^2 \right) \right] \right]_i$$

The angular velocities ω_1 and ω_2 are functions of the velocity of the centerpoint and angular velocity of the platform as derived in Section 3.4

$$\omega_1 = \frac{[\underline{V}_c + (\underline{\omega} \times \underline{R}_{pc})] \cdot \underline{s}_2}{L} \quad ; \quad \omega_2 = \frac{[\underline{V}_c + (\underline{\omega} \times \underline{R}_{pc})] \cdot \underline{s}_{23}}{L}$$

The partial derivative of this term of the kinetic energy can then be written as

$$\frac{\partial}{\partial \dot{q}_j} \left(\sum_i^6 \left[\frac{M_e}{2} \left(\underline{V}_e \cdot \underline{V}_e \right) \right]_i \right) = \sum_i^6 \left[M_e \left[\dot{E} \frac{\partial \dot{E}}{\partial \dot{q}_j} + E^2 \left(\omega_1 \frac{\partial \omega_1}{\partial \dot{q}_j} + \omega_2 \frac{\partial \omega_2}{\partial \dot{q}_j} \right) \right] \right]_i$$

where the partial derivative of the angular velocities ω_1 and ω_2 are given by

$$\frac{\partial \omega_1}{\partial \dot{q}_j} = \frac{1}{L} \left[\frac{\partial \underline{V}_c}{\partial \dot{q}_j} + \left(\frac{\partial \underline{\omega}}{\partial \dot{q}_j} \times \underline{R}_{pc} \right) \right] \cdot \underline{s}_2$$

$$\frac{\partial \omega_2}{\partial \dot{q}_j} = \frac{1}{L} \left[\frac{\partial \underline{V}_c}{\partial \dot{q}_j} + \left(\frac{\partial \underline{\omega}}{\partial \dot{q}_j} \times \underline{R}_{pc} \right) \right] \cdot \underline{s}_{23}$$

Once the partial derivatives of the kinetic energy have been derived, the time derivative of the resulting expression must be determined. This is a very tedious and time consuming process since the vectors $\underline{R}_{pc}$, $\underline{s}_2$ and $\underline{s}_2$ are time dependent functions of the location of the platform. Similar complications arise when obtaining the partial derivatives of the kinetic energy and the potential energy expressions with respect to the displacement variables since there are many terms which are not simple functions of the independent displacement variables.

The Lagrangian method has been successfully applied to serial kinematic chains and the explicit equations of motion have been obtained for some serial manipulators [13, 14]. The main reason is that the velocities and positions of all the rigid bodies of the system, which are required for the kinetic and potential energy expressions, can be written as simple functions of the independent displacement variables and their first time derivatives. In the case of the platform the velocities and positions of the rigid bodies are not simple functions of the location and velocity of the platform as shown in Sections 3.3 and 3.4. This complicates the process of obtaining the partial derivatives required for the equations of motion.

5.1.3 Kane's Method

The method used in this thesis for deriving the dynamic model is what is known as Kane's Method for Dynamic Analysis [27]. A brief explanation of how to use this method is given in the appendix of this thesis. The equations of motion for the dynamic model for

a system with "w" elements (bodies & particles) and "n" degrees of freedom can be obtained by using the following equation

$$\sum_{j=1}^{w} \left(\frac{\partial \underline{V}_j}{\partial u_k} \cdot \{ \underline{F}_j - \underline{F}_j^* \} \right) + \sum_{j=1}^{w} \left(\frac{\partial \underline{\omega}_j}{\partial u_k} \cdot \{ \underline{T}_j - \underline{T}_j^* \} \right) = 0; \quad k = 1, 2, ..., n \quad (1)$$

where $\underline{F}_j^*$ and $\underline{T}_j^*$ are the Inertial Force and Torque respectively, and can be calculated by

$$\underline{F}_j^* = m_j \underline{A}_j \quad \& \quad \underline{T}_j^* = \underline{\alpha}_j \cdot \underline{I}_j^{\pi} + \underline{\omega}_j \times \underline{I}_j^{\pi} \cdot \underline{\omega}_j$$

This equation must be setup for each of the degrees of freedom of the system. In order to obtain the dynamic model, expressions for the following terms for each body must be determined

$\dfrac{\partial \underline{V}_j}{\partial u_k}$, the velocity partial derivative of body "j" respect to the kth generalized speed

$\dfrac{\partial \underline{\omega}_j}{\partial u_k}$, the angular velocity partial derivative of body "j"respect to the kth generalized speed

$\underline{F}_j$, the resultant force vector acting on body "j" at a given point "c"

$\underline{T}_j$, the resultant torque vector acting on body "j", about the point "c"

$\underline{A}_j$, the acceleration vector of body "j" at a given point "c"

m_j, the mass of body j

$\underline{\omega}_j$, the angular velocity vector of body "j"

$\underline{\alpha}_j$, the angular acceleration vector of body "j"

$\underline{I}_j^{\pi}$, the inertia dyadic of body "j", about the point "c"

5.2 Mobility Analysis

The first step in setting up the equations of motion is to determine the degrees of freedom of the spatial parallel manipulator or platform. The platform (see Figure 5.1)

itself has 6 degrees of freedom since it is a rigid body in space free to move when all the six actuators are operational. Each connector adds on three more degrees of freedom as outlined in Section 2.5 and shown in Figure 5.2. Since there are six connectors, the system has a total of 24 degrees of freedom .

The next step is to select the generalized coordinates required to completely describe the system configuration. Six variables are required in order to locate the platform in space. The vector $\underline{C}$ will be used to describe the location of the centerpoint of the platform, which accounts for three of the degrees of freedom. The rotation matrix [R] will be used to describe the orientation of the platform in space, which accounts for the other three degrees of freedom for the platform. A detailed description of $\underline{C}$ and [R] is given in Sections 3.1, 3.3 and 3.6.
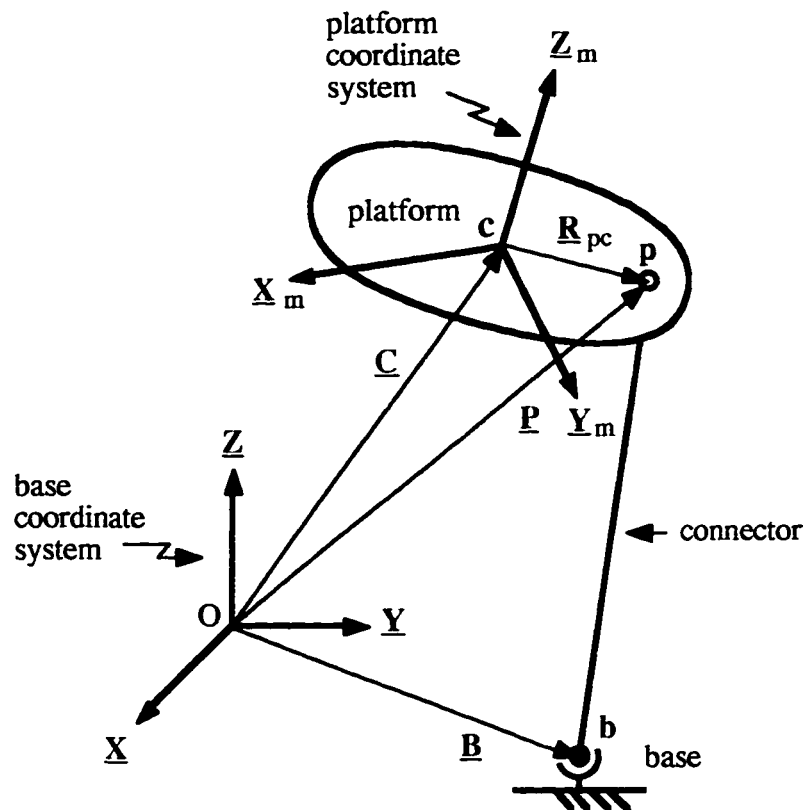
Figure 5.1 - Spatial Platform

Each connector requires three generalized coordinates in order to describe its configuration (see Figure 5.2). The first one is the actuator displacement, E. The second is the displacement at the point joining the connector to the coupling stage, H. The third is the displacement between the decoupling damper and the decoupling spring, D, as shown in figure 5.2. In summary, the generalized coordinates used to describe the complete system are (the letter "q" will used to designate the generalized coordinates)
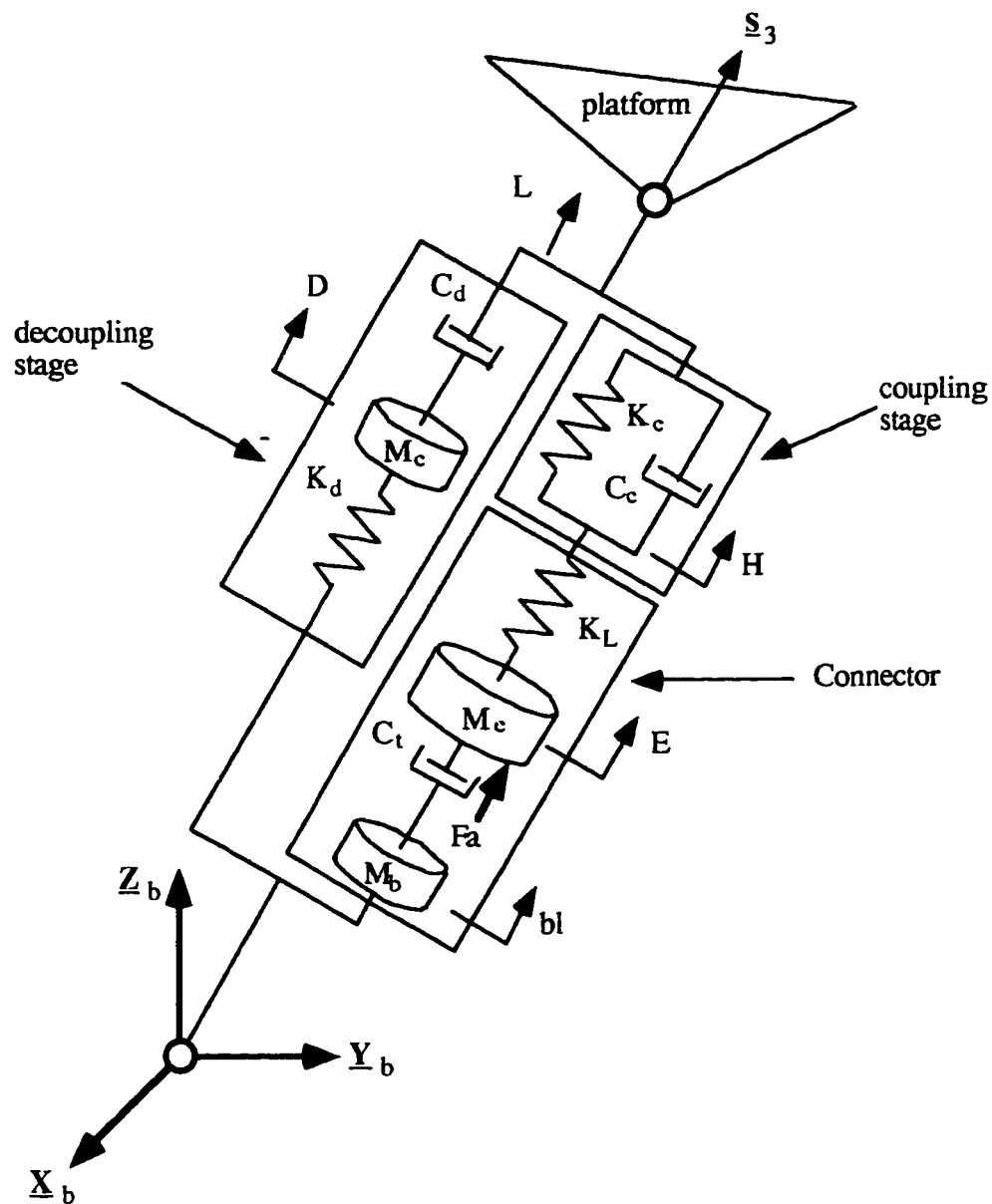
Figure 5.2 - Connector Model with Generalized Coordinates

$$(q_1)_i = (E)_i; \quad (q_2)_i = (H)_i; \quad (q_3)_i = (D)_i$$

where the letter "i" indicates the number of the connector, $i = 1$ to 6. The platform will be described using the following Generalized Coordinates

$$\underline{C} = [\, X_c, Y_c, Z_c \,] \Rightarrow q_{19} = X_c, \quad q_{20} = Y_c, \quad q_{21} = Z_c$$

$$[R] = f(\, \theta_x, \theta_y, \theta_z \,) \Rightarrow q_{22} = \theta_x, q_{23} = \theta_y, q_{24} = \theta_z$$

5.3 Generalized Speeds, Velocity and Acceleration Analysis

The next step is the selection of the Generalized Speeds. These are variables used to describe the velocity of each body in the system and are a function of the Generalized Coordinates and their first time derivatives. Although there are more than one possible set of Generalized Speeds, the number of elements in each set must be equal to the number of Generalized Coordinates.

5.3.1 Generalized Speeds

The letter "u" is used to designate the Generalized Speeds, which are functions of the Generalized Coordinates and their first time derivatives. A simple choice is to use the first time derivative of each Generalized Coordinate, q_j, as the Generalized Speed u_j. For each connector they will be the first time derivatives of the Generalized Coordinates E, H & D

$$(u_1)_i = \frac{d}{dt}(E)_i; \quad (u_2)_i = \frac{d}{dt}(H)_i; \quad (u_3)_i = \frac{d}{dt}(D)_i$$

The Generalized Speeds of the vector $\underline{C}$ are the first time derivatives of the centerpoint coordinates

$$(C_x) = V_{cx} = u_{19}, \quad \frac{d}{dt}(C_y) = V_{cy} = u_{20}, \quad \frac{d}{dt}(C_z) = V_{cz} = u_{21}$$

The elements of the platform's angular velocity vector $\underline{\omega} = [\,\omega_x,\,\omega_y,\,\omega_z\,]^T$ about the axes of the Base Coordinate System are used as the Generalized Speeds of the rotation matrix $[\mathbf{R}]$ and thus

$$\omega_x = u_{22}, \quad \omega_y = u_{23}, \quad \omega_x = u_{24}$$

5.3.2 Velocity Analysis

Each of the bodies on the connector will have a similar expression for their velocity vectors and the same expression for their angular velocity vectors. The angular velocity vector for the rigid bodies of the connector is given by (see Section 3.4)

$$\underline{\omega}_{12} = \frac{[(\underline{V}_c \cdot \underline{s}_2) + \underline{\omega} \cdot (\underline{R}_{pc} \times \underline{s}_2)]}{L}\,\underline{s}_1 + \frac{[(\underline{V}_c \cdot \underline{s}_{23}) + \underline{\omega} \cdot (\underline{R}_{pc} \times \underline{s}_{23})]}{L}\,\underline{s}_2 \quad (2)$$

The velocity vectors of the base mass, the decoupling stage mass and the actuator mass, (see Section 3.4) are given respectively by

$$\underline{V}_b = \frac{bl}{L}\,[(\underline{V}_c \cdot \underline{s}_2) + \underline{\omega} \cdot (\underline{R}_{pc} \times \underline{s}_2)]\,\underline{s}_2 +$$

$$\frac{bl}{L}\,[(\underline{V}_c \cdot \underline{s}_{23}) + \underline{\omega} \cdot (\underline{R}_{pc} \times \underline{s}_{23})]\,\underline{s}_{23} \quad (3)$$

$$\underline{V}_d = \dot{D}\underline{s}_3 + \frac{D}{L}\,[(\underline{V}_c \cdot \underline{s}_2) + \underline{\omega} \cdot (\underline{R}_{pc} \times \underline{s}_2)]\,\underline{s}_2 +$$

$$\frac{D}{L}\,[(\underline{V}_c \cdot \underline{s}_{23}) + \underline{\omega} \cdot (\underline{R}_{pc} \times \underline{s}_{23})]\,\underline{s}_{23} \quad (4)$$

$$\underline{V}_e = \dot{E}\underline{s}_3 + \frac{E}{L}\,[(\underline{V}_c \cdot \underline{s}_2) + \underline{\omega} \cdot (\underline{R}_{pc} \times \underline{s}_2)]\,\underline{s}_2 +$$

$$\frac{E}{L} \left[\left(\underline{V}_c \cdot \underline{S}_{23} \right) + \underline{\omega} \cdot \left(\underline{R}_{pc} \times \underline{S}_{23} \right) \right] \underline{S}_{23} \qquad (5)$$

Using the definitions for $\underline{S}_1$, $\underline{S}_2$ and $\underline{S}_{23}$ given in Section 3.3, the angular velocity vector $\underline{\omega}_{12}$ can also be written in terms of the Generalized Speeds defined above

$$\underline{\omega}_{12} = \frac{u_{19}}{L} \cdot \begin{pmatrix} 0 \\ -s_{3z} \cdot s_{23x} \\ s_{23x} \cdot s_{3y} \end{pmatrix} + \frac{u_{20}}{L} \cdot \begin{pmatrix} -s_{3z} \\ -s_{3z} \cdot s_{23y} \\ s_{23y} \cdot s_{3y} \end{pmatrix} + \frac{u_{21}}{L} \cdot \begin{pmatrix} s_{3y} \\ -s_{3z} \cdot s_{23z} \\ s_{23z} \cdot s_{3y} \end{pmatrix} +$$

$$\frac{u_{22}}{L} \cdot \begin{bmatrix} R_{pcy} \cdot s_{3y} + R_{pcz} \cdot s_{3z} \\ \left(R_{pcz} \cdot s_{23y} - R_{pcy} \cdot s_{23z} \right) \cdot s_{3z} \\ \left(R_{pcy} \cdot s_{23z} - R_{pcz} \cdot s_{23y} \right) \cdot s_{3y} \end{bmatrix} + \frac{u_{23}}{L} \cdot \begin{bmatrix} -\left(R_{pcx} \cdot s_{3y} \right) \\ \left(R_{pcx} \cdot s_{23z} - R_{pcz} \cdot s_{23x} \right) \cdot s_{3z} \\ \left(R_{pcz} \cdot s_{23x} - R_{pcx} \cdot s_{23z} \right) \cdot s_{3y} \end{bmatrix} +$$

$$\frac{u_{24}}{L} \cdot \begin{bmatrix} -R_{pcx} \cdot s_{3z} \\ \left(R_{pcy} \cdot s_{23x} - R_{pcx} \cdot s_{23y} \right) \cdot s_{3z} \\ \left(R_{pcx} \cdot s_{23y} - R_{pcy} \cdot s_{23x} \right) \cdot s_{3y} \end{bmatrix} \qquad (6)$$

The velocity vectors $\underline{V}_b$, $\underline{V}_d$ and $\underline{V}_e$ can also be written in terms of the generalized speeds defined above

$$\underline{V}_b = u_{19} \cdot \frac{bl}{L} \cdot \begin{bmatrix} \left(s_{23x} \right)^2 \\ s_{23y} \cdot s_{23x} \\ s_{23z} \cdot s_{23x} \end{bmatrix} + u_{20} \cdot \frac{bl}{L} \cdot \begin{bmatrix} s_{23y} \cdot s_{23x} \\ \left(s_{3z} \right)^2 + \left(s_{23y} \right)^2 \\ s_{23y} \cdot s_{23z} - s_{3z} \cdot s_{3y} \end{bmatrix} +$$

$$u_{21} \cdot \frac{bl}{L} \cdot \begin{bmatrix} s_{23z} \cdot s_{23x} \\ s_{23y} \cdot s_{23z} - s_{3z} \cdot s_{3y} \\ \left(s_{3y} \right)^2 + \left(s_{23z} \right)^2 \end{bmatrix} +$$

$$u_{22} \cdot \frac{bl}{L} \cdot \begin{bmatrix} \left(R_{pcy} \cdot s_{23z} - R_{pcz} \cdot s_{23y} \right) \cdot s_{23x} \\ \left(s_{23z} \cdot s_{23y} - s_{3y} \cdot s_{3z} \right) \cdot R_{pcy} - \left[\left(s_{3z} \right)^2 + \left(s_{23y} \right)^2 \right] \cdot R_{pcz} \\ \left[\left(s_{3y} \right)^2 + \left(s_{23z} \right)^2 \right] \cdot R_{pcy} + \left(s_{3y} \cdot s_{3z} - s_{23z} \cdot s_{23y} \right) \cdot R_{pcz} \end{bmatrix} +$$

$$u_{23} \cdot \frac{bl}{L} \cdot \begin{bmatrix} \left(R_{pcz} \cdot s_{23x} - R_{pcx} \cdot s_{23z} \right) \cdot s_{23x} \\ \left(s_{3y} \cdot s_{3z} - s_{23y} \cdot s_{23z} \right) \cdot R_{pcx} + s_{23x} \cdot s_{23y} \cdot R_{pcz} \\ \left[- \left(s_{23z} \right)^2 - \left(s_{3y} \right)^2 \right] \cdot R_{pcx} + s_{23x} \cdot s_{23z} \cdot R_{pcz} \end{bmatrix} +$$

$$u_{24} \cdot \frac{bl}{L} \cdot \begin{bmatrix} \left(R_{pcx} \cdot s_{23y} - R_{pcy} \cdot s_{23x} \right) \cdot s_{23x} \\ \left[\left(s_{3z} \right)^2 + \left(s_{23y} \right)^2 \right] \cdot R_{pcx} - s_{23x} \cdot s_{23y} \cdot R_{pcy} \\ \left(s_{23y} \cdot s_{23z} - s_{3y} \cdot s_{3z} \right) \cdot R_{pcx} - s_{23x} \cdot s_{23z} \cdot R_{pcy} \end{bmatrix} \qquad (7)$$

$$\underline{V}_d = u_3 \cdot \begin{pmatrix} s_{3x} \\ s_{3y} \\ s_{3z} \end{pmatrix} + u_{19} \cdot \frac{E}{L} \cdot \begin{bmatrix} \left(s_{23x} \right)^2 \\ s_{23y} \cdot s_{23x} \\ s_{23z} \cdot s_{23x} \end{bmatrix} +$$

$$u_{20} \cdot \frac{D}{L} \cdot \begin{bmatrix} s_{23y} \cdot s_{23x} \\ \left(s_{3z} \right)^2 + \left(s_{23y} \right)^2 \\ s_{23y} \cdot s_{23z} - s_{3z} \cdot s_{3y} \end{bmatrix} + u_{21} \cdot \frac{D}{L} \cdot \begin{bmatrix} s_{23z} \cdot s_{23x} \\ s_{23y} \cdot s_{23z} - s_{3z} \cdot s_{3y} \\ \left(s_{3y} \right)^2 + \left(s_{23z} \right)^2 \end{bmatrix} +$$

$$u_{22} \cdot \frac{D}{L} \cdot \begin{bmatrix} \left(R_{pcy} \cdot s_{23z} - R_{pcz} \cdot s_{23y} \right) \cdot s_{23x} \\ \left(s_{23z} \cdot s_{23y} - s_{3y} \cdot s_{3z} \right) \cdot R_{pcy} - \left[\left(s_{3z} \right)^2 + \left(s_{23y} \right)^2 \right] \cdot R_{pcz} \\ \left[\left(s_{3y} \right)^2 + \left(s_{23z} \right)^2 \right] \cdot R_{pcy} + \left(s_{3y} \cdot s_{3z} - s_{23z} \cdot s_{23y} \right) \cdot R_{pcz} \end{bmatrix} +$$

$$u_{23} \cdot \frac{D}{L} \cdot \begin{bmatrix} \left(R_{pcz} \cdot s_{23x} - R_{pcx} \cdot s_{23z}\right) \cdot s_{23x} \\ \left(s_{3y} \cdot s_{3z} - s_{23y} \cdot s_{23z}\right) \cdot R_{pcx} + s_{23x} \cdot s_{23y} \cdot R_{pcz} \\ \left[-\left(s_{23z}\right)^2 - \left(s_{3y}\right)^2\right] \cdot R_{pcx} + s_{23x} \cdot s_{23z} \cdot R_{pcz} \end{bmatrix} +$$

$$u_{24} \cdot \frac{D}{L} \cdot \begin{bmatrix} \left(R_{pcx} \cdot s_{23y} - R_{pcy} \cdot s_{23x}\right) \cdot s_{23x} \\ \left[\left(s_{3z}\right)^2 + \left(s_{23y}\right)^2\right] \cdot R_{pcx} - s_{23x} \cdot s_{23y} \cdot R_{pcy} \\ \left(s_{23y} \cdot s_{23z} - s_{3y} \cdot s_{3z}\right) \cdot R_{pcx} - s_{23x} \cdot s_{23z} \cdot R_{pcy} \end{bmatrix} \qquad (8)$$

$$\underline{V}_e = u_1 \cdot \begin{pmatrix} s_{3x} \\ s_{3y} \\ s_{3z} \end{pmatrix} + u_{19} \cdot \frac{E}{L} \cdot \begin{bmatrix} \left(s_{23x}\right)^2 \\ s_{23y} \cdot s_{23x} \\ s_{23z} \cdot s_{23x} \end{bmatrix} +$$

$$u_{20} \cdot \frac{E}{L} \cdot \begin{bmatrix} s_{23y} \cdot s_{23x} \\ \left(s_{3z}\right)^2 + \left(s_{23y}\right)^2 \\ s_{23y} \cdot s_{23z} - s_{3z} \cdot s_{3y} \end{bmatrix} + u_{21} \cdot \frac{E}{L} \cdot \begin{bmatrix} s_{23z} \cdot s_{23x} \\ s_{23y} \cdot s_{23z} - s_{3z} \cdot s_{3y} \\ \left(s_{3y}\right)^2 + \left(s_{23z}\right)^2 \end{bmatrix} +$$

$$u_{22} \cdot \frac{E}{L} \cdot \begin{bmatrix} \left(R_{pcy} \cdot s_{23z} - R_{pcz} \cdot s_{23y}\right) \cdot s_{23x} \\ \left(s_{23z} \cdot s_{23y} - s_{3y} \cdot s_{3z}\right) \cdot R_{pcy} - \left[\left(s_{3z}\right)^2 + \left(s_{23y}\right)^2\right] \cdot R_{pcz} \\ \left[\left(s_{3y}\right)^2 + \left(s_{23z}\right)^2\right] \cdot R_{pcy} + \left(s_{3y} \cdot s_{3z} - s_{23z} \cdot s_{23y}\right) \cdot R_{pcz} \end{bmatrix} +$$

$$u_{23} \cdot \frac{E}{L} \cdot \begin{bmatrix} \left(R_{pcz} \cdot s_{23x} - R_{pcx} \cdot s_{23z}\right) \cdot s_{23x} \\ \left(s_{3y} \cdot s_{3z} - s_{23y} \cdot s_{23z}\right) \cdot R_{pcx} + s_{23x} \cdot s_{23y} \cdot R_{pcz} \\ \left[-\left(s_{23z}\right)^2 - \left(s_{3y}\right)^2\right] \cdot R_{pcx} + s_{23x} \cdot s_{23z} \cdot R_{pcz} \end{bmatrix} +$$

$$u_{24} \cdot \frac{E}{L} \cdot \begin{bmatrix} \left(R_{pcx} \cdot s_{23y} - R_{pcy} \cdot s_{23x} \right) \cdot s_{23x} \\ \left[\left(s_{3z} \right)^2 + \left(s_{23y} \right)^2 \right] \cdot R_{pcx} - s_{23x} \cdot s_{23y} \cdot R_{pcy} \\ \left(s_{23y} \cdot s_{23z} - s_{3y} \cdot s_{3z} \right) \cdot R_{pcx} - s_{23x} \cdot s_{23z} \cdot R_{pcy} \end{bmatrix} \qquad (9)$$

Using the Generalized Speeds defined previously, the angular velocity and the velocity vectors for the platform are given by

$$\underline{V}_c = \begin{pmatrix} u_{19} \\ u_{20} \\ u_{21} \end{pmatrix} \qquad \underline{\omega} = \begin{pmatrix} u_{22} \\ u_{23} \\ u_{24} \end{pmatrix} \qquad (10)$$

5.3.3 Acceleration Analysis

As derived in Section 3.5, the angular acceleration vector $\underline{\alpha}_{12}$ for all the rigid bodies of the connector is given by

$$\underline{\alpha}_{12} = \alpha_1 \underline{s}_1 + \alpha_2 \underline{s}_2 + \omega_1 \omega_2 \left[\underline{s}_2 \times \underline{s}_1 \right] \qquad (11)$$

The acceleration vector for the mass M_b can be written as

$$\underline{A}_b = bl \left[\alpha_1 \underline{s}_2 + \alpha_2 \underline{s}_{23} + \omega_1 \omega_2 \left(\underline{s}_1 \cdot \underline{s}_3 \right) \underline{s}_2 \right] \qquad (12)$$

The acceleration vector for the decoupling stage mass M_d can be written as

$$\underline{A}_d = \ddot{D}\, \underline{s}_3 + 2\dot{D}\left(\omega_1 \underline{s}_2 + \omega_2 \underline{s}_{23} \right) + D\left(\alpha_1 \underline{s}_2 + \alpha_2 \underline{s}_{23} \right) +$$

$$D \left[2\omega_1 \omega_2 \left(\underline{s}_1 \cdot \underline{s}_3 \right) \underline{s}_2 + \omega_1^2 \left(\underline{s}_1 \cdot \underline{s}_3 \right) \underline{s}_1 - \left(\omega_1^2 + \omega_2^2 \right) \underline{s}_3 \right] \qquad (13)$$

The acceleration vector for the actuator mass M_e can be written as

$$\underline{A}_e = \ddot{E}\, \underline{s}_3 + 2\dot{E}\left(\omega_1 \underline{s}_2 + \omega_2 \underline{s}_{23} \right) + E\left(\alpha_1 \underline{s}_2 + \alpha_2 \underline{s}_{23} \right) +$$

$$E\left[2\omega_1\omega_2(\underline{s}_1 \cdot \underline{s}_3)\underline{s}_2 + \omega_1^2(\underline{s}_1 \cdot \underline{s}_3)\underline{s}_1 - (\omega_1^2 + \omega_2^2)\underline{s}_3 \right] \qquad (14)$$

The angular acceleration and acceleration vectors for the platform are given by

$$\underline{A}_c = \begin{pmatrix} A_{cx} \\ A_{cy} \\ A_{cz} \end{pmatrix} \qquad \underline{\alpha} = \begin{pmatrix} \alpha_x \\ \alpha_y \\ \alpha_z \end{pmatrix} \qquad (15)$$

5.4 Velocity and Angular Velocity Partial Derivatives

One of the distinctive features of Kane's Method is the use of the velocity and angular velocity partial derivatives of each body with respect to the generalized speeds. These partial derivatives define the directions of the instantaneous translational and rotational displacement of each body. A more complete explanation is given in the appendix.

As shown in Section 3.4, the connector angular velocity vector $\underline{\omega}_{12}$ can be written as

$$\underline{\omega}_{12} = \left[(\underline{V}_c \cdot \underline{s}_2)\underline{s}_1 + (\underline{V}_c \cdot \underline{s}_{23})\underline{s}_2 \right] \frac{1}{L} +$$

$$\left[(\underline{\omega} \cdot (\underline{R}_{pc} \times \underline{s}_2))\underline{s}_1 + (\underline{\omega} \cdot (\underline{R}_{pc} \times \underline{s}_{23}))\underline{s}_2 \right] \frac{1}{L}$$

This angular velocity vector is a function of the Generalized Speeds u_{19}, u_{20}, u_{21}, u_{22}, u_{23} & u_{24} as shown in equation (6). The angular velocity partial derivatives for these bodies with respect to the generalized speeds u_1 through u_3 are (k = 1 to 3)

$$\frac{\delta\left(\underline{\omega}_{12}\right)}{\delta u_k} = 0 \qquad (16)$$

The angular velocity partial derivatives the generalized speeds u_{19} through are u_{24}

$$\frac{\delta\underline{\omega}_{12}}{\delta u_{19}} = [s_{2x}\,\underline{s}_1 + s_{23x}\,\underline{s}_2]\,\frac{1}{L} \tag{17}$$

$$\frac{\delta\underline{\omega}_{12}}{\delta u_{20}} = [s_{2y}\,\underline{s}_1 + s_{23y}\,\underline{s}_2]\,\frac{1}{L} \tag{18}$$

$$\frac{\delta\underline{\omega}_{12}}{\delta u_{21}} = [s_{2z}\,\underline{s}_1 + s_{23z}\,\underline{s}_2]\,\frac{1}{L} \tag{19}$$

$$\frac{\delta\underline{\omega}_{12}}{\delta u_{22}} = [\underline{s}_1(\mathbf{R}_{pc}\times\underline{s}_2)_x + \underline{s}_2(\mathbf{R}_{pc}\times\underline{s}_{23})_x]\,\frac{1}{L} \tag{20}$$

$$\frac{\delta\underline{\omega}_{12}}{\delta u_{23}} = [\underline{s}_1(\mathbf{R}_{pc}\times\underline{s}_2)_y + \underline{s}_2(\mathbf{R}_{pc}\times\underline{s}_{23})_y]\,\frac{1}{L} \tag{21}$$

$$\frac{\delta\underline{\omega}_{12}}{\delta u_{24}} = [\underline{s}_1(\mathbf{R}_{pc}\times\underline{s}_2)_z + \underline{s}_2(\mathbf{R}_{pc}\times\underline{s}_{23})_z]\,\frac{1}{L} \tag{22}$$

where $(\mathbf{R}_{pc}\times\underline{s}_2)_{x,y,z}$ are the respective x, y and z components of the vector product of the vectors $\mathbf{R}_{pc}$ and $\underline{s}_2$; and $(\mathbf{R}_{pc}\times\underline{s}_{23})_{x,y,z}$ are the respective x, y and z components of the vector product of the vectors $\mathbf{R}_{pc}$ and $\underline{s}_{23}$. These velocity partial derivatives can be also be written in their expanded form

$$\frac{\delta\left(\underline{\omega}_{12}\right)}{\delta u_{19}} = \frac{1}{L}\cdot\begin{pmatrix} 0 \\ -s_{23x}\cdot s_{3z} \\ s_{23x}\cdot s_{3y} \end{pmatrix} \tag{17.a}$$

$$\frac{\delta\left(\underline{\omega}_{12}\right)}{\delta u_{20}} = \frac{1}{L}\cdot\begin{pmatrix} -s_{3z} \\ -s_{23y}\cdot s_{3z} \\ s_{23y}\cdot s_{3y} \end{pmatrix} \tag{18.a}$$

$$\frac{\delta\left(\underline{\omega}_{12}\right)}{\delta u_{21}} = \frac{1}{L} \cdot \begin{pmatrix} s_{3y} \\ -s_{23z} \cdot s_{3z} \\ s_{23z} \cdot s_{3y} \end{pmatrix} \qquad (19.a)$$

$$\frac{\delta\left(\underline{\omega}_{12}\right)}{\delta u_{22}} = \frac{1}{L} \cdot \begin{bmatrix} R_{pcy} \cdot s_{3y} + R_{pcz} \cdot s_{3z} \\ \left(R_{pcz} \cdot s_{23y} - R_{pcy} \cdot s_{23z}\right) \cdot s_{3z} \\ \left(R_{pcy} \cdot s_{23z} - R_{pcz} \cdot s_{23y}\right) \cdot s_{3y} \end{bmatrix} \qquad (20.a)$$

$$\frac{\delta\left(\underline{\omega}_{12}\right)}{\delta u_{23}} = \frac{1}{L} \cdot \begin{bmatrix} -R_{pcx} \cdot s_{3y} \\ \left(R_{pcx} \cdot s_{23z} - R_{pcz} \cdot s_{23x}\right) \cdot s_{3z} \\ \left(R_{pcz} \cdot s_{23x} - R_{pcx} \cdot s_{23z}\right) \cdot s_{3y} \end{bmatrix} \qquad (21.a)$$

$$\frac{\delta\left(\underline{\omega}_{12}\right)}{\delta u_{24}} = \frac{1}{L} \cdot \begin{bmatrix} -R_{pcx} \cdot s_{3z} \\ \left(R_{pcy} \cdot s_{23x} - R_{pcx} \cdot s_{23y}\right) \cdot s_{3z} \\ \left(R_{pcx} \cdot s_{23y} - R_{pcy} \cdot s_{23x}\right) \cdot s_{3y} \end{bmatrix} \qquad (22.a)$$

The velocity partial derivatives of the base mass with respect to the Generalized Speeds u_1 through u_3 of each connector ($k = 1$ to 3) are

$$\frac{\delta\left(\underline{V}_b\right)}{\delta u_k} = 0 \qquad (23)$$

Using the expression for $\underline{V}_b$ derived in Section 3.4 and the definitions of the Generalized Speeds, the velocity partial derivatives of $\underline{V}_b$ with respect to the Generalized Speeds u_{19} through u_{24} can be written as

$$\frac{\delta \underline{V}_b}{\delta u_{19}} = \begin{bmatrix} s_{2x} \underline{s}_2 + s_{23x} \underline{s}_{23} \end{bmatrix} \frac{bl}{L} \qquad (24)$$

$$\frac{\delta \underline{V}_b}{\delta u_{20}} = \left[s_{2y} \underline{s}_2 + s_{23y} \underline{s}_{23} \right] \frac{bl}{L} \tag{25}$$

$$\frac{\delta \underline{V}_b}{\delta u_{21}} = \left[s_{2z} \underline{s}_2 + s_{23z} \underline{s}_{23} \right] \frac{bl}{L} \tag{26}$$

$$\frac{\delta \underline{V}_b}{\delta u_{22}} = \left[\underline{s}_2 (\underline{R}_{pc} \times \underline{s}_2)_x + \underline{s}_{23} (\underline{R}_{pc} \times \underline{s}_{23})_x \right] \frac{bl}{L} \tag{27}$$

$$\frac{\delta \underline{V}_b}{\delta u_{23}} = \left[\underline{s}_2 (\underline{R}_{pc} \times \underline{s}_2)_y + \underline{s}_{23} (\underline{R}_{pc} \times \underline{s}_{23})_y \right] \frac{bl}{L} \tag{28}$$

$$\frac{\delta \underline{V}_b}{\delta u_{24}} = \left[\underline{s}_2 (\underline{R}_{pc} \times \underline{s}_2)_z + \underline{s}_{23} (\underline{R}_{pc} \times \underline{s}_{23})_z \right] \frac{bl}{L} \tag{29}$$

These velocity partial derivatives can also be written in their expanded form

$$\frac{\delta (\underline{V}_b)}{\delta u_{19}} = \frac{bl}{L} \cdot \begin{bmatrix} (s_{23x})^2 \\ s_{23y} \cdot s_{23x} \\ s_{23z} \cdot s_{23x} \end{bmatrix} \tag{24.a}$$

$$\frac{\delta (\underline{V}_b)}{\delta u_{20}} = \frac{bl}{L} \cdot \begin{bmatrix} s_{23y} \cdot s_{23x} \\ (s_{3z})^2 + (s_{23y})^2 \\ s_{23y} \cdot s_{23z} - s_{3z} \cdot s_{3y} \end{bmatrix} \tag{25.a}$$

$$\frac{\delta (\underline{V}_b)}{\delta u_{21}} = \frac{bl}{L} \cdot \begin{bmatrix} s_{23z} \cdot s_{23x} \\ s_{23y} \cdot s_{23z} - s_{3z} \cdot s_{3y} \\ (s_{3y})^2 + (s_{23z})^2 \end{bmatrix} \tag{26.a}$$

$$\frac{\delta\left(\underline{V}_b\right)}{\delta u_{22}} = \frac{bl}{L} \cdot \begin{bmatrix} \left(R_{pcy} \cdot s_{23z} - R_{pcz} \cdot s_{23y}\right) \cdot s_{23x} \\ \left(s_{23z} \cdot s_{23y} - s_{3y} \cdot s_{3z}\right) \cdot R_{pcy} - \left[\left(s_{3z}\right)^2 + \left(s_{23y}\right)^2 \right] \cdot R_{pcz} \\ \left[\left(s_{3y}\right)^2 + \left(s_{23z}\right)^2 \right] \cdot R_{pcy} + \left(s_{3y} \cdot s_{3z} - s_{23z} \cdot s_{23y}\right) \cdot R_{pcz} \end{bmatrix} \qquad (27.a)$$

$$\frac{\delta\left(\underline{V}_b\right)}{\delta u_{23}} = \frac{bl}{L} \cdot \begin{bmatrix} \left(R_{pcz} \cdot s_{23x} - R_{pcx} \cdot s_{23z}\right) \cdot s_{23x} \\ \left(s_{3y} \cdot s_{3z} - s_{23y} \cdot s_{23z}\right) \cdot R_{pcx} + s_{23x} \cdot s_{23y} \cdot R_{pcz} \\ \left[-\left(s_{23z}\right)^2 - \left(s_{3y}\right)^2 \right] \cdot R_{pcx} + s_{23x} \cdot s_{23z} \cdot R_{pcz} \end{bmatrix} \qquad (28.a)$$

$$\frac{\delta\left(\underline{V}_b\right)}{\delta u_{24}} = \frac{bl}{L} \cdot \begin{bmatrix} \left(R_{pcx} \cdot s_{23y} - R_{pcy} \cdot s_{23x}\right) \cdot s_{23x} \\ \left[\left(s_{3z}\right)^2 + \left(s_{23y}\right)^2 \right] \cdot R_{pcx} - s_{23x} \cdot s_{23y} \cdot R_{pcy} \\ \left(s_{23y} \cdot s_{23z} - s_{3y} \cdot s_{3z}\right) \cdot R_{pcx} - s_{23x} \cdot s_{23z} \cdot R_{pcy} \end{bmatrix} \qquad (29.a)$$

The velocity partial derivatives of the velocity vector $\underline{V}_d$ with respect to the Generalized Speeds u_1 and u_2 of each connector are given by

$$\frac{\delta\left(\underline{V}_d\right)}{\delta u_1} = 0 \qquad\qquad \frac{\delta\left(\underline{V}_d\right)}{\delta u_2} = 0 \qquad\qquad (30)$$

The velocity partial derivative of the velocity vector $\underline{V}_d$ with respect to the generalized speed u_3 of each connector is given by

$$\frac{\delta\left(\underline{V}_d\right)}{\delta u_3} = \begin{pmatrix} s_{3x} \\ s_{3y} \\ s_{3z} \end{pmatrix} \qquad\qquad (31)$$

The velocity partial derivative of the velocity vector $\underline{V}_e$ with respect to the Generalized Speeds u_1 of each connector is given by

$$\frac{\delta\left(\underline{V}_e\right)}{\delta u_1} = \begin{pmatrix} s_{3x} \\ s_{3y} \\ s_{3z} \end{pmatrix} \tag{32}$$

The velocity partial derivatives of the velocity vector $\underline{V}_e$ with respect to the Generalized Speeds u_1 and u_2 of each connector are given by

$$\frac{\delta\left(\underline{V}_e\right)}{\delta u_2} = 0 \qquad \frac{\delta\left(\underline{V}_e\right)}{\delta u_3} = 0 \tag{33}$$

The velocity partial derivatives of the velocity vectors $\underline{V}_d$ and $\underline{V}_e$ with respect to the Generalized Speeds u_{19} through u_{24} are the similar to those for the velocity vector $\underline{V}_b$, the difference is that instead of bl the displacements D and E are used.

The velocity partial derivatives of the centerpoint velocity vector $\underline{V}_c$ with respect to the Generalized Speeds u_{19} through u_{21} are

$$\frac{\delta\left(\underline{V}_c\right)}{\delta u_{19}} = \begin{pmatrix} 1 \\ 0 \\ 0 \end{pmatrix} \qquad \frac{\delta\left(\underline{V}_c\right)}{\delta u_{20}} = \begin{pmatrix} 0 \\ 1 \\ 0 \end{pmatrix} \qquad \frac{\delta\left(\underline{V}_c\right)}{\delta u_{21}} = \begin{pmatrix} 0 \\ 0 \\ 1 \end{pmatrix} \tag{34}$$

The angular velocity partial derivatives of the angular velocity vector $\underline{\omega}$ with respect to the Generalized Speeds u_{22} through u_{24} are

$$\frac{\delta\left(\underline{\omega}\right)}{\delta u_{22}} = \begin{pmatrix} 1 \\ 0 \\ 0 \end{pmatrix} \qquad \frac{\delta\left(\underline{\omega}\right)}{\delta u_{20}} = \begin{pmatrix} 0 \\ 1 \\ 0 \end{pmatrix} \qquad \frac{\delta\left(\underline{\omega}\right)}{\delta u_{21}} = \begin{pmatrix} 0 \\ 0 \\ 1 \end{pmatrix} \tag{35}$$

The velocity and angular partial derivatives of the platform with respect to the remaining Generalized Speeds are zero.

5.5 Setting up the Dynamic Model

As stated in equation 1, the dynamic model for a system with "w" bodies and "n" degrees of freedom can be generated by using the following equation

$$\sum_{j=1}^{w} (\frac{\partial \mathbf{V}_j}{\partial u_k} \cdot \{ \mathbf{F}_j - \mathbf{F}_j^* \}) + \sum_{j=1}^{w} (\frac{\partial \omega_j}{\partial u_k} \cdot \{ \mathbf{T}_j - \mathbf{T}_j^* \}) = 0; \quad k = 1, 2, ..., n$$

this equation can be simplified somewhat by using the following expressions

$$\mathbf{F}_j' = \mathbf{F}_j - m_j \mathbf{A}_j \tag{36.a}$$

$$\mathbf{T}_j' = \mathbf{T}_j - \left[(\underline{\alpha}_j \cdot \mathbf{Ij}^{\cdot \cdot}) + (\underline{\omega}_j \times \mathbf{Ij}^{\cdot \cdot} \cdot \underline{\omega}_j) \right] \tag{36.b}$$

where expressions for the resultant forces $\mathbf{F}_j$, torques $\mathbf{T}_j$, angular velocities $\underline{\omega}_j$,

accelerations $\underline{\mathbf{A}}_j$ and angular accelerations $\underline{\alpha}_j$ for each of the bodies of the spatial parallel

manipulator system are given in Chapters 3 and 4. Equation (1) can now be written as

$$\sum_{j=1}^{w} (\frac{\partial \mathbf{V}_j}{\partial u_k} \cdot \mathbf{F}_j') + \sum_{j=1}^{w} (\frac{\partial \omega_j}{\partial u_k} \cdot \mathbf{T}_j') = 0; \quad k = 1, 2, ..., n \tag{37}$$

The force term is known as the effective force, $\mathbf{F}'_j$; the torque term is known as the effective torque, $\mathbf{T}'_j$.

5.5.1 Formulating the Dynamic Model

The spatial parallel manipulator system has 19 bodies (the platform and three bodies for each connector) and 24 degrees of freedom (w = 19 & n = 24). By using the above expression, the model of the spatial platform can be generated. This model has 24

equations. The general form of the kth equation of motion for the spatial platform is

$$\sum_{i=1}^{6} \left[\left(\frac{(\partial \mathbf{V}_e)_i}{\partial u_k} \cdot (\mathbf{F}'_e)_i \right) + \left(\frac{(\partial \omega_{12})_i}{\partial u_k} \cdot (\mathbf{T}'_e)_i \right) \right] +$$

$$\sum_{i=1}^{6} \left[\left(\frac{(\partial \mathbf{V}_d)_i}{\partial u_k} \cdot (\mathbf{F}'_d)_i \right) + \left(\frac{(\partial \omega_{12})_i}{\partial u_k} \cdot (\mathbf{T}'_d)_i \right) \right] +$$

$$\sum_{i=1}^{6} \left[\left(\frac{(\partial \mathbf{V}_b)_i}{\partial u_k} \cdot (\mathbf{F}'_b)_i \right) + \left(\frac{(\partial \omega_{12})_i}{\partial u_k} \cdot (\mathbf{T}'_b)_i \right) \right] +$$

$$\left[\frac{\partial \mathbf{V}_c}{\partial u_k} \cdot \mathbf{F}'_c + \frac{\partial \omega}{\partial u_k} \cdot \mathbf{T}'_c \right] = 0 \qquad (38)$$

where the letter "i" designates the ith connector ($i = 1$ to 6). The first six terms of this equation describe the motion of the mass M_e, the second six terms describe the motion of the mass M_d, the third six terms describe the motion of the mass M_b, and the last term describes the motion of the platform itself.

Although the use of equation (38) for setting up the model may seem to be very time consuming and tedious, it becomes rather simple since many of the velocity and angular velocity partial derivatives are zero. For the first degrees of freedom of each connector (6 dof in total) all the velocity and angular velocity partial derivatives are zero except the velocity partial derivative of the velocity vector $\mathbf{V}_e$ as indicated in equation (32). The equation of motion for the first degree of freedom of each connector, which generates the first six equations of motion, can be written as

$$\left(\frac{(\partial \mathbf{V}_e)_i}{\partial u_k} \cdot (\mathbf{F}'_e)_i \right) = 0; \quad \text{for } i = 1 \text{ to } 6 \qquad (39)$$

The equations of motion for the second degree of freedom of each connector is zero since the effective forces for this degree of freedom are zero (there is no mass at the point

of displacement H). This is a problem since the dynamic model requires 24 equations. This problem will solved by defining some auxiliary equations later.

For the third degree of freedom of each connector, all the velocity and angular velocity partial derivatives are zero except the velocity partial derivatives of the velocity vector $\underline{V}_d$ as indicated in equation (31). The equations of motion for this degrees of freedom, which generates the next six equations of motion, is given by

$$\left(\frac{(\partial \underline{V}_d)_i}{\partial u_k} \cdot \left(\underline{F}'_d \right)_i \right) = 0; \quad \text{for } i = 1 \text{ to } 6 \tag{40}$$

The equations of motion for the last degrees of freedom are more complicated since most of the velocity and angular velocity partial derivatives are not zero as was the case in the connector degrees of freedom. The general equation of motion for the last six degrees of freedom, which describes the translation and rotation of the platform about the X, Y, Z axes is given by (for k = 19 to 24)

$$\sum_{i=1}^{6} \left(\frac{(\partial \underline{V}_e)_i}{\partial u_k} \cdot \left(\underline{F}'_e \right)_i \right) + \sum_{i=1}^{6} \left(\frac{(\partial \underline{V}_d)_i}{\partial u_k} \cdot \left(\underline{F}'_d \right)_i \right) + \sum_{i=1}^{6} \left(\frac{(\partial \underline{V}_b)_i}{\partial u_k} \cdot \left(\underline{F}'_b \right)_i \right) +$$

$$\sum_{i=1}^{6} \left[\frac{(\partial \underline{\omega}_{12})_i}{\partial u_k} \cdot \left(\underline{T}'_e + \underline{T}'_d + \underline{T}'_b \right)_i \right] + \frac{\partial \underline{V}_c}{\partial u_k} \cdot \underline{F}'_c + \frac{\partial \underline{\omega}}{\partial u_k} \cdot \underline{T}'_c = 0$$

Since the velocity partial derivatives of $\underline{\omega}$ for the Generalized Speeds u_{19}, u_{20} and u_{21} are zero, the general equation of motion for the translation of the platform can be written as (for k = 19 to 21)

$$\sum_{i=1}^{6} \left(\frac{(\partial \underline{V}_e)_i}{\partial u_k} \cdot \left(\underline{F}'_e \right)_i \right) + \sum_{i=1}^{6} \left(\frac{(\partial \underline{V}_d)_i}{\partial u_k} \cdot \left(\underline{F}'_d \right)_i \right) + \sum_{i=1}^{6} \left(\frac{(\partial \underline{V}_b)_i}{\partial u_k} \cdot \left(\underline{F}'_b \right)_i \right) +$$

$$\sum_{i=1}^{6} \left[\frac{(\partial \underline{\omega}_{12})_i}{\partial u_k} \cdot \left(\underline{T}'_e + \underline{T}'_d + \underline{T}'_b \right)_i \right] + \frac{\partial \underline{V}_c}{\partial u_k} \cdot \underline{F}'_c = 0 \tag{41}$$

Since the velocity partial derivatives of $\underline{V}_c$ for the Generalized Speeds u_{22}, u_{23} and u_{24} are zero, the general equation of motion for the translation of the platform can be written as (for $k = 22$ to 24)

$$\sum_{i=1}^{6} \left(\frac{(\partial \underline{V}_e)_i}{\partial u_k} \cdot \left(\underline{F}'_e \right)_i \right) + \sum_{i=1}^{6} \left(\frac{(\partial \underline{V}_d)_i}{\partial u_k} \cdot \left(\underline{F}'_d \right)_i \right) + \sum_{i=1}^{6} \left(\frac{(\partial \underline{V}_b)_i}{\partial u_k} \cdot \left(\underline{F}'_b \right)_i \right) +$$

$$\sum_{i=1}^{6} \left[\frac{(\partial \underline{\omega}_{12})_i}{\partial u_k} \cdot \left(\underline{T}'_e + \underline{T}'_d + \underline{T}'_b \right)_i \right] + \frac{\partial \underline{\omega}}{\partial u_k} \cdot \underline{T}'_c = 0 \qquad (42)$$

5.5.2 Effective Forces

The difference between the resultant force acting on a given body, $\underline{F}_j$, and its inertial force, $m_j \underline{A}_j$, is known as the effective force, $\underline{F}'_j$. The resultant forces acting on each bodies of the spatial manipulator were derived in Chapter 4, the accelerations for each body were derived in Chapter 3. The effective forces for the platform and the bodies on each connector are given by

$$\underline{F}'_e = \underline{F}_e - M_e \underline{A}_e \qquad (43)$$

$$\underline{F}'_d = \underline{F}_d - M_d \underline{A}_d \qquad (44)$$

$$\underline{F}'_b = \underline{F}_b - M_b \underline{A}_b \qquad (45)$$

$$\underline{F}'_c = \underline{F}_c - M_p \underline{A}_c \qquad (46)$$

These equations can expanded using the expressions for the resultant forces and accelerations derived in Sections 4.6 and 3.5 respectively

$$\underline{F}'_e = \left[F_a - C_t \dot{E} - K_L \delta_L \right] \underline{s}_3 - \left[M_e g \right] \underline{k} -$$

$$M_e \ddot{E} \underline{s}_3 - 2 M_e \dot{E} \left(\omega_1 \underline{s}_2 + \omega_2 \underline{s}_{23} \right) - M_e E \left(\alpha_1 \underline{s}_2 + \alpha_2 \underline{s}_{23} \right) -$$

$$M_e E\left(2\omega_1 \omega_2(\underline{s}_1 \cdot \underline{s}_3)\underline{s}_2 + \omega_1^2(\underline{s}_1 \cdot \underline{s}_3)\underline{s}_1 - \left(\omega_1^2 + \omega_2^2\right)\underline{s}_3 \right) \quad (47)$$

$$\underline{F}'_d = \left[-C_d(\dot{D} - \dot{L}) - K_d \delta_d \right] \underline{s}_3 - \left[M_d g \right] \underline{k} -$$

$$M_d \ddot{D}\, \underline{s}_3 - 2 M_d \dot{D}\left(\omega_1 \underline{s}_2 + \omega_2 \underline{s}_{23} \right) - M_d D\left(\alpha_1 \underline{s}_2 + \alpha_2 \underline{s}_{23} \right) -$$

$$M_d D\left(2\omega_1 \omega_2(\underline{s}_1 \cdot \underline{s}_3)\underline{s}_2 + \omega_1^2(\underline{s}_1 \cdot \underline{s}_3)\underline{s}_1 - \left(\omega_1^2 + \omega_2^2\right)\underline{s}_3 \right) \quad (48)$$

$$\underline{F}'_b = \left[C_t \dot{E}_i - F_r \right] \underline{s}_3 - \left[M_b g \right] \underline{k} - M_b bl\left(\alpha_1 \underline{s}_2 + \alpha_2 \underline{s}_{23} \right) -$$

$$M_b bl\left(2\omega_1 \omega_2(\underline{s}_1 \cdot \underline{s}_3)\underline{s}_2 + \omega_1^2(\underline{s}_1 \cdot \underline{s}_3)\underline{s}_1 - \left(\omega_1^2 + \omega_2^2\right)\underline{s}_3 \right) \quad (49)$$

$$\underline{F}'_c = \left[\underline{F}_g + \underline{F}_{ext} + \sum_{i=1}^{6} F_1 \underline{s}_3 \right] - M_p \underline{A}_c \quad (50)$$

5.5.3 Effective Torques

The difference between the resultant torque acting on a given body, $\underline{T}_j$, and its inertial torque, $m_j \underline{A}_j$, is known as the effective torque, $\underline{T}'_j$. The resultant torques acting on each body of the spatial manipulator were derived in Sections 4.4 and 4.5, the angular velocities and accelerations for each body were derived in Section 3.4 and 3.5. The effective torques for the platform and the bodies on each connector are given by

$$\underline{T}'_e = \underline{T}_e - \left[\underline{\alpha}_{12} \cdot \mathbf{Ie}'' + \underline{\omega}_{12} \times \mathbf{Ie}'' \cdot \underline{\omega}_{12} \right] \quad (51)$$

$$\underline{T}'_d = \underline{T}_d - \left[\underline{\alpha}_{12} \cdot \mathbf{Id}'' + \underline{\omega}_{12} \times \mathbf{Id}'' \cdot \underline{\omega}_{12} \right] \quad (52)$$

$$\underline{T}'_b = \underline{T}_b - \left[\underline{\alpha}_{12} \cdot \mathbf{Ib}'' + \underline{\omega}_{12} \times \mathbf{Ib}'' \cdot \underline{\omega}_{12} \right] \quad (53)$$

$$\mathbf{T}'_c = \left[\mathbf{T}_{ext} + \sum_{i=1}^{6} F_l \, \underline{S}_{o3} \right] - \left[\underline{\alpha} \cdot \mathbf{Ip}^{\text{"}} + \underline{\omega} \times \mathbf{Ip}^{\text{"}} \cdot \underline{\omega} \right] \qquad (54)$$

where Ie", Id", Ib" and Ip" are the body inertia dyadics (see the appendix).

5.5.4 Inertia Dyadics

The inertial properties of a rigid body in space are usually described using the inertia tensor. A more compact and useful method is the inertia dyadic [27]. A dyadic is a juxtaposition of vectors, a inertia dyadic is the use of a dyadic to describe the inertia of a rigid body. The inertia dyadic for a body can be defined in term of its principal axes and principal inertias, as explained in detail in the appendix. The principal axes $\underline{S}_{23}$, $\underline{S}_2$ and $\underline{S}_3$ for each of the rigid bodies on the connector are shown in figure 5.3. The inertia dyadic for the base inertia, decoupling stage inertia and the actuator inertia are given by

$$\mathbf{Ib}^{\text{"}} = \mathbf{Ib}_{xx} \left[\underline{S}_{23} \right] \left[\underline{S}_{23} \right] + \mathbf{Ib}_{yy} \left[\underline{S}_2 \right] \left[\underline{S}_2 \right] + \mathbf{Ib}_{zz} \left[\underline{S}_3 \right] \left[\underline{S}_3 \right] \qquad (55)$$

$$\mathbf{Id}^{\text{"}} = \mathbf{Id}_{xx} \left[\underline{S}_{23} \right] \left[\underline{S}_{23} \right] + \mathbf{Id}_{yy} \left[\underline{S}_2 \right] \left[\underline{S}_2 \right] + \mathbf{Id}_{zz} \left[\underline{S}_3 \right] \left[\underline{S}_3 \right] \qquad (56)$$

$$\mathbf{Ie}^{\text{"}} = \mathbf{Ie}_{xx} \left[\underline{S}_{23} \right] \left[\underline{S}_{23} \right] + \mathbf{Ie}_{yy} \left[\underline{S}_2 \right] \left[\underline{S}_2 \right] + \mathbf{Ie}_{zz} \left[\underline{S}_3 \right] \left[\underline{S}_3 \right] \qquad (57)$$

where $\mathbf{Ie}_{xx}$, $\mathbf{Id}_{xx}$, $\mathbf{Ib}_{xx}$, $\mathbf{Ie}_{yy}$, $\mathbf{Id}_{yy}$, $\mathbf{Ib}_{yy}$, $\mathbf{Ie}_{zz}$, $\mathbf{Id}_{zz}$ and $\mathbf{Ib}_{zz}$ are the principal moments of inertia of the connector rigid bodies. The inertia dyadic for the platform is given by

$$\mathbf{Ip}^{\text{"}} = \mathbf{Ip}_{xx} \left[\underline{X}_m \right] \left[\underline{X}_m \right] + \mathbf{Ip}_{yy} \left[\underline{Y}_m \right] \left[\underline{Y}_m \right] + \mathbf{Ip}_{zz} \left[\underline{Z}_m \right] \left[\underline{Z}_m \right] \qquad (58)$$

where $\mathbf{Ip}_{xx}$, $\mathbf{Ip}_{yy}$ and $\mathbf{Ip}_{zz}$ are the principal moments of inertia of the platform.
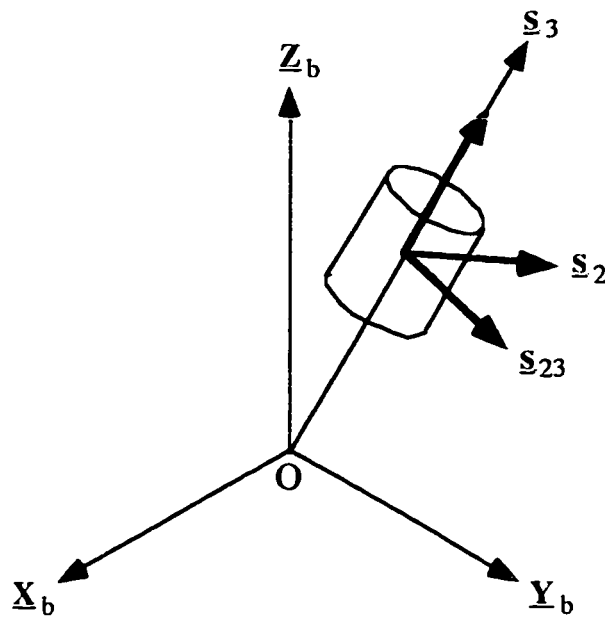
Figure 5.3 - Principal Axes

5.6 Deriving the Equations of Motion

The dynamic model of the platform system is described by 24 equations of motions. These equations are obtained by using equation (1) for each of the degrees of freedom of the system.

5.6.1 Equation of Motion for the mass M_e

The equation of motion for the mass M_e can be obtained by using equations (32), (39) and (47)

$$\left(\frac{(\partial \underline{V}_e)_i}{\partial u_k} \cdot \left(\underline{F}'_e \right)_i \right) = \left(\left[F_a - C_t \dot{E} - K_1 \delta_1 \right] \underline{s}_3 - \left[M_e g \right] \underline{k} \right) \cdot \underline{s}_3$$

$$\left(- M_e \ddot{E} \underline{s}_3 - 2 M_e \dot{E} \left(\omega_1 \underline{s}_2 + \omega_2 \underline{s}_{23} \right) - M_e E \left(\alpha_1 \underline{s}_2 + \alpha_2 \underline{s}_{23} \right) \right) \cdot \underline{s}_3 +$$

$$\left(- M_e E \left(2 \omega_1 \omega_2 \left(\underline{s}_1 \cdot \underline{s}_3 \right) \underline{s}_2 + \omega_1^2 \left(\underline{s}_1 \cdot \underline{s}_3 \right) \underline{s}_1 - \left(\omega_1^2 + \omega_2^2 \right) \underline{s}_3 \right) \right) \cdot \underline{s}_3 = 0$$

Figure 5.4 - Hooke Joint at the base of the connector

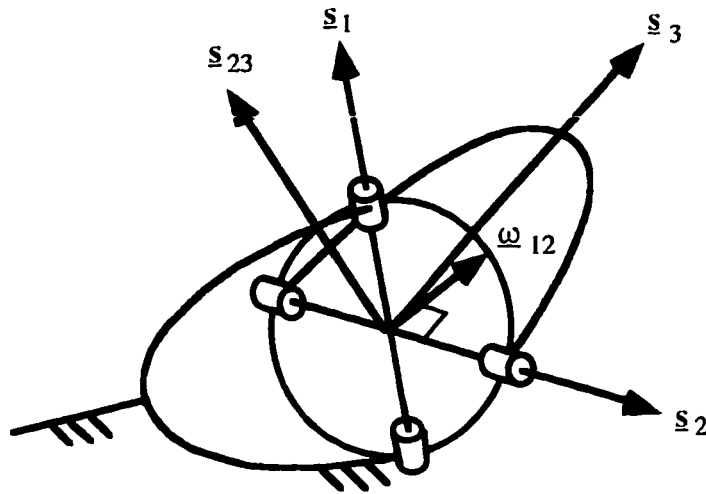As mentioned in Sections 3.3 and 3.4 the vector $\underline{s}_1$, which has been selected to be parallel to the fixed $\underline{X}$ axis, describes the first axis of the Hooke joint of the HPS serial manipulator (see Figure 5.4). The vector $\underline{s}_2$ describes the second axis of the Hooke joint and is the resultant of the vector product of $\underline{s}_1$ and $\underline{s}_3$. The vector $\underline{s}_3$ is parallel to the connector itself and $\underline{s}_{23}$ is the resultant of the vector product of $\underline{s}_2$ and $\underline{s}_3$. The evaluation of all the equations of motion will required the following scalar products

$$\underline{s}_1 \cdot \underline{s}_2 ; \quad \underline{s}_1 \cdot \underline{s}_{23} ; \quad \underline{s}_1 \cdot \underline{s}_3 ; \quad \underline{s}_2 \cdot \underline{s}_3 ; \quad \underline{s}_{23} \cdot \underline{s}_3 ; \quad \underline{s}_{23} \cdot \underline{s}_2$$

Since the vectors $\underline{s}_1$ and $\underline{s}_2$ are perpendicular, and $\underline{s}_2 , \underline{s}_3$,and $\underline{s}_{23}$ are mutually perpendicular the following scalar products zero

$$\underline{s}_2 \cdot \underline{s}_3 = 0; \quad \underline{s}_{23} \cdot \underline{s}_3 = 0; \quad \underline{s}_{23} \cdot \underline{s}_2 = 0; \quad \underline{s}_1 \cdot \underline{s}_2 = 0 \qquad (59)$$

Since the vector $\underline{s}_1$ is parallel to the $\underline{X}$ axis, the remaining scalar products are

$$\underline{s}_1 \cdot \underline{s}_{23} = s_{23x} ; \quad \underline{s}_1 \cdot \underline{s}_3 = s_{3x} \qquad (60)$$

By using equations (59) and (60), the equation of motion for M_e can be simplified to

$$F_a = M_e \left[\ddot{E} + g \, s_{3z} + E \omega_1^2 (s_{3x})^2 - E \left(\omega_1^2 + \omega_2^2 \right) \right] + C_t \dot{E} + K_L \delta_L \quad (61)$$

The first term on the right hand side indicates that the actuator has to accelerate the mass M_e. This acceleration is the sum of the body's own acceleration, the gravitational acceleration and the centrifugal acceleration. The actuator also has to move against the friction force its generates and has to deform the K_L spring.

5.6.2 Equation of Motion for the mass M_d

The equation of motion for the mass M_d can be obtained using equations (31), (40) and (49)

$$\left(\frac{(\partial \underline{V}_d)_i}{\partial u_k} \cdot \left(\underline{F}_d' \right)_i \right) = \left(\left[- C_d (\dot{D} - \dot{L}) - K_d \delta_d \right] \underline{s}_3 - \left[M_d g \, \underline{k} \right) \cdot \underline{s}_3 + \right.$$

$$\left(- M_d \ddot{D} \, \underline{s}_3 - 2 M_d \dot{D} (\omega_1 \underline{s}_2 + \omega_2 \underline{s}_{23}) - M_d D (\alpha_1 \underline{s}_2 + \alpha_2 \underline{s}_{23}) \right) \cdot \underline{s}_3 +$$

$$\left(- M_d D \left(2 \omega_1 \omega_2 (\underline{s}_1 \cdot \underline{s}_3) \underline{s}_2 + \omega_1^2 (\underline{s}_1 \cdot \underline{s}_3) \underline{s}_1 - (\omega_1^2 + \omega_2^2) \underline{s}_3 \right) \right) \cdot \underline{s}_3 = 0$$

Using the equations (59) and (60), this equation can be simplified to

$$M_d \left[\ddot{D} + g \, s_{3z} + D \omega_1^2 (s_{3x})^2 - D \left(\omega_1^2 + \omega_2^2 \right) \right] + C_d (\dot{D} - \dot{L}) + K_d \delta_d = 0 \quad (62)$$

Although the decoupling stage does not have an actuator to move its mass, the energy is supplied by external sources such as the rotation of the connector which produce the centrifugal terms and the extension of the decoupling damper. These forces move the decoupling stage against gravity , accelerate the decoupling stage mass, and move the decoupling stage mass against its friction and stiffness element .

5.6.3 Platform Equations of Motion

The platform equations of motion can be divided into two types: those that produce the translation of the platform and those that produce the rotation of the platform. The general forms of the platform equations of motion are given by equations (41) and (42). Equation (41) must be evaluated for the generalized speed u_{19}, u_{20} and u_{21}; and equation (42) must be evaluated for the generalized speed u_{22}, u_{23} and u_{24}.

5.6.3.1 Translation along the X, Y and Z axes

The general equation of motion for the translation of the platform along the X Y and Z axes is given by (k =19, 20 and 21)

$$\sum_{i=1}^{6} \left(\frac{(\partial \underline{V}_e)_i}{\partial u_k} \cdot \left(\underline{F}'_e \right)_i \right) + \sum_{i=1}^{6} \left(\frac{(\partial \underline{V}_d)_i}{\partial u_k} \cdot \left(\underline{F}'_d \right)_i \right) + \sum_{i=1}^{6} \left(\frac{(\partial \underline{V}_d)_i}{\partial u_k} \cdot \left(\underline{F}'_d \right)_i \right) +$$

$$\sum_{i=1}^{6} \left[\frac{(\partial \underline{\omega}_{12})_i}{\partial u_k} \cdot \left(\underline{T}'_e + \underline{T}'_d + \underline{T}'_b \right)_i \right] + \frac{\partial \underline{V}_c}{\partial u_k} \cdot \underline{F}'_c = 0 \tag{63}$$

The first three terms of the above equation can be evaluated using equations (24), (25) and (26) for the velocity partial derivatives with respect to the generalized speeds u_{19}, u_{20} and u_{21}. These velocity partial derivatives have the following general forms

$$\frac{\partial \underline{V}_b}{\partial u_k} = \frac{bl}{L} [U_k \underline{S}_2 + Q_k \underline{S}_{23}]$$

$$\frac{\partial \underline{V}_d}{\partial u_k} = \frac{D}{L} [U_k \underline{S}_2 + Q_k \underline{S}_{23}]$$

$$\frac{\partial \underline{V}_e}{\partial u_k} = \frac{E}{L} [U_k \underline{S}_2 + Q_k \underline{S}_{23}]$$

where $U_{19} = s_{2x}$, $U_{20} = s_{2y}$, $U_{21} = s_{2z}$ and $Q_{19} = s_{23x}$, $Q_{20} = s_{23y}$, $Q_{21} = s_{23z}$.

Using these general forms for the velocity partial derivatives, the first three terms of equation (63) can be expanded to

$$\sum_{i=1}^{6} \left(\frac{(\partial \underline{V}_e)_i}{\partial u_k} \cdot \left(\underline{F}'_e \right)_i \right) + \sum_{i=1}^{6} \left(\frac{(\partial \underline{V}_d)_i}{\partial u_k} \cdot \left(\underline{F}'_d \right)_i \right) + \sum_{i=1}^{6} \left(\frac{(\partial \underline{V}_b)_i}{\partial u_k} \cdot \left(\underline{F}'_b \right)_i \right) =$$

$$\sum_{i=1}^{6} \left(\left[F_a - C_t \dot{E} - K_L \delta_L \right] \underline{s}_3 - \left[M_e g \right] \underline{k} \right) \cdot \frac{E}{L} \left[U_k \underline{s}_2 + Q_k \underline{s}_{23} \right] +$$

$$\sum_{i=1}^{6} \left(- M_e \ddot{E} \, \underline{s}_3 - 2 M_e \dot{E} \left(\omega_1 \underline{s}_2 + \omega_2 \underline{s}_{23} \right) \right) \cdot \frac{E}{L} \left[U_k \underline{s}_2 + Q_k \underline{s}_{23} \right] +$$

$$\sum_{i=1}^{6} - M_e E \left(\alpha_1 \underline{s}_2 + \alpha_2 \underline{s}_{23} + 2 \omega_1 \omega_2 (\underline{s}_1 \cdot \underline{s}_3) \underline{s}_2 \right) \cdot \frac{E}{L} \left[U_k \underline{s}_2 + Q_k \underline{s}_{23} \right] +$$

$$\sum_{i=1}^{6} \left(- M_e E \left(\omega_1^2 (\underline{s}_1 \cdot \underline{s}_3) \underline{s}_1 - \left(\omega_1^2 + \omega_2^2 \right) \underline{s}_3 \right) \right) \cdot \frac{E}{L} \left[U_k \underline{s}_2 + Q_k \underline{s}_{23} \right] +$$

$$\sum_{i=1}^{6} \left(\left[- C_d (\dot{D} - \dot{L}) - K_d \delta_d \right] \underline{s}_3 - \left[M_d g \right] \underline{k} \right) \cdot \frac{D}{L} \left[U_k \underline{s}_2 + Q_k \underline{s}_{23} \right] +$$

$$\sum_{i=1}^{6} \left(- M_d \ddot{D} \, \underline{s}_3 - 2 M_d \dot{D} \left(\omega_1 \underline{s}_2 + \omega_2 \underline{s}_{23} \right) \right) \cdot \frac{D}{L} \left[U_k \underline{s}_2 + Q_k \underline{s}_{23} \right] +$$

$$\sum_{i=1}^{6} - M_d D \left(\alpha_1 \underline{s}_2 + \alpha_2 \underline{s}_{23} + 2 \omega_1 \omega_2 (\underline{s}_1 \cdot \underline{s}_3) \underline{s}_2 \right) \cdot \frac{D}{L} \left[U_k \underline{s}_2 + Q_k \underline{s}_{23} \right] +$$

$$\sum_{i=1}^{6} \left(- M_d D \left(\omega_1^2 (\underline{s}_1 \cdot \underline{s}_3) \underline{s}_1 - \left(\omega_1^2 + \omega_2^2 \right) \underline{s}_3 \right) \right) \cdot \frac{D}{L} \left[U_k \underline{s}_2 + Q_k \underline{s}_{23} \right] +$$

$$\sum_{i=1}^{6} \left(\left[C_t \dot{E} - F_r \right] \underline{s}_3 - \left[M_b g \right] \underline{k} \right) \cdot \frac{bl}{L} \left[U_k \underline{s}_2 + Q_k \underline{s}_{23} \right] +$$

$$\sum_{i=1}^{6} - M_b bl \left(\alpha_1 \underline{s}_2 + \alpha_2 \underline{s}_{23} + 2 \omega_1 \omega_2 (\underline{s}_1 \cdot \underline{s}_3) \underline{s}_2 \right) \cdot \frac{bl}{L} \left[U_k \underline{s}_2 + Q_k \underline{s}_{23} \right] +$$

$$\sum_{i=1}^{6} \left(- M_b bl \left(\omega_1^2 (\underline{s}_1 \cdot \underline{s}_3) \underline{s}_1 - \left(\omega_1^2 + \omega_2^2 \right) \underline{s}_3 \right) \right) \cdot \frac{bl}{L} \left[U_k \underline{s}_2 + Q_k \underline{s}_{23} \right]$$

As given by equation (59), the above equation can be simplified considerably by the fact that many of the scalar products required for its evaluation are zero

$$\underline{s}_2 \cdot \underline{s}_3 = \underline{s}_{23} \cdot \underline{s}_3 = \underline{s}_{23} \cdot \underline{s}_2 = \underline{s}_1 \cdot \underline{s}_2 = 0;$$

The equation of motion can then be written as

$$\sum_{i=1}^{6} - g \left[\frac{[M_e E + M_d D + M_b bl]}{L} \left[U_k s_{2z} + Q_k s_{23z} \right] \right]_i -$$

$$\sum_{i=1}^{6} \left[\frac{2 [M_e \dot{E} E + M_d \dot{D} D]}{L} \left[U_k \omega_1 + Q_k \omega_2 \right] \right]_i -$$

$$\sum_{i=1}^{6} \left[\frac{[M_e E^2 + M_d D^2 + M_b bl^2]}{L} \left[U_k \alpha_1 + Q_k \alpha_2 \right] \right]_i -$$

$$\sum_{i=1}^{6} \left[\frac{[M_e E^2 + M_d D^2 + M_b bl^2]}{L} 2 U_k \omega_1 \omega_2 s_{3x} \right]_i +$$

$$\sum_{i=1}^{6} \left[\frac{[M_e E^2 + M_d D^2 + M_b bl^2]}{L} Q_k \omega_1^2 s_{3x} s_{23x} \right]_i \qquad (64)$$

The fourth term of equation (63) can be evaluated by using equations (17), (18) and (19) for the angular velocity partial derivatives with respect to the generalized speeds u_{19}, u_{20} and u_{21}. These angular velocity partial derivatives have the following general form

$$\frac{\partial \underline{\omega}_{12}}{\partial u_k} = \frac{1}{L}[\ U_k \underline{s}_1 + Q_k \underline{s}_2]$$

where $U_{19} = s_{2x}$, $U_{20} = s_{2y}$, $U_{21} = s_{2z}$ and $Q_{19} = s_{23x}$, $Q_{20} = s_{23y}$, $Q_{21} = s_{23z}$

Using the expression for the effective torques given in equations (51), (52), and (53), the fourth term of equation (61) can be written as

$$\sum_{i=1}^{6} \left[\frac{(\partial \underline{\omega}_{12})_i}{\partial u_k} \cdot \left(\underline{T}'_e + \underline{T}'_d + \underline{T}'_b \right)_i \right] =$$

$$\sum_{i=1}^{6} \frac{(\partial \underline{\omega}_{12})_i}{\partial u_k} \cdot \left[-\left[(\underline{\alpha}_{12})_i \cdot (\underline{II}'')_i + (\underline{\omega}_{12})_i \times (\underline{II}'')_i \cdot (\underline{\omega}_{12})_i \right] \right]$$

where II'' is the sum of all the mass dyadics of the rigid bodies on the connector. Using equations (55), (56) and (57) and the generalized form of the angular velocity partial derivative, the above equation can be expanded to

$$\sum_{i=1}^{6} -II_{xx}\left((\underline{\alpha}_{12})_i \cdot (\underline{s}_{23})_i \right)\left((\underline{s}_{23})_i \cdot \left(\frac{U_k \underline{s}_1 + Q_k \underline{s}_2}{L} \right)_i \right) -$$

$$\sum_{i=1}^{6} II_{xx}\left[\left(\frac{U_k \underline{s}_1 + Q_k \underline{s}_2}{L} \right)_i \cdot \left((\underline{\omega}_{12})_i \times (\underline{s}_{23})_i \right) \right] \left[(\underline{s}_{23})_i \cdot (\underline{\omega}_{12})_i \right] -$$

$$\sum_{i=1}^{6} II_{yy}\left((\underline{\alpha}_{12})_i \cdot (\underline{s}_2)_i \right)\left((\underline{s}_2)_i \cdot \left(\frac{U_k \underline{s}_1 + Q_k \underline{s}_2}{L} \right)_i \right) -$$

$$\sum_{i=1}^{6} \Pi_{yy} \left[\left(\frac{U_k \underline{S}_1 + Q_k \underline{S}_2}{L} \right)_i \cdot \left((\underline{\omega}_{12})_i \times (\underline{S}_2)_i \right) \right] \left[(\underline{S}_2)_i \cdot (\underline{\omega}_{12})_i \right]$$

$$\sum_{i=1}^{6} \Pi_{zz} \left((\underline{\alpha}_{12})_i \cdot (\underline{S}_3)_i \right) \left((\underline{S}_3)_i \cdot \left(\frac{U_k \underline{S}_1 + Q_k \underline{S}_2}{L} \right)_i \right) -$$

$$\sum_{i=1}^{6} \Pi_{zz} \left[\left(\frac{U_k \underline{S}_1 + Q_k \underline{S}_2}{L} \right)_i \cdot \left((\underline{\omega}_{12})_i \times (\underline{S}_3)_i \right) \right] \left[(\underline{S}_3)_i \cdot (\underline{\omega}_{12})_i \right]$$

The principal moments of inertia of the rigid bodies about the X and Y axes are equal. By using equation (59), which states that many of the scalar products required for evaluating the above equation are zero, this part of the equation of motion can be simplified to

$$-\sum_{i=1}^{6} \left[U_k \left(\frac{\alpha_1}{L} \left(\Pi_{zz} s_{3x}^2 + \Pi_{xx} s_{23x}^2 \right) + \frac{2\omega_1 \omega_2 s_{23x} s_{3x}}{L} (\Pi_{zz} - \Pi_{xx}) \right) \right]_i -$$

$$\sum_{i=1}^{6} \left[Q_k \frac{\alpha_2}{L} \Pi_{xx} \right]_i - \sum_{i=1}^{6} \left[Q_k \frac{\omega_1^2}{L} s_{23y} s_{3x} (\Pi_{xx} - \Pi_{zz}) \right]_i \qquad (65)$$

Using equation (50) and the fact that the platform angular velocity partial derivatives for the generalized speeds u_{19}, u_{20}, and u_{21} are zero, the last term of the general equation of motion can be written as

$$\frac{\partial \underline{V}_c}{\partial u_k} \cdot \left[\underline{F}_g + \underline{F}_{ext} + \sum_{i=1}^{6} (F_1 \underline{S}_3)_i - M_p \underline{A}_c \right]$$

The equation of motion for translation along the X axis is given by (k = 19,
$U_{19} = s_{2x}$ and $Q_{19} = s_{23x}$)

$$\sum_{i=1}^{6} (F_L s_{3x})_i = M_p A_{cx} + F_{ext,\, x} +$$

$$\sum_{i=1}^{6} g\left[\frac{\left[M_e E + M_d D + M_b bl\right]}{L}\left[s_{23x}\, s_{23z}\right]\right]_i +$$

$$\sum_{i=1}^{6} \left[\frac{2\left[M_e \dot{E} E + M_d \dot{D} D\right]}{L}\, s_{23x}\, \omega_2\right]_i +$$

$$\sum_{i=1}^{6} \left[\frac{\left[M_e E^2 + M_d D^2 + M_b bl^2\right]}{L}\, s_{23x}\, \alpha_2\right]_i +$$

$$\sum_{i=1}^{6} \left[\frac{\left[M_e E^2 + M_d D^2 + M_b bl^2\right]}{L}\, \omega_1^2\, s_{3x}\, s_{23x}^2\right]_i +$$

$$\sum_{i=1}^{6} \left[s_{23x}\, s_{3x}\frac{\omega_1^2}{L}\left(II_{xx} - II_{zz}\right)\right]_i + \sum_{i=1}^{6} \left[s_{23x}\frac{\alpha_2}{L}\, II_{xx}\right]_i \qquad (66)$$

Analogously, the equation of motion along the Y axis can be written as ($k = 20$,
$U_{20} = s_{2y}$ and $Q_{20} = s_{23y}$)

$$\sum_{i=1}^{6} \left(F_L\, s_{3y}\right)_i = M_p A_{cy} + F_{ext,\, y} +$$

$$\sum_{i=1}^{6} g\left[\frac{\left[M_e E + M_d D + M_b bl\right]}{L}\left[s_{2y}\, s_{2z} + s_{23y}\, s_{23z}\right]\right]_i +$$

$$\sum_{i=1}^{6} \left[\frac{2\left[M_e \dot{E} E + M_d \dot{D} D\right]}{L}\left[s_{2y}\, \omega_1 + s_{23y}\, \omega_2\right]\right]_i +$$

$$\sum_{i=1}^{6} \left[\frac{\left[M_e E^2 + M_d D^2 + M_b bl^2\right]}{L}\left[s_{2y}\, \alpha_1 + s_{23y}\, \alpha_2\right]\right]_i +$$

$$\sum_{i=1}^{6}\left[\left[\frac{\left[M_eE^2+M_dD^2+M_bbl^2\right]}{L}\right]\left[2\,\omega_1\,\omega_2\,s_{3x}\,s_{2y}+\omega_1^2\,s_{3x}\,s_{23x}\,s_{23y}\right]\right]_i+$$

$$\sum_{i=1}^{6}\left[s_{2y}\,\frac{\alpha_1}{L}\left(\Pi_{zz}\,s_{3x}^2+\Pi_{xx}\,s_{23x}^2\right)\right]_i+\sum_{i=1}^{6}\left[s_{23y}\,\frac{\alpha_2}{L}\,\Pi_{xx}\right]_i+$$

$$\sum_{i=1}^{6}\left[2s_{2y}\,\frac{\omega_1\,\omega_2\,s_{23x}\,s_{3x}}{L}\,\left(\Pi_{zz}-\Pi_{xx}\right)\right]_i+$$

$$\sum_{i=1}^{6}\left[s_{23y}s_{3x}\,\frac{\omega_1^2}{L}\left(\Pi_{xx}-\Pi_{zz}\right)\right]_i \tag{67}$$

Analogously, the equation of motion along the Z axis can be written as

$$\sum_{i=1}^{6}\left(F_L\,s_{3z}\right)_i = M_pA_{cz}+M_pg+F_{ext,z}+$$

$$\sum_{i=1}^{6}g\left[\frac{\left[M_eE+M_dD+M_bbl\right]}{L}\left[s_{2z}^2+s_{23z}^2\right]\right]_i+$$

$$\sum_{i=1}^{6}\left[\frac{2\left[M_e\dot{E}E+M_d\dot{D}D\right]}{L}\left[s_{2z}\omega_1+s_{23z}\omega_2\right]\right]_i+$$

$$\sum_{i=1}^{6}\left[\frac{\left[M_eE^2+M_dD^2+M_bbl^2\right]}{L}\left[s_{2z}\alpha_1+s_{23z}\alpha_2\right]\right]_i+$$

$$\sum_{i=1}^{6}\left[\frac{\left[M_eE^2+M_dD^2+M_bbl^2\right]}{L}\left[2\,\omega_1\,\omega_2\,s_{3x}\,s_{2z}+\omega_1^2\,s_{3x}\,s_{23x}\,s_{23z}\right]\right]_i+$$

$$\sum_{i=1}^{6} \left[s_{2z} \frac{\alpha_1}{L} \left(\Pi_{zz} s_{3x}^2 + \Pi_{xx} s_{23x}^2 \right) \right]_i + \sum_{i=1}^{6} \left[s_{23z} \frac{\alpha_2}{L} \Pi_{xx} \right]_i +$$

$$\sum_{i=1}^{6} \left[2 s_{2z} \frac{\omega_1 \omega_2 s_{23x} s_{3x}}{L} \left(\Pi_{zz} - \Pi_{xx} \right) \right]_i +$$

$$\sum_{i=1}^{6} \left[s_{23z} s_{3x} \frac{\omega_1^2}{L} \left(\Pi_{xx} - \Pi_{zz} \right) \right]_i \tag{68}$$

Using the fact that the coefficients U_k and Q_k are the components of the vectors $\underline{s}_2$ and $\underline{s}_{23}$, the equations of motion for the translation of the platform along the X, Y and Z axes can be combined into a single vector equation

$$\sum_{i=1}^{6} \left(F L \underline{s}_3 \right)_i = M_p \left(\underline{A}_c + g\underline{k} \right) + \underline{F}_{ext} + \underline{F}_{gr} + \underline{F}_{tan} + \underline{F}_{cor} + \underline{F}_{centr} \tag{69}$$

where the vector $\underline{F}_{gr}$, the connector gravitational force vector, describes the forces applied to the platform by the gravitational acceleration acting on the masses M_e, M_d and M_b

$$\underline{F}_{gr} = \sum_{i=1}^{6} \left[\frac{g \left[M_e E + M_d D + M_b bl \right]}{L} \left[s_{2z} \underline{s}_2 + s_{23z} \underline{s}_{23} \right] \right]_i \tag{69.a}$$

The connector tangential acceleration force vector, $\underline{F}_{tan}$, describes the forces applied to the platform by the angular acceleration $\underline{\alpha}_{12}$ acting on the rigid bodies of the connector

$$\underline{F}_{tan} = \sum_{i=1}^{6} \left[\frac{M_e E^2 + M_d D^2 + M_b bl^2 + \Pi_{xx} s_{23x}^2 + \Pi_{zz} s_{3x}^2}{L} \alpha_1 \underline{s}_2 \right]_i +$$

$$\sum_{i=1}^{6} \left[\frac{M_e E^2 + M_d D^2 + M_b bl^2 + II_{xx}}{L} \alpha_2 \underline{S}_{23} \right]_i \qquad (69.b)$$

The connector Coriolis acceleration force vector, $\underline{F}_{cor}$, describes the forces applied to the platform by the Coriolis acceleration acting on the rigid bodies on the connector

$$\underline{F}_{cor} = \sum_{i=1}^{6} \left[\frac{2[M_e \dot{E} E + M_d \dot{D} D]}{L} [\omega_1 \underline{S}_2 + \omega_2 \underline{S}_{23}] \right]_i \qquad (69.c)$$

The connector centrifugal acceleration force vector, $\underline{F}_{cent}$, describes the forces applied to the platform by the centrifugal acceleration acting on the rigid bodies on the connector

$$\underline{F}_{cent} = \sum_{i=1}^{6} \left[\frac{s_{3x} s_{23x} \left(M_e E^2 + M_d D^2 + M_b bl^2 \right)}{L} \omega_1^2 \underline{S}_{23} \right]_i +$$

$$\sum_{i=1}^{6} \left[\frac{2 s_{3x} \left(M_e E^2 + M_d D^2 + M_b bl^2 \right)}{L} \omega_1 \omega_2 \underline{S}_2 \right]_i +$$

$$\sum_{i=1}^{6} \left[\frac{s_{3x} s_{23x} (II_{xx} - II_{zz})}{L} \omega_1^2 \underline{S}_{23} \right]_i +$$

$$\sum_{i=1}^{6} \left[\frac{2 s_{23x} s_{3x} (II_{zz} - II_{xx})}{L} \omega_1 \omega_2 \underline{S}_2 \right]_i \qquad (69.d)$$

5.6.3.2 Rotation about the X, Y and Z axes

The general equation of motion for the rotations about the X, Y and Z axes is given by (k = 22, 23 and 24)

$$\sum_{i=1}^{6} \left(\frac{(\partial \underline{V}_e)_i}{\partial u_k} \cdot \left(\underline{F}'_e \right)_i \right) + \sum_{i=1}^{6} \left(\frac{(\partial \underline{V}_d)_i}{\partial u_k} \cdot \left(\underline{F}'_d \right)_i \right) + \sum_{i=1}^{6} \left(\frac{(\partial \underline{V}_d)_i}{\partial u_k} \cdot \left(\underline{F}'_d \right)_i \right) +$$

$$\sum_{i=1}^{6} \left[\frac{(\partial \underline{\omega}_{12})_i}{\partial u_k} \cdot \left(\underline{T}'_e + \underline{T}'_d + \underline{T}'_b \right)_i \right] + \frac{\partial \underline{\omega}}{\partial u_k} \cdot \underline{T}'_c = 0 \tag{70}$$

The first three terms of the above equation can be evaluated using equations (27), (28) and (29) for the velocity partial derivatives with respect to the generalized speeds u_{22}, u_{23} and u_{24}. These velocity partial derivatives have the following general forms

$$\frac{\partial \underline{V}_b}{\partial u_k} = \frac{bl}{L} \left[U_k \underline{s}_2 + Q_k \underline{s}_{23} \right]$$

$$\frac{\partial \underline{V}_d}{\partial u_k} = \frac{D}{L} \left[U_k \underline{s}_2 + Q_k \underline{s}_{23} \right]$$

$$\frac{\partial \underline{V}_e}{\partial u_k} = \frac{E}{L} \left[U_k \underline{s}_2 + Q_k \underline{s}_{23} \right]$$

where the coefficients U_k and Q_k are given by

$$\begin{bmatrix} U_{22} \\ U_{23} \\ U_{24} \end{bmatrix} = \left(\underline{R}_{pc} \times \underline{s}_2 \right) = \begin{bmatrix} R_{pcy}\, s_{2z} - R_{pcz}\, s_{2y} \\ R_{pcz}\, s_{2x} - R_{pcx}\, s_{2z} \\ R_{pcx}\, s_{2y} - R_{pcy}\, s_{2x} \end{bmatrix}$$

$$\begin{bmatrix} Q_{22} \\ Q_{23} \\ Q_{24} \end{bmatrix} = \left(\underline{R}_{pc} \times \underline{s}_{23} \right) = \begin{bmatrix} R_{pcy}\, s_{23z} - R_{pcz}\, s_{23y} \\ R_{pcz}\, s_{23x} - R_{pcx}\, s_{23z} \\ R_{pcx}\, s_{23y} - R_{pcy}\, s_{23x} \end{bmatrix}$$

The fourth term of equation (70) can be evaluated using equations (20), (21) and (22) for the angular velocity partial derivatives with respect to the generalized speeds u_{22}, u_{23} and u_{24}. These velocity partial derivatives have the following general forms

$$\frac{\partial \omega\, 12}{\partial u_k} = \frac{1}{L}[\, U_k \underline{s}_1 + Q_k \underline{s}_2]$$

Using equation (54), the fifth term of equation (70) can be written as

$$\frac{\partial \omega}{\partial u_k} \cdot \mathbf{T}'_c = \frac{\partial \omega}{\partial u_k} \cdot \left[\, \mathbf{T}_{ext} + \sum_{i=1}^{6} (F_l \underline{s}_{o3})_i - \underline{\alpha} \cdot Ip' + (\underline{\omega} \times Ip' \cdot \underline{\omega})\right]$$

Given the fact that these velocity partial derivatives have the same structure as the velocity partial derivatives with respect to the generalized speeds u_{19}, u_{20} and u_{21}, equation (70) can be simplified using a derivation parallel to the one outlined in the previous section. The equation of motion for the rotations about the X, Y and Z axes can be written as

$$\sum_{i=1}^{6} (F_L \underline{s}_{o3})_i = \mathbf{T}_{ext} + \mathbf{T}'_p + \mathbf{T}_{gr} + \mathbf{T}_{tan} + \mathbf{T}_{cor} + \mathbf{T}_{centr} \qquad (71)$$

where $\mathbf{T}_{ext}$ is the external torque applied to the platform. $\mathbf{T}'_p$ is the inertial torque of the platform which is given by

$$\mathbf{T}'_p = \frac{\partial \omega}{\partial u_k} \cdot \left[\, \underline{\alpha} \cdot \mathbf{I}_p + (\underline{\omega} \times \mathbf{I}_p \cdot \underline{\omega})\right] \qquad (71.a)$$

The connector gravitational torque vector, $\mathbf{T}_{gr}$, describes the torques applied to the platform caused by the gravitational acceleration acting on the rigid bodies of the connector

$$\mathbf{T}_{gr} = \sum_{i=1}^{6} \left[\, \frac{g[\, M_e E + M_d D + M_b bl\,]}{L}\, s_{2z}(\underline{R}_{pc} \times \underline{s}_2)\right]_i +$$

$$\sum_{i=1}^{6} \left[\, \frac{g[\, M_e E + M_d D + M_b bl\,]}{L}\, s_{23z}(\underline{R}_{pc} \times \underline{s}_{23})\right]_i \qquad (71.b)$$

The connector tangential acceleration torque vector, $\mathbf{T}_{tan}$, describes the torques applied to the platform by the angular acceleration $\underline{\alpha}_{12}$ acting on the rigid bodies of the connector

$$\mathbf{T}_{tan} = \sum_{i=1}^{6} \left[\frac{M_e E^2 + M_d D^2 + M_b bl^2 + II_{xx} s_{23x}^2 + II_{zz} s_{3x}^2}{L} \alpha_1 \left(\mathbf{R}_{pc} \times \underline{s}_2\right) \right]_i +$$

$$\sum_{i=1}^{6} \left[\frac{M_e E^2 + M_d D^2 + M_b bl^2 + II_{xx}}{L} \alpha_2 \left(\mathbf{R}_{pc} \times \underline{s}_{23}\right) \right]_i \qquad (71.c)$$

The connector Coriolis acceleration torque vector, $\mathbf{T}_{cor}$, describes the torques applied to the platform by the Coriolis acceleration acting on the rigid bodies of the connector

$$\mathbf{T}_{cor} = \sum_{i=1}^{6} \left[\frac{2\left[M_e \dot{E} E + M_d \dot{D} D\right]}{L} \left[\omega_1 \left(\mathbf{R}_{pc} \times \underline{s}_2\right) + \omega_2 \left(\mathbf{R}_{pc} \times \underline{s}_{23}\right) \right] \right]_i \qquad (71.d)$$

The connector centrifugal acceleration torque vector, $\mathbf{T}_{cent}$, describes the torques applied to the platform by the centrifugal acceleration acting on the rigid bodies on the connector

$$\mathbf{T}_{cent} = \sum_{i=1}^{6} \left[\frac{s_{3x} s_{23x} \left(M_e E^2 + M_d D^2 + M_b bl^2\right)}{L} \omega_1^2 \left(\mathbf{R}_{pc} \times \underline{s}_{23}\right) \right]_i +$$

$$\sum_{i=1}^{6} \left[\frac{2 s_{3x} \left(M_e E^2 + M_d D^2 + M_b bl^2\right)}{L} \omega_1 \omega_2 \left(\mathbf{R}_{pc} \times \underline{s}_2\right) \right]_i +$$

$$\sum_{i=1}^{6} \left[\frac{s_{3x} \left(II_{xx} - II_{zz}\right)}{L} \omega_1^2 \left(\mathbf{R}_{pc} \times \underline{s}_{23}\right) \right]_i +$$

$$\sum_{i=1}^{6} \left[\frac{s_{23x} s_{3x} \left(II_{zz} - II_{xx}\right)}{L} \omega_1 \omega_2 \left(\mathbf{R}_{pc} \times \underline{s}_2\right) \right]_i \qquad (71.e)$$

5.6.4 Summary of the Equations of Motion for the Platform

The equations of motion describing the platform translation and rotation, equations (69) and (71), can be combined into one single vectorial equation

$$\sum_{i=1}^{6} \left(F_l \, \hat{\underline{S}}_3 \right)_i = \widehat{\underline{W}}_{ext} + \widehat{\underline{W}}_p + \widehat{\underline{W}}_{gr} + \widehat{\underline{W}}_{tan} + \widehat{\underline{W}}_{cor} + \widehat{\underline{W}}_{cent} \qquad (72)$$

where the vector $\hat{\underline{S}}_3$ is the Plücker line coordinates of each of the connectors.

The vector $\widehat{\underline{W}}_{ext}$, the external wrench, describes the forces and torques applied to the platform from external sources such as the cutting forces generated in milling operations.

The vector $\widehat{\underline{W}}_p$, the platform inertial and gravitational wrench, quantifies the forces generated by the acceleration of the platform

$$\widehat{\underline{W}}_p = \begin{bmatrix} M_p(\underline{A}_c + \underline{g}) \\ \underline{\alpha} \cdot \underline{I}_p + \left(\underline{\omega} \times \underline{I}_p \cdot \underline{\omega} \right) \end{bmatrix} \qquad (72.a)$$

The connector gravitational wrench $\widehat{\underline{W}}_{gr}$ describes the forces and torques applied on the platform by the gravitational acceleration acting on the rigid bodies of the connector

$$\widehat{\underline{W}}_{gr} = \sum_{i=1}^{6} \left[\frac{g \left[M_e E + M_d D + M_b bl \right]}{L} \, s_{2z} \hat{\underline{S}}_2 \right]_i +$$

$$\sum_{i=1}^{6} \left[\frac{g \left[M_e E + M_d D + M_b bl \right]}{L} \, s_{23z} \hat{\underline{S}}_{23} \right]_i \qquad (72.b)$$

where the vectors are

$$\hat{\underline{S}}_2 = \begin{bmatrix} \underline{s}_2 \\ \underline{R}_{pc} \times \underline{s}_2 \end{bmatrix} \quad ; \quad \hat{\underline{S}}_{23} = \begin{bmatrix} \underline{s}_{23} \\ \underline{R}_{pc} \times \underline{s}_{23} \end{bmatrix} \qquad (72.c)$$

The connector tangential acceleration wrench $\widehat{\underline{W}}_{tan}$ determines the forces and torques applied to the platform by the inertial forces produced by the angular acceleration $\underline{\alpha}_{12}$ acting on the rigid bodies of the connector

$$\widehat{\underline{W}}_{tan} = \sum_{i=1}^{6} \left[\frac{M_e E^2 + M_d D^2 + M_b bl^2 + \Pi_{xx} s_{23x}^2 + \Pi_{zz} s_{3x}^2}{L} \alpha_1 \dot{\underline{S}}_2 \right]_i +$$

$$\sum_{i=1}^{6} \left[\frac{M_e E^2 + M_d D^2 + M_b bl^2 + \Pi_{xx}}{L} \alpha_2 \widehat{\underline{S}}_{23} \right]_i \qquad (72.d)$$

The connector Coriolis acceleration wrench $\widehat{\underline{W}}_{cor}$ determines the forces and torques applied to the platform by the inertial forces produced by the Coriolis acceleration acting on the rigid bodies of the connector

$$\widehat{\underline{W}}_{cor} = \sum_{i=1}^{6} \left[\frac{2 \left[M_e \dot{E} E + M_d \dot{D} D \right]}{L} \left[\omega_1 \dot{\underline{S}}_2 + \omega_2 \dot{\underline{S}}_{23} \right] \right]_i \qquad (72.e)$$

The connector centrifugal acceleration wrench $\widehat{\underline{W}}_{cent}$ determines the forces and torques applied to the platform by the inertial forces produced by the centrifugal acceleration acting on the rigid bodies of the connector

$$\widehat{\underline{W}}_{cent} = \sum_{i=1}^{6} \left[\frac{s_{3x} s_{23x} \left(M_e E^2 + M_d D^2 + M_b bl^2 \right)}{L} \omega_1^2 \dot{\underline{S}}_{23} \right]_i +$$

$$\sum_{i=1}^{6} \left[\frac{2 s_{3x} \left(M_e E^2 + M_d D^2 + M_b bl^2 \right)}{L} \omega_1 \omega_2 \widehat{\underline{S}}_2 \right]_i +$$

$$\sum_{i=1}^{6} \left[\frac{s_{3x} \left(\Pi_{xx} - \Pi_{zz} \right)}{L} \omega_1^2 \dot{\underline{S}}_{23} \right]_i +$$

$$\sum_{i=1}^{6} \left[\frac{s_{23x} \, s_{3x} \, (\Pi_{zz} - \Pi_{xx})}{L} \, \omega_1 \omega_2 \hat{\underline{S}}_2 \right]_i \qquad (72.f)$$

Equation (72) illustrates the high degree of coupling that exits in the platform equations of motion. Each connector will have to produce a force that is a function of the location and motion of the other connectors and the platform. The dynamic coupling is a function of the system parameters such as connector length, moment of inertias and masses. For light loads, the connectors do not have to be so strong which reduces the connector masses and moment of inertias. For heavy loads, the connectors must be stronger and consequently their masses and moments of inertias are increased. Therefore platforms designed for heavy loads will exhibit a higher degree of coupling than the platform designed for light loads.

The dynamic coupling is also a consequence of the motion of the platform, which determines the velocity and acceleration of the connectors. In high speed applications the connector velocity and acceleration increase and the coupling will be more significant. In low speed applications, the connector velocity and acceleration are smaller and the coupling caused by the tangential acceleration, Coriolis acceleration and centrifugal acceleration may not be not an important factor. The gravitational acceleration will cause coupling regardless of the motion of the platform and should be a concern for any type of application.

5.7 Dynamic Model Validation

A major issue when modeling a dynamic system is to be able to determine whether or not the model itself is correct. This requires a comparison with another method such as Newton's 2nd Law or Lagrange's Equation. The equations of motion of the manipulator will be verified using Newton's 2nd Law.

5.7.1 Equation of Motion for the mass M_e

The sum of forces acting on the mass M_e was determined in Section 4.6

$$\underline{F}_e = \left[F_a - C_t \dot{E} - K_L \delta_L \right] \underline{s}_3 - \left[M_e g \right] \underline{k}$$

The sum of forces must be equal to the mass M_e multiplied by its acceleration. The acceleration vector, which was determined in Section 3.5, is given by

$$\underline{A}_e = \ddot{E} \, \underline{s}_3 + 2 \dot{E} (\omega_1 \underline{s}_2 + \omega_2 \underline{s}_{23}) + E (\alpha_1 \underline{s}_2 + \alpha_2 \underline{s}_{23}) +$$

$$E \left(2 \omega_1 \omega_2 (\underline{s}_1 \cdot \underline{s}_3) \underline{s}_2 + \omega_1^2 (\underline{s}_1 \cdot \underline{s}_3) \underline{s}_1 - (\omega_1^2 + \omega_2^2) \underline{s}_3 \right)$$

The force is equal to the product of the acceleration and the mass

$$F_a \, \underline{s}_3 = \left[C_t \dot{E} + K_L \delta_L \right] \underline{s}_3 + M_e g \, \underline{k} + M_e \ddot{E} \, \underline{s}_3 + 2 M_e \dot{E} (\omega_1 \underline{s}_2 + \omega_2 \underline{s}_{23}) +$$

$$M_e E \left(\alpha_1 \underline{s}_2 + \alpha_2 \underline{s}_{23} + 2 \omega_1 \omega_2 (\underline{s}_1 \cdot \underline{s}_3) \underline{s}_2 + \omega_1^2 (\underline{s}_1 \cdot \underline{s}_3) \underline{s}_1 - (\omega_1^2 + \omega_2^2) \underline{s}_3 \right)$$

This equation can be divided into a component parallel to the connector and a component perpendicular to the connector. The parallel component is

$$F_a = C_t \dot{E} + K_L \delta_L \cdot M_e \left[\ddot{E} + g \, s_{3z} + E (\omega_1^2 \, s_{3x}^2 - (\omega_1^2 + \omega_2^2)) \right]$$

This equation described the motion of the mass M_e along the connector. It is the same as equation (61) which is the equation of motion derived by using Kane's Method.

The component perpendicular to the connector generates an equilibrant force at the point joining the connector with the platform. This will be covered in the verification of the platform equations of motion.

5.7.2 Equation of Motion for the mass M_d

The sum of forces acting on the mass M_d was determined in Section 4.6

$$\underline{F}_d = \left[-C_d(\dot{D} - \dot{L}) - K_d \delta_d \right] \underline{s}_3 - [M_d g] \underline{k}$$

The sum of forces must be equal to the product of the mass and the acceleration. The acceleration vector, which was determined in Section 3.5, is given by

$$\underline{A}_d = \ddot{D}\,\underline{s}_3 + 2\dot{D}(\omega_1 \underline{s}_2 + \omega_2 \underline{s}_{23}) + D(\alpha_1 \underline{s}_2 + \alpha_2 \underline{s}_{23}) +$$

$$D\left(2\omega_1 \omega_2 (\underline{s}_1 \cdot \underline{s}_3)\underline{s}_2 + \omega_1^2 (\underline{s}_1 \cdot \underline{s}_3)\underline{s}_1 - (\omega_1^2 + \omega_2^2)\underline{s}_3 \right)$$

The force is equal to the product of this acceleration and the mass

$$\left[-C_d(\dot{D} - \dot{L}) - K_d \delta_d \right] \underline{s}_3 = M_d g \underline{k} + M_d \ddot{D}\,\underline{s}_3 + 2 M_d \dot{D}(\omega_1 \underline{s}_2 + \omega_2 \underline{s}_{23}) +$$

$$M_d D\left(\alpha_1 \underline{s}_2 + \alpha_2 \underline{s}_{23} + 2\omega_1 \omega_2 (\underline{s}_1 \cdot \underline{s}_3)\underline{s}_2 + \omega_1^2 (\underline{s}_1 \cdot \underline{s}_3)\underline{s}_1 - (\omega_1^2 + \omega_2^2)\underline{s}_3 \right)$$

As done in the previous section, this equation can be divided into a component parallel to the connector and a component perpendicular to the connector. The parallel component is

$$\left[-C_d(\dot{D} - \dot{L}) - K_d \delta_d \right] = M_d \left[\ddot{D} + g\,s_{3z} + D(\omega_1^2 \, s_{3x}^2 - (\omega_1^2 + \omega_2^2)) \right]$$

This equation described the motion of the decoupling stage mass along the connector. It is the same as equation (62) which is the equation of motion for the mass M_d, derived using Kane's Method.

The component perpendicular to the connector generates an equilibrant force at the point joining the connector with the platform. This will be covered in the verification of the platform equations of motion.

5.7.3 Equations of Motion of the Platform

The sum of forces on the platform is given by

$$\underline{F}_p = \underline{F}_{ext} - M_p g + \sum_{i=1}^{6} \underline{F}_L$$

Where $\underline{F}_{ext}$ is the external force applied on the platform, and $\underline{F}_L$ is the force that each connector applies to the platform. This last force can also be divided into two components

$$\underline{F}_L = \underline{F}'_L + \underline{F}''_L$$

Where $\underline{F}'_L$ is the parallel force component which is applied by each of the connectors to the platform along the direction of the connector, $\underline{s}_3$. This force is generated by the coupling stage stiffness and damper along with the decoupling damper as discussed in Section 4.6. The expression for this force is given by

$$\underline{F}'_L = \left[C_d(\dot{D} - \dot{L}) + C_c(\dot{H} - \dot{L}) + K_c \delta_c \right] \underline{s}_3 \tag{73}$$

The perpendicular force $\underline{F}''_L$ is applied by each of the connectors to the platform along a direction perpendicular to the connector. This force is generated by the gravitational, Coriolis, centrifugal and angular acceleration components acting on the rigid bodies of each connector. The acceleration of any rigid body on the connector at a distance $\underline{U}$ from the base, as shown in figure 5.5, is given by

$$\underline{A} = g\,\underline{k} + \ddot{U}\,\underline{s}_3 + 2\dot{U}(\omega_1\underline{s}_2 + \omega_2\underline{s}_{23}) + U(\alpha_1\underline{s}_2 + \alpha_2\underline{s}_{23}) +$$

$$U\left(2\omega_1\omega_2(\underline{s}_1 \cdot \underline{s}_3)\underline{s}_2 + \omega_1^2(\underline{s}_1 \cdot \underline{s}_3)\underline{s}_1 - (\omega_1^2 + \omega_2^2)\underline{s}_3 \right) \tag{74}$$

The inertial force of a body is the product of its mass and acceleration. The inertial force of the mass M on the connector is given by
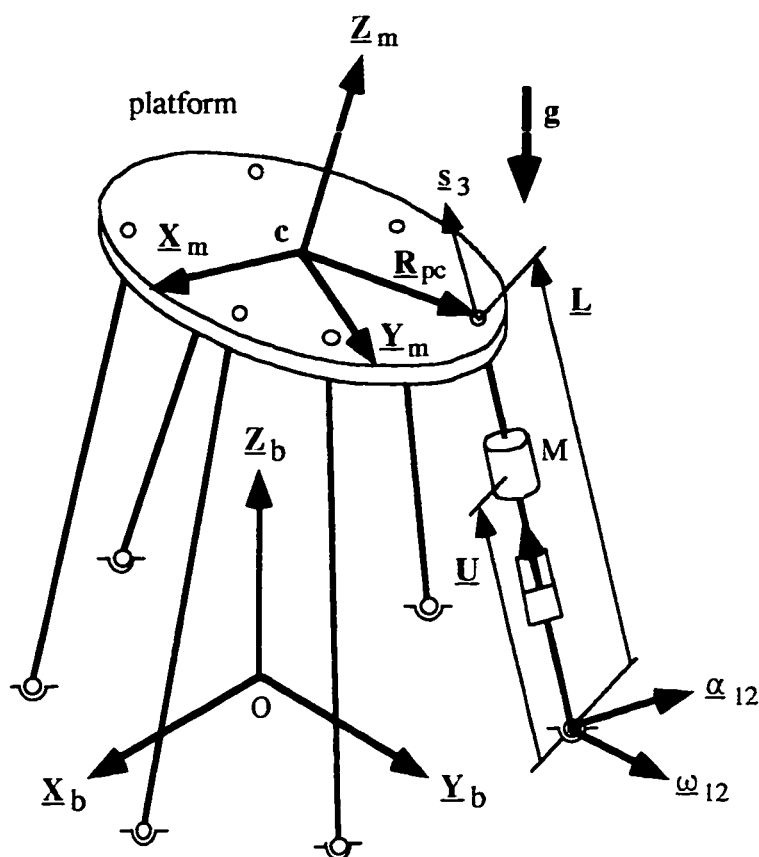
Figure 5.5 - Platform and connector with Rigid Body

$$\underline{F}_I = - M\underline{A} = - M\left[g\underline{k} + \ddot{U}\underline{s}_3 + 2\dot{U}(\omega_1\underline{s}_2 + \omega_2\underline{s}_{23}) + U(\alpha_1\underline{s}_2 + \alpha_2\underline{s}_{23})\right] -$$

$$MU\left(2\omega_1\omega_2(\underline{s}_1 \cdot \underline{s}_3)\underline{s}_2 + \omega_1^2(\underline{s}_1 \cdot \underline{s}_3)\underline{s}_1 - \left(\omega_1^2 + \omega_2^2\right)\underline{s}_3\right) \quad (75)$$

The inertial torque of a body is generated by its angular velocity and acceleration

$$\underline{T}_I = - \underline{\alpha}_{12} \cdot I'' - \underline{\omega}_{12} \times I'' \cdot \underline{\omega}_{12}$$

where I'' is the inertia dyadic of the body. Using the expressions for the inertia dyadic given in equations (56), (57) and (58), the inertial torque can be written as

$$\underline{T}_I = II_{xx}\left[\underline{\alpha}_{12} \cdot \underline{s}_{23}\right]\underline{s}_{23} + II_{xx}\left[\underline{\omega}_{12} \times \underline{s}_{23}\right]\left[\underline{s}_{23} \cdot \underline{\omega}_{12}\right] +$$

$$\Pi_{xx} \left[\underline{\alpha}_{12} \cdot \underline{s}_2 \right] \underline{s}_2 + \Pi_{xx} \left[\underline{\omega}_{12} \times \underline{s}_2 \right] \left[\underline{s}_2 \cdot \underline{\omega}_{12} \right] +$$

$$\Pi_{zz} \left[\underline{\alpha}_{12} \cdot \underline{s}_3 \right] \underline{s}_3 + \Pi_{zz} \left[\underline{\omega}_{12} \times \underline{s}_3 \right] \left[\underline{s}_3 \cdot \underline{\omega}_{12} \right] \qquad (76)$$

The inertial force $\underline{F}_I$ produces a torque about the base of the connector (see Figure 5.6)

$$U \underline{s}_3 \times \underline{F}_I$$

This torque together with the inertial torque $\underline{T}_I$ will be balanced by the torque produced by the force $\underline{F}''_L$ as shown in figures 5.5 and 5.6

$$L \underline{s}_3 \times \underline{F}''_L = (U \underline{s}_3 \times \underline{F}_I) + \underline{T}_I$$
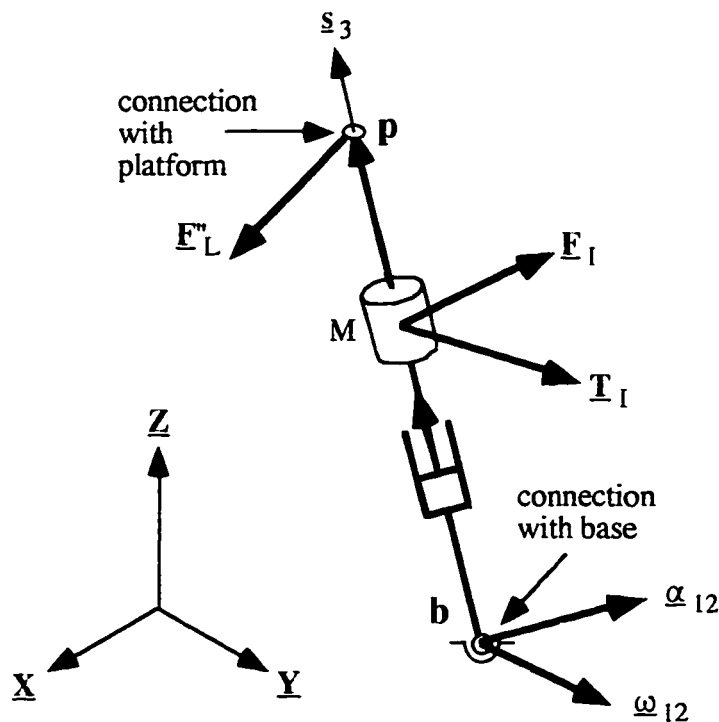
Figure 5.6 - Forces and Torques acting on the connector

The force $\underline{F}''_L$ can be determined by taking the vector product of $\underline{s}_3$ and the above equation

$$\underline{s}_3 \times \left[L\underline{s}_3 \times \underline{F}''_L \right] = \underline{s}_3 \times \left[(U\underline{s}_3 \times \underline{F}_I) + \underline{T}_I \right]$$

which gives the following expression for $\underline{F}''_L$

$$\underline{F}''_L = \frac{-\underline{s}_3 \times \left[(U\underline{s}_3 \times \underline{F}_I) + \underline{T}_I \right]}{L}$$

This force can be expanded by using to the expressions for the inertial force and torque, equations (75) and (76)

$$\underline{F}''_L = \left[\frac{gMU}{L} \left[s_{2z}\underline{s}_2 + s_{23z}\underline{s}_{23} \right] \right] +$$

$$\left[\frac{MU^2 + I_{xx} s_{23x}^2 + I_{zz} s_{3x}^2}{L} \alpha_1\underline{s}_2 + \frac{MU^2 + I_{xx}}{L} \alpha_2\underline{s}_{23} \right] +$$

$$\left[\frac{2M\dot{U}U}{L} \left[\omega_1\underline{s}_2 + \omega_2\underline{s}_{23} \right] \right] +$$

$$\left[\frac{2s_{3x} MU^2 + 2s_{23x} s_{3x} (I_{zz} - I_{xx})}{L} \omega_1\omega_2\underline{s}_2 \right] +$$

$$\left[\frac{s_{3x} s_{23x} (MU^2 + I_{xx} - I_{zz})}{L} \omega_1^2\underline{s}_{23} \right] \qquad (77)$$

The sum of forces on the platform, which is equal to the product of its acceleration and mass, can now be written as

$$\underline{F}_{ext} - M_p\underline{g} + \sum_{i=1}^{6} \underline{F}'_L + \sum_{i=1}^{6} \underline{F}''_L = M_p\underline{A}_c$$

The above equation can be rewritten using all the rigid bodies of the connector

$$\sum_{i=1}^{6} (F_L \, \underline{s}_3)_i = \underline{F}_{ext} + M_p \underline{A}_c + M_p \underline{g} +$$

$$\sum_{i=1}^{6} \left[\frac{g [M_e E + M_d D + M_b bl]}{L} \left[s_{2z} \underline{s}_2 + s_{23z} \underline{s}_{23} \right] \right]_i +$$

$$\sum_{i=1}^{6} \left[\frac{M_e E^2 + M_d D^2 + M_b bl^2 + II_{xx} \, s_{23x}^2 + II_{zz} \, s_{3x}^2}{L} \, \alpha_1 \underline{s}_2 \right]_i +$$

$$\sum_{i=1}^{6} \left[\frac{M_e E^2 + M_d D^2 + M_b bl^2 + II_{xx}}{L} \, \alpha_2 \underline{s}_{23} \right]_i +$$

$$\sum_{i=1}^{6} \left[\frac{2 [M_e \dot{E} E + M_d \dot{D} D]}{L} [\omega_1 \underline{s}_2 + \omega_2 \underline{s}_{23}] \right]_i +$$

$$\sum_{i=1}^{6} \left[\frac{2 s_{3x} (M_e E^2 + M_d D^2 + M_b bl^2)}{L} \, \omega_1 \omega_2 \underline{s}_2 \right]_i +$$

$$\sum_{i=1}^{6} \left[\frac{2 s_{23x} \, s_{3x} (II_{zz} - II_{xx})}{L} \, \omega_1 \omega_2 \underline{s}_2 \right]_i +$$

$$\sum_{i=1}^{6} \left[\frac{s_{3x} \, s_{23x} (M_e E^2 + M_d D^2 + M_b bl^2)}{L} \, \omega_1^2 \underline{s}_{23} \right]_i +$$

$$\sum_{i=1}^{6} \left[\frac{s_{23x} \, s_{3x} (II_{xx} - II_{zz})}{L} \, \omega_1^2 \underline{s}_{23} \right]_i$$

This is the same equation (69) obtained by using Kane's Method.

The sum of torques about the platform center of gravity can be written in the form (see figure 5.7)

$$\underline{T}_{ext} + \sum_{i=1}^{6} \underline{R}_{pc} \times \underline{F}'_{L} + \sum_{i=1}^{6} \underline{R}_{pc} \times \underline{F}''_{L} = \underline{\alpha} \cdot Ip'' + \underline{\omega} \times Ip'' \cdot \underline{\omega}$$

where the $\underline{T}_{ext}$ is the external torque applied to the platform and the right hand side of the equation is the inertial torque of the platform. Using the expressions derived previously for the forces $\underline{F}'_{L}$ and $\underline{F}''_{L}$, the above equation can be expanded to

$$\sum_{i=1}^{6} (F_{L} \underline{S}_{o3})_i = \underline{T}_{ext} + \underline{\alpha} \cdot Ip'' + \underline{\omega} \times Ip'' \cdot \underline{\omega} +$$

$$\sum_{i=1}^{6} \left[\frac{g [M_e E + M_d D + M_b bl]}{L} \underline{R}_{pc} \times [s_{2z} \underline{S}_2 + s_{23z} \underline{S}_{23}] \right]_i +$$

$$\sum_{i=1}^{6} \left[\frac{M_e E^2 + M_d D^2 + M_b bl^2 + \Pi_{xx} s_{23x}^2 + \Pi_{zz} s_{3x}^2}{L} \underline{R}_{pc} \times \alpha_1 \underline{S}_2 \right]_i +$$
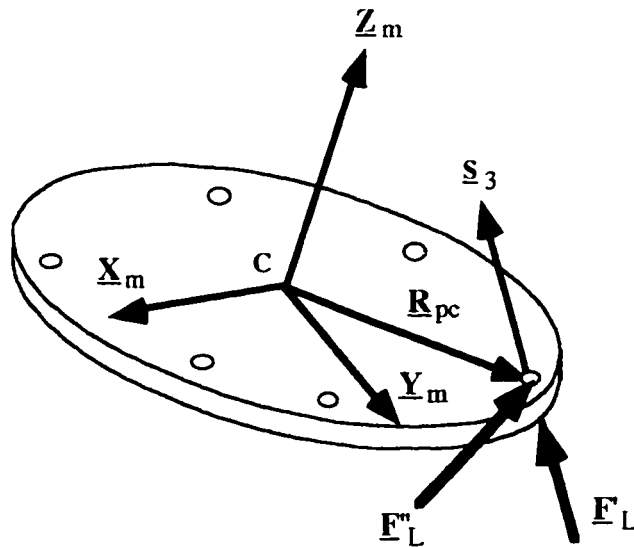

Figure 5.7 - Connector Forces acting on the platform

$$\sum_{i=1}^{6} \left[\frac{M_e E^2 + M_d D^2 + M_b bl^2 + \Pi_{xx}}{L} \underline{R}_{pc} \times \alpha_2 \underline{S}_{23} \right]_i +$$

$$\sum_{i=1}^{6} \left[\frac{2 \left[M_e \dot{E} E + M_d \dot{D} D \right]}{L} \underline{R}_{pc} \times \left[\omega_1 \underline{S}_2 + \omega_2 \underline{S}_{23} \right] \right]_i +$$

$$\sum_{i=1}^{6} \left[\frac{2 s_{3x} \left(M_e E^2 + M_d D^2 + M_b bl^2 \right)}{L} \underline{R}_{pc} \times \omega_1 \omega_2 \underline{S}_2 \right]_i +$$

$$\sum_{i=1}^{6} \left[\frac{2 s_{23x} s_{3x} \left(\Pi_{zz} - \Pi_{xx} \right)}{L} \underline{R}_{pc} \times \omega_1 \omega_2 \underline{S}_2 \right]_i +$$

$$\sum_{i=1}^{6} \left[\frac{s_{3x} s_{23x} \left(M_e E^2 + M_d D^2 + M_b bl^2 \right)}{L} \underline{R}_{pc} \times \omega_1^2 \underline{S}_{23} \right]_i +$$

$$\sum_{i=1}^{6} \left[\frac{s_{23x} s_{3x} \left(\Pi_{xx} - \Pi_{zz} \right)}{L} \underline{R}_{pc} \times \omega_1^2 \underline{S}_{23} \right]_i$$

This is the same as equation (71) which was derived using Kane's Method. The validation of the equations of motion is complete and it has been demonstrated that the same results are obtained using two different formulations.

5.8 Summary

Kane's Method has proven to be an effective formulation for obtaining the explicit equations of motion for a parallel manipulator. This method is more effective for parallel manipulators than Lagrange's formulation. One of the main reasons is that setting up the equations of motion with Lagrange requires several operations with the velocity and displacement expressions as outlined in section 5.1[13, 26]. These expressions are rather elaborate for parallel manipulators (see Section 3.4), as compared to serial manipulators for which Lagrange has proven to an effective formulation technique. Kane's Method uses the

velocity expression for obtaining the velocity partial derivatives which was shown here to be a simple task. This partial derivatives turn out to be the coefficients of the velocity equations.

Kane's Method is similar to the Newton-Euler formulation since both methods require a force and torque analysis. The main reason that Kane's Method was used instead is that it is a more systematic formulation, which uses the velocity and angular velocity partial derivatives for eliminating the workless constraints. In the Newton-Euler formulation these constraints have to be eliminated by combining equations, a non systematic process which can prove to be difficult and time consuming. The Newton-Euler formulation was used here to validate the equations of motion which have already been derived using Kane's Method. The results obtained using Kane's Method offered the insight for setting up the equations of motion with Newton-Euler, which saved a considerable amount of work. This insight would not be available if the Newton-Euler formulation was used from the outset.

This work proves that selection of the formulation method is very important consideration for dynamic modeling. This selection is heavily influenced by the type of kinematic chain the manipulator is based on (serial or parallel kinematic chain).

CHAPTER 6
DYNAMIC SIMULATION ALGORITHM

Once the dynamic model has been derived, a simulation algorithm can be developed. The objective is to determine the required actuator forces, power and frequency response for a given spatial parallel manipulator and the required task. Parameters such as dimensions, platform mass, connector stiffness and transmission damping coefficients (see Chapter 2 for more details on all the parameters) will be specified.

The first part of the simulation will determine the kinematic state of the connectors (positions, velocities and accelerations) using the motion or task description of the platform. The second part of the simulation will determine the forces and moments acting on the system and will determine the required actuator response for the desired task.

6.1 Motion and Task Planning

There are different types of task that the manipulator can perform. The platform can be required to carry a load or to counteract an external force such as those generated when machining. In this case the external force and torque are specified along with the desired output resultant force and torque. This is also known as force control. The platform can also be required to move a body through a prescribed motion such as that of a flight simulator. This type of task requires motion control. Another applications might require the platform to operate in a combined or hybrid force/motion control mode. Polishing a lens or machining a complex contour requires that the platform controls the contact forces between the end effector and the workpiece while at the same time executing a given motion profile.

Although more emphasis is given to the areas of motion and hybrid control, the simulation algorithm is designed to use any of the mentioned tasks as the input.

128

6.2 Inverse Kinematic Simulation Algorithm

The inverse kinematic analysis will be done in two parts. Firstly it is necessary to determine the motion of the platform (location, velocity and acceleration) based on the motion planning parameters. Secondly part of the inverse kinematic analysis will determine the motion of each connector. Most of the equations used in this section have been derived and discussed in detail in Chapter 3.

6.2.1 Platform Inverse Kinematics

Two basic platform motions (see Section 3.6) will be considered for the inverse kinematic analysis. The first is a rectilinear motion and the second is a curvilinear motion. For both cases the initial position of the centerpoint c, $\underline{C}_o$, and the initial orientation of the platform, $[R]_o$, will be specified. Using these initial quantities, the initial position of any point on the platform can be determined by

$$\underline{P}_o = \underline{C}_o + [R]_o \underline{R}_{pc/m} \tag{1}$$

where $\underline{R}_{pc/m}$ is the position vector of point p with respect to centerpoint c defined with respect to the moving coordinate frame as explained in Section 3.2. This vector is a constant which is determined by the platform dimensions.

6.2.1.1 Rectilinear Motion

The parameters required to specify a rectilinear motion are the total displacement ΔS, the axis of translation $\underline{w}$ (see Figure 6.1) and the time period T (see Section 3.6). The position, velocity and acceleration of any point p on the platform can be determined by

$$\underline{P}(t) = \underline{C}_o + [R]_o \underline{R}_{pc/m} + \frac{\Delta S}{2}\left[1 - \cos\left(\frac{\pi t}{T}\right)\right]\underline{w} \tag{2}$$

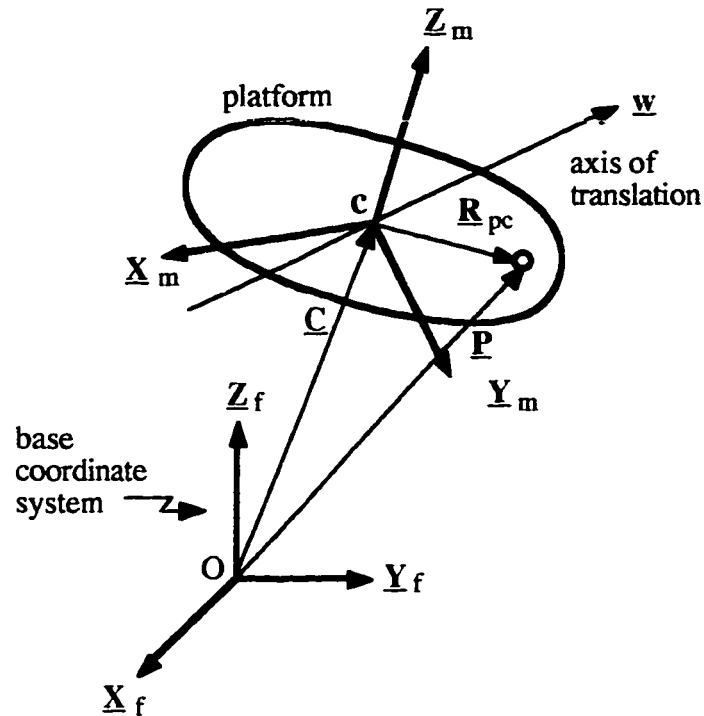$$\underline{V}_p(t) = \frac{\Delta S}{2}\frac{\pi}{T}\sin\left(\frac{\pi t}{T}\right)\underline{w} \tag{3}$$

Figure 6.1 - Rectilinear Motion

$$\underline{A}_p(t) = \frac{\Delta S}{2}\left(\frac{\pi}{T}\right)^2 \cos\left(\frac{\pi t}{T}\right)\underline{w}$$ (4)

For this type of motion, the orientation of the platform remains constant and the rotation matrix is not used.

6.2.1.2 Rotational Motion

The parameters required to specify a rotational motion are the total angular displacement $\Delta\theta$, the axis of rotation $\underline{s}$, the distance r_c from the centerpoint c to the axis of rotation (see Figure 6.2), and the time period T as mentioned in Section 3.6. The position, velocity and acceleration of any point on the platform can be determined by

$$\underline{P} = \underline{P}_o + \underline{R}_{pc}$$ (5)

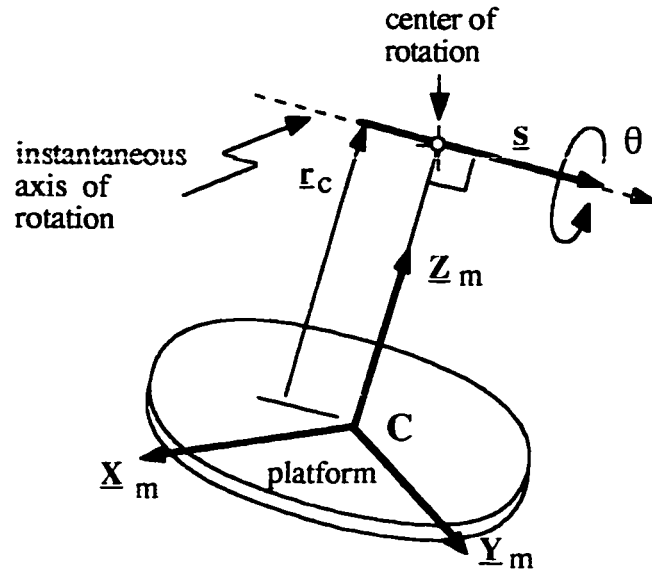Figure 6.2 - Curvilinear Motion

$$\underline{V}_p = \left[\left(\, \underline{r}_c - \underline{R}_{pc}\right) \times \underline{\omega} \right] \tag{6}$$

$$\underline{A}_p = \underline{\omega} \times \left[\left(\, \underline{r}_c - \underline{R}_{pc}\right) \times \underline{\omega} \right] + \left(\, \underline{r}_c - \underline{R}_{pc}\right) \times \underline{\alpha} \tag{7}$$

where $\underline{\theta}$, $\underline{\omega}$ and $\underline{\alpha}$ are the platform angular displacement, velocity and acceleration vectors

$$\underline{\theta}\,(t) = \frac{\Delta\theta}{2}\left[\, 1 - \cos\left(\frac{\pi t}{T}\right)\right]\underline{s} \tag{8}$$

$$\underline{\omega}\,(t) = \frac{\Delta\theta\,\pi}{2\,T}\left[\sin\left(\frac{\pi t}{T}\right)\right]\underline{s} \tag{9}$$

$$\underline{\alpha}\,(t) = \frac{\Delta\theta\,\pi^2}{2\,T^2}\left[\cos\left(\frac{\pi t}{T}\right)\right]\underline{s} \tag{10}$$

The relative position vector $\underline{R}_{pc}$, which changes as the platform moves, is determined by

$$\underline{R}_{pc} = \left[\, R\,\right]_o \left[\, R\,\right]\underline{R}_{pc/m} \tag{11}$$

where $[R]_o$ describes the initial orientation of the platform, $\underline{R}_{pc/m}$ is the relative position vector with respect to the moving coordinate frame, and $[R]$ is the rotation matrix

$$[R] = \begin{bmatrix} s_x{}^2\,vsn\,\theta + \cos\theta & s_x\,s_y\,vsn\,\theta - s_z\sin\theta & s_x\,s_z\,vsn\,\theta + s_y\sin\theta \\ s_x\,s_y\,vsn\,\theta + s_z\sin\theta & s_y{}^2\,vsn\,\theta + \cos\theta & s_y\,s_z\,vsn\,\theta - s_x\sin\theta \\ s_x\,s_z\,vsn\,\theta - s_y\sin\theta & s_y\,s_z\,vsn\,\theta + s_x\sin\theta & s_z{}^2\,vsn\,\theta + \cos\theta \end{bmatrix} \quad (12)$$

6.2.2 Connector Inverse Kinematics

The Plücker line coordinates for each connector can be determined by using the following equation

$$\underline{S}_3 = \frac{[\,\underline{P} - \underline{B}\,]}{|\underline{P} - \underline{B}|} \quad ; \quad \underline{S}_{o3} = \frac{\underline{B} \times [\,\underline{P} - \underline{B}\,]}{|\underline{P} - \underline{B}|} \quad (13)$$

where $\underline{P}$ is determined using equation (2) or (5) depending on the type of motion ; and $\underline{B}$ is the position of the connection with the base. The length of a connector is given by

$$L = |\underline{P} - \underline{B}| \quad (14)$$

The velocity of point p on the connector can be determined using either equation (3) or (6). The velocity of the prismatic joint in the connector can be determined by

$$\underline{V}_3 = (\,\underline{V}_p \cdot \underline{S}_3\,)\,\underline{S}_3 \quad (15)$$

The angular velocity of the Hooke joint located at the base of the connector is given by

$$\underline{\omega}_{12} = \underline{\omega}_1 + \underline{\omega}_2 \quad (16)$$

where the components of this vector are given by (see Sections 3.3 and 3.4)

$$\underline{\omega}_1 = \left(\frac{\underline{V}_p \cdot \underline{S}_2}{L}\right)\underline{S}_1 \quad (17)$$

$$\underline{\omega}_2 = \left(\frac{\underline{V}_p \cdot \underline{S}_{23}}{L} \right) \underline{S}_2 \qquad (18)$$

The acceleration of point **p** on the connector can be determined using either equation (4) or (7). The acceleration of the prismatic joint in the connector can be determined by

$$\underline{A}_3 = \left(\underline{A}_p^* \cdot \underline{S}_3 \right) \underline{S}_3 \qquad (19)$$

where $\underline{A}^*_p$ is given by

$$\underline{A}_p^* = \underline{A}_p - \omega_1^2 \left(\underline{S}_1 \times \underline{S}_{o1} \right) - \omega_2^2 \left(\underline{S}_2 \times \underline{S}_{o2} \right) -$$

$$2\omega_1 \underline{S}_1 \times \left(\omega_2 \underline{S}_{o2} + V_3 \underline{S}_3 \right) - 2\omega_2 \underline{S}_2 \times V_3 \underline{S}_3 \qquad (20)$$

The angular acceleration of the Hooke joint located at the base of the connector is given by

$$\underline{\alpha}_{12} = \underline{\alpha}_1 + \underline{\alpha}_2 + \omega_1 \omega_2 \left(\underline{S}_1 \times \underline{S}_2 \right) \qquad (21)$$

The angular accelerations $\underline{\alpha}_1$ and $\underline{\alpha}_2$ are given by

$$\underline{\alpha}_1 = \left(\frac{\underline{A}_p^* \cdot \underline{S}_2}{L} \right) \underline{S}_1 \qquad (22)$$

$$\underline{\alpha}_2 = \left(\frac{\underline{A}_p^* \cdot \underline{S}_{23}}{L} \right) \underline{S}_2 \qquad (23)$$

6.3 Equations of Motion for the Manipulator

The equations of motion were derived in Chapter 5. Since the system has 24 degrees of freedom, the dynamic model must have 24 equations of motion. The dynamic behavior of the platform is described by the following set of equations

$$\sum_{i=1}^{6} \left(F_L \, \hat{\underline{S}}_3 \right)_i = \hat{\underline{W}}_{ext} + \hat{\underline{W}}_p + \hat{\underline{W}}_{gr} + \hat{\underline{W}}_{tan} + \hat{\underline{W}}_{cor} + \hat{\underline{W}}_{cent} \qquad (24)$$

where the dual vector $\hat{\underline{S}}_3$ contains the Plücker line coordinates of each of the connectors.

The vector $\hat{\underline{W}}_{ext}$, the external wrench, represents the forces and torques applied to the

platform from external sources such as the cutting forces generated in milling operations.

The platform inertial and gravitational wrench, $\hat{\underline{W}}_p$, quantifies the forces and torques

generated by the gravitational acceleration, the angular velocity and the angular acceleration

of the platform

$$\hat{\underline{W}}_p = \begin{bmatrix} M_p(\underline{A}_c + g) \\ \underline{\alpha} \cdot I_p'' + (\underline{\omega} \times I_p'' \cdot \underline{\omega}) \end{bmatrix} \qquad (24.a)$$

The connector gravitational wrench, $\hat{\underline{W}}_{gr}$, quantifies the forces and torques applied to the

platform by the gravitational acceleration acting on the rigid bodies of the connector

$$\hat{\underline{W}}_{gr} = \sum_{i=1}^{6} \left[\frac{g[M_e E + M_d D + M_b bl]}{L} \, s_{2z} \hat{\underline{S}}_2 \right]_i +$$

$$\sum_{i=1}^{6} \left[\frac{g[M_e E + M_d D + M_b bl]}{L} \, s_{23z} \hat{\underline{S}}_{23} \right]_i \qquad (24.b)$$

where $\hat{\underline{S}}_2$ and $\hat{\underline{S}}_{23}$ are the given by:

$$\hat{\underline{S}}_2 = \begin{bmatrix} \underline{s}_2 \\ \underline{R}_{pc} \times \underline{s}_2 \end{bmatrix} \quad ; \quad \hat{\underline{S}}_{23} = \begin{bmatrix} \underline{s}_{23} \\ \underline{R}_{pc} \times \underline{s}_{23} \end{bmatrix} \qquad (24.c)$$

The connector tangential acceleration wrench, $\hat{\underline{W}}_{tan}$, describes the forces and torques

applied to the platform by the angular acceleration $\underline{\alpha}_{12}$ acting on the rigid bodies of the connector

$$\widehat{\underline{W}}_{tan} = \sum_{i=1}^{6} \left[\frac{M_e E^2 + M_d D^2 + M_b bl^2 + \Pi_{xx} s_{23x}^2 + \Pi_{zz} s_{3x}^2}{L} \alpha_1 \underline{\hat{S}}_2 \right]_i +$$

$$\sum_{i=1}^{6} \left[\frac{M_e E^2 + M_d D^2 + M_b bl^2 + \Pi_{xx}}{L} \alpha_2 \underline{\hat{S}}_{23} \right]_i \qquad (24.d)$$

The connector Coriolis acceleration wrench, $\widehat{\underline{W}}_{cor}$, quantifies the forces and torques applied to the platform by the Coriolis acceleration acting on the rigid bodies of the connector

$$\widehat{\underline{W}}_{cor} = \sum_{i=1}^{6} \left[\frac{2 \left[M_e \dot{E} E + M_d \dot{D} D \right]}{L} \left[\omega_1 \underline{\hat{S}}_2 + \omega_2 \underline{\hat{S}}_{23} \right] \right]_i \qquad (24.e)$$

The connector centrifugal acceleration wrench, $\widehat{\underline{W}}_{cor}$, represents the forces and torques applied to the platform by the centrifugal acceleration acting on the rigid bodies of the connector

$$\widehat{\underline{W}}_{cent} = \sum_{i=1}^{6} \left[\frac{s_{3x} s_{23x} \left(M_e E^2 + M_d D^2 + M_b bl^2 \right)}{L} \omega_1^2 \underline{\hat{S}}_{23} \right]_i +$$

$$\sum_{i=1}^{6} \left[\frac{2 s_{3x} \left(M_e E^2 + M_d D^2 + M_b bl^2 \right)}{L} \omega_1 \omega_2 \underline{\hat{S}}_2 \right]_i +$$

$$\sum_{i=1}^{6} \left[\frac{s_{3x} \left(\Pi_{xx} - \Pi_{zz} \right)}{L} \omega_1^2 \underline{\hat{S}}_{23} \right]_i +$$

$$\sum_{i=1}^{6} \left[\frac{s_{23x} \, s_{3x} \, (\Pi_{zz} - \Pi_{xx})}{L} \, \omega_1 \omega_2 \hat{S}_2 \right]_i \qquad (24.f)$$

The equation of motion for the mass M_d is

$$M_d \left[\ddot{D} + g \, s_{3z} + D \omega_1^2 (s_{3x})^2 - D \left(\omega_1^2 + \omega_2^2 \right) \right] + C_d \left(\dot{D} - \dot{L} \right) + K_d \delta_d = 0 \qquad (25)$$

where the first time derivative of the length of the connector L is equal to the velocity of the prismatic joint of the connector

$$\dot{L} = V_3$$

The equation of motion for the mass M_e is

$$F_a = M_e \left[\ddot{E} + g \, s_{3z} + E \omega_1^2 (s_{3x})^2 - E \left(\omega_1^2 + \omega_2^2 \right) \right] + C_t \dot{E} + K_1 \delta_1 \qquad (26)$$

The last six equations of motion can be obtained by using the auxiliary equations derived in Chapter 4

$$F_L = C_d (\dot{D} - \dot{L}) + C_c (\dot{H} - \dot{L}) + K_c \delta_c \qquad (27)$$

$$K_L \delta_L = C_c (\dot{H} - \dot{L}) + K_c \delta_c \qquad (28)$$

These auxiliary equations can be used eliminate the displacement δ_L from equation (26) and relate the connector forces to the actuator forces. First use equation (28) to eliminate the coupling stage displacement and velocity from equation (27)

$$F_L = C_d (\dot{D} - \dot{L}) + K_L \delta_L$$

Now rearranging in terms of the displacement δ_L

$$K_L \delta_L = F_L - C_d (\dot{D} - \dot{L})$$

By substituting the above equation into equation (26) and rearranging, the following expression for the connector force F_L is obtained

$$F_L = Fa - C_t \dot{E} + C_d(\dot{D} - \dot{L}) + M_e \left[E \left(\omega_1^2 (1 - (s_{3x})^2) + \omega_2^2 \right) - \ddot{E} - g s_{3z} \right] \quad (29)$$

Which can also be written in terms of the actuator force

$$Fa = F_L + M_e \left[\ddot{E} + g s_{3z} - E \left(\omega_1^2 (1 - (s_{3x})^2) + \omega_2^2 \right) \right] + C_t \dot{E} - C_d(\dot{D} - \dot{L})$$

This equation indicates that the actuator has not only has to produce the required connector force, it also has to accelerate the mass M_e and work against the decoupling damper and the internal friction of the actuator.

6.4 Development of the Dynamic Simulation Software

The objective of this algorithm is to determine the required actuator forces, power and frequency response for a given spatial parallel manipulator performing a desired motion or task. Parameters such as the dimensions, platform mass, connector stiffness and transmission damping coefficients (see Chapter 2 for more details on all the parameters) must be specified by the user. The numerical algorithm for the computer simulation of the inverse dynamic behavior will be developed.

6.4.1 Static Solution

The initial or static conditions must be calculated before the running the dynamic simulation. The initial conditions consist of the position and orientation of the platform; the length and orientation of each of the connectors; the position of the rigid bodies on each connector; and the initial actuator forces. The initial position and orientation of the platform are specified before running the simulation program, with this information the connector lengths and orientations can be determined. The length of the fixed mass of the connector,

bl , is a fixed length and is determined when designing the connectors. The initial positions of the actuator and decoupling stage (as described by the displacements E and D) and the actuator forces can be determined by a static analysis of the manipulator.

The equations of motion can be used for the static analysis of the manipulator by simply setting all the velocities and acceleration to zero (except of the gravitational acceleration). The connector static forces can thus be calculated using equation which reduces to

$$\sum_{i=1}^{6} \left(F_L \hat{\underline{S}}_3 \right)_i = \begin{bmatrix} \underline{F}_{ext}(0) \\ \underline{T}_{ext}(0) \end{bmatrix} + \begin{bmatrix} M_p g \\ 0 \end{bmatrix} \tag{30}$$

Here $\underline{F}_{ext}(0)$ and $\underline{T}_{ext}(0)$ are the static external force and torque vectors, which depend on the desired task as outlined in Chapter 4. Equation (30) is a system of six scalar equations that can be solved to determine the static connector forces F_L. The static actuator displacement can be solved by using the static connector forces and equations (27) and (28)

$$E = \left(L - l_{Lo} - l_{co} \right) + \frac{F_L}{K_c + K_L} \tag{31}$$

where l_{lo} and l_{co} are the the free length of the K_L and K_c respectively. The decoupling stage static displacement is given by

$$D = l_{db} - \frac{M_d g \, s_{3z}}{K_d} \tag{32}$$

where l_{do} is the free length of K_c. The static actuator forces can be determined by using equation (29) with all the velocities set to zero

$$Fa = F_L + M_e g \, s_{3z} \tag{33}$$

For a dynamic simulation, the static solution is equivalent to the initial conditions when the initial velocities and accelerations are very small.

6.4.2 External Wrench

The expressions for the external forces and torques were derived in Section 4.2. For the mirror polishing task the external wrench is calculated using

$$\widehat{\underline{W}}_{ext} = \begin{bmatrix} -F_n(\underline{Z}_m + \mu\underline{t}) \\ a\underline{Z}_m \times (-F_n\mu\underline{t}) \end{bmatrix} \tag{34}$$

where F_n is the normal or contact force, μ is the coefficient of friction, "a" is the distance from the point of contact to the centerpoint of the platform, and $\underline{t}$ is the direction of travel. For a rectilinear motion the axis of translation $\underline{w}$ is the direction of travel, for curvilinear motion the direction of travel is given by

$$\underline{t} = \underline{Z}_m \times \underline{s}$$

The external wrench for machining is given by

$$\widehat{\underline{W}}_{ext} = \begin{bmatrix} -F_{cutting}\,\underline{t} \\ a\underline{Z}_m \times (-F_{cutting}\,\underline{t}) \end{bmatrix} \tag{35}$$

where $F_{cutting}$ is the cutting force.

6.4.3 Numerical Solution

The equations of motion are a set of nonlinear differential equations. The analytical solutions for these type of equations can prove to be tedious and complex as well as the implementation of the numerical solutions [28]. An alternate approach is to use some approximate method which involves difference equations and to use small time steps.

One of these approaches is the Euler Method for numerically solving the differential equations. This method involves calculating a new estimate for the highest order time derivative based on previous values of the other derivatives. The new estimate for the highest time derivative is then used to calculate new estimates for the lower order time derivatives. Using the equation of motion for the decoupling stage, given by equation

(25), the new estimate for the acceleration can be written as

$$\ddot{D}_{new} = \frac{M_d \, D_{old}\left[\left(\omega_{1,\,new}^2 + \omega_{2,\,new}^2\right) - \omega_{1,\,new}^2 \left(s_{3x,\,new}\right)^2\right]}{M_d} -$$

$$\frac{M_d g \, s_{3z,\,new} + C_d\left(\dot{D}_{old} - V_{3,\,new}\right) + K_d \delta_{d,\,old}}{M_d} \tag{36}$$

New values are used for the angular velocities ω_1 and ω_2, for the connector velocity V_3 and the line coordinates $\underline{s}_3$ since these can be determined by the inverse kinematic analysis. The use of the latest values will improve the estimate for the acceleration. Using this new estimate for the acceleration, a new estimate for the velocity and displacement of the decoupling stage can be obtained

$$\dot{D}_{new} = \ddot{D}_{new} \, \Delta t + \dot{D}_{old} \tag{37}$$

$$D_{new} = \dot{D}_{new} \, \Delta t + D_{old} \tag{38}$$

where Δt is the time step or increment used in the numerical method. The size of the time step selected must be 5 to 10 times smaller than the shortest event to be considered [29]. Using the equation of motion for the connector's equivalent mass, given by equation (29), the new estimate for the acceleration can be written as

$$\ddot{E}_{new} = \frac{Fa_{old} - F_{1,\,old} - C_t \, \dot{E}_{old} - C_d\left(\dot{D}_{old} - V_{3,\,new}\right)}{M_e} +$$

$$\left[E_{old}\left(\omega_{1\,new}^2\left(1 - \left(s_{3x,\,new}\right)^2\right) + \omega_{2,\,new}^2\right) - g \, s_{3z,\,new}\right] \tag{39}$$

Using this new estimate for the acceleration, a new estimate for the velocity and displacement of the actuator can be obtained

$$\dot{E}_{new} = \ddot{E}_{new}\, \Delta t + \dot{E}_{old} \qquad (40)$$

$$E_{new} = \dot{E}_{new}\, \Delta t + E_{old} \qquad (41)$$

The new values for the connector forces F_L can be determined by using equation (24)

$$\sum_{i=1}^{6} \left(F_{L,\,new}\,\hat{\underline{S}}_{3,\,new} \right)_i = \widehat{\underline{W}}_{ext,\,new} + \widehat{\underline{W}}_{p,\,new} + \widehat{\underline{W}}_{gr,\,new} +$$

$$\widehat{\underline{W}}_{tan,\,new} + \widehat{\underline{W}}_{cor,\,new} + \widehat{\underline{W}}_{cent,\,new} \qquad (42)$$

The six wrenches on the right hand side of this equation are given by

$$\widehat{\underline{W}}_{p,\,new} = \begin{bmatrix} M_p(\underline{A}_{c,\,new} + \mathbf{g}) \\ \underline{\alpha}_{new} \cdot I_p{}^n + (\underline{\omega}_{new} \times I_p{}^n \cdot \underline{\omega}_{new}) \end{bmatrix} \qquad (42.a)$$

$$\widehat{\underline{W}}_{gr,\,new} = \sum_{i=1}^{6} \left[\frac{g\,[\,M_e E_{new} + M_d D_{new} + M_b\,bl\,]}{L_{new}}\; s_{2z,\,new}\,\hat{\underline{S}}_{2,\,new} \right]_i +$$

$$\sum_{i=1}^{6} \left[\frac{g\,[\,M_e E_{new} + M_d D_{new} + M_b\,bl\,]}{L}\; s_{23z,\,new}\,\hat{\underline{S}}_{23,\,new} \right]_i \qquad (42.b)$$

$$\widehat{\underline{W}}_{tan,\,new} = \sum_{i=1}^{6} \left[\frac{M_e E^2_{new} + M_d D^2_{new} + M_b\,bl^2}{L_{new}}\; \alpha_{1,\,new}\,\hat{\underline{S}}_{2,\,new} \right]_i +$$

$$\sum_{i=1}^{6} \left[\frac{\Pi_{xx}\,s_{23x,\,new}{}^2 + \Pi_{zz}\,s_{3x,\,new}{}^2}{L_{new}}\; \alpha_{1,\,new}\,\hat{\underline{S}}_{2,\,new} \right]_i +$$

$$\sum_{i=1}^{6} \left[\frac{M_e E^2_{new} + M_d D^2_{new} + M_b\,bl^2 + \Pi_{xx}}{L_{new}}\; \alpha_{2,\,new}\,\hat{\underline{S}}_{23,\,new} \right]_i \qquad (42.c)$$

$$\widehat{\underline{W}}_{cor,\ new} = \sum_{i=1}^{6} \left[\frac{2\left[M_e \dot{E}_{new}\ E_{new} \right]}{L_{new}} \left[\omega_{1,\ new}\ \underline{S}_{2,\ new} + \omega_{2,\ new}\ \underline{S}_{23,\ new} \right] \right]_i +$$

$$\sum_{i=1}^{6} \left[\frac{2\left[M_d \dot{D}_{new}\ D_{new} \right]}{L_{new}} \left[\omega_{1,\ new}\ \widehat{\underline{S}}_{2,\ new} + \omega_{2,\ new}\ \underline{S}_{23,\ new} \right] \right]_i \qquad (42.d)$$

$$\widehat{\underline{W}}_{cent,\ new} = \sum_{i=1}^{6} \left[\frac{s_{3x,\ new}\ s_{23x,\ new}\left(M_e E_{new}^2 \right)}{L_{new}} \omega_{1,\ new}^2\ \widehat{\underline{S}}_{23,\ new} \right]_i +$$

$$\sum_{i=1}^{6} \left[\frac{s_{3x,\ new}\ s_{23x,\ new}\left(M_d D_{new}^2 + M_b\ bl^2 \right)}{L_{new}} \omega_{1,\ new}^2\ \underline{S}_{23,\ new} \right]_i +$$

$$\sum_{i=1}^{6} \left[\frac{2 s_{3x,\ new}\left(M_e E_{new}^2 + M_d D_{new}^2 + M_b\ bl^2 \right)}{L_{new}} \omega_{1,\ new}\ \omega_{2,\ new}\ \widehat{\underline{S}}_{2,\ new} \right]_i +$$

$$\sum_{i=1}^{6} \left[\frac{s_{3x,\ new}\left(\Pi_{xx} - \Pi_{zz} \right)}{L_{new}} \omega_{1,\ new}^2\ \widehat{\underline{S}}_{23,\ new} \right]_i +$$

$$\sum_{i=1}^{6} \left[\frac{s_{3x,\ new}\ s_{23x,\ new}\left(\Pi_{zz} - \Pi_{xx} \right)}{L} \omega_{1,\ new}\ \omega_{2,\ new}\ \widehat{\underline{S}}_{2,\ new} \right]_i \qquad (42.e)$$

Once the wrenches are calculated, the connector forces are determined by solving equation (42) using a numerical solution for a system of linear equations [28].

The new estimate for the actuator force can be calculated with the equation (29)

$$Fa_{new} = F_{L,\ new} + C_t\ \dot{E}_{new} - C_d\left(\dot{D}_{new} - V_{3,\ new} \right) + M_e\ \ddot{E}_{new} +$$

$$M_e\left[g\ s_{3z,\ new} + E_{new}\left(\omega_{1,\ new}^2 \left(\left(s_{3x,\ new} \right)^2 - 1 \right) - \omega_{2,\ new}^2 \right) \right] \qquad (43)$$

The required power output/input for each actuator can be calculated using the following equation

$$\text{Power}_{new} = Fa_{new}\,\dot{E}_{new} \qquad (44)$$

6.5 The Dynamic Simulation Software

Prior to executing the manipulator dynamic simulation software, the user has to provide the motion and task planning parameters; the geometric parameters such as the base and platform dimensions; and system parameters such as mass and moments of inertia, spring constants and damping coefficients.

The simulation software was implemented by using the following steps

Part A - Static or Initial Position Solution - The system initial forces and connector location are determined by

1- Calculate the static connector endpoint position using equation (2).

2- Calculate the static connector line coordinates and length using equations (13) and (14)

3- Calculate the static connector forces using equation (30).

4- Calculate the initial displacements E and D using equations (31) and (32).

5- Calculate the static actuator forces using equation (33).

Part B - Dynamic Solution: The actuator force requirements are determined based on the desired motion and task. The initial time is set to $t = 0$.

Part B.1 - Inverse Kinematics: The connector location, velocity and acceleration are calculated using the motion planning parameters.

6- For rectilinear motion determine the connector end point position, velocity and acceleration using equations (2), (3) and (4).

7- For curvilinear motion determine the connector end point position, velocity and acceleration using equations (5) through (12).

8- Calculate the connector line coordinates and length using equations (13) and (14).

9- Calculate the connector velocity vector $\underline{V}_3$ using equation (15).

10- Calculate the connector angular velocity vector $\underline{\omega}_{12}$ using equations (16) to (18).

11- Calculate the connector acceleration vector $\underline{A}_3$ using equation (19).

12- Calculate the connector angular acceleration vector $\underline{\alpha}_{12}$ using equations (20) to (23).

Part B.2 - Inverse Dynamics: The actuator force and power required to generate the desired motion are calculated.

13- Calculate the new acceleration, velocity and displacement of decoupling stage using equations (36) to (38).

14- Calculate the new acceleration, velocity and displacement of actuator using equations (39) to (41).

15- Calculate the external wrench using equation (35).

16- Calculate the new connector forces using equations (42) and (42.a) through (42.e).

17- Calculate the new actuator forces using equation (43).

18- Calculate the actuator power requirements using equation (44).

19- Increase the the time to $t = t + \Delta t$, go to step 6.

The total simulation algorithm is outlined in Figure 6.3. This is the basis for the dynamic simulation software developed using ANSI C [28, 30] as part of this research project and will be further discussed in Chapter 7.
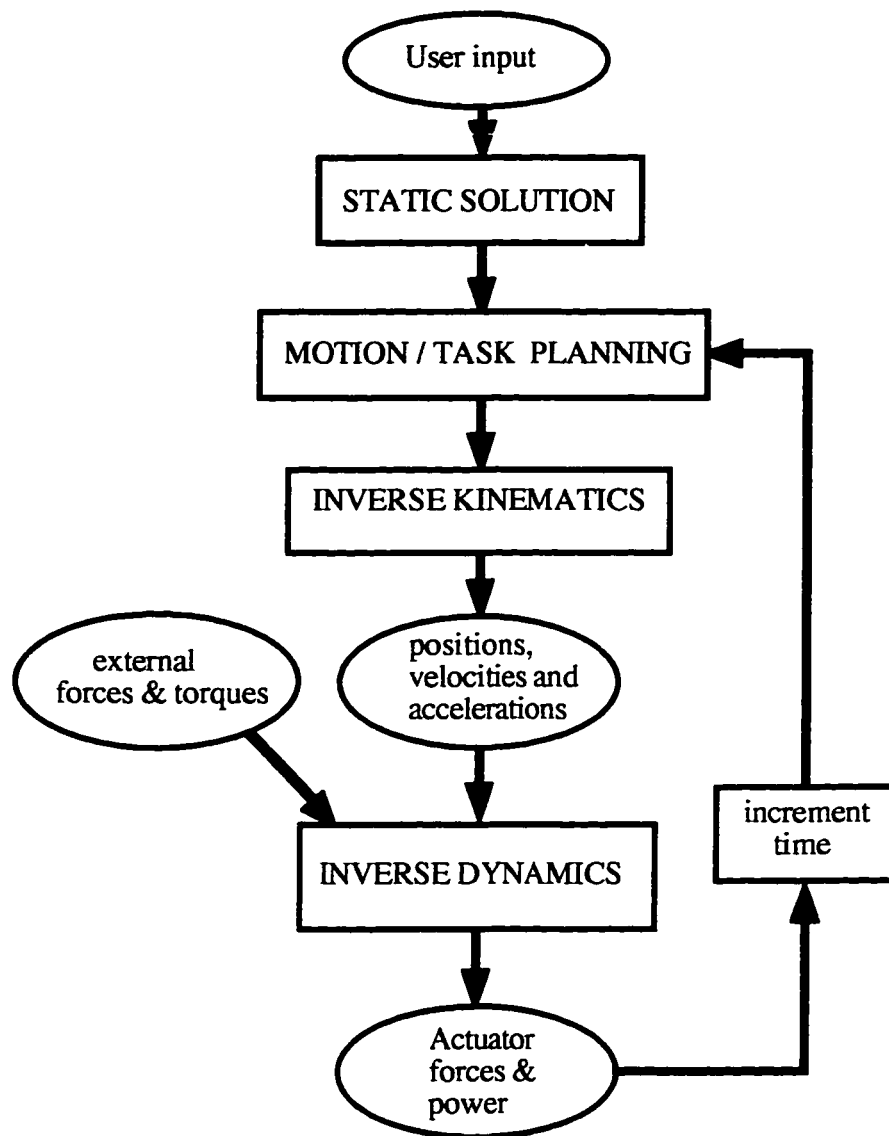
Figure 6.3 - Dynamic Simulation Software

CHAPTER 7
TESTING AND RESULTS

The dynamic simulation software allows the the designer to determine the actuator requirements for a manipulator performing a desired task or motion. The first goal of testing this software is to gain some understanding of the dynamic behavior of parallel manipulators. As indicated in Chapter 5, section 5.6, the dynamic model can be written as:

$$\sum_{i=1}^{6} \left(F_1 \, \hat{\underline{S}}_3 \right)_i = \widehat{\underline{W}}_{ext} + \widehat{\underline{W}}_p + \widehat{\underline{W}}_{gr} + \widehat{\underline{W}}_{tan} + \widehat{\underline{W}}_{cor} + \widehat{\underline{W}}_{cent}$$

The last four terms of this equations describe the coupling effects between the connectors. These terms can be grouped into an equivalent coupling wrench as:

$$\widehat{\underline{W}}_{couple} = \widehat{\underline{W}}_{gr} + \widehat{\underline{W}}_{tan} + \widehat{\underline{W}}_{cor} + \widehat{\underline{W}}_{cent}$$

This coupling wrench is a function of the system geometry, the system parameters and the desired motion or task to be implemented with the platform:

$$\widehat{\underline{W}}_{couple} = \sum_{i}^{6} f\left(\left[\hat{\underline{S}}_3, \, \underline{\omega}_{12}, \, \underline{\alpha}_{12}, \, E, \, \dot{E}, \, D, \, \dot{D}, \, bl, \, L, \, M_e, \, M_d, \, M_{bl}, \, Ie", \, Id", \, Ib" \right]_i \right)$$

The actuator requirements (forces, power and frequency response) are a function of the coupling wrench and therefore a function of the geometry, the system parameters such as masses and spring constants, and the desired motion or task.

The test results will help to gain some understanding of the dynamic behavior of the system. Since the equations of motion are a function of so many different parameters, it is very difficult to asses the effect of all the possible parameter variations. This is why only

146

some combinations will be tested, enough to understand the dynamics of the system and help identify some relevant factors affecting such behavior.

The second objective is to demonstrate the usefulness of this software as integral part of a CAE tool for the design of parallel manipulators as mentioned in Section 1.4. By evaluating the effect of different parameters on the dynamic behavior of the system, this software will assist the designer in the process of developing a parallel manipulator.

7.1 System Geometrical Description

The system geometry is determined by the location of the connector base and end points, which are a function of the platform and base dimensions, and the reference location of the platform with respect to the base as mentioned in Section 3.3. The connector base point B is the point at which the connector and the base are joined together by a Hooke joint. The connector end point P is the the point at which the connector and the platform are joined together by a spherical joint.

The geometry of the base and platform can be described in different ways [9, 10, 11] such as the one shown in Figure 7.1 which describes a general six-six platform. The designation six-six indicates that each base point is at different location, and each end point is at different location (no common points). All the base points are on a circle of radius r_b.
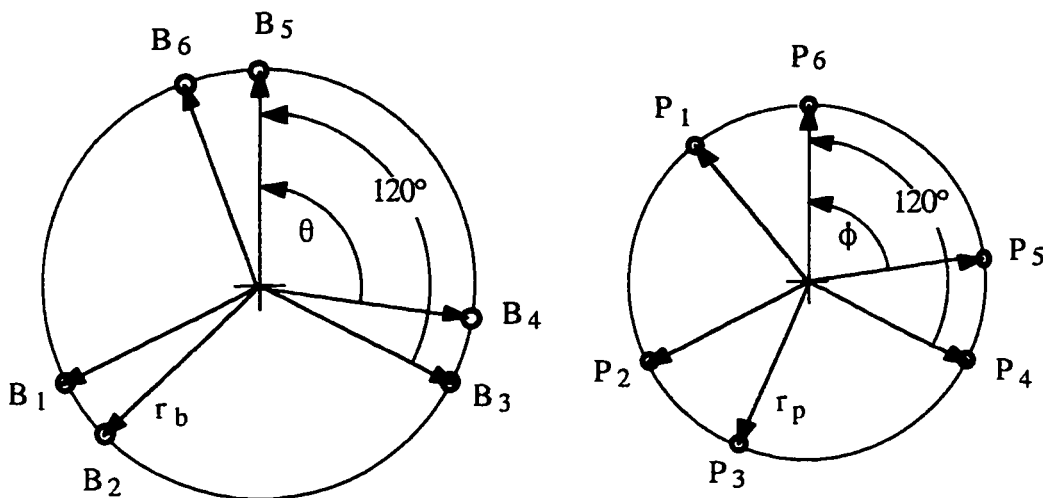
Figure 7.1 - Base and Platform Geometry
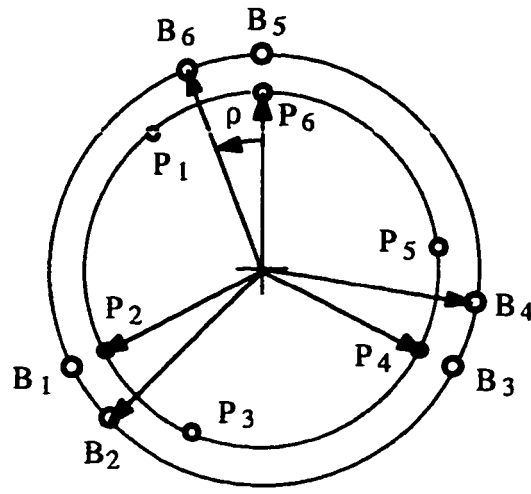
Figure 7.2 - Orientation of the platform with respect to the base

The location of each base point is determined by the radius r_b and the angle θ as shown in

Figure 7.1. A similar arrangement is used for each end point position on the platform. In

the case of the platform, the radius r_p and the angle ϕ are used. The location of the

platform with respect to the base is specified by the angle ρ as shown in Figure 7.2.

The geometry used for testing the dynamic simulation algorithm is shown in Figure 7.3.

This geometry has been proposed by [2, 16] and its simplifies the forward kinematic

analysis considerably. All the base and end points are located on the sides or vertices of

equilateral triangles. The geometry is determined by the dimension called SIDE and the

scaling factors BSIDE, TSCALE and TSIDESCALE as shown in Figure 7.4. The

connecting arrangement is shown in Figure 7.5. The reference or home position of the

platform with respect to the base is determined by locating the platform parallel to the base.

The centerpoint of the platform is at a distance H along the $\underline{Z}$ axis as shown in Figure 7.6.

This distance is a function of SIDE and the scaling factor HSCALE. The following values

for SIDE and the scaling factor are used for all the simulation test cases: SIDE = 4 ft ,

BSCALE = 1.05, TSIDESCALE = 0.625 and TSCALE = 0.55. The geometry of the

system will be varied by changing the reference position using the scaling factor HSCALE.
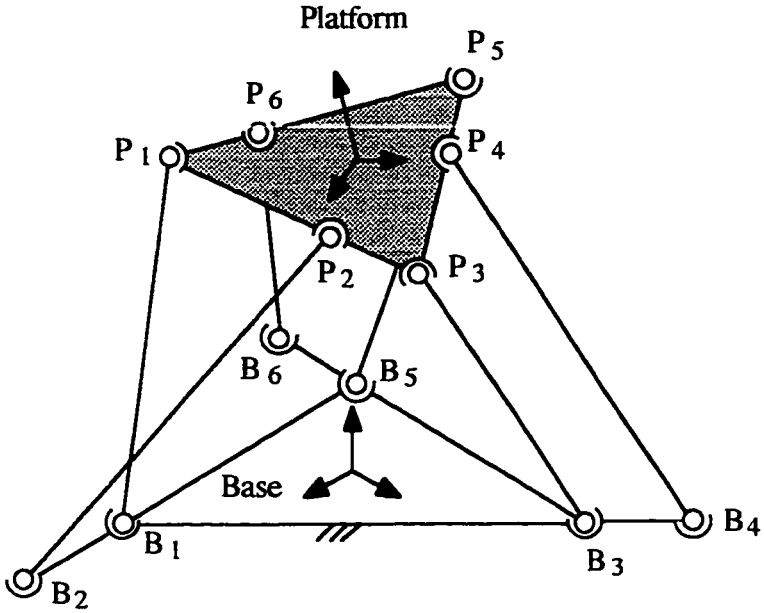
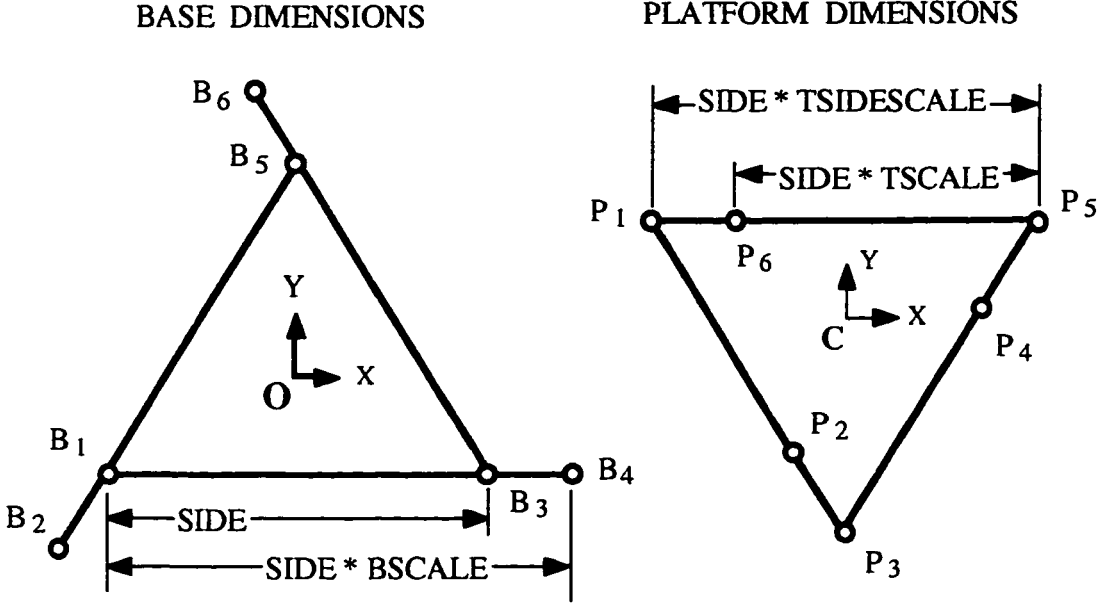Figure 7.3 - Manipulator Geometry used for testing

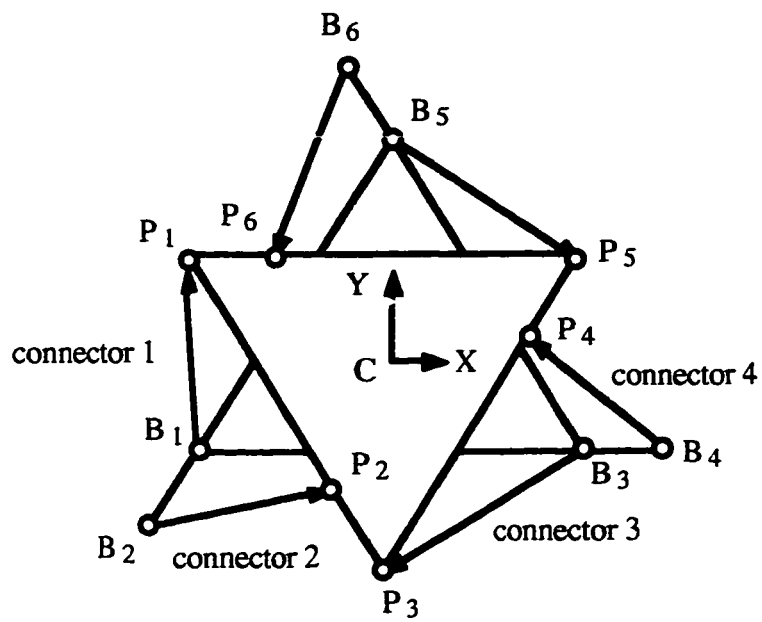Figure 7.4 - Base and platform geometry used for testing

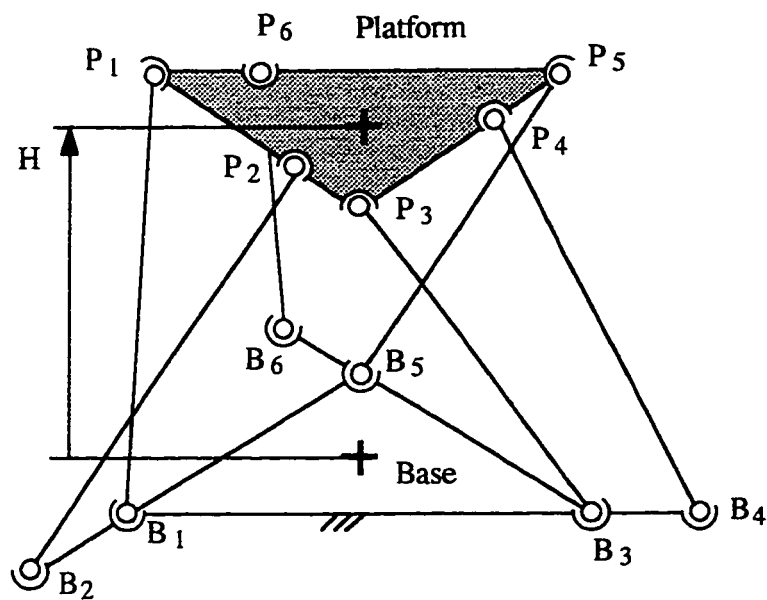Figure 7.5 - Top View of the base and platform geometry used for testing

Figure 7.6 - Platform reference position

In general all the base points are constrained to be in the same plane. An interesting possibility is to locate the base points on different planes as shown in Figure 7.7. In this particular arrangement, three base points are in one plane and the remaining three base points are in another plane. For the test cases three of the base points will be in one plane, the other three will be in parallel plane at a distance b as shown in Figure 7.8. The location of the base points will be similar to the geometry used for when all the points are coplanar as shown in Figure 7.8.

In summary, the geometric variations that will be used for the testing of the software are changes of the platform reference height H and changes in the distance between base point planes, b. The change of the values H and b will change the connector line coordinates $\underline{s}_3$ and the connector unit vectors $\underline{s}_2$ and $\underline{s}_{23}$ as mentioned in Section 3.3. This affects the actuator requirements since many of the terms of the equations of motion are functions of these unit vectors. These variations are by no means the only possible geometric variations, there are infinite combinations of geometric variations that can be used. These tests are conducted to understand some of the relationships between the geometric parameters and the dynamic behavior of the system.

7.2 System Parameters

As mentioned previously, the system parameters include the masses and the moment of inertia of the platform and the connector rigid bodies; the spring constants of the coupling stage, the decoupling stage and the connector itself; and the damping coefficients of the coupling and decoupling stages (see Chapter 2). As in the case of the manipulator geometry there are an infinite number of combinations of these parameters that can be used for testing the dynamic simulation algorithm, but such wide range of tests is beyond the scope of this project. The purpose here is to vary some of the system parameters in order to understand their effects on the actuator requirements.
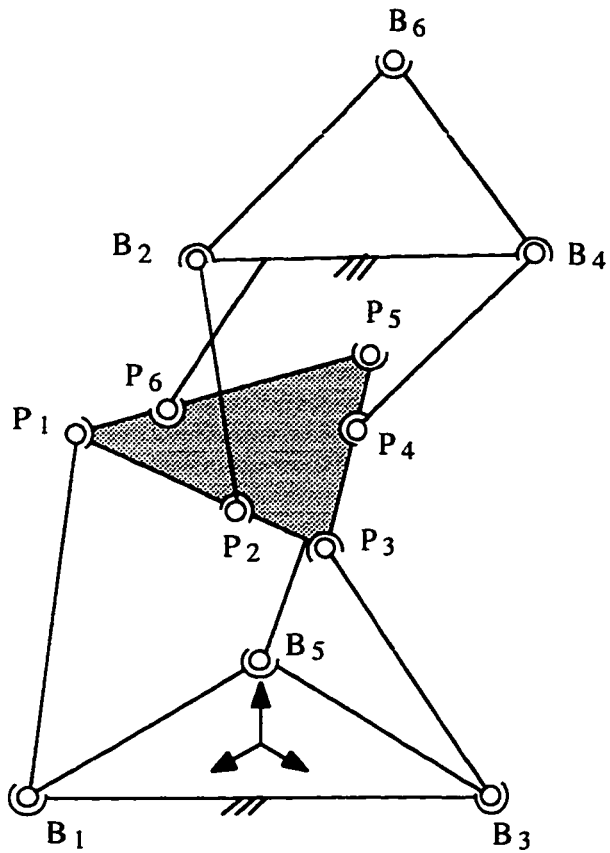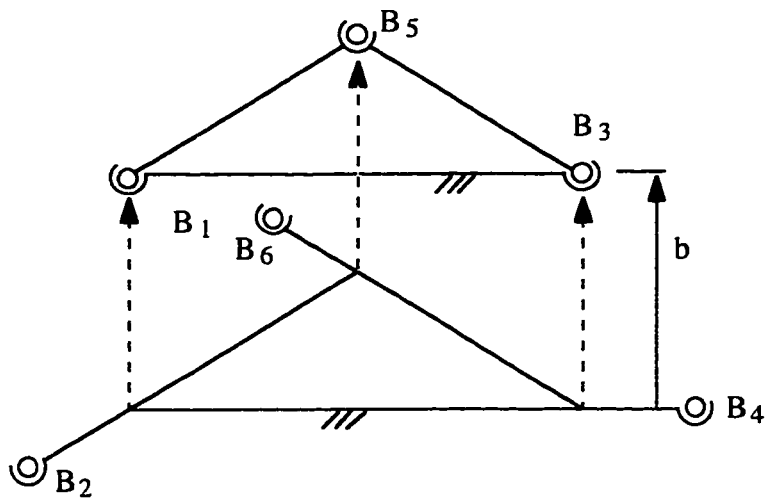
Figure 7.7 - Relocated base points

Figure 7.8 - Location of base points in two parallel planes

7.2.1 Inertial Parameters

The platform mass and moment of inertia are determined by modeling the platform as a thin disk made out of aluminum with a radius of 1.5 ft and 0.5 inches thick. These dimensions are in proportion with the dimensions of the base and platform selected. Using this information, the inertial parameters of the platform are

$$M_p = 50 \text{ lbs}; \quad Ip_{zz} = 30 \text{ lbf - ft}^2; \quad Ip_{xx} = Ip_{yy} = 60 \text{ lbf - ft}^2$$

The inertial parameters for the actuator and the decoupling stage damper present more of a challenge to determine. The main reason is that these parameters depend on the actuator dimensions and requirements which in turn depend on the results of the dynamic simulation. This problem will be circumvented by making a conservative assumption. The decoupling damper will be assumed to be solid steel cylinder of 2.5 inches in diameter and 8 inches long. The actuator moving mass and fixed mass will be assumed to be a solid steel cylinder of 2.5 inches in diameter and 4 inches long. Using these assumptions, the inertial parameters for these elements are

$$M_e = M_b = 7.5 \text{ lbs}; \quad Ib_{zz} = Ie_{zz} = 1 \text{ lbf - ft}^2; \quad Ib_{xx} = Ie_{xx} = Ie_{yy} = 2 \text{ lbf - ft}^2$$

$$M_d = 15 \text{ lbs}; \quad Id_{zz} = 2 \text{ lbf - ft}^2; \quad Id_{xx} = Id_{yy} = 4 \text{ lbf - ft}^2$$

One of the objectives of using such conservative estimates is to obtain the worst case actuator requirements.

7.2.2 Spring Constants and Damping Coefficients

The type of tasks used for the simulation tests do not involve high frequency disturbances (see Section 2.5), therefore the decoupling stage will be deactivated. The values used for the spring constant and the damping coefficient of decoupling stage are

$$C_d = 0 \frac{\text{lbf}}{\text{ft - sec}} \quad ; \quad K_d \Rightarrow \infty$$

Since the decoupling stage is deactivated, the decoupling stage mass does not change its displacement D along the direction $\underline{s}_3$. The decoupling stage is located at 1.25 ft from the base of the connector which is enough to accommodate the height, base and platform dimensions.

The tasks used for testing do not require implicit force control, therefore the coupling stage is also deactivated (see Section 2.5). The connector will also be assumed to be infinitely rigid and the transmission will assumed to be frictionless. The reason for neglecting the actuator/transmission friction is that upon further examination and some initial results of the dynamic simulation, it was determined that the actuator model to be incomplete. The main reason being that most actuators are not back drivable or present very high resistance to externally imposed motions (specifically the hydraulic actuators). More descriptive actuator models should be considered in future work.

The net effect of deactivating the coupling stage and making the connector extremely stiff is that the velocity and acceleration of the actuator will be the same as the $\underline{V}_3$ and $\underline{A}_3$ terms derived in Sections 3.4 and 3.5 respectively. The displacement E is then given by

$$E = L - l_{lo}$$

where l_{lo} is the free length of K_L, which is in this case is assumed to be 1.25 ft long.

7.3 Motion and Task Planning for Testing

Two different types of motions or tasks are used for testing the dynamic simulation software. The platform will be used in a machining process to support and move a 150 lb workpiece. A full groove will be cut with a four tooth end mill as explained in Section 4.1.2. The cutting force is assumed to be 200 lbf and the workpiece is to be taken through rectilinear and curvilinear motions as explained in Chapter 3, section 3.6.

7.3.1 Rectilinear Motion

The first motion to be used for machining the workpiece is a rectilinear motion parallel to the XY plane at a distance H from the base as shown in Figure 7.9, along the axis of translation $\underline{w}$ which is at an angle θ with the $\underline{X}$ axis as shown in Figure 7.10. The platform starts moving from point $\underline{C}_o$, moves a distance of ΔS along the direction of
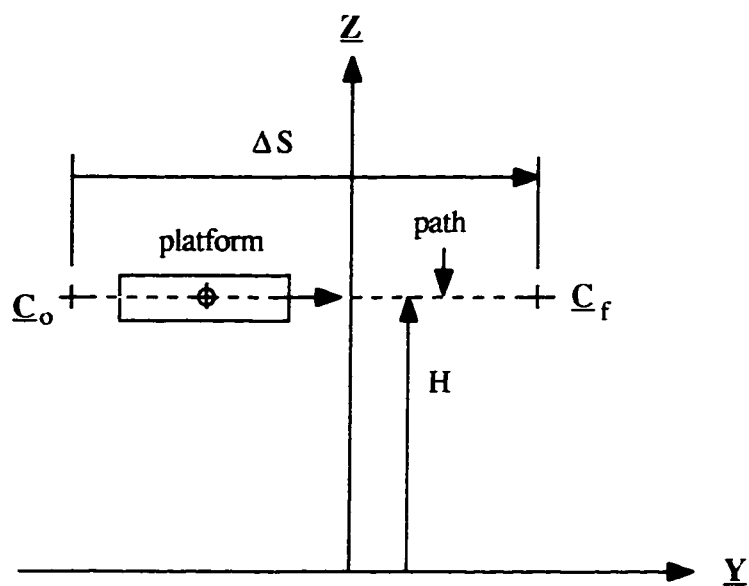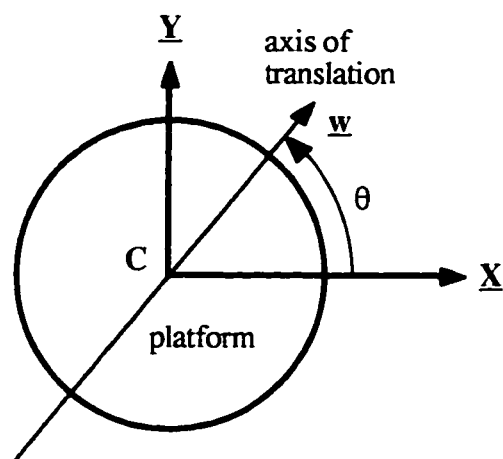
Figure 7.9 - Rectilinear Motion for machining
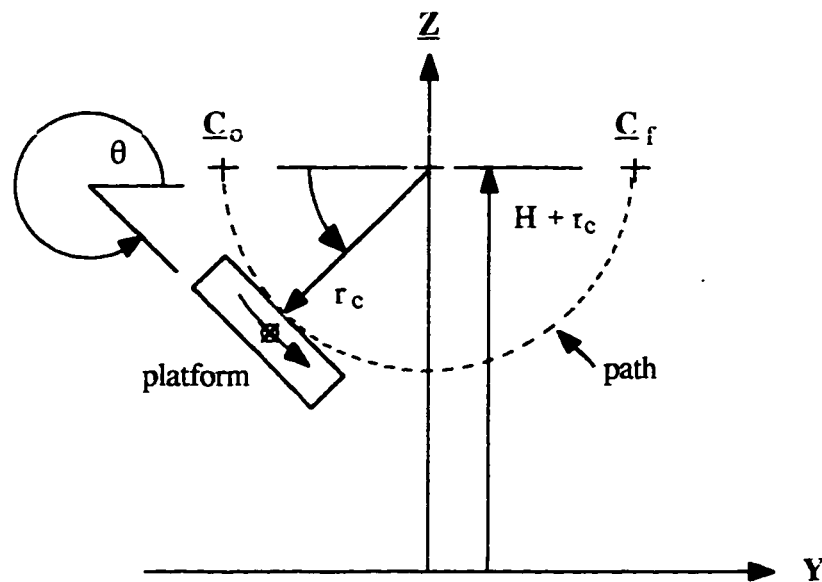
Figure 7.10 - Axis of Translation for the Platform

Figure 7.11 - Curvilinear Motion for Machining

motion in a period of time T and completes its motion at point $\underline{C}_f$. The workpiece will be machined throughout the complete motion.

7.3.2 Curvilinear Motion

The second motion to be used for machining the workpiece is a curvilinear motion in the YZ plane. The radius of curvature r_c is 0.5 ft, the axis of rotation $\underline{s}$ is parallel to the $\underline{X}$ axis and intersects the $\underline{Z}$ axis at a distance $H + r_c$ from the base as shown in Figure 7.11. The initial orientation of the platform is $-90°$, and it rotates $180°$ in a period of time T to end at a orientation of $+90°$. The workpiece will be machined throughout the complete motion and the cutting forces are tangent to the path at all times.

7.4 Test Cases, Results and Discussion

As mentioned before, there are many combinations of parameters that can be used when testing the dynamic simulation software. One of the objectives of the testing is to gain some insight of the dynamic behavior of the platform, not to test as many combinations of parameters as possible. The effect of geometric variations will be explored by changing the

height H and the distance b as discussed in section 7.1. The effect of variations in the system parameters will be evaluated by increasing the mass and moment of inertia of the connector rigid bodies. The effects of variations of the motion planning parameters will be examined by reducing the time period T required for completing the motion, and by changing the type of motion (rectilinear and curvilinear) used.

The required actuator forces will be calculated for each test by the simulation program and displayed. One important condition is that the actuator force requirements must not exceed the maximum force capacity. When this happens, the system is operating in an condition known as an actuator singularity and the desired motion cannot be produced by the manipulator. The possibility of this condition happening will be monitored using the actuator force index λ which is determined by

$$\lambda = \left[\frac{F_{max} - |F|}{F_{max}} \right] \times 100$$

where F_{max} is the maximum force capacity of the actuators and F is the required actuator force. The above equation is similar to the definition of some performance indices used in the area of control theory [29]. The use of the force index λ allows all the actuators of the manipulator to be compared on the same dimensionless scale which might be somewhat difficult by just using the actuator force plots. The force index simplifies identifying actuator saturation; the smaller the force index, the closer the actuator is to being saturated. This index also allows the designer to avoid overdesigning or underdesigning when selecting the actuators.

The determinant of the Manipulator Jacobian [J_m] is also an indicator of possible actuator saturation. When the determinant is zero, the actuators cannot generate the desired motion as discussed in Section 4.5 and will saturate. As the determinant increases in magnitude the less likely the actuators will saturate in general. Since the determinant has units of length^3, it will be divided by the maximum value of the determinant to eliminate the units. Therefore it will become a dimensionless indicator of actuator saturation for the

complete manipulator. This will be a combined inidicator of the effectiveness of all the actuators of the manipulator. This simplifies the task of comparing manipulator designs.

7.4.1 Test Cases with Geometric Variations

The first test cases involve a rectilinear motion of the platform as discussed in section 7.3.1. In the first group of tests the height of the platform was increased from 1 ft to 5 ft, the distance b is zero and the time period T is 30 seconds. The results of these tests are shown in Figure 7.12.

For the rectilinear motion it can be seen that as the height is increased there is a increase in the force requirements for most of the actuators, although actuators 5 and 6 show a reduction in force requirements. This is seen more clearly in the force index plots. This suggests that the general force requirements increase with the height. The lower the height, the greater the s_{3x} and s_{3y} components of each connector as shown in Figure 7.13. This means that the horizontal force components are greater which are desirable for balancing the effect of a horizontal external load, such as the cutting force. The disadvantage is that the connectors will be closer to a configuration where will be partially working against other connectors. The extreme case is when the height is close to zero. When two connectors are totally opposite to each other, one of them is redundant.

As the height increases, the connectors will have greater vertical force components as shown in Figure 7.14 and the possibility of having opposite connectors is virtually eliminated. The disadvantage is that when the connectors have large vertical components the platform will be become very weak in the horizontal plane and very large actuator forces are required to balance an external horizontal load, such a the cutting force. Therefore the platform height should not be increased too much. The effects of further increasing the height of the platform in a rectilinear motion are shown in figure 7.15. It can be seen that the actuator requirements increase as the height is increased. The definition of a what is considered a low or high platform depends on the other factors such as the type of motion and the type of external loads applied.
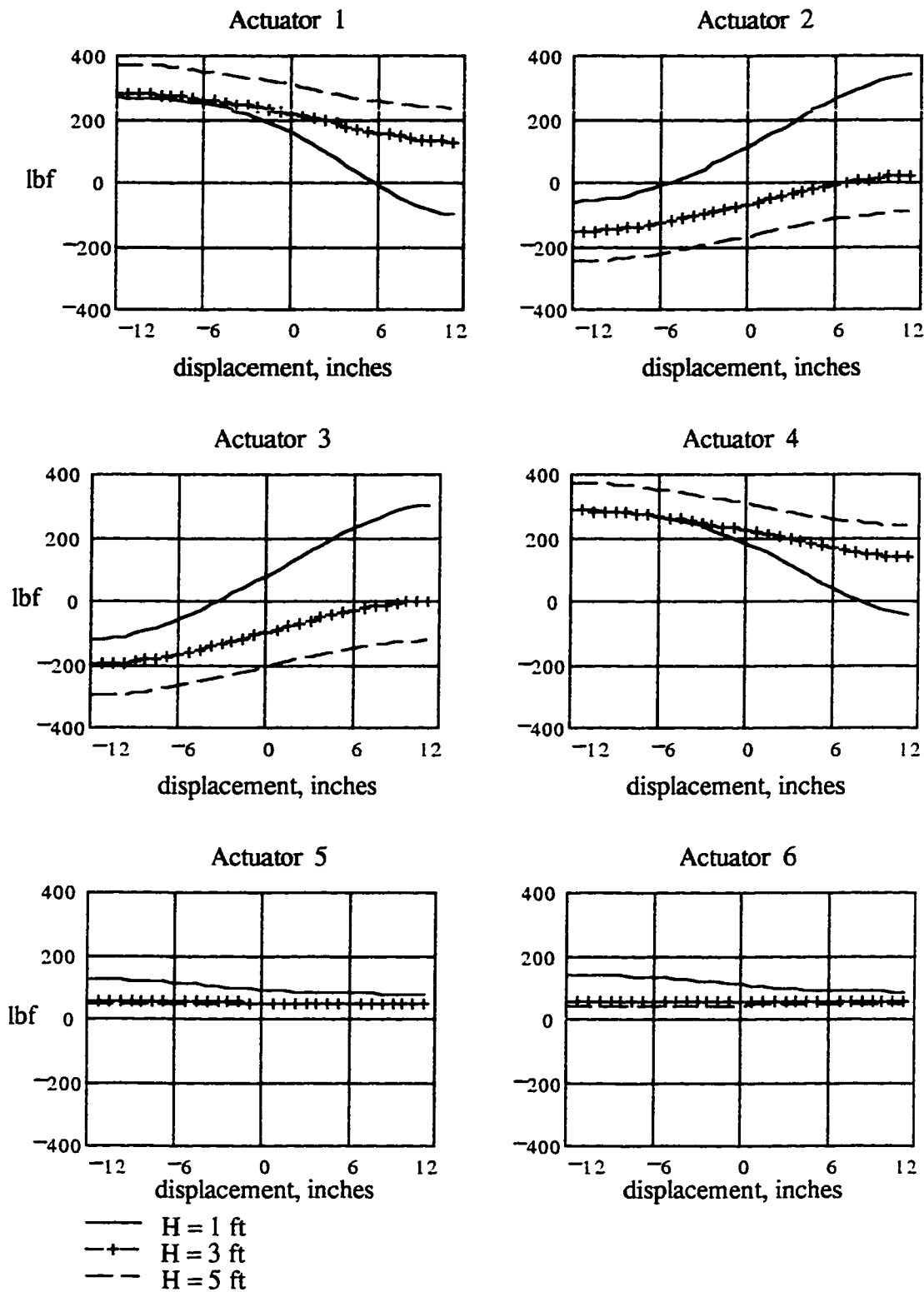
Actuator 1

displacement, inches

Actuator 2

displacement, inches

Actuator 3

displacement, inches

Actuator 4

displacement, inches

Actuator 5

displacement, inches

Actuator 6

displacement, inches

$H = 1$ ft
$H = 3$ ft
$H = 5$ ft

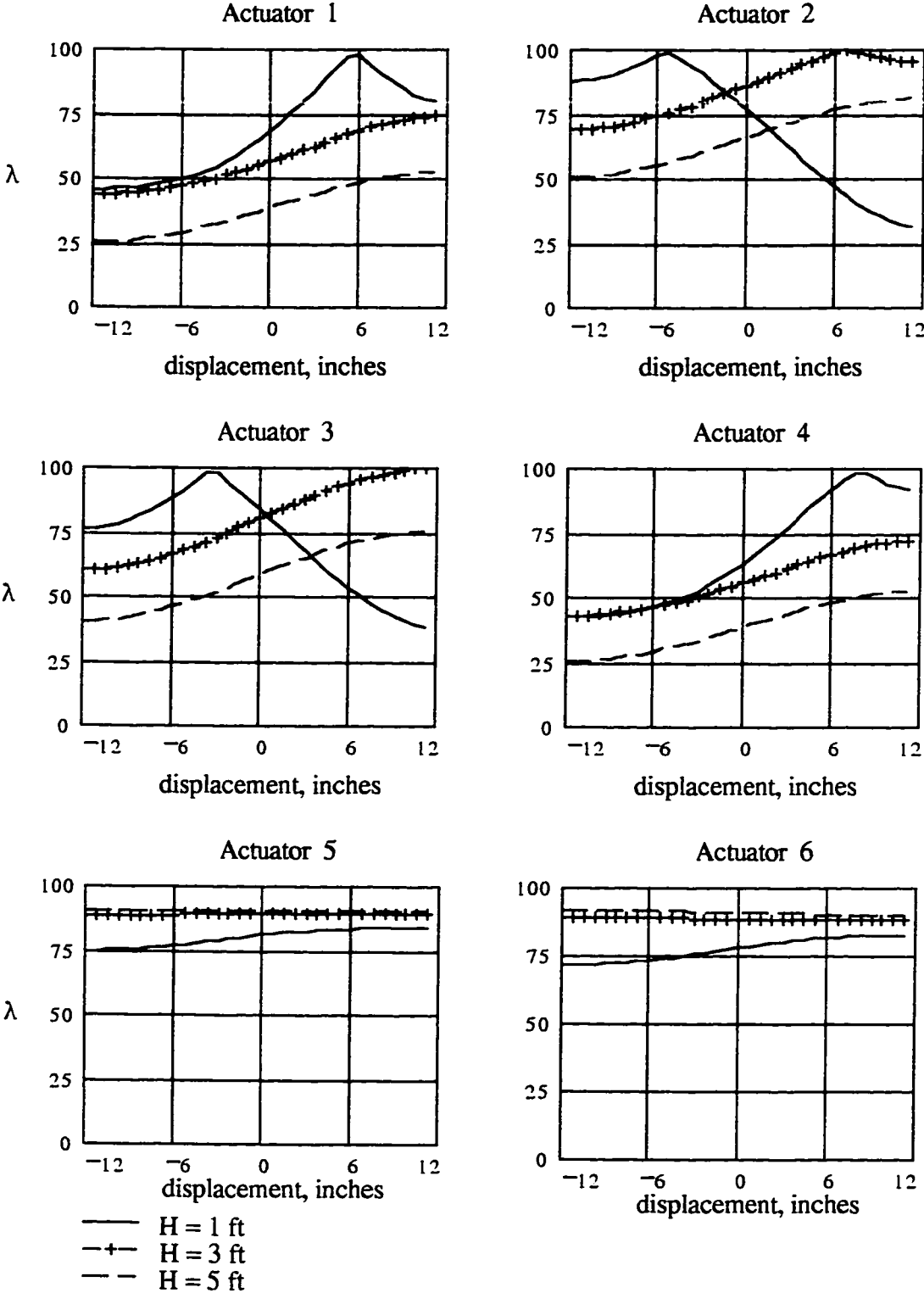Figure 7.12a - Effects of platform height on the actuator forces, rectilinear motion

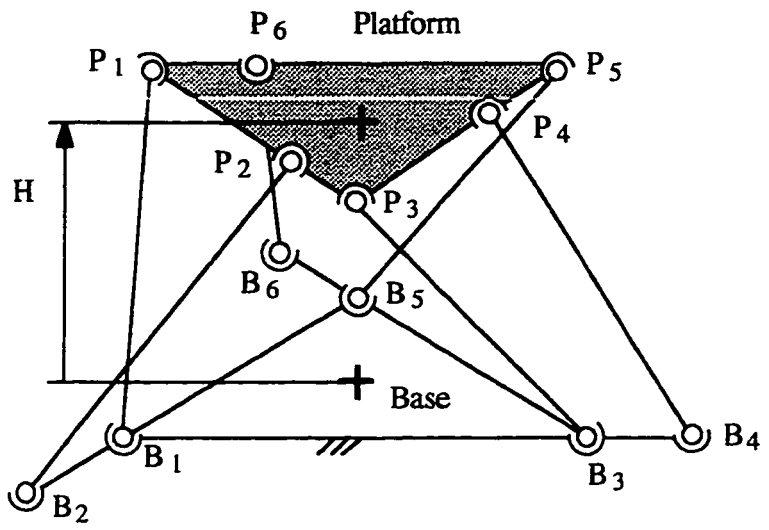Figure 7.12b - Effects of platform height on the force index λ, rectilinear motion
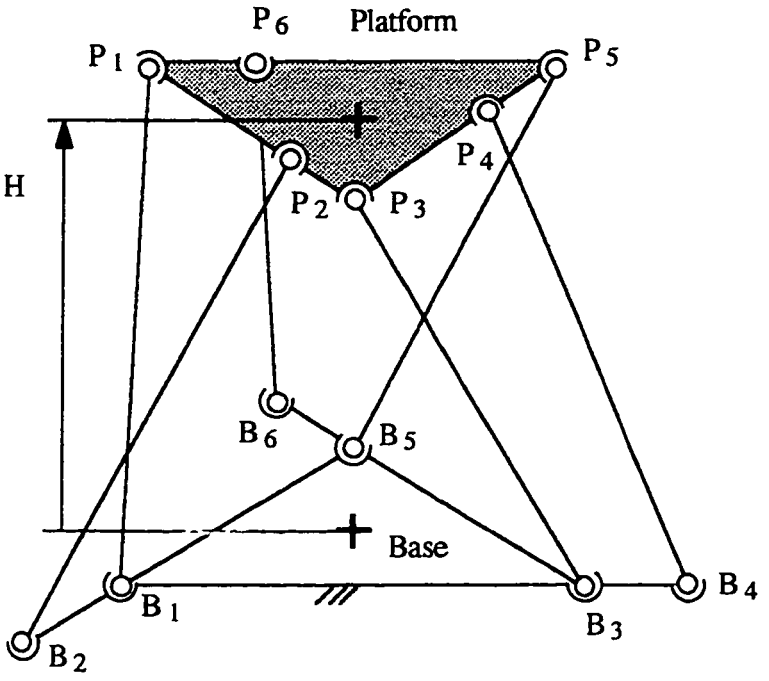
Figure 7.13 - Platform at low heights
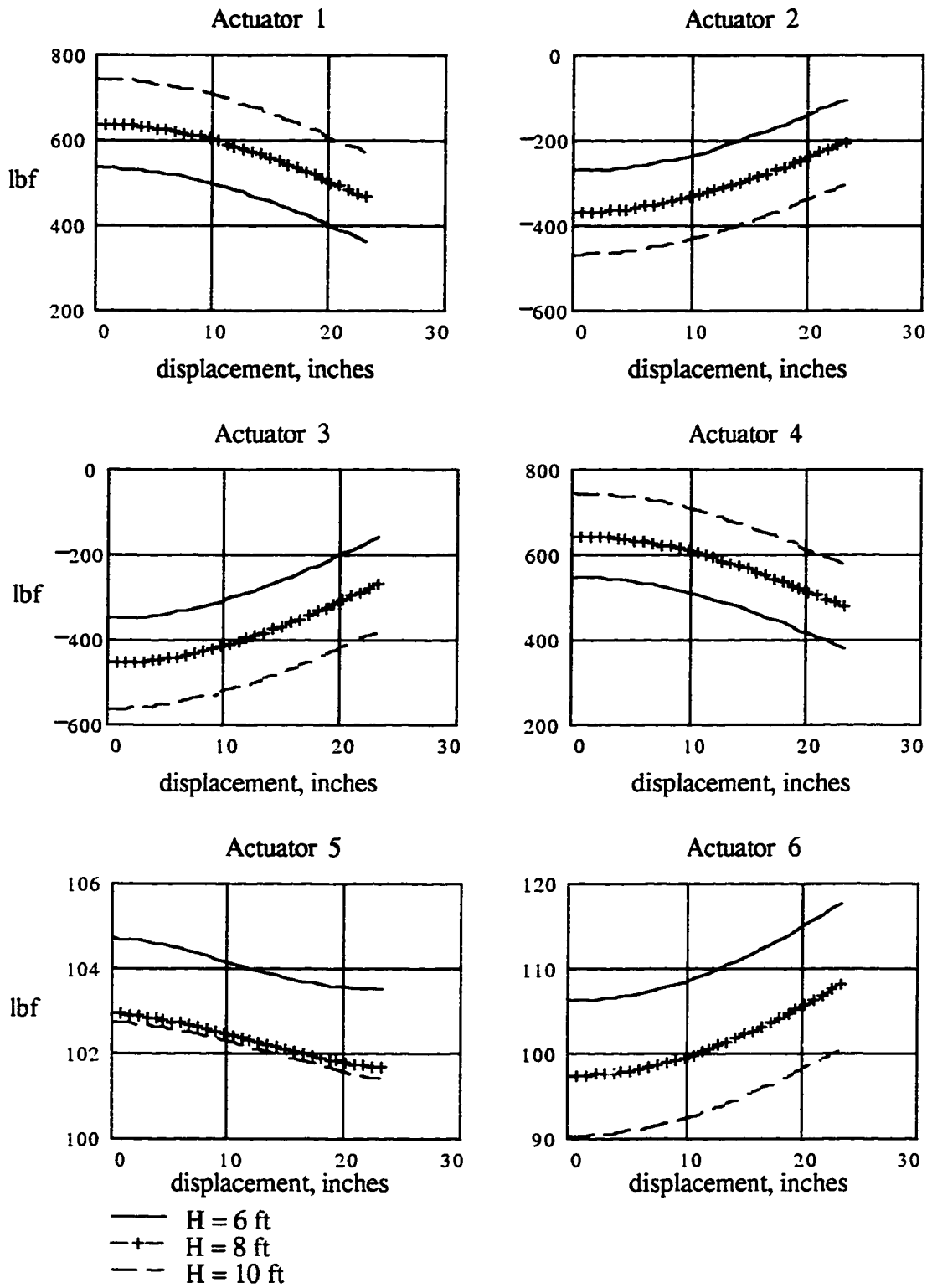

Figure 7.14 - Platform at greater height

Actuator 1

lbf

800

600

400

200

0   10   20   30

displacement, inches

Actuator 2

0

⁻200

⁻400

⁻600

0   10   20   30

displacement, inches

Actuator 3

lbf

0

⁻200

⁻400

⁻600

0   10   20   30

displacement, inches

Actuator 4

800

600

400

200

0   10   20   30

displacement, inches

Actuator 5

106

104

lbf

102

100

0   10   20   30

displacement, inches

Actuator 6

120

110

100

90

0   10   20   30

displacement, inches

——— H = 6 ft
—+— H = 8 ft
— — H = 10 ft

Figure 7.15 - The effects of further increases of the height of the platform

The second test case uses the curvilinear motion described in section 7.3.2 and the reference height of the platform is increased from 2 ft to 4 ft, the distance b is zero and the time period T is 15 seconds. The results of these tests are shown in Figure 7.17.

The effects of changing the height for the curvilinear motion are totally different from the results obtained for the rectilinear motion. For the curvilinear motion as the height is increased, the overall force requirements are lowered. The improvement is more noticeable in actuators 2 and 3 when the platform is at the initial orientation of - 90° and the final orientation of + 90°. The location of the platform close to the initial location is shown in Figure 7.16. In this orientation the cutting force and the weight of the platform are pushing the platform downwards. The greater height makes the connector vertical components greater, which can then balance out the external and gravitational loads more effectively.
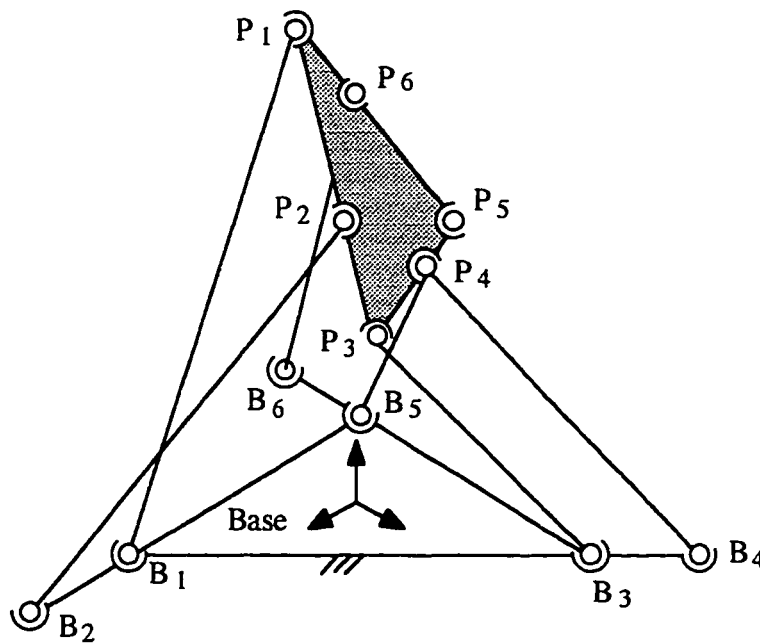

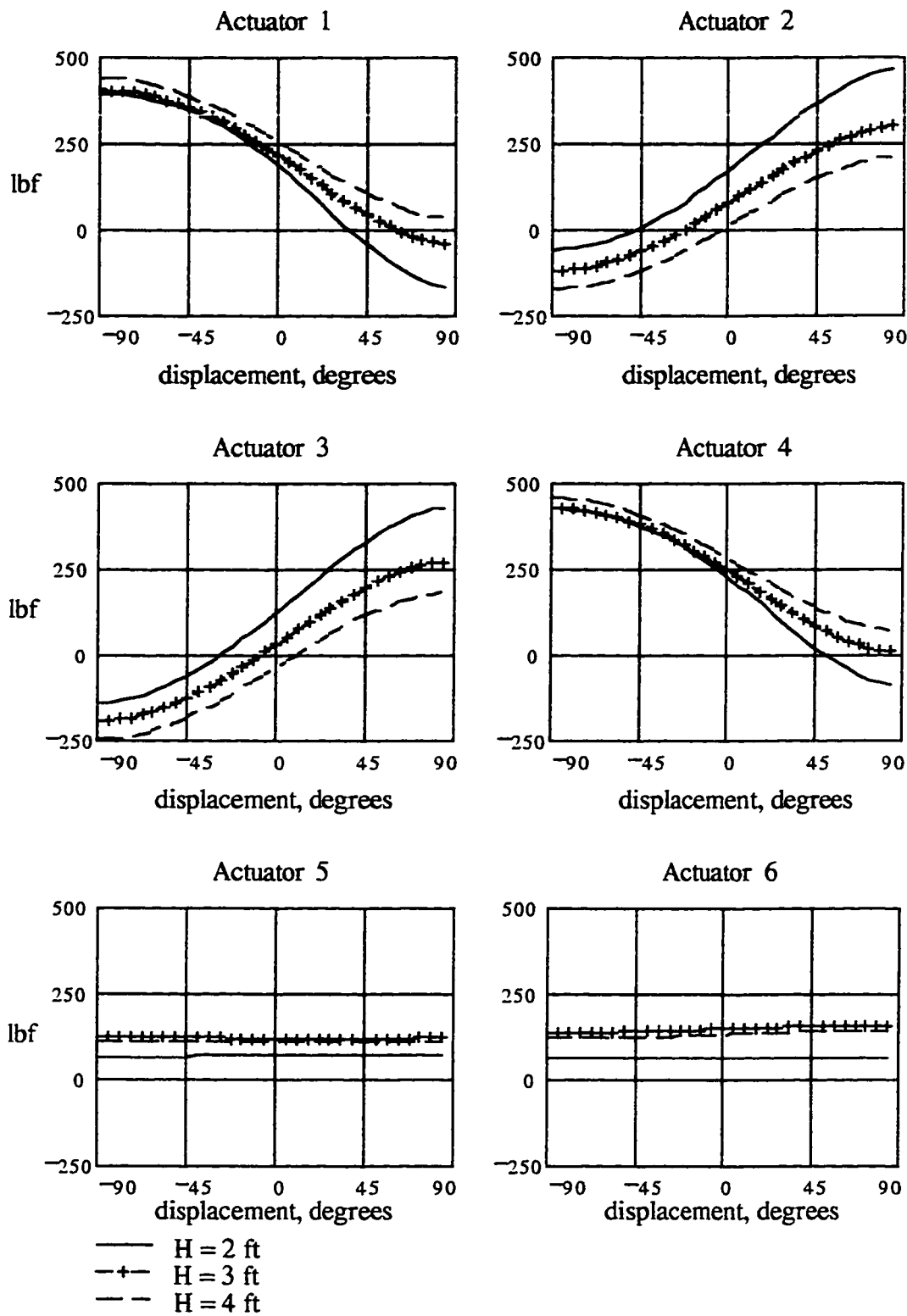Figure 7.16 - Platform close to the initial position for the curvilinear motion

Actuator 1

Actuator 2

Actuator 3

Actuator 4

Actuator 5

Actuator 6

——— H = 2 ft
—+— H = 3 ft
— — H = 4 ft

Figure 7.17a - Effects of the platform height on the actuator forces, curvilinear motion

Actuator 1

Actuator 2

Actuator 3

Actuator 4

Actuator 5

Actuator 6

λ

displacement, degrees

------ H = 2 ft

—+— H = 3 ft

— — H = 4 ft
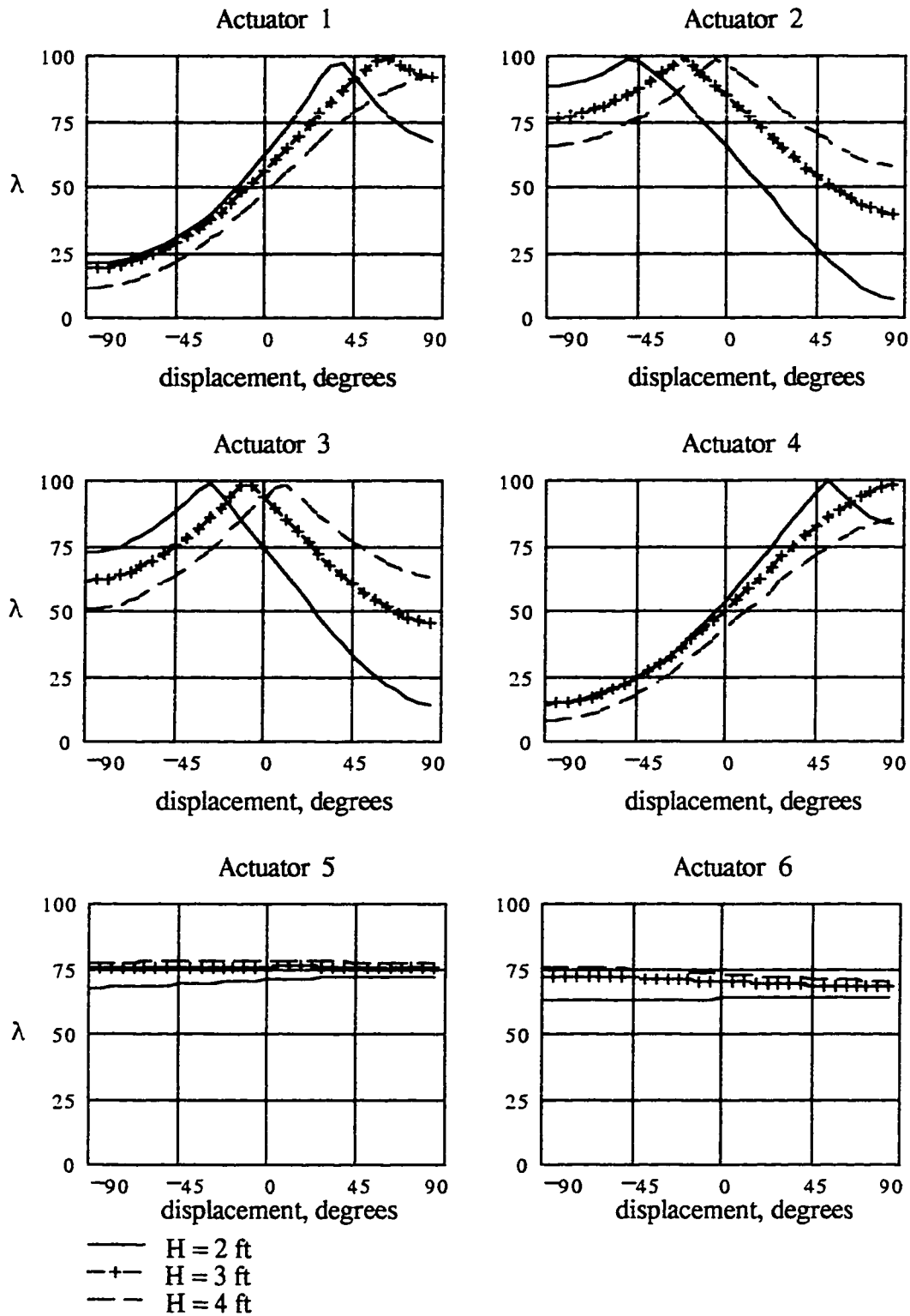
Figure 7.17b - Effects of the platform height on the force index λ, curvilinear motion

The next set of tests consist of changing the distance b (as shown in figure 7.18) while keeping the platform at a fixed height of 2 ft and the time period T equal to 30 seconds. The results of the rectilinear and curvilinear motions are shown in Figures 7.19 and 7.20 respectively.

These plots indicate that the greater the distance b between the planes, the greater the general actuator force requirements. The increase of the distance b increases the horizontal force components for the connectors in the higher plane. This allows the platform to balance the horizontal load with less force, but at the same time it locates the connectors in a configuration where they are partially working against each other. The extreme case is when the distance b is equal to the height H. In this case the three connectors are completely horizontal and will be balancing the external load and partially working against each other. The force indices change with the type of motion. For the rectilinear motion the actuators 2, 4 and 6, which are not relocated by the factor b, have lower indices. For the curvilinear motion the actuators 1, 3 and 5, which are relocated by the factor b, have
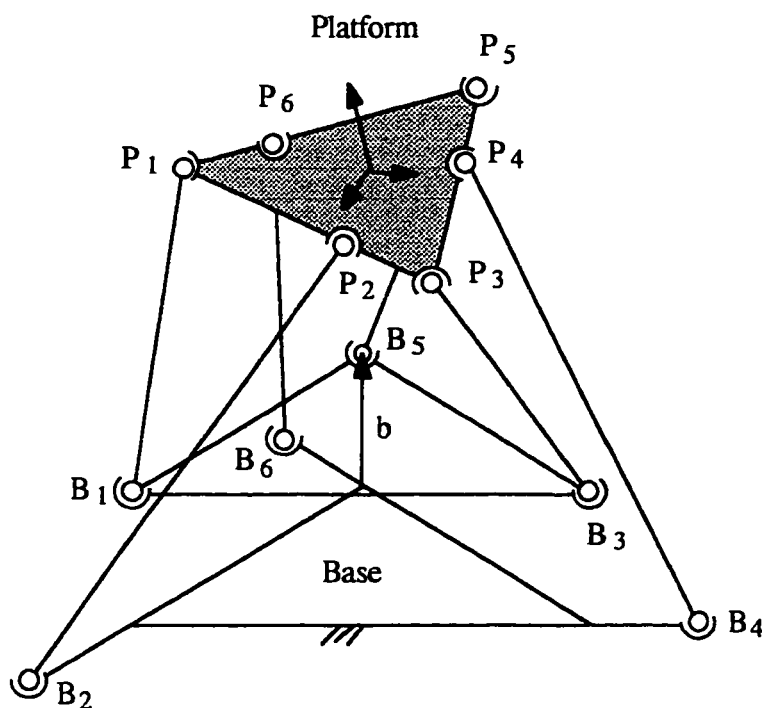

Figure 7.18 - Platform with base points in two parallel planes

lower indices. This illustrates the fact that a much greater number of tests is required in order to better understand the effects of geometric variations. The main reason for such behavior is the complex relationship between the connector forces (and actuator forces), the line coordinates and the geometry of the system which can be observed in the equations of motion
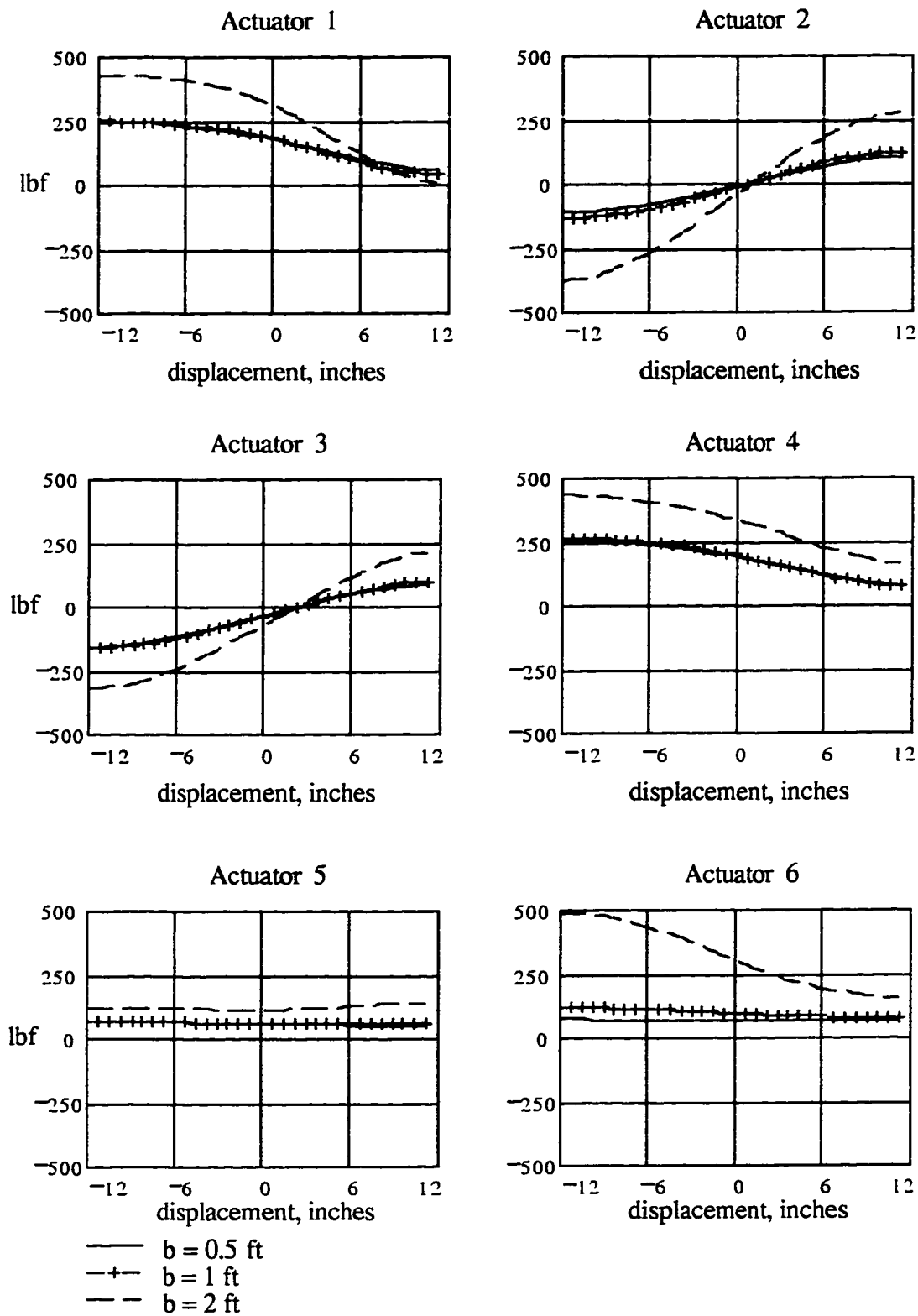
$$\sum_{i=1}^{6} \left(F_l \, \widehat{\underline{S}}_3 \right)_i = \widehat{\underline{W}}_{ext} + \widehat{\underline{W}}_p + \widehat{\underline{W}}_{gr} + \widehat{\underline{W}}_{tan} + \widehat{\underline{W}}_{cor} + \widehat{\underline{W}}_{cent}$$

where the line coordinates are given by

$$\left(\widehat{\underline{S}} \right)_i = \left(\begin{array}{c} \underline{s}_3 \\ \underline{R}_{pc} \times \underline{s}_3 \end{array} \right)_i$$

The direction $\underline{s}_3$ is a function of the position of the base points and the end points as mentioned in Section 3.3. The relative position vector $\underline{R}_{pc}$ is a function of the dimensions and the orientation of the platform. Therefore since the vectors $\underline{s}_3$ and $\underline{R}_{pc}$ are functions of so many parameters, it is difficult to determine the effect on one parameter on the behavior of the system. The great amount of combinations of geometric parameters makes difficult to generalize the above observations. This is problem is further compounded by other factors such as the type of external loads.

The effects of changing the axis of translation $\underline{w}$ for the rectilinear motion are shown in Figure 7.21 and 7.22. This axis is determined by the value of the angle θ as shown in Figure 7.10. The values used are $\theta = 0°$ (the $\underline{X}$ axis), $30°$, $60°$, $90°$ (the $\underline{Y}$ axis), $120°$ and $150°$. The height used was 2 ft and the time period was set to 30 seconds. These results indicate that the forces requirements change as the direction changes but no general pattern is seen in these results. Although no pattern can be observed it is important to use different direction of motion when designing a manipulator to establish the actuator force requirements.

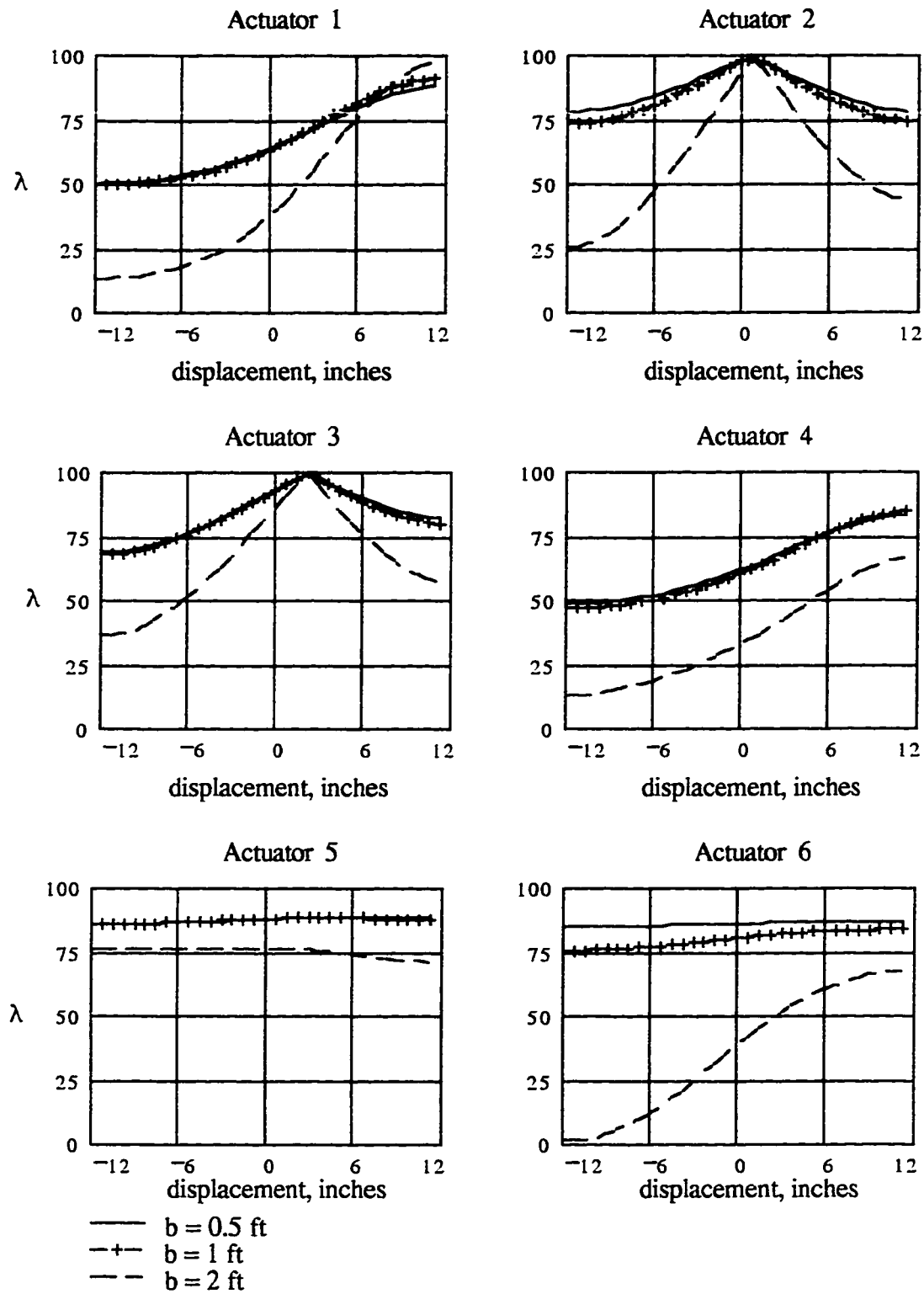Figure 7.19a - Effects of the distance b on the actuator forces, rectilinear motion

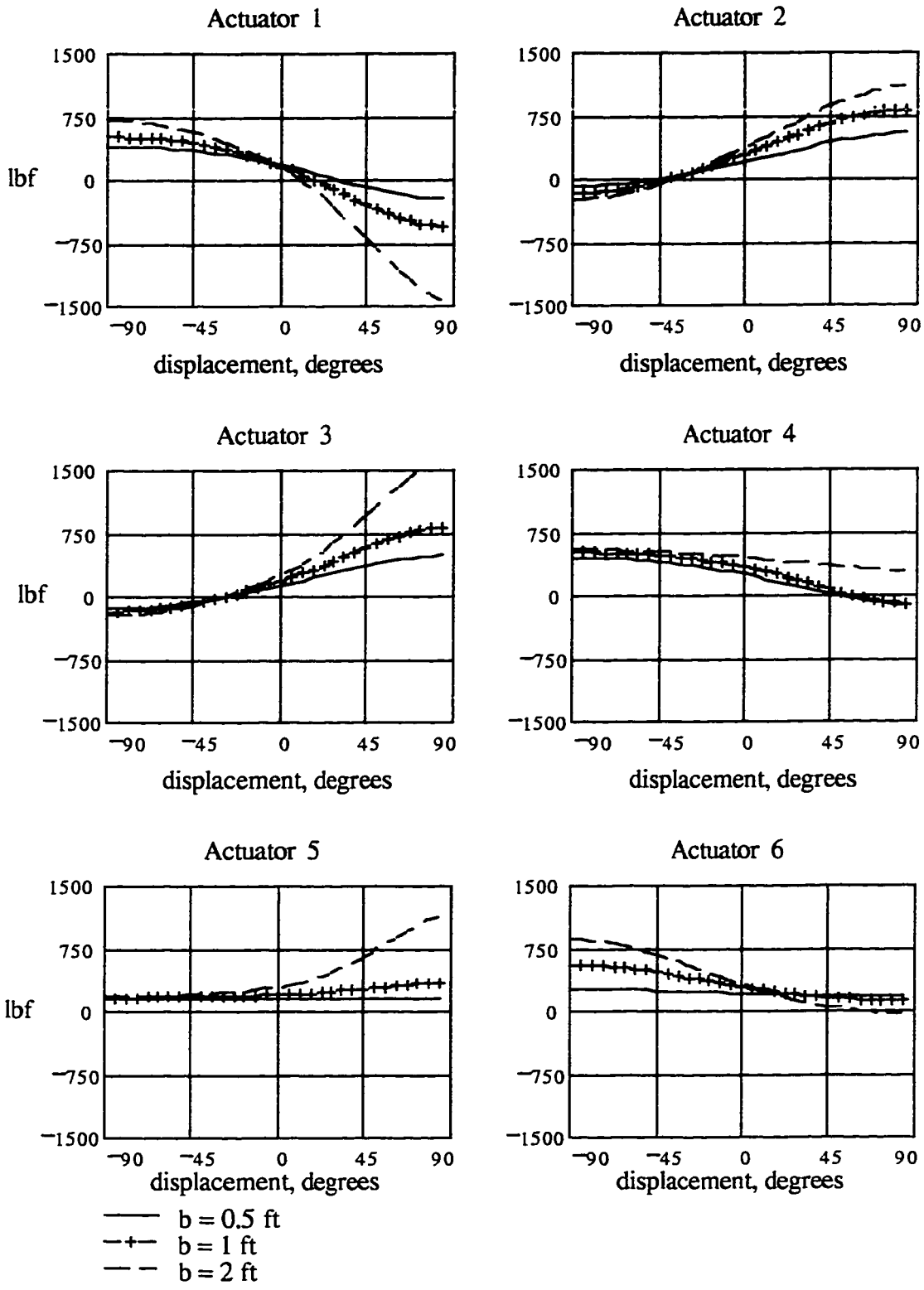Figure 7.19b - Effects of the distance b on the force index λ, rectilinear motion

Actuator 1

Actuator 2

Actuator 3

Actuator 4

Actuator 5

Actuator 6

——— b = 0.5 ft
—+— b = 1 ft
— — b = 2 ft

Figure 7.20a - Effects of the distance b on the actuator requirements, curvilinear motion

Actuator 1

Actuator 2

displacement, degrees

displacement, degrees

Actuator 3

Actuator 4

displacement, degrees

displacement, degrees

Actuator 5

Actuator 6

displacement, degrees

displacement, degrees
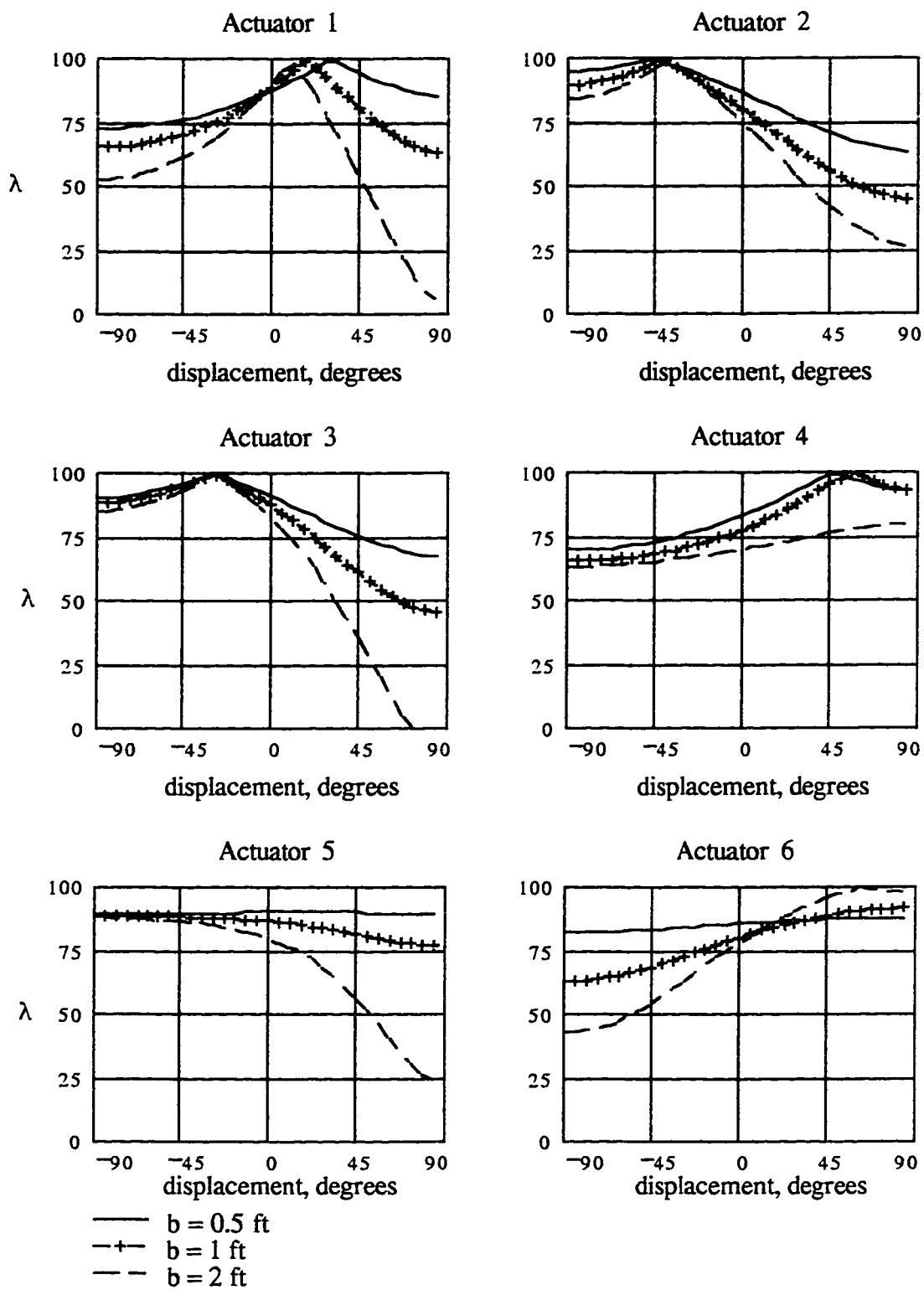
——— b = 0.5 ft
—+— b = 1 ft
— — b = 2 ft

Figure 7.20b - Effects of the distance b on the force index λ, curvilinear motion

7.4.2 Test Cases with Variations of the Direction of Motion

The effects of changing the axis of translation $\underline{w}$ for the rectilinear motion are shown in Figure 7.21 and 7.22. This axis is determined by the value of the angle θ as shown in Figure 7.10. The values used are $\theta = 0°$ (the $\underline{X}$ axis), $30°, 60°, 90°$ (the $\underline{Y}$ axis), $120°$ and $150°$. The height used was 2 ft and the time period was set to 30 seconds. These results indicate that the forces requirements change as the direction changes but no general pattern is seen in these results. Although no pattern can be observed it is important to use different direction of motion when designing a manipulator to establish the actuator force requirements.

As mentioned previously, the magnitude of determinant of the Manipulator Jacobian $[\mathbf{J}_m]$ is another way of checking for actuator saturation. It was used here to asses the effects of changing the axis of translation $\underline{w}$ for rectilinear motions. The determinant is calculated and shown in figure 7.23. Using this as an indicator, the best or most effective directions of motion are θ is equal to $30°$ and $90°$. This is difficult to verify with the force index plots since some of the indices improve at these angles and others decrease as shown in Figures 7.21 and 7.22. Based on these results, it can be said that the determinant of the $[\mathbf{J}_m]$ may not be an accurate indicator of the effectiveness of the actuators.

One of the possible reasons for the disparity in the observations is that the determinant is a combined or composite indicator which takes into account all the actuators while the force index λ is an indicator of the effectiveness of an individual actuator. Another important consideration is that the determinant is used for calculating the connector forces

$$ \{ F_L \} = [\mathbf{J}_m]^{-1} \left(\widehat{\underline{W}}_{ext} + \widehat{\underline{W}}_p + \widehat{\underline{W}}_{gr} + \widehat{\underline{W}}_{tan} + \widehat{\underline{W}}_{cor} + \widehat{\underline{W}}_{cent} \right) $$

Once the connector forces are known, the actuator forces can be determined using (see Section 6.3)

$$ Fa = F_L + M_e \left[\ddot{E} + g \, s_{3z} - E \left(\omega_1^2 \left(1 - (s_{3x})^2 \right) + \omega_2^2 \right) \right] + C_t \dot{E} + C_d (\dot{D} - \dot{L}) $$

It is clear that the actuator, in addition to producing the connector force F_L, has to accelerate the mass M_e and work against the decoupling damper and the internal friction of the actuator. Therefore its is possible to have actuator saturation even if the connector force F_L is considerably low. The determinant is not capable of predicting such situations.

The advantage of using the determinant is that it is a single index that groups all the actuators together. This simplifies the evaluation of the manipulator considerably when compared to the use of the individual forces indices. More research is required in order to correlate the value of the determinant and the effectiveness of the actuators.

The fourth set of tests were conducted using variations of the time period T. The shorter the time period, the faster the platform moves. The results of the tests for the rectilinear and curvilinear motions are shown in Figure 7.24 and 7.25 respectively. It can be seen that the reduction of the time period form 30 seconds to 5 seconds does not produce any noticeable changes in the force requirements. The reduction to a time period of 1 second produces some changes of the force requirements, although not the dramatic changes expected from a reduction by a factor of 30 of the time period.

The platform moves faster as the time period used is shorter, and the velocity and acceleration of the connectors will increase. This will increase the magnitude of the tangential, Coriolis and centrifugal coupling wrenches of the connectors since they are functions of the kinematic state of the system among other things (see Section 5.6)

$$\widehat{W}_{tan} + \widehat{W}_{cor} + \widehat{W}_{cent} = \sum_i^6 f\left(\left[\ \omega_{12}, \alpha_{12}, \dot{E}, \dot{D}, \dots\ \right]_i\right)$$

Since these wrenches are a function of the kinematic state, one would expect a noticeable increase in the actuator force requirements as the platform moves faster. This trend is not observed in the test results. One possible explanation is that the magnitudes of the angular velocities and acceleration vectors are small for the motions tested. These values are shown for the curvilinear motion in Figures 7.26 and 7.27.
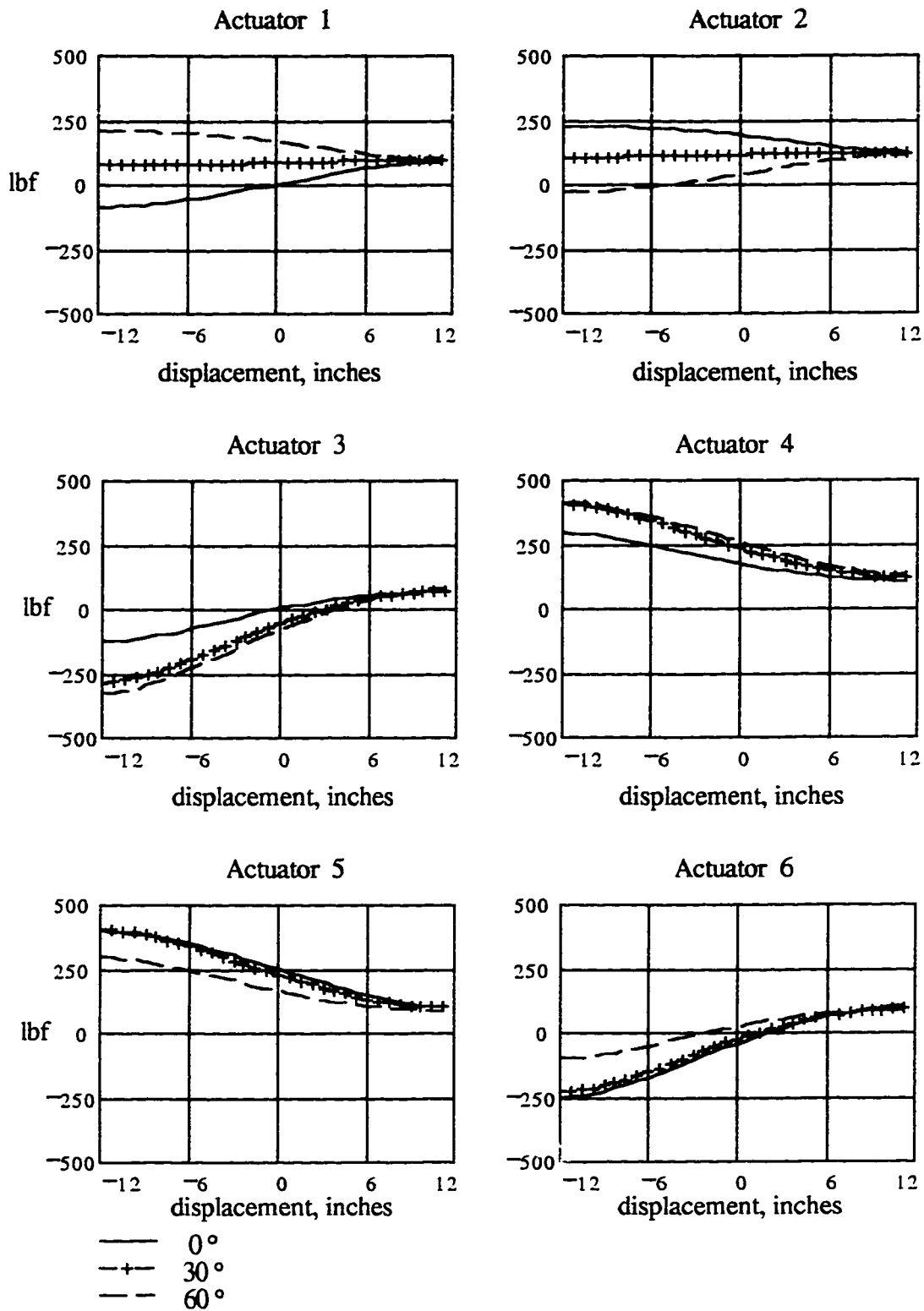
Figure 7.21a - Effects of the axis of translation $\underline{w}$ on the actuator forces, $\theta = 0°$, $30°$ and $60°$, rectilinear motion
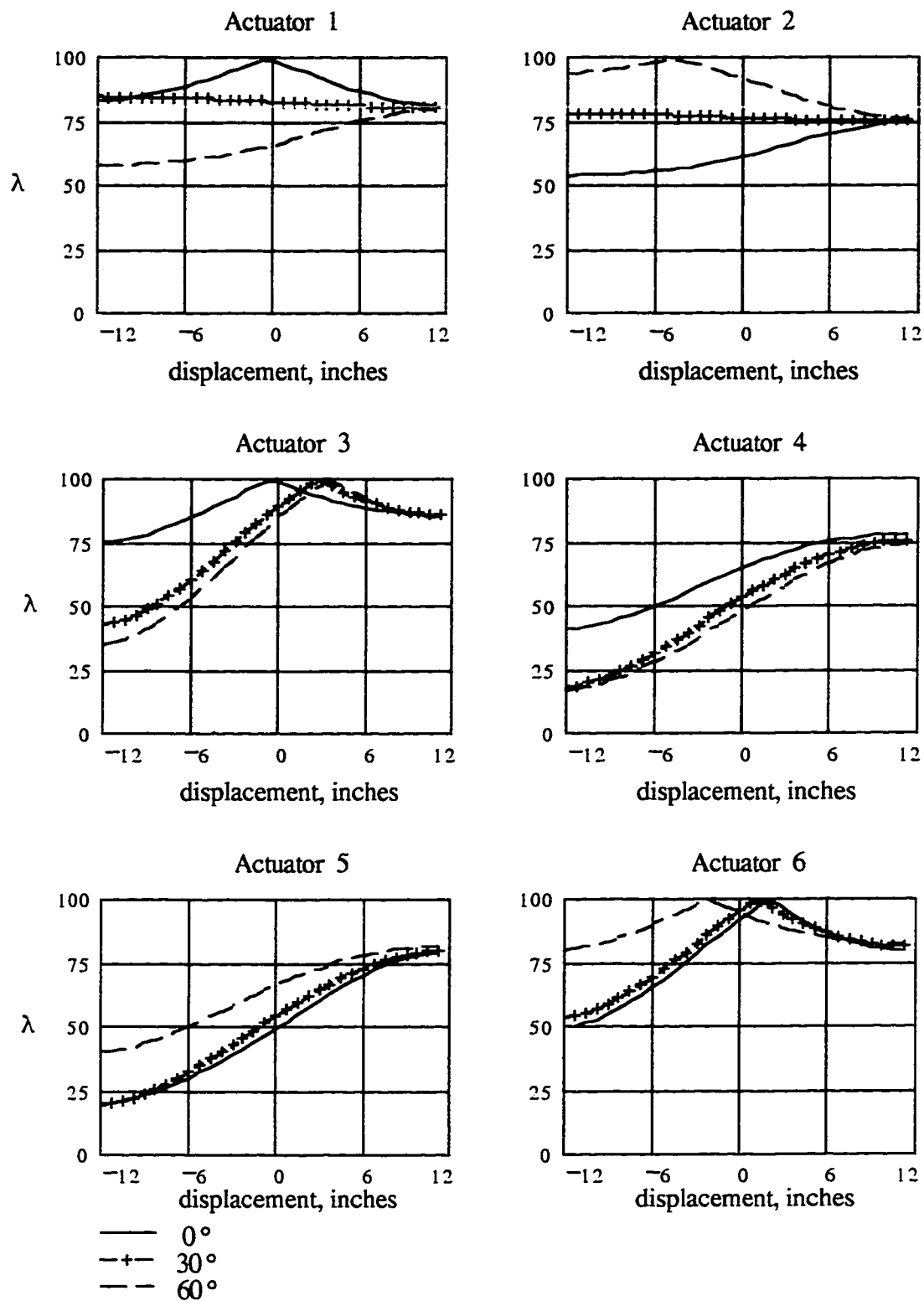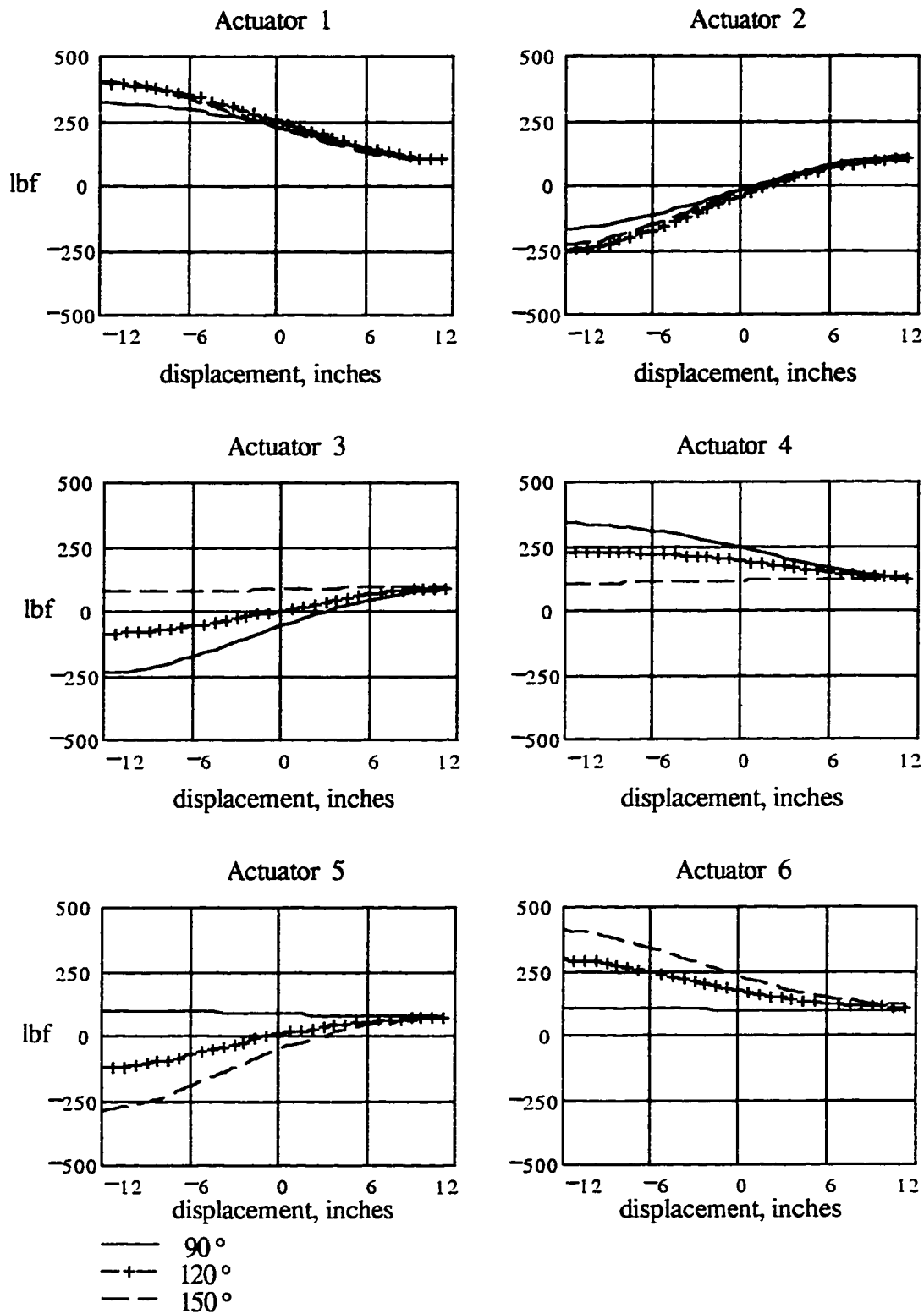
175

Actuator 1

Actuator 2

Actuator 3

Actuator 4

Actuator 5

Actuator 6

—— 0°
—+— 30°
— — 60°

Figure 7.21b - Effects of the axis of translation $\underline{w}$ on the force index λ, $\theta = 0°$, $30°$ and $60°$, rectilinear motion

Actuator 1
Actuator 2
Actuator 3
Actuator 4
Actuator 5
Actuator 6

— 90°
—+— 120°
— — 150°

Figure 7.22a - Effects of the axis of translation w on the actuator forces, θ = 90°, 120° and 150°, rectilinear motion

Actuator 1

λ

displacement, inches

Actuator 2

displacement, inches

Actuator 3

λ

displacement, inches

Actuator 4

displacement, inches

Actuator 5

λ

displacement, inches

Actuator 6

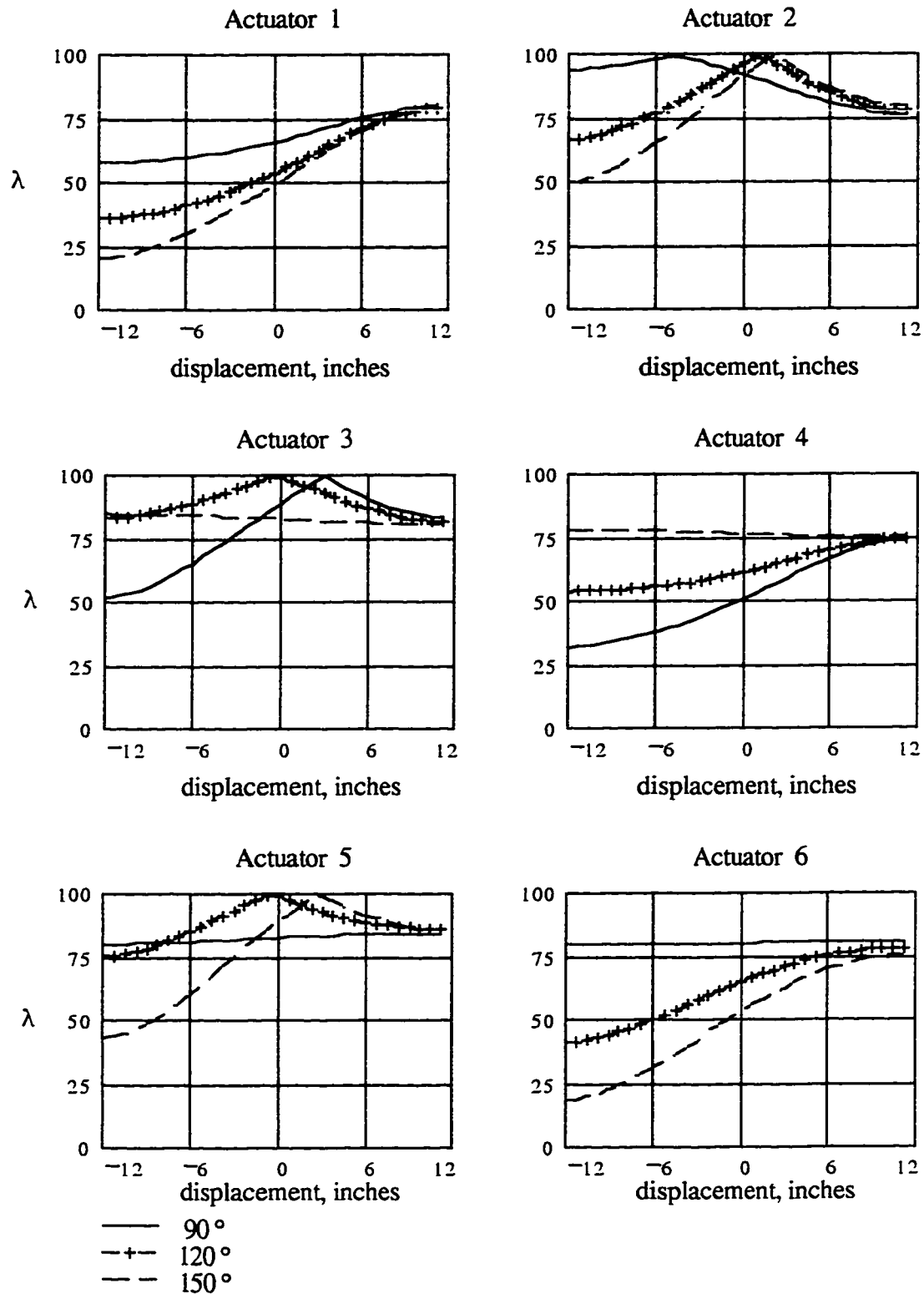displacement, inches

——— 90°
—+— 120°
— — 150°

Figure 7.22b - Effects of the axis of translation $\underline{w}$ on the force index λ, θ = 90°, 120° and 150°, rectilinear motion
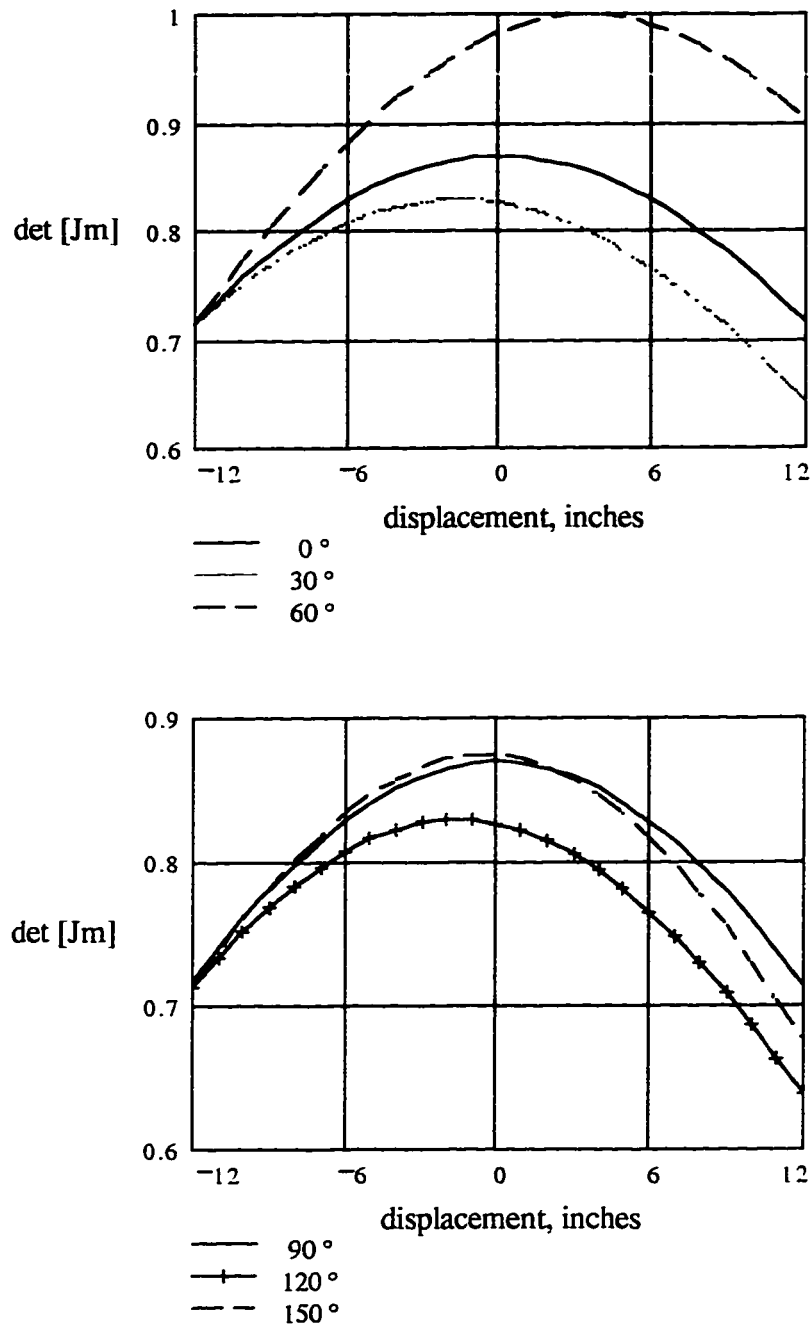
Figure 7.23 - The determinant of [J m] for the rectilinear motion in different directions

7.4.3 Variations in the Time Period

The fourth set of tests were conducted using variations of the time period T. The shorter the time period, the faster the platform moves. The results of the tests for the rectilinear and curvilinear motions are shown in Figure 7.24 and 7.25 respectively. It can be seen that the reduction of the time period form 30 seconds to 5 seconds does not produce any noticeable changes in the force requirements. The reduction to a time period of 1 second produces some changes of the force requirements, although not the dramatic changes expected from a reduction by a factor of 30 of the time period.

The platform moves faster as the time period used is shorter, and the velocity and acceleration of the connectors will increase. This will increase the magnitude of the tangential, Coriolis and centrifugal coupling wrenches of the connectors since they are functions of the kinematic state of the system among other things (see Section 5.6)

$$\widehat{\underline{W}}_{tan} + \widehat{\underline{W}}_{cor} + \widehat{\underline{W}}_{cent} = \sum_{i}^{6} f([\ \underline{\omega}_{12}, \underline{\alpha}_{12}, \dot{E}, \dot{D}, \dots\ ]_i)$$

Since these wrenches are a function of the kinematic state, one would expect a noticeable increase in the actuator force requirements as the platform moves faster. This trend is not observed in the test results. One possible explanation is that the magnitudes of the angular velocities and acceleration vectors are small for the motions tested. These values are shown for the curvilinear motion in Figures 7.26 and 7.27. It can be noticed that for the time periods of 15 and 5 seconds the angular velocities and accelerations are less than 1 rad/sec and 1 rad/sec ^{2} respectively. It is only for a time period of 1 second that these values become somewhat significant. Note that these are the magnitudes and the signs are not included. The sign of the angular velocities and accelerations determined the signs of some of the terms in the coupling wrench. Therefore the effect of an increase of one angular acceleration might be canceled by the decrease of another angular acceleration.

Another factor to take into account how the values for the time periods and displacements for actual applications compare to the values used for testing. The time period of 1 second means that the platform is moving a average rate of 1200 in / min which is higher than the feed rates possible with existing technology (< 1000 in / min) [25].
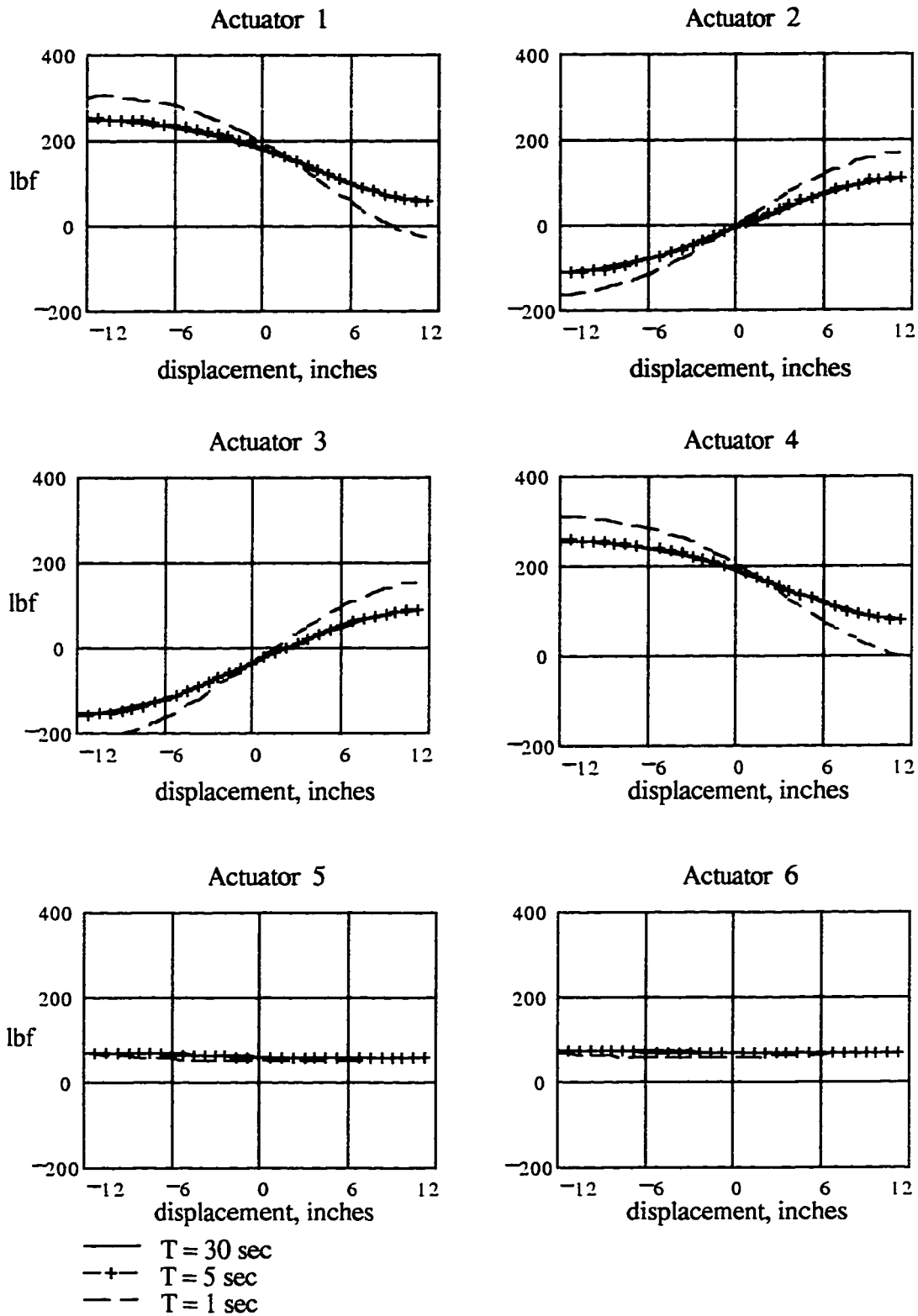
Actuator 1

Actuator 2

Actuator 3

Actuator 4

Actuator 5

Actuator 6

T = 30 sec
T = 5 sec
T = 1 sec

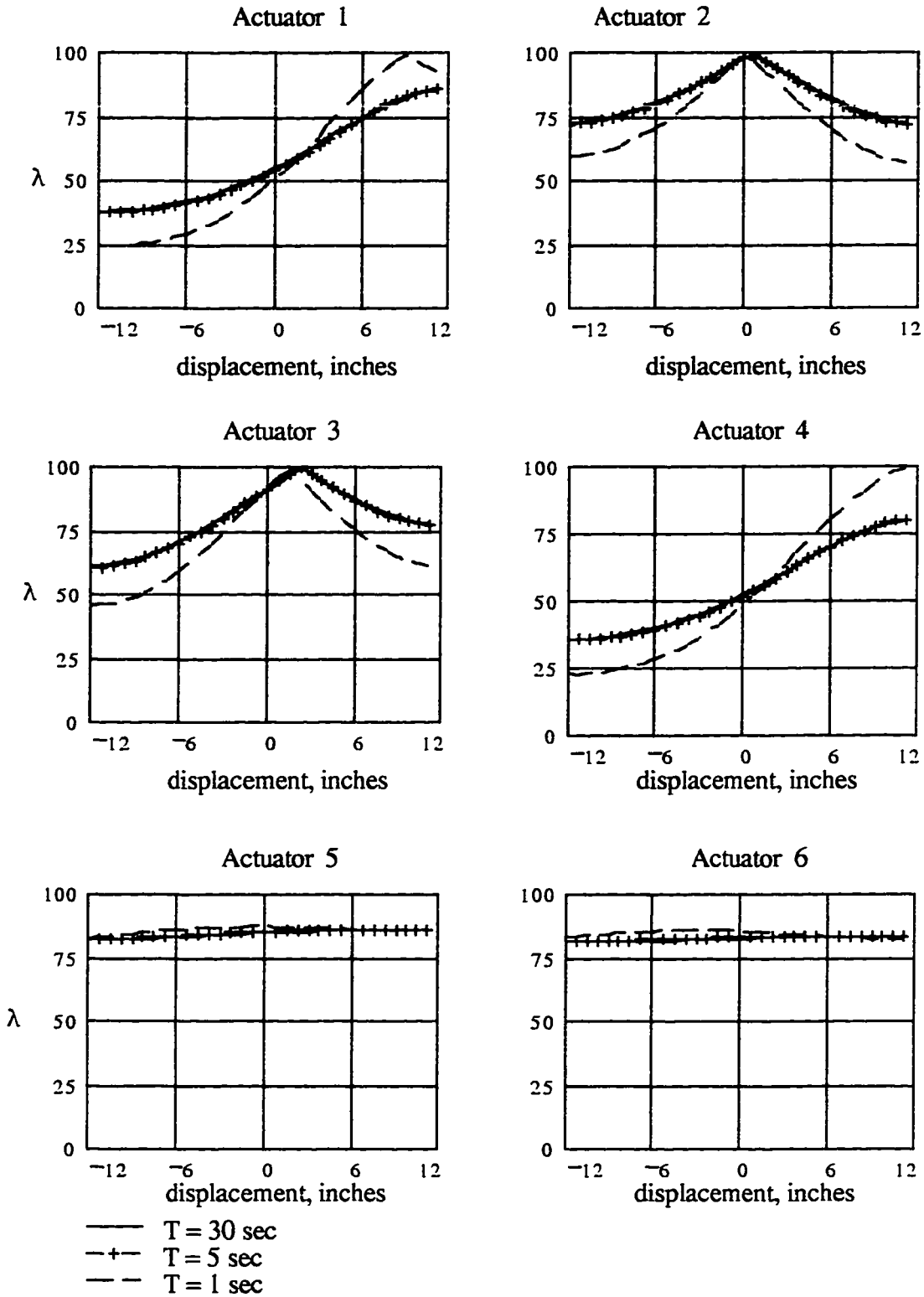Figure 7.24a - Effects of the time period on the actuator forces, rectilinear motion

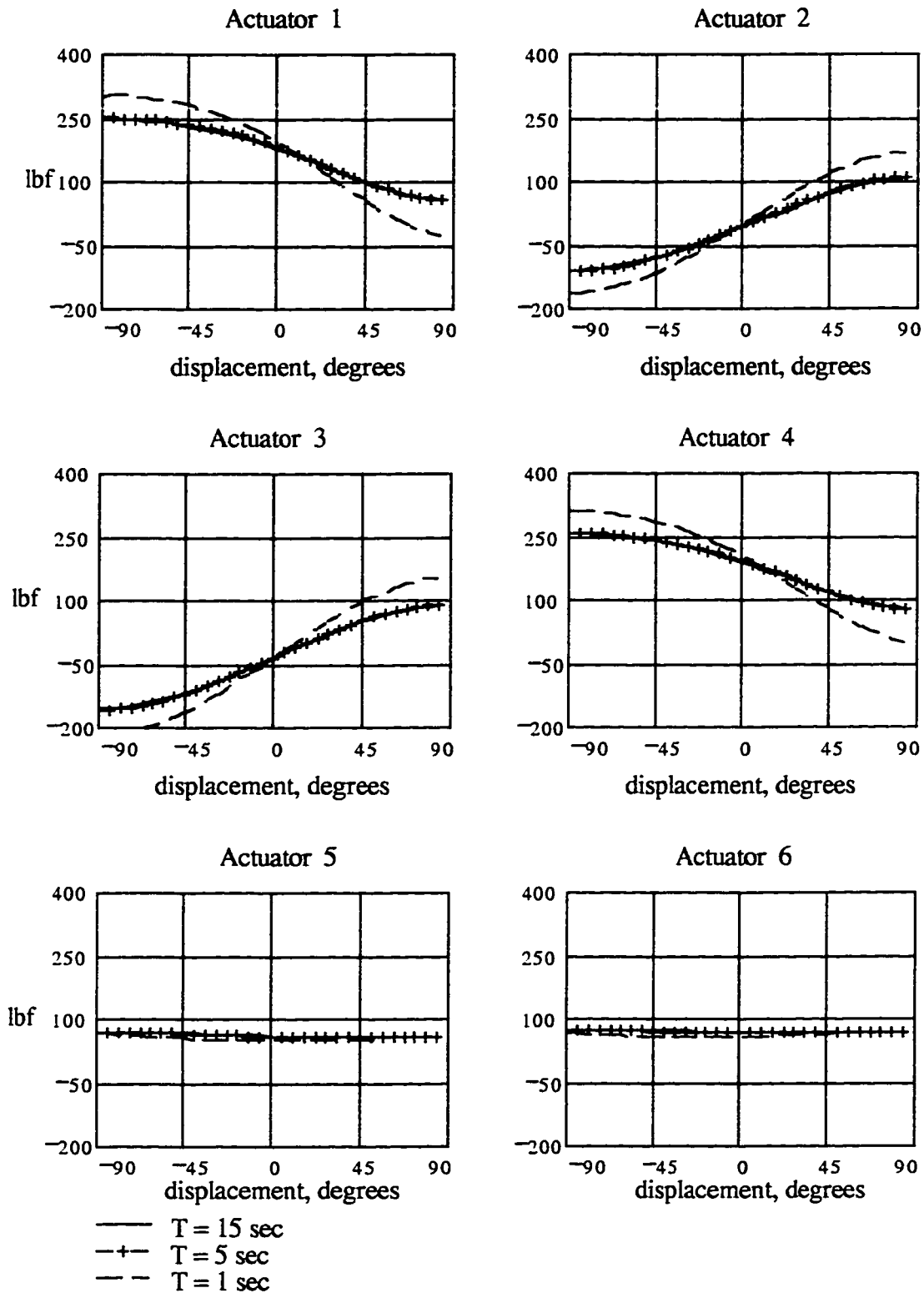Figure 7.24b - Effects of the time period on the force index λ, rectilinear motion

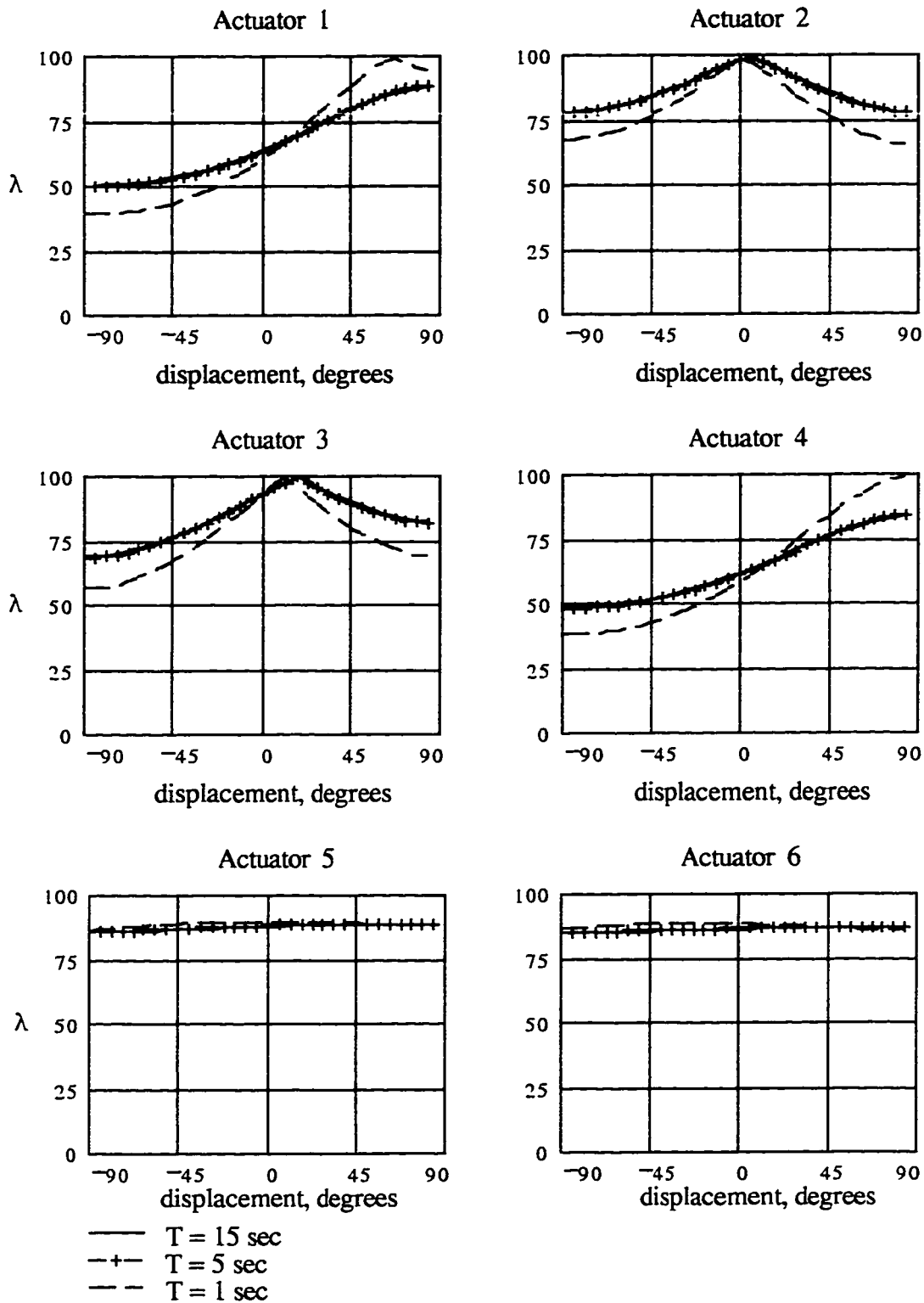Figure 7.25a - Effects of the time period on the actuator forces, curvilinear motion

Actuator 1

Actuator 2

Actuator 3

Actuator 4

Actuator 5

Actuator 6

—— T = 15 sec
—+— T = 5 sec
— — T = 1 sec

Figure 7.25b - Effects of the time period on the force index λ, curvilinear motion

connector 1

rad/sec

displacement, degrees

connector 2

displacement, degrees

connector 3

rad/sec

displacement, degrees

connector 4

displacement, degrees

connector 5

rad/sec

displacement, degrees

connector 6

displacement, degrees

————— T = 15 sec
—+— T = 5 sec
— — T = 1 sec
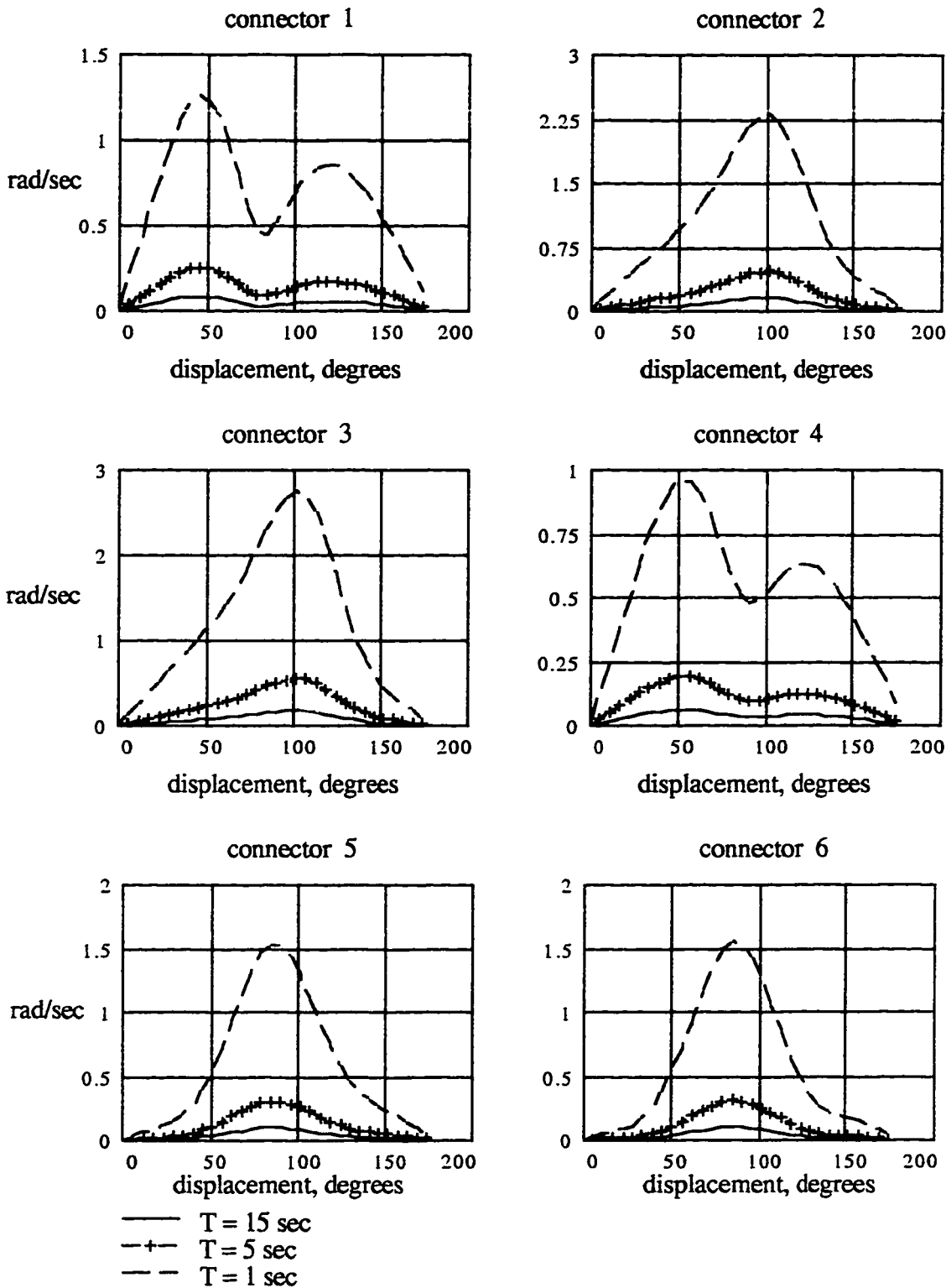
Figure 7.26 - Connector Angular Velocities as a function of the time period T

connector 1

rad/sec ^{2}

displacement, degrees

connector 2

displacement, degrees

connector 3

rad/sec ^{2}

displacement, degrees

connector 4

displacement, degrees

connector 5

rad/sec ^{2}

displacement, degrees

connector 6

displacement, degrees
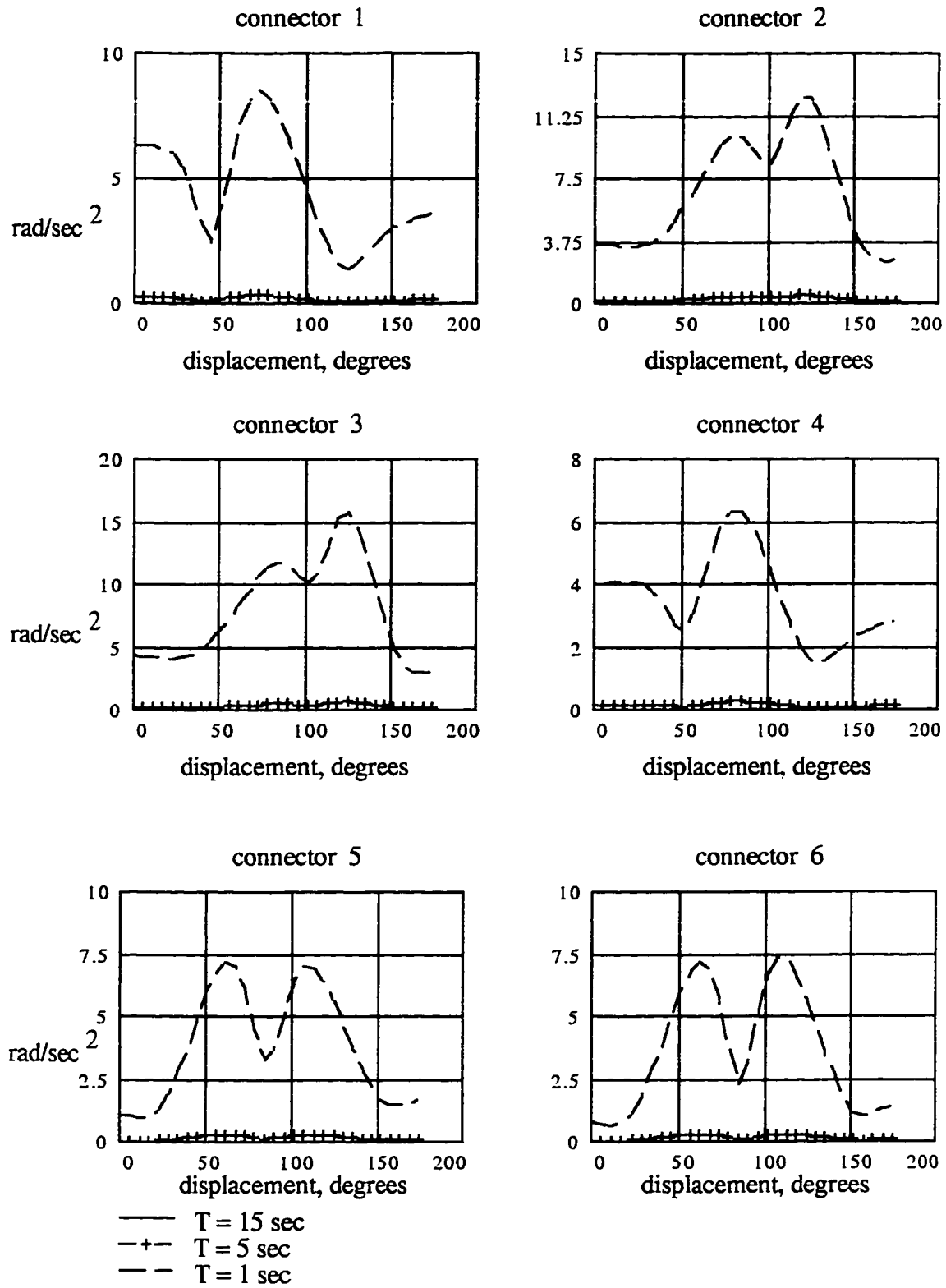
——— T = 15 sec
—+— T = 5 sec
— — T = 1 sec

Figure 7.27 - Connector Angular Accelerations as a function of the time period T

7.4.4 Test Cases with Variations of Inertial Properties

The effects of the connector masses and moments of inertia on the dynamic behavior of is explored in the last set of tests. The platform height is set to 2 ft, the distance b is zero and the time period is 30 seconds. The masses and inertias are multiplied by a factor of 1, 3 and 5 (indicated by the notation M x 1, M x 3 and M x 5). The results of the rectilinear and curvilinear motions are shown in Figures 7.28 and 7.29 respectively.

It can be seen that as the inertial properties are increased, the general actuator force requirements increase. The greatest increases are seen for the actuators 2, 3, 5 and 6 where the force requirements register more than a 100% increase. This suggests that the inertial parameters have a significant effect on the dynamic behavior of the system. All the coupling terms in the equations of motion are functions of these inertial parameters as shown in Section 5.6. Since for the motions used for testing generate small values for the connector angular velocity and acceleration vectors, the only numerically significant coupling term left is the gravitational wrench. This term is a function of the gravitational acceleration and the geometry of the system. These results indicate that the gravitational terms are relevant in the dynamic behavior of the system regardless of the speed of the platform and should be considered when designing and controlling a parallel manipulator.

Once more these observations are based on some simple test cases, and in order to study general trends much more testing is required. If the gravitational coupling is found to a sole significant coupling factor, the manipulator can be designed to reduce this effect through mass balancing.

7.5 Summary

These observations are base on a small group of tests. The equations of motion are functions of a great set of factors (see Section 5.6) that can be changed. This underlines the great importance of more testing with different sets of geometric parameters, system parameters, motions and tasks in order to carefully study the effects of coupling.

These results provide some insight to the dynamic behavior of a platform system and how its is affected by different factors. Much more testing is required using different

combinations of parameters. One of the useful aspects of these results is that it gives the researcher some idea of the parameters that should be changed and analyzed such as the connector masses and the relocation of the base points.
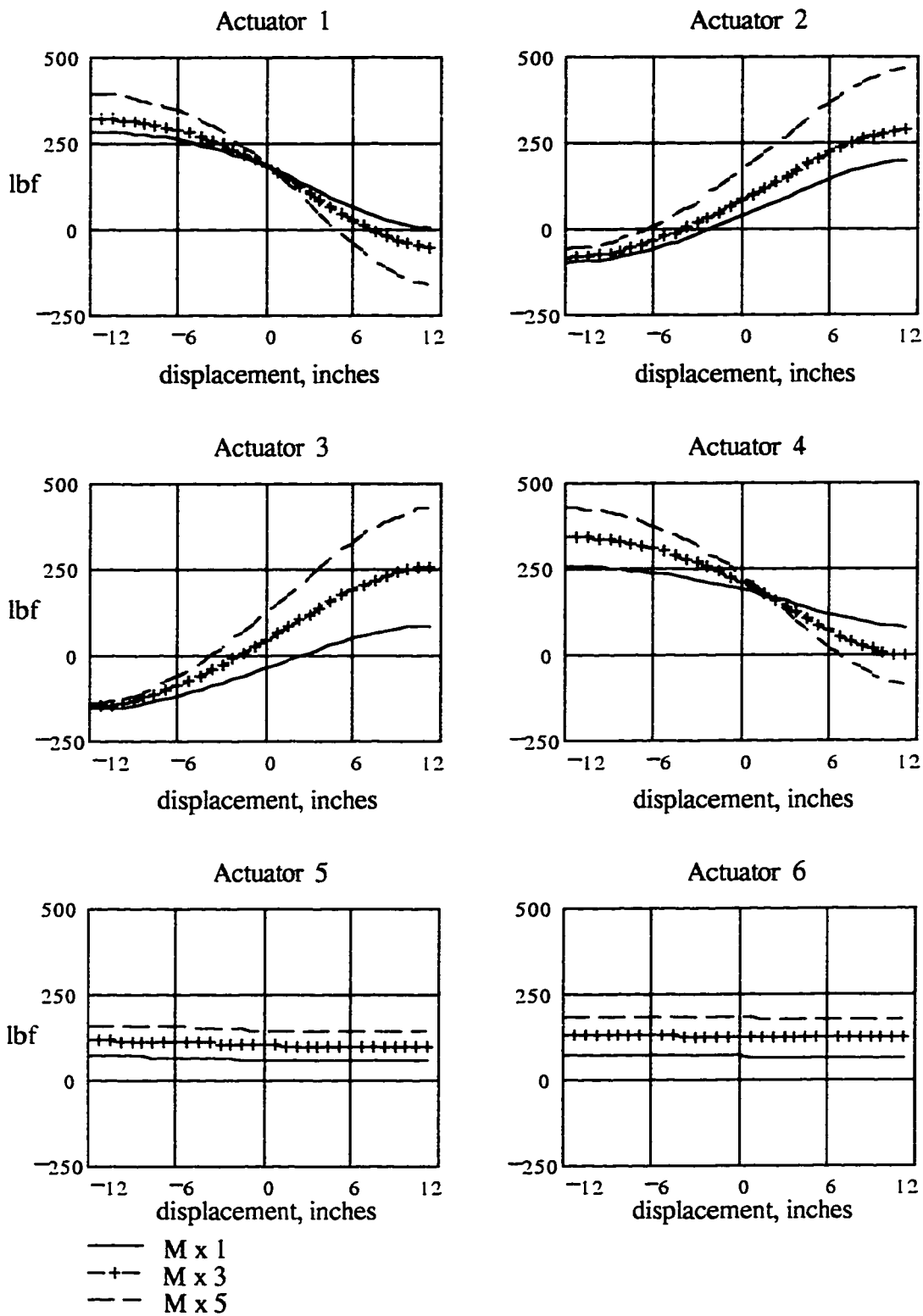
Actuator 1

Actuator 2

Actuator 3

Actuator 4

Actuator 5

Actuator 6

——— M x 1
—+— M x 3
— — M x 5

Figure 7.28a - Effects of the mass and inertial parameters on the actuator forces, rectilinear motion

Actuator 1

λ

100
75
50
25
0

−12 −6 0 6 12

displacement, inches

Actuator 2

100
75
50
25
0

−12 −6 0 6 12

displacement, inches

Actuator 3

λ

100
75
50
25
0

−12 −6 0 6 12

displacement, inches

Actuator 4

100
75
50
25
0

−12 −6 0 6 12

displacement, inches

Actuator 5

λ

100
75
50
25
0

−12 −6 0 6 12

displacement, inches

Actuator 6

100
75
50
25
0

−12 −6 0 6 12

displacement, inches

——— M x 1
—+— M x 3
— — M x 5
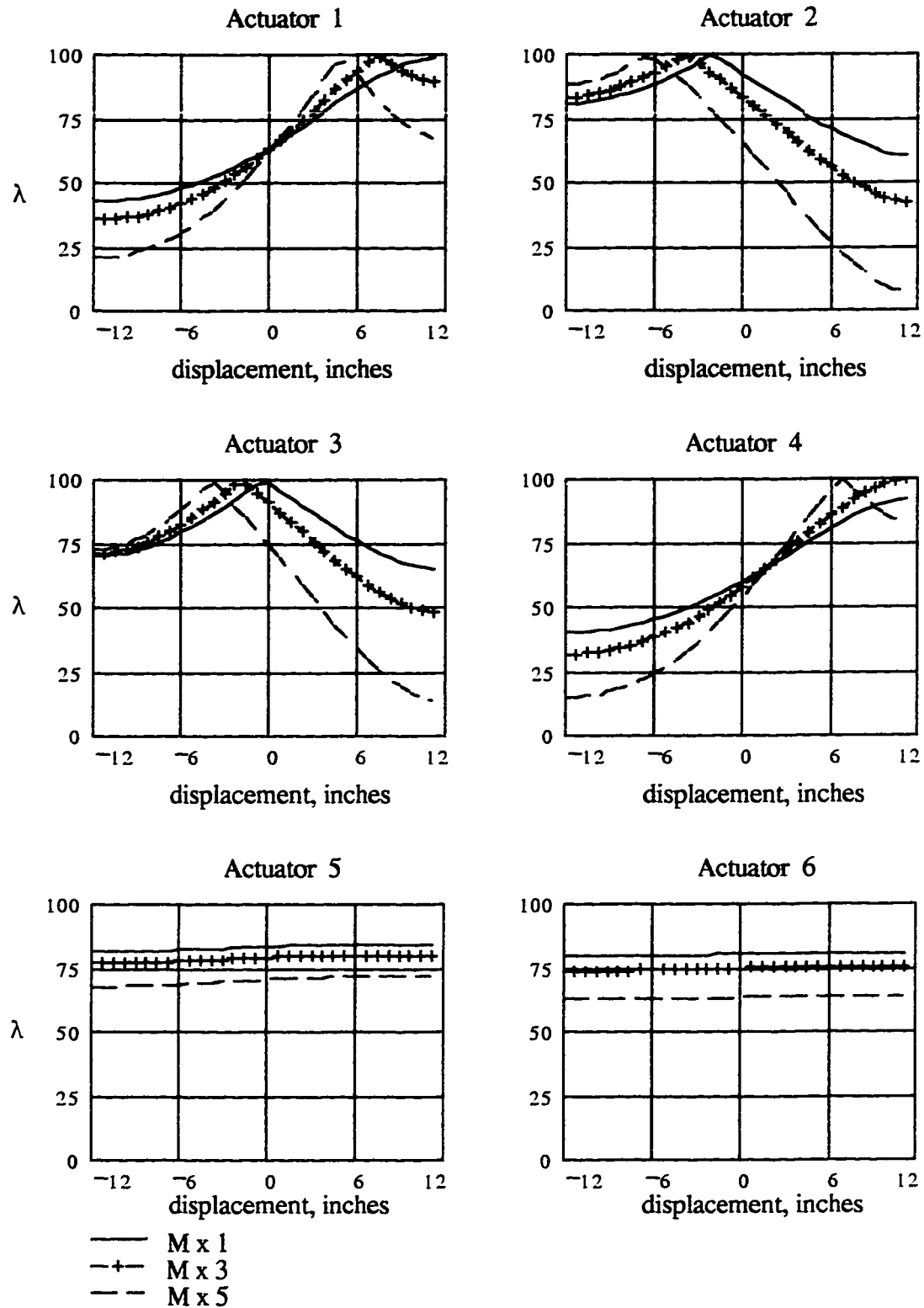
Figure 7.28b - Effects of the mass and inertial parameters on the force index λ, rectilinear motion

Actuator 1

lbf

displacement, degrees

Actuator 2

displacement, degrees

Actuator 3

lbf

displacement, degrees

Actuator 4

displacement, degrees

Actuator 5

lbf

displacement, degrees

Actuator 6

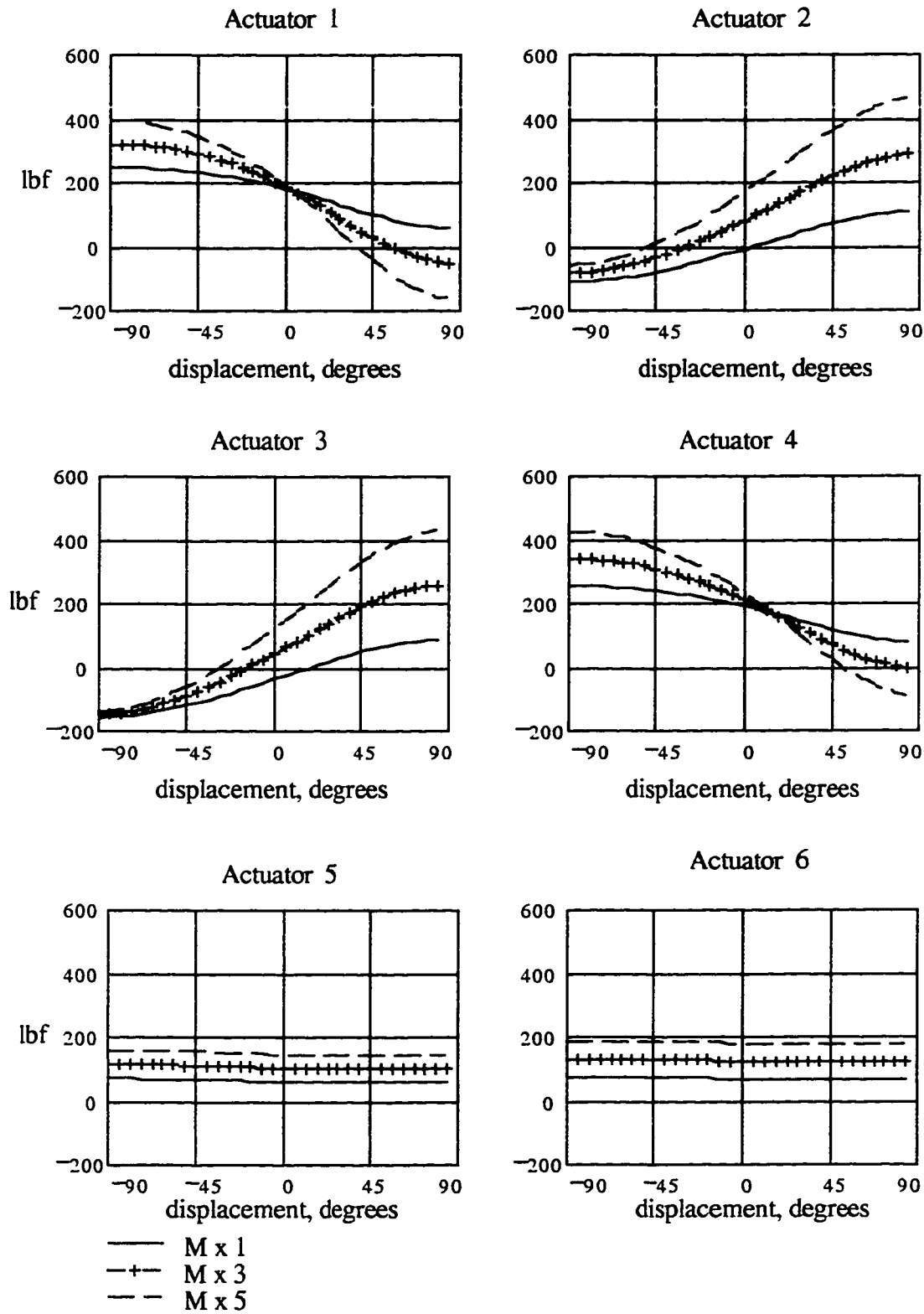displacement, degrees

——— M x 1
—+— M x 3
— — M x 5

Figure 7.29a - Effects of the mass and inertial parameters on the actuator forces, curvilinear motion
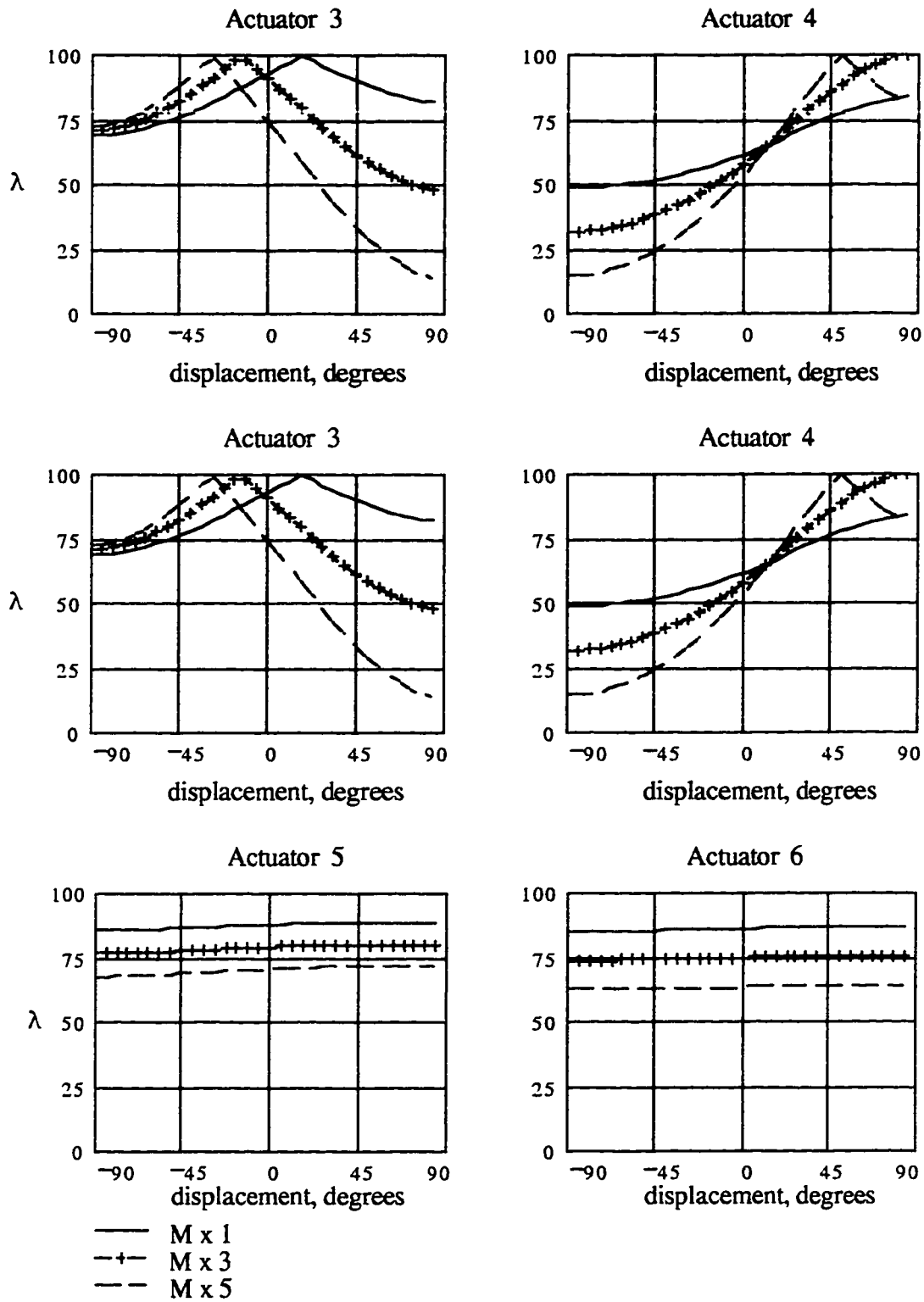
Figure 7.29b - Effects of the mass and inertial parameters on the force index λ, curvilinear motion

CHAPTER 8
CONCLUSIONS AND RECOMMENDATIONS

Although more work is needed in the area of dynamics of parallel manipulator, many useful observations and recommendations have been obtained from this research which constitutes a major step towards the development of the Computer Assisted Engineering tool for the design and analysis of parallel manipulators.

8.1 Developing the Dynamic Model

The explicit equations of motion for the parallel manipulator have been determined and used for developing a computer simulation of the dynamic behavior.

8.1.1 Selection of a Formulation Method

In this research Kane's Method has been successfully applied in the development of the explicit equations of motion for a parallel manipulator. The usefulness of a given formulation method seems to be related to the type of kinematic chain upon which the manipulator is based on. Lagrange's Method has been used successfully for the modeling serial manipulators, while not so for parallel manipulators.

Both the Newton-Euler formulation and Kane's Method require explicit force and torque expressions. These are obtained from free-body diagrams of each of the rigid bodies of the system. For serial manipulators, the force and torque expressions can prove to be difficult to obtain [7, 8, 9, 10]. Since the links or rigid bodies are in series, the forces and torques are not a simple sum of the individual joint contributions. On the other hand, the force and torque analysis is relatively simple for parallel manipulators. For the parallel manipulators, the end effector force and torque is produced by all the connectors working together.

192

The Lagrange formulation, which does not need a force and torque analysis of the system, requires explicit expressions for the velocity and position of each joint. These expressions, which must be in terms of the system generalized coordinates, are used for the kinetic and potential energy expressions. For serial manipulators they are simple to obtain since the motion of the links is additive [13, 14, 31]. On the other hand, the expressions for a parallel manipulator, as shown in Sections 3.4 and 3.5, are very complicated. This quickly complicates the derivation of the dynamic model as outlined in Section 5.1. This is the main reason that the explicit equations of motion for parallel manipulators have not been derived using Lagrange's formulation which appears to be virtually impossible [8, 9].

Therefore the selection of the method is more than a choice of the analyst, it is greatly influenced by the type of kinematic chain used in the manipulator. For serial manipulators where the force and torque expression can become somewhat elaborate but the velocity and position expression are relative simple to obtain, Lagrange's formulation is better. For parallel manipulators, where the force analysis is relatively simple compared to the position and velocity analysis, Kane's Method works better.

8.1.2 Use of the Explicit Dynamic Model

The dynamic model or equations of motion of a manipulator can be used for the forward and inverse dynamic analysis. Some understanding of the dynamic behavior can be gained by using a computer simulation based on this model. This can be achieved regardless if the explicit equations of motion are available. The great advantage of having the explicit dynamic model is that general observations can be made without having to run a great number of numerical simulations.

The coupling between the connectors is a good example of the usefulness of the explicit equations of motion. This coupling is quoted as being negligible or that it can be corrected using adaptive control systems [10, 11]. It may well be that the combination of manipulator parameters and motions used did not cause serious coupling effects [10, 11]. On the contrary, the dynamic model derived in Chapter 5 indicates that for the general case there is a high degree of coupling between the connectors of the system. This is caused by

the gravitational, tangential, Coriolis and centrifugal accelerations of the connectors. The numerical simulations of Chapter 7 indicate that for the test cases quoted the most significant coupling is caused by the gravitational acceleration. It is conceivable that future applications will required faster platform motions in which the other coupling terms become relevant and cannot be neglected as has been done previously [10, 11].

The explicit equations of motion allow the designer to select manipulator parameters that can minimize or eliminate the coupling effects of the connectors which has thus far been done for serial manipulators [13, 14].

Another important use of the explicit dynamic model is in the design of the control system. The approach that has been used is to consider the coupling effects as uncertainties or errors which can be minimized using control systems [10, 11]. This may well be satisfactory when the coupling effects are minimal but not valid for fast motions with high coupling effects. A more effective approach is to use the dynamic model to predict the coupling effects and include these effects in the control commands to the actuators. This will in general create a more precise system with a faster time of response [13, 14, 26].

8.2 Dynamic Behavior of Parallel Manipulators

The results of Chapter 7 provide some understanding of the dynamic behavior and how its affected by different variations of parameters.

The first observation that can be made is that the geometry has a great effect on the dynamic behavior of the manipulator. Factors such as the reference height, the axis of translation and the type of motion used clearly affect the actuator requirements. However since there so many parameters it is difficult to establish any trend as shown in the tests of Chapter 7 and more testing with different sets of parameters is recommended.

As mentioned before, the explicit equations of motion indicate the high degree of coupling between the connectors. However, the motions used for testing did not create significant coupling effects except for the gravitational coupling. Other coupling terms are a function of the location and motion of the platform, while the gravitational coupling is only a function of the location of the platform. If this is valid for great range of tests, a

approximate dynamic model can be used

$$\sum_{i=1}^{6} \left(F_1 \, \widehat{\underline{S}}_3 \right)_i = \widehat{\underline{W}}_{ext} + \widehat{\underline{W}}_p + \widehat{\underline{W}}_{gr}$$

This approximate model would neglect all the coupling terms except for the gravitational coupling. This approximate model could be included in real time control system with minimal computational overhead since the most time consuming terms to calculate are omitted. It is important to recall that this is a useful approach only for motions where the other coupling terms are not numerically significant (see Section 6.5).

8.3 Recommendations

This research is one of the first steps towards the ultimate goal of developing a design / analysis tool for parallel manipulators. Much more work must be done before reaching such goal.

8.3.1 Dynamic Modeling

The equations of motion of a manipulator can be written in what is known as the standard form in which all the displacements, velocities and accelerations are written in terms of the generalized coordinates and their time derivatives [13, 14]

$$\underline{F} = [\, H(q) \,] \, \ddot{q} + \dot{q}^T [\, C(q) \,] \, \dot{q} + [\, K(q) \,] \, q + G(q)$$

where $\underline{F}$ is the actuator force / torque vector; $q = [\, q_1, q_1 \, ... \,]^T$ is vector of the generalized coordinates, $[\, H(q) \,]$ is the manipulator equivalent inertia tensor, $[\, C(q) \,]$ is the damping, Coriolis acceleration and centrifugal acceleration matrix, $[\, K(q) \,]$ is the stiffness matrix; and $G(q)$ is the gravitational forces vector. The dynamic behavior of a manipulator can be understood better by obtaining the inertia tensor $[\, H(q) \,]$ [13, 14]. In order to convert the equations of motion derived in Chapter 5 to the standard form, all the angular velocity and acceleration terms of the connectors must be written in terms of the platform coordinates,

velocity and acceleration. This will involve a considerable amount of work because of the length the expressions for the angular velocities and accelerations of the connectors (see Sections 3.4 and 3.5). Nevertheless is may be worth the effort since it will possibly provide more insight of the dynamic behavior and indicate how to simplify the dynamics by designing the manipulator.

8.3.2 Testing

More testing is required in order to make general statements about the dynamic behavior of parallel manipulators. In order to do so, more work should be done in the area of motion and task planning. Most of the motion planning for manipulators consist of the path planning of a given point on the end effector [13, 32]. This is not sufficient for planning the motion of a parallel manipulator where its orientation is also an important factor. Therefore a mathematical description of actual tasks should be developed to be used as part of the input for the dynamic simulation software.

A comparison of alternative platforms designed to perform the same motion or tasks is an important issue. An actuator force index was used to compare the tests of Chapter 7 which is essentially a dimensionless performance index. This index indicates when an individual actuator saturates but does not indicate for how long its saturates and does not take into account the rest of the actuators. The designer has to compare all the force index plots for one design with all the force index plots of a competing design in order to select the best. Therefore there is a need for performance indices that can evaluate the combined effect all of the actuators and can be used to quickly compare different designs in an objective way. These indices could use factors such as power consumption and time of saturation as indicators.

8.3.3 Design

It is highly desirable to simplify the equations of motion by redesigning the manipulator or by using a different motion. If more testing indicates that the most significant coupling term is the gravitational coupling, then the manipulator can be redesigned to minimize it. The gravitational coupling term, as derived in Chapter 5, is given by

$$\widehat{\underline{W}}_{gr} = \sum_{i=1}^{6} \left[\frac{g \left[M_e E + M_d D + M_b bl \right]}{L} \left(s_{2z} \widehat{\underline{S}}_2 + s_{23z} \widehat{\underline{S}}_{23} \right) \right]_i$$

This is caused by the gravitational acceleration pulling the rigid bodies of the connector. This term can be reduced by using a balancing mass, m, at a distance U below the base of the connector as shown in Figure 8.1. The gravitational wrench can now be written as

$$\widehat{\underline{W}}_{gr} = \sum_{i=1}^{6} \left[\frac{g \left[M_e E + M_d D + M_b bl - m U \right]}{L} \left(s_{2z} \widehat{\underline{S}}_2 + s_{23z} \widehat{\underline{S}}_{23} \right) \right]_i$$

The main problem is how to select the mass m and the distance U to reduce or eliminate the gravitational coupling. Fixing the mass, the distance U can be calculated by

$$U = \frac{M_e E + M_d D + M_b bl}{m}$$

The limitation of this equation is that the displacement E and D are not constant. In order to minimize the effects of the variations of E and D, the equation can be expressed in a modified form

$$U = \frac{M_e E_{ave} + M_d D_{ave} + M_b bl}{m}$$

where E_{ave} and D_{ave} are the average values of the displacements E and D.

One important consideration is that the balancing mass can only reduced the effects of the gravitational coupling. The use of the balancing mass will increase the effects of the
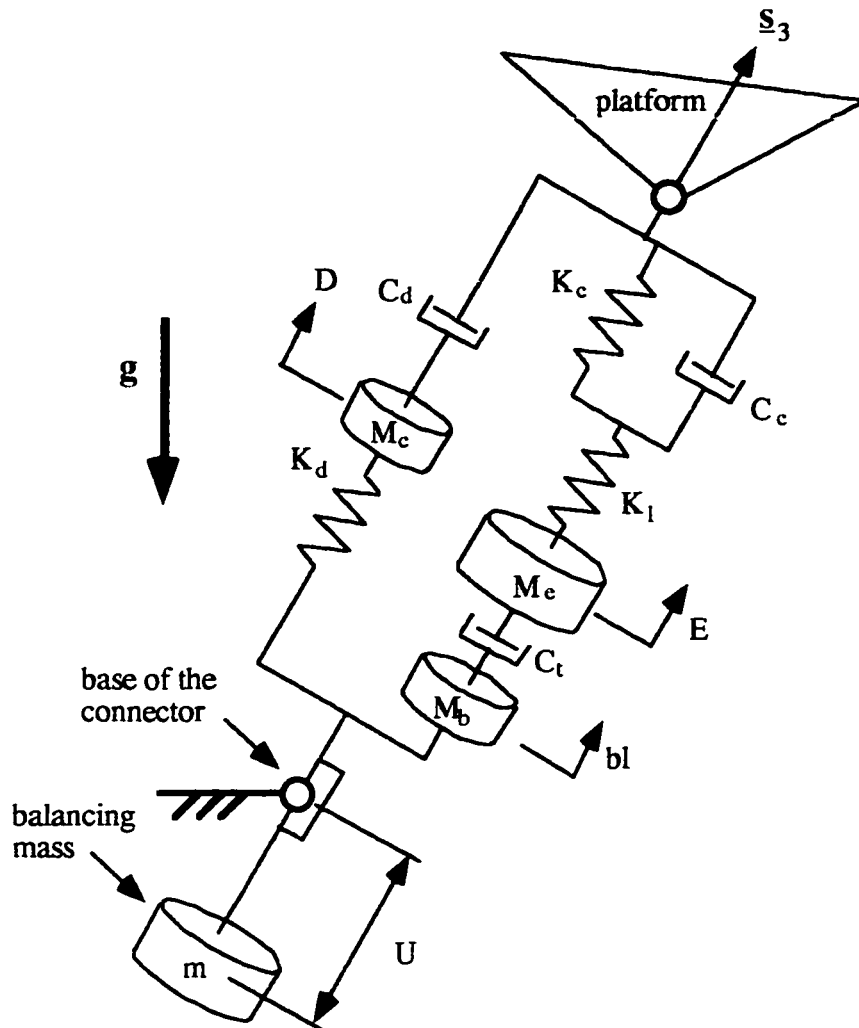
Figure 8.1 - Connector with balancing mass.

tangential, Coriolis and centrifugal accelerations. Therefore it is important to determine if these coupling effects are minor before using a balancing mass.

8.4 Summary

The following are the most important findings and recommendations stemming from this research

1 - Kane's Method is an efficient method for deriving the equations of motion for a parallel manipulator.

2 - The equations of motion indicate that there is a high degree of coupling between the connectors. This coupling is caused by the gravitational, tangential, Coriolis, centrifugal accelerations acting upon the connectors.

3 - The initial results from the dynamic simulations indicate that for the test motions used the most significant coupling is caused by gravity. The magnitude of the connector velocity and acceleration vectors are relatively small for the motions tested.

4 - The explicit equations of motion are useful for designing a manipulator with an improved or simplified dynamic behavior. One possibility is to use mass balancing to minimize the effects of gravity of the connectors.

APPENDIX
KANE'S METHOD FOR DYNAMIC ANALYSIS

The objective of this document is to give the reader a basic idea of how Kane's Formulation or Method is used to obtain the equations of motion of a multibody system. It is by no means a complete description of Kane's method.

The equations of motion for the dynamic model for a system with "w" elements (bodies and particles) and "n" degrees of freedom can be obtained by using the following equation:

$$\sum_{j=1}^{w} \left(\frac{\partial \underline{V}_j}{\partial u_k} \cdot \{ \underline{F}_j - \underline{F}_j^* \} \right) + \sum_{j=1}^{w} \left(\frac{\partial \underline{\omega}_j}{\partial u_k} \cdot \{ \underline{T}_j - \underline{T}_j^* \} \right) = 0; \quad k = 1, 2, ..., n \quad (1)$$

This equation must be setup for each of the degrees of freedom. In order to obtain the system's dynamic model, expressions for the following terms for each body must be determined:

$\frac{\partial \underline{V}_j}{\partial u_k}$, the velocity partial derivative of body "j" respect to the kth generalized speed

$\frac{\partial \underline{\omega}_j}{\partial u_k}$, the angular velocity partial derivative of body "j" respect to the kth generalized speed

$\underline{F}_j$, the resultant force vector acting on body "j" at a given point "c"

$\underline{T}_j$, the resultant torque vector acting on body "j", about the point "c"

$\underline{A}_j$, the acceleration vector of body "j" at a given point "c"

m_j, the mass of body j

$\underline{\omega}_j$, the angular velocity vector of body "j"

$\underline{\alpha}_j$, the angular acceleration vector of body "j"

Ij^* , the inertia dyadic of body "j", about the point "c"

200

1 Generalized Coordinate and Generalized Speeds

A Generalized Coordinate is a position or displacement variable used to describe a degree of freedom. The set of Generalized Coordinates is not unique, more than one can be used to describe the configuration of a system. The number of Generalized Coordinates must be equal to the degrees of freedom of the system (n)

$$\mathbf{q} = (\ q_1, q_2, \dots q_r, \dots q_n\ ) \Rightarrow \text{set of generalized coordinates}$$

A Generalized Speed is a function of the the Generalized Coordinates and their first time derivatives of the Generalized Coordinates. The Generalized Speeds are not unique, more than one set of Generalized Speeds can be used to describe a system. The number of Generalized Speeds must also be equal to the degrees of freedom of the system (n)

$$\mathbf{u} = (\ u_1, u_2, \dots u_r, \dots u_n\ ) \Rightarrow \text{set of generalized speeds}$$

The selection of a given set of Generalized Speeds and coordinates can simplify the derivation of the equations of motion of a system. How to select a set that will simplify the analysis is not immediately obvious, it is more a case of experience. This is illustrated in Example 1.

Example 1 - Determine the degrees of freedom, the Generalized Coordinates and the Generalized Speeds for the system shown in Figure 1.

Solution: The system has 2 degrees of freedom. The configuration of the system can be completely described once the angular position of each link is specified. Different sets of Generalized Coordinates (each must have two elements) can be used to describe the system, some of them are

$$\text{Set 1} \Rightarrow q_1 = x_a \ \& \ q_2 = x_b \ ; \quad \text{Set 2} \Rightarrow q_1 = y_a \ \& \ q_2 = y_b$$

$$\text{Set 3} \Rightarrow q_1 = \theta_1 \ \& \ q_2 = \theta_2 \ ; \quad \text{Set 4} \Rightarrow q_1 = \theta_1 \ \& \ q_2 = \theta_1 - \theta_2$$
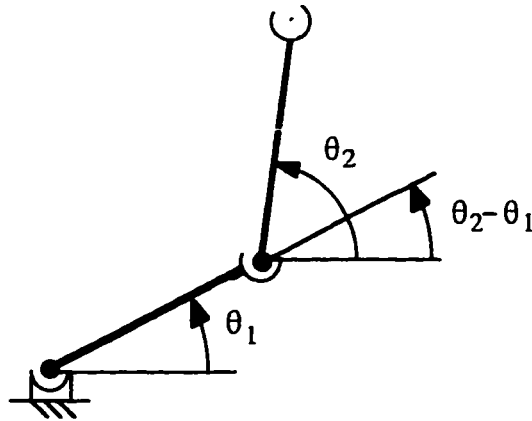
Figure 1 - System for Example 1

Different sets of Generalized Speeds (each must have two elements) can also be used to describe the system, some of them are

$$\text{Set 1} \Rightarrow u_1 = \frac{dx_a}{dt} \ \& \ u_2 = \frac{dx_b}{dt} \quad ; \quad \text{Set 2} \Rightarrow u_1 = \frac{dy_a}{dt} \ \& \ u_2 = \frac{dy_b}{dt}$$

$$\text{Set 3} \Rightarrow u_1 = \frac{d\theta_1}{dt} \ \& \ u_2 = \frac{d\theta_2}{dt} \quad ; \quad \text{Set 4} \Rightarrow u_1 = \frac{d\theta_1}{dt} \ \& \ u_2 = \frac{d\theta_2}{dt} - \frac{d\theta_1}{dt}$$

Any of the above sets can be used to define the Generalized Coordinates and the Generalized Speeds (for instance Set 1 of the Generalized Coordinates and set 4 of the Generalized Speeds can be used). Some of the sets will make the dynamic modeling easier in terms of the work required to derive the model. How to select the optimal set of Generalized Coordinates and speeds is mostly a matter of experience.

2 Velocity Partials and Angular Velocity Partials

The partial derivative of the velocity and the angular velocity are also known as the partial velocity and the partial angular velocity respectively [27]. The use of the terms "partial velocity" and "partial angular velocity" is confusing since it implies that these quantities are velocities and they must have velocity units. This is not the case and it is easier to call them the velocity partials and the angular velocity partials.

Expressions for the velocity at a given point in the body (the translational velocity) and the angular velocity of each body of the system must be determined in order to derive the velocity and angular velocity partials. The velocities and angular velocities will be expressed in terms of the Generalized Coordinates and Generalized Speeds. The velocity and the angular velocity of a given body can be written as a function of the Generalized Coordinates, Generalized Speeds and time

$$\underline{V}_i = f(q_1, q_2, ...q_n; u_1, u_2, ...u_n; t) \quad \& \quad \underline{\omega}_i = h(q_1, q_2, ...q_n; u_1, u_2, ...u_n; t)$$

In most cases, the velocity of a body is a function of the Generalized Coordinates and the Generalized Speeds which are implicit functions of time. The velocity partial derivatives and the angular velocity partial derivatives are obtained by taking the derivatives of the velocity and angular velocity vectors respect to each Generalized Speed. It will be shown that the velocity partials and the angular velocity partials are simply the coefficients of the Generalized Speeds in the expressions for the velocity and angular velocity vectors. Example 2 illustrates how to determine the velocity partials and angular velocity partials for a simple system as shown in Figure 1.

Example 2 - Determine the velocity and angular velocity partials for the system shown in Figure 1. Solution :

i - Define the Generalized Coordinates - In order to describe the system, two Generalized Coordinates are required since the system has two degrees of freedom. One possible choice is to use the angle between each link and the positive X axis

$$q_1 = \theta_1 \quad \& \quad q_2 = \theta_2$$

ii - Define the Generalized Speeds - Two Generalized Speeds are required, for which there are different options. In this case the two following possible sets will be used for the system

$$\text{Set } 1 : u_1 = \omega_1 ; u_2 = \omega_2 \qquad \text{Set } 2 : u_1 = \omega_1 ; u_2 = \omega_2 - \omega_1$$

where ω_1 and ω_2 are the time derivatives of the Generalized Coordinates.

iii - Find an expression for the velocity vector and angular velocity vector of each body of the system. These must be a function of the Generalized Speeds and Coordinates. The velocity of each link of the system at a given point must be determined. Point "a" will be used for link 1 and point "b" will be used for link 2

For the first set of Generalized Speeds, the velocities can be written as -

$$\underline{V}_1 = L_1 u_1 \, (-\sin\theta_1 \, \underline{i} + \cos\theta_1 \, \underline{j}); \qquad \underline{\omega}_1 = u_1 \, \underline{k}$$

$$\underline{V}_2 = L_1 u_1 \, (-\sin\theta_1 \, \underline{i} + \cos\theta_1 \, \underline{j}) + L_2 u_2 \, (-\sin\theta_2 \, \underline{i} + \cos\theta_2 \, \underline{j}); \qquad \underline{\omega}_2 = u_2 \, \underline{k}$$

The velocity partials and angular velocity partials can now be determined

$$\frac{\partial \underline{V}_1}{\partial u_1} = L_1 \, (-\sin\theta_1 \, \underline{i} + \cos\theta_1 \, \underline{j}) ; \qquad \frac{\partial \underline{V}_1}{\partial u_2} = 0$$

$$\frac{\partial \underline{V}_2}{\partial u_1} = L_1 \, (-\sin\theta_1 \, \underline{i} + \cos\theta_1 \, \underline{j}) ; \qquad \frac{\partial \underline{V}_2}{\partial u_2} = L_2 \, (-\sin\theta_2 \, \underline{i} + \cos\theta_2 \, \underline{j})$$

$$\frac{\partial \underline{\omega}_1}{\partial u_1} = \underline{k} ; \qquad \frac{\partial \underline{\omega}_1}{\partial u_2} = 0 ; \qquad \frac{\partial \underline{\omega}_2}{\partial u_1} = 0 ; \qquad \frac{\partial \underline{\omega}_2}{\partial u_2} = \underline{k}$$

For the second set of Generalized Speeds, the velocities can be written as -

$$\underline{V}_1 = L_1 u_1 \, (-\sin\theta_1 \, \underline{i} + \cos\theta_1 \, \underline{j})$$

$$\underline{V}_2 = L_1 u_1 \, (-\sin\theta_1 \, \underline{i} + \cos\theta_1 \, \underline{j}) + L_2 \, (u_1 - u_2) \, (-\sin\theta_2 \, \underline{i} + \cos\theta_2 \, \underline{j})$$

$$\underline{\omega}_1 = u_1 \, \underline{k}; \qquad \underline{\omega}_2 = (u_1 - u_2) \, \underline{k}$$

The velocity partials and angular velocity partials for this set of Generalized Speeds are

$$\frac{\partial \underline{V}_1}{\partial u_1} = L_1 \left(-\sin\theta_1 \, \underline{i} + \cos\theta_1 \, \underline{j}\right) ; \quad \frac{\partial \underline{V}_1}{\partial u_2} = 0$$

$$\frac{\partial \underline{V}_2}{\partial u_1} = L_1 \left(-\sin\theta_1 \, \underline{i} + \cos\theta_1 \, \underline{j}\right) + L_2 \left(-\sin\theta_2 \, \underline{i} + \cos\theta_2 \, \underline{j}\right)$$

$$\frac{\partial \underline{V}_2}{\partial u_2} = L_2 \left(\sin\theta_2 \, \underline{i} - \cos\theta_2 \, \underline{j}\right)$$

$$\frac{\partial \underline{\omega}_1}{\partial u_1} = \underline{k} ; \quad \frac{\partial \underline{\omega}_1}{\partial u_2} = 0 ; \quad \frac{\partial \underline{\omega}_2}{\partial u_1} = \underline{k} ; \quad \frac{\partial \underline{\omega}_2}{\partial u_2} = -\underline{k}$$

Note that the velocity and angular velocity partials do not have velocity units. The velocity partial derivatives have length units if the Generalized Speed is an angular velocity; and are dimensionless if the Generalized Speed is a translational velocity. The angular velocity partial derivatives are dimensionless. The selection of the set of Generalized Speeds will not affect the final form of the equations of motion. It will determine the amount of work that the analyst has to do in order to set up the dynamic model. In this problem the first set simplifies the expressions for the velocity partials which will also simplify the amount of work required to obtain the equations of motion. The velocity of each body can be expressed in terms of the Generalized Speeds and the velocity partials and angular velocity partials

$$\underline{V}_j = \sum_{k=1}^{n} \frac{\partial \underline{V}_j}{\partial u_k} \, u_k$$

The velocity partials and the angular velocity partials can be thought of as the base vectors in which the velocity of a body is expressed in. They are the directions in which the instantaneous motion is taking place at a given moment. If the velocity of body j does not depend on the rth Generalized Speed, the rth velocity partial of that body is zero.

3 Resultant Forces & Resultant Torques

The resultant forces and torques acting upon each body **j** of the system must be determined in order to obtain the equations of motion . It is very important that all the forces acting on a body be defined respect to a common point j. Although the point j for each body can be arbitrarily selected, it is more useful to define this point at the center of gravity of body **j**.

The resultant force and torque that act upon body **j** of the system can be written as

$$\mathbf{F}_i = \mathbf{F}_{ej} + \mathbf{F}_{cj} + \mathbf{F}_{fj} \quad \& \quad \mathbf{T}_j = \mathbf{T}_{ej} + \mathbf{T}_{cj} + \mathbf{T}_{fj}$$

where $\mathbf{F}_{ej}$ and $\mathbf{T}_{ej}$ are the external forces and torques; $\mathbf{F}_{cj}$ and $\mathbf{T}_{cj}$ are the contact forces and torques; and $\mathbf{F}_{fj}$ and $\mathbf{T}_{fj}$ are the field effect forces and torques.

The external forces and torques are all the inputs to the system that are generated by actuators such as motors and hydraulic pistons; or by disturbances such as chattering in milling and turning.

The contact or interaction forces are the forces and torques that are caused by the interaction of body j with other adjacent bodies. These can be divided into two categories: workless constraints and contributing forces. Noncontributing or workless constraint forces do not increase or decrease the energy of the system since they act parallel to directions along which there is no motion. A typical case is the normal force between a body and the surface. The body is moving tangent to the surface and the contact force is acting perpendicular to the surface, a direction in which there is no motion. These forces are also known as reciprocal forces, constraint forces, or workless forces. Although they can be included in the force expression without any loss of generality, it is not necessary to include these forces (or torques) in the resultant force (or torque) expression because once they are multiplied by the velocity partials and angular velocity partials (the base vectors for the body's motion) as required by equation (1) they will be eliminated.

The contributing interaction forces are generated between bodies that are connected by nonrigid elements such as elastic springs and viscous dampers. They act along the

direction of motion and will change the energy level of the system. Other connection forces such as those produced by dry friction and nonlinear elastic elements can also exist between two bodies. The force generated by these connections will be a function of the Generalized Coordinates and/or the Generalized Speeds.

Field forces and torques are those forces and torques caused by the action of a force field such as a magnetic force field or a gravitational field. Although the gravitational field is the most common type, there are some case in which the magnetic field has a considerable effect on a body such as in the case of magnetic bearings. The force or torque generated by gravity is given by

$$\underline{F}_{fj} = - M_j \, g \, \underline{e} \; ; \qquad \underline{T}_{fj} = (- M_j \, g \, \underline{e}) \times (\underline{r}_{j/cg})$$

where $\underline{e}$ is the direction of the gravitational field, and $\underline{r}_{j/cg}$ is the distance from the center of gravity to the point of reference. The torque caused by gravity is zero when the center of gravity is selected as the reference point

The resultant force and torque acting on a rigid body will be determined for the system of Example 3.

Example 3 - Determine the resultant forces and torques acting on the rigid body shown in Figure 2.

Solution - Assume that friction between the body and the inclined plane is zero and that all forces intersect the center of gravity of the rigid body.

i - Make a free body diagram for the rigid body as shown in Figure 3. There all types of forces acting on the rigid body. There is an external force F, there is the effect of gravity, there is a workless constraint acting normal to the inclined plane and there are contact forces produced by the spring and the damper.

ii - Add up all the forces acting on the rigid body - Since all the forces intersect the center of gravity, the resultant torque is zero. To simplify the force analysis, the forces will be added in the $\underline{t}$ and $\underline{n}$ directions.
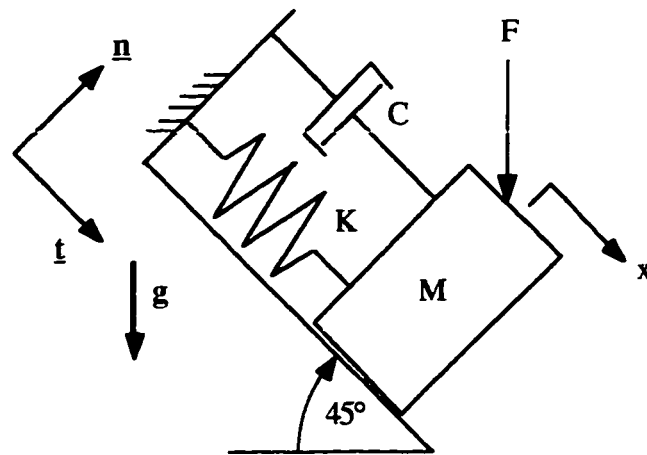
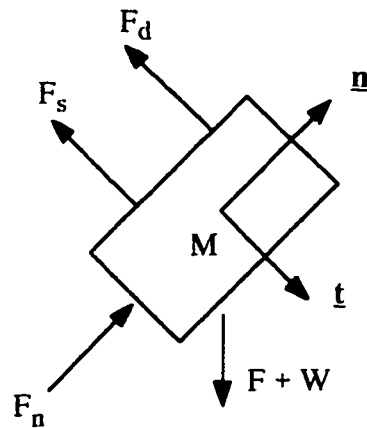Figure 2 - Example of a system with interaction forces

Figure 3 - Free-Body Diagram for example 3

Forces in the $\underline{t}$ direction

$$\sum F = (F + W)\cos 45°\underline{t} - (C\dot{x} + Kx)\underline{t}$$

Forces in the $\underline{n}$ direction

$$\sum F = F_n\underline{n} - (F + W)\cos 45°\underline{n}$$

where W is the weight of the mass M.

4 Resultant Inertial Forces and Resultant Inertial Torques

The resultant inertial force and torque acting on body j have are given by as

$$\underline{F}_j^* = - m_j \underline{A}_j \quad \& \quad \underline{T}_j^* = - \underline{\alpha}_j \cdot \mathbf{I}_j^{''} - \underline{\omega}_j \times \mathbf{I}_j^{''} \cdot \underline{\omega}_j$$

the acceleration vector and angular acceleration vector of body j at point j must be expressed as a function of the Generalized Coordinates, the Generalized Speeds and their time derivatives. Once the Inertia Dyadic, the acceleration and angular acceleration vectors of body j have been determined the resultant inertial force and torque can be easily calculated using the above equation.

4.1 Inertia Dyadic

The inertia dyadic is an alternate way of describing the inertia of a body. This section describes what is a dyad, a dyadic and how these can be used for describing the inertia of a rigid body. A dyad is an operator that is formed by the juxtaposition of any given number of vectors. As an example, given vectors $\underline{A}$ and $\underline{B}$, the dyad $\underline{A}\,\underline{B}$ is defined as

$$\underline{A} = \begin{bmatrix} A_x \\ A_y \\ A_z \end{bmatrix} \quad \& \quad \underline{B} = \begin{bmatrix} B_x \\ B_y \\ B_z \end{bmatrix} \quad \text{the dyad} \quad \underline{A}\,\underline{B} = \begin{bmatrix} A_x \\ A_y \\ A_z \end{bmatrix}\begin{bmatrix} B_x \\ B_y \\ B_z \end{bmatrix}$$

Note that the dyad is neither a scalar product nor a vector product of the vectors involved, these vectors are just grouped together. One of the properties of a dyad is that when the scalar product of a dyad $\underline{A}\,\underline{B}$ and a vector $\underline{u}$ is taken, another vector is always obtained. The resultant vector depends of the order of the multiplication

$$\underline{v} = \underline{u} \cdot \underline{A}\,\underline{B} \quad ; \quad \underline{w} = \underline{A}\,\underline{B} \cdot \underline{u} \quad \text{where } \underline{v} \neq \underline{w}$$

A dyadic, Q", is a sum of dyads

$$Q^{''} = \underline{A}\,\underline{B} + \underline{C}\,\underline{D} + \underline{E}\,\underline{F} \ \dots$$

The inertia of a rigid body can be described by using an inertia matrix or tensor [I]. This is defined respect to a set of mutually perpendicular axes (such as $\underline{n}_1, \underline{n}_2$ & $\underline{n}_3$ of Figure 4)

$$(I_{123}) = \begin{pmatrix} I_{11} & I_{12} & I_{13} \\ I_{21} & I_{22} & I_{23} \\ I_{31} & I_{32} & I_{33} \end{pmatrix}$$

One of the limitations of using the inertia matrix [I_{123}] is that it must be rederived if the inertia of the body is to be described with respect to another set of axes (such as $\underline{n}_a, \underline{n}_b$ & $\underline{n}_c$ of Figure 4). A better way to describe the inertial properties of a rigid body is by using the inertia dyadic I''. The dyadic I'' can be defined in terms of the inertia matrix of the rigid body, [I_{123}] (which is defined in terms of the axes $\underline{n}_1, \underline{n}_2$ & $\underline{n}_3$), and the axes $\underline{n}_1, \underline{n}_2$ & $\underline{n}_3$

$$I'' = I_1\,\underline{n}_1 + I_2\,\underline{n}_2 + I_3\,\underline{n}_3 \qquad (51)$$

where I_1, I_2 & I_3 are the columns of the inertia matrix [I_{123}]. This can also be written as

$$I'' = \begin{bmatrix} I_{11} \\ I_{21} \\ I_{31} \end{bmatrix}\begin{bmatrix} n1_x \\ n1_y \\ n1_z \end{bmatrix} + \begin{bmatrix} I_{12} \\ I_{22} \\ I_{32} \end{bmatrix}\begin{bmatrix} n2_x \\ n2_y \\ n2_z \end{bmatrix} + \begin{bmatrix} I_{13} \\ I_{23} \\ I_{33} \end{bmatrix}\begin{bmatrix} n3_x \\ n3_y \\ n3_z \end{bmatrix}$$

The inertia dyadic can be used to determine the elements of the inertia matrix, [I_{abc}], defined with respect to any set of axes (such as $\underline{n}_a, \underline{n}_b$ & $\underline{n}_c$ in figure 3)

$$[I_{abc}] = [\,\underline{n}_a \cdot I'', \underline{n}_b \cdot I'', \underline{n}_c \cdot I''\,]$$

This can be also written as

$$I_a = \underline{n}_a \cdot I'' = \underline{n}_a \cdot I_1\,\underline{n}_1 + \underline{n}_a \cdot I_2\,\underline{n}_2 + \underline{n}_a \cdot I_3\,\underline{n}_3$$

$$I_b = \underline{n}_b \cdot I'' = \underline{n}_b \cdot I_1\,\underline{n}_1 + \underline{n}_b \cdot I_2\,\underline{n}_2 + \underline{n}_b \cdot I_3\,\underline{n}_3$$
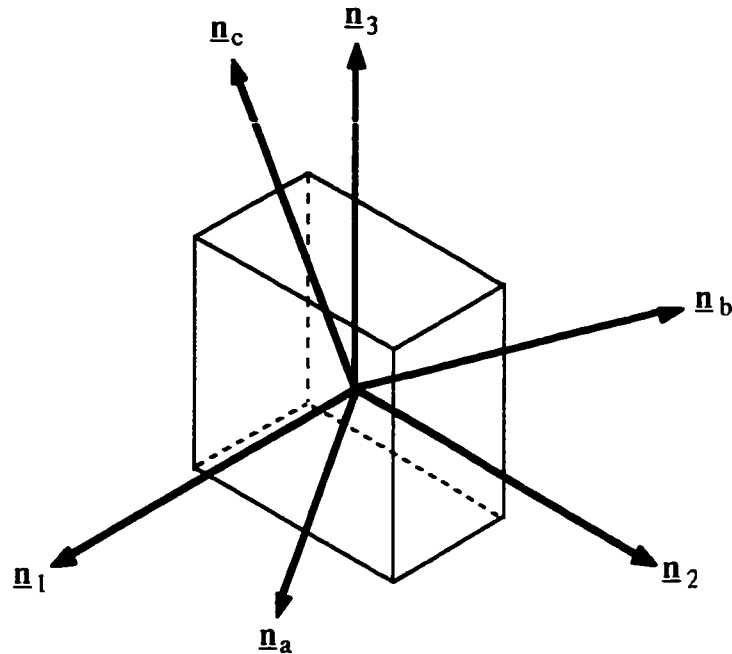
Figure 4 - Different sets of reference axes

$$I_c = \underline{n}_c \cdot I'' = \underline{n}_c \cdot I_1 \underline{n}_1 + \underline{n}_c \cdot I_2 \underline{n}_2 + \underline{n}_c \cdot I_3 \underline{n}_3$$

where I_a, I_b & I_c are the columns of the inertia matrix $[I_{abc}]$.

A simple way to determine the inertia dyadic of a rigid body is by using the moment of inertia about the principal axes of the body

$$I''_j = I_{xx} \underline{n}_x \underline{n}_x + I_{yy} \underline{n}_y \underline{n}_y + I_{zz} \underline{n}_z \underline{n}_z$$

where I_{xx}, I_{yy} & I_{zz} are the principal moments of inertia; and $\underline{n}_x$, $\underline{n}_y$ and $\underline{n}_z$ are unit vectors describing the orientation of the principal axes of the rigid body. The inertia dyadic for body j in terms of the principal axes can also be written in its expanded form as

$$I''_j = I_{xx} \begin{bmatrix} nx_x \\ nx_y \\ nx_z \end{bmatrix} \begin{bmatrix} nx_x \\ nx_y \\ nx_z \end{bmatrix} + I_{yy} \begin{bmatrix} ny_x \\ ny_y \\ ny_z \end{bmatrix} \begin{bmatrix} ny_x \\ ny_y \\ ny_z \end{bmatrix} + I_{zz} \begin{bmatrix} nz_x \\ nz_y \\ nz_z \end{bmatrix} \begin{bmatrix} nz_x \\ nz_y \\ nz_z \end{bmatrix}$$

Although the Inertia Dyadic is independent of the orientation of coordinate frame, it depends on the location of the origin of the coordinate frame in a similar way as the inertia tensor. The Theorem of Parallel Axes, which is used to determine the inertia tensor for any origin location, also applies to Inertia Dyadics

$$\mathbf{I}"_{j/a} = \mathbf{I}"_{j/c} + \mathbf{I}"_{a/c}$$

where $\mathbf{I}"_{j/a}$ is the Inertia Dyadic of body j about an arbitrary point a, $\mathbf{I}"_{j/c}$ is the Inertia Dyadic of body j about its center of gravity c, and $\mathbf{I}"_{a/c}$ is the change in Inertia Dyadic produced by the change of reference point from c to a. This third term depends on the relative position vector of point "a" with respect to c, and on the mass of body j.

Example 4 - Using the concept of Inertia Dyadic, determine the inertia matrix for the body shown in Figure 5 respect to the XYZ frame. The principal moments of inertia are given by (for a thin disk)

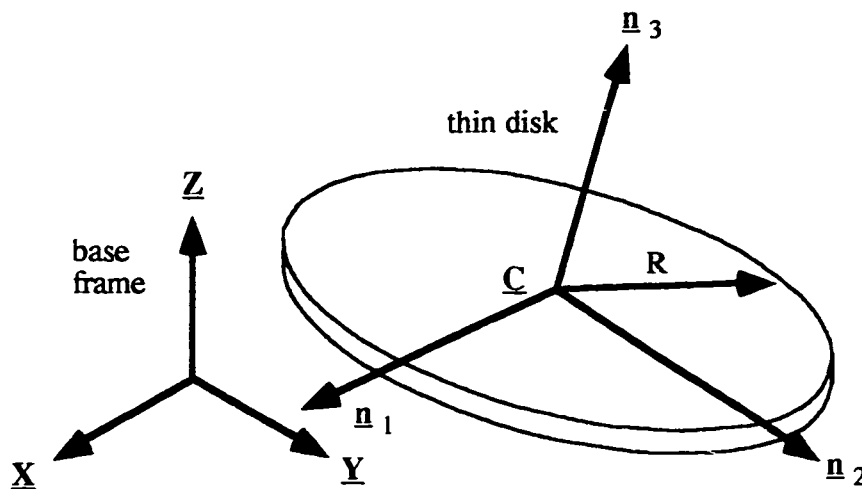$$I_{zz} = 0.5\, m\, R^2 ; \qquad I_{xx} = I_{yy} = 0.25\, m\, R^2$$

Figure 5 - System for Example 4

The orientation of the rigid body is described by the unit vectors $\underline{n}_1$, $\underline{n}_2$ and $\underline{n}_3$

$$\underline{n}_1 = \begin{bmatrix} 0.866 \\ 0.50 \\ 0 \end{bmatrix} \qquad \underline{n}_2 = \begin{bmatrix} -0.353 \\ 0.612 \\ 0.707 \end{bmatrix} \qquad \underline{n}_3 = \begin{bmatrix} 0.353 \\ -0.612 \\ 0.707 \end{bmatrix}$$

The principal axes and moments of inertia will be used to determine the Inertia Dyadic for this body

$$\mathbf{I}'' = I_{xx} \begin{bmatrix} 0.866 \\ 0.50 \\ 0 \end{bmatrix}\begin{bmatrix} 0.866 \\ 0.50 \\ 0 \end{bmatrix} + I_{yy} \begin{bmatrix} -0.353 \\ 0.612 \\ 0.707 \end{bmatrix}\begin{bmatrix} -0.353 \\ 0.612 \\ 0.707 \end{bmatrix} + I_{zz} \begin{bmatrix} 0.353 \\ -0.612 \\ 0.707 \end{bmatrix}\begin{bmatrix} 0.353 \\ -0.612 \\ 0.707 \end{bmatrix}$$

The inertia matrix or tensor respect to the XYZ frame can be determined by using the following equation

$$[\mathbf{I}] = [\underline{X} \cdot \mathbf{I}'', \underline{Y} \cdot \mathbf{I}'', \underline{Z} \cdot \mathbf{I}'']$$

Each column of the inertia matrix or tensor is given by

$$\underline{X} \cdot \mathbf{I}'' = \left(I_{xx}\begin{bmatrix} 1 \\ 0 \\ 0 \end{bmatrix} \cdot [\underline{n}_1][\underline{n}_1] + I_{yy}\begin{bmatrix} 1 \\ 0 \\ 0 \end{bmatrix} \cdot [\underline{n}_2][\underline{n}_2] + I_{zz}\begin{bmatrix} 1 \\ 0 \\ 0 \end{bmatrix} \cdot [\underline{n}_3][\underline{n}_3] \right)$$

$$\underline{Y} \cdot \mathbf{I}'' = \left(I_{xx}\begin{bmatrix} 0 \\ 1 \\ 0 \end{bmatrix} \cdot [\underline{n}_1][\underline{n}_1] + I_{yy}\begin{bmatrix} 0 \\ 1 \\ 0 \end{bmatrix} \cdot [\underline{n}_2][\underline{n}_2] + I_{zz}\begin{bmatrix} 0 \\ 1 \\ 0 \end{bmatrix} \cdot [\underline{n}_3][\underline{n}_3] \right)$$

$$\underline{Z} \cdot \mathbf{I}'' = \left(I_{xx}\begin{bmatrix} 0 \\ 0 \\ 1 \end{bmatrix} \cdot [\underline{n}_1][\underline{n}_1] + I_{yy}\begin{bmatrix} 0 \\ 0 \\ 1 \end{bmatrix} \cdot [\underline{n}_2][\underline{n}_2] + I_{zz}\begin{bmatrix} 0 \\ 0 \\ 1 \end{bmatrix} \cdot [\underline{n}_3][\underline{n}_3] \right)$$

Substituting the values of the moments of inertia and the unit vectors $\underline{n}_1$, $\underline{n}_2$ and $\underline{n}_3$, the inertia tensor respect to the XYZ frame is

$$[\mathbf{I}] = m\,R^2 \begin{bmatrix} 0.281 & -0.0514 & 0.0625 \\ -0.0514 & 0.344 & -0.108 \\ 0.0625 & -0.108 & 0.375 \end{bmatrix}$$

The following example shows how to determine the inertial forces and torques, using the definition given before and the Inertia Dyadic.

Example 5 - Determine the inertial forces and torques acting on each link in Figure 1

Solution

i - First determine the acceleration and angular acceleration vectors for both links. These can be found by taking the time derivative of the velocity and angular velocity vectors which were found in example 2

$$\underline{V}_1 = L_1\, u_1\, (-\sin\theta_1\, \underline{i} + \cos\theta_1\, \underline{j})$$

$$\underline{V}_2 = L_1\, u_1\, (-\sin\theta_1\, \underline{i} + \cos\theta_1\, \underline{j}) + L_2\, u_2\, (-\sin\theta_2\, \underline{i} + \cos\theta_2\, j)$$

$$\underline{\omega}_1 = u_1\, \underline{k}; \quad \underline{\omega}_2 = u_2\, \underline{k}$$

The accelerations and angular accelerations for bodies 1 and 2 are

Acceleration of Body 1 at point a, and the angular acceleration of Body 1

$$\underline{A}_1 = L_1\, \frac{du_1}{dt}\, (-\sin\theta_1\, \underline{i} + \cos\theta_1\, \underline{j}) + L_1\, u_1\, \omega_1\, (-\cos\theta_1\, \underline{i} - \sin\theta_1\, \underline{j})$$

$$\underline{\alpha}_1 = \frac{du_1}{dt}\, \underline{k}$$

Acceleration of Body 2 at point b, and the angular acceleration of Body 2

$$\underline{A}_2 = \underline{A}_1 + L_2\, \frac{du_2}{dt}\, (-\sin\theta_2\, \underline{i} + \cos\theta_2\, \underline{j}) + L_2\, u_2\, \omega_2\, (-\cos\theta_2\, \underline{i} - \sin\theta_2\, \underline{j})$$

$$\underline{\alpha}_2 = \frac{du_2}{dt}\, \underline{k}$$

ii - Using the fact that the Generalized Speeds u_1 and u_2 are the angular velocity of links 1 and 2 respectively, the resultant inertial forces calculated by using the expressions derived above are

$$\mathbf{F}_1^* = M_1 L_1 \alpha_1 (\sin\theta_1 \mathbf{i} - \cos\theta_1 \mathbf{j}) + M_1 L_1 \omega_1^2 (\cos\theta_1 \mathbf{i} + \sin\theta_1 \mathbf{j})$$

$$\mathbf{F}_2^* = -M_2 \mathbf{A}_1 + M_2 L_2 \alpha_2 (\sin\theta_2 \mathbf{i} - \cos\theta_2 \mathbf{j}) + M_2 L_2 \omega_2^2 (\cos\theta_2 \mathbf{i} + \sin\theta_2 \mathbf{j})$$

iii - In the planar case the angular velocity and acceleration vectors are perpendicular to the plane. The unit vectors $\mathbf{n}_1$ and $\mathbf{n}_2$ are in the plane and the unit vector $\mathbf{n}_3$ is perpendicular to the plane. Therefore the following scalar and vector products are zero

$$\underline{\alpha}_j \cdot [\mathbf{n}_1] = \underline{\alpha}_j \cdot [\mathbf{n}_2] = \underline{\omega}_j \cdot [\mathbf{n}_1] = \underline{\omega}_j \cdot [\mathbf{n}_2] = \underline{\omega}_j \times [\mathbf{n}_3] = 0$$

The first term of both inertial torques can be simplified to

$$\underline{\alpha}_j \cdot \mathbf{Ij}'' = I_{xx} \underline{\alpha}_j \cdot [\mathbf{n}_1][\mathbf{n}_1] + I_{yy} \underline{\alpha}_j \cdot [\mathbf{n}_2][\mathbf{n}_2] + I_{zz} \underline{\alpha}_j \cdot [\mathbf{n}_3][\mathbf{n}_3] = I_{zz} \alpha_j \mathbf{k}$$

The second term of each inertial torque can be simplified to

$$\underline{\omega}_j \times \mathbf{Ij}'' \cdot \underline{\omega}_j = I_{xx} \underline{\omega}_j \times [\mathbf{n}_1][\mathbf{n}_1] \cdot \underline{\omega}_j + I_{yy} \underline{\omega}_j \times [\mathbf{n}_2][\mathbf{n}_2] \cdot \underline{\omega}_j +$$

$$I_{zz} \underline{\omega}_j \times [\mathbf{n}_3][\mathbf{n}_3] \cdot \underline{\omega}_j = 0$$

Therefore the resultant inertial torques for links 1 and 2 are

$$\mathbf{T}_1^* = -\alpha_1 I_{Z1} \mathbf{k} \quad \& \quad \mathbf{T}_2^* = -\alpha_2 I_{Z2} \mathbf{k}$$

6 Steps for using Kane's Method

In order to derive the dynamic model of a system using Kane's Method, the following steps must be completed

1 - Determine the degrees of freedom of the system to be analyzed, n

2 - Select the Generalized Coordinates (must be an independent set which has n terms)

3 - Define the n Generalized Speeds for the system. These must functions of the Generalized Coordinates and their first time derivatives.

4 - Write expressions for the velocity, angular velocity, acceleration and angular acceleration of each body in the system in terms of the n Generalized Coordinates and the n Generalized Speeds defined in steps 2 and 3.

5 - Obtain the velocity partials and angular velocity partials of the equations from step 4.

6 - Obtain the resultant force and torque acting on each body.

7 - Calculate the resultant inertial force and torque acting on each body.

8 - Setup the n equations of motion using equation (1)

These steps will be used in the examples that follow.

Example 6 - Obtain the dynamic model for the system shown in figure 6 using the steps outlined above.

step 1 - The system has one degree of freedom.

step 2 - The displacement of mass M, x, will be used as the Generalized Coordinate.

step 3 - The first time derivative of x will be used as the Generalized Speed.

$$q_1 = x \qquad \& \qquad u_1 = \frac{dx}{dt}$$

step 4 - The angular velocity and angular acceleration are zero since the system only has translational motion. The velocity and acceleration for the mass M are given by

$$V = u_1 \, \mathbf{i} \quad ; \quad A = \frac{du_1}{dt} \, \mathbf{i}$$
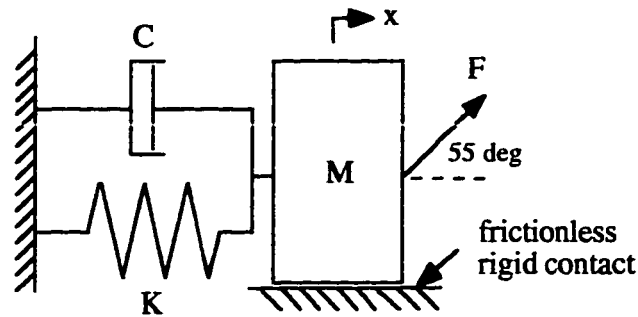
Figure 6 - System for example 6

step 5 - The angular velocity partial is zero since the angular velocity is zero. The velocity partial derivative with respect to the Generalized Speed is

$$\frac{\partial \underline{V}}{\partial u_1} = \underline{i} \qquad \frac{\partial \underline{\omega}}{\partial u_1} = 0$$

step 6 - The resultant torque for this system is zero since all the forces are assumed to go through the center of gravity of the mass. The resultant force acting on the body is given by

$$\underline{F}_1 = F \cos(55^\circ) \underline{i} - Kx \underline{i} - C \frac{dx}{dt} \underline{i} + F \sin(55^\circ) \underline{j} + Fn \underline{j} \quad ; \quad \underline{T}_1 = 0$$

step 7 - The resultant inertial torque for this system is zero since the angular acceleration is zero. The resultant inertial force acting on the body is given by

$$\underline{F}_1^* = M \frac{d^2x}{dt^2} \underline{i} \quad ; \quad \underline{T}_1^* = 0$$

step 8 - The equation of motion is given by equation (1)

$$\frac{\partial \underline{V}}{\partial u_1} \left(\underline{F}_1 - \underline{F}_1^* \right) = 0$$

Using the expressions for the velocity partial derivative, the resultant force and the inertial

force derived in previous steps the equation of motion can be written as

$$\underline{i} \cdot \left[\left(F \cos(55^\circ)\, \underline{i} - Kx\, \underline{i} - C \frac{dx}{dt}\, \underline{i} + F \sin(55^\circ)\, \underline{j} + Fn\, \underline{j} \right) - M \frac{d^2x}{dt^2}\, \underline{i} \right]$$

The equation of motion can be simplified to

$$0.5735\, F = M \frac{d^2x}{dt^2} + C \frac{dx}{dt} + Kx$$

Notice that the workless contact force, F_n, is eliminated from the equation once the scalar product is taken with the velocity partial derivative (which define the directions of motion). For this example, the equation could be obtained with less effort using Newton's 2nd Law. For more complicated problems, Kane's Method is more efficient for setting up the dynamic model.

Example 7 - Obtain the dynamic model for the system shown in figure 7

For simplicity, the unit vectors $\underline{t}$ and $\underline{n}$ will be used to describe the forces and motion.

step 1 - Determine the degrees of freedom of the system: By inspection it can be seen that this system has two degrees of freedom.

step 2 - Select the Generalized Coordinates : The displacements X_a and X_b will be used as the Generalized Coordinates. These are sufficient to locate all the parts of the system.

$$q_1 = X_a \qquad \& \qquad q_2 = X_b$$

step 3 - Define the n Generalized Speeds for the system: The following set of Generalized Speeds will be used -

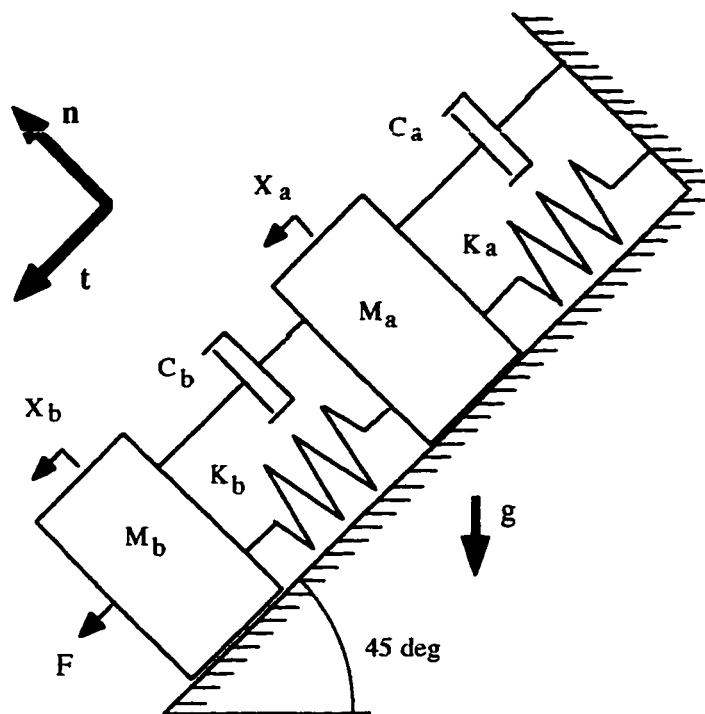$$u_1 = \frac{dX_a}{dt} \; ; \; u_2 = \frac{dX_b}{dt} - \frac{dX_a}{dt}$$

Figure 7 - An inclined 2 DOF system

step 4 - The angular velocities and angular accelerations are zero there is only translational motion. The velocities and accelerations for the masses M_a & M_b are given by

$$\underline{V}_a = u_1 \, \underline{t} \ ; \quad \underline{V}_b = u_2 \, \underline{t} + u_1 \, \underline{t} \ ; \quad \underline{A}_a = \frac{du_1}{dt} \, \underline{t} \ ; \quad \underline{A}_b = \frac{du_2}{dt} \, \underline{t} + \frac{du_1}{dt} \, \underline{t}$$

step 5 - Obtain the velocity partial derivatives and the angular velocity partial derivatives

$$\frac{\partial \underline{V}_a}{\partial u_1} = \underline{t} \ ; \quad \frac{\partial \underline{V}_a}{\partial u_2} = 0 \ ; \quad \frac{\partial \underline{V}_b}{\partial u_1} = \underline{t} \ ; \quad \frac{\partial \underline{V}_b}{\partial u_2} = \underline{t}$$

step 6 - Obtain the resultant force and torque acting on each body: Only the resultant forces will be determined since there are no torques acting upon the system. There are contributing interaction forces generated by the springs and viscous dampers acting on the system, a workless constraint from the contact of the bodies with the inclined plane, an

external force acting on M_b and the gravitational field acting on both bodies.

The forces acting on body "a" are

external forces: $F_{ea} = 0$

contact forces: $F_{ca} = C_b u_2 \underline{t} - C_a u_1 \underline{t} + K_b (X_b - X_a) \underline{t} - K_a X_a \underline{t} + F_{na} \underline{n}$

field forces: $F_{fa} = 0.707 M_a g \underline{t} - 0.707 M_a g \underline{n}$

The resultant force acting of body "a" is

$$F_a = 0.707 M_a g (\underline{t} - \underline{n}) + C_b u_2 \underline{t} - C_a u_1 \underline{t} + K_b (X_b - X_a) \underline{t} - K_a X_a \underline{t} + F_{na} \underline{n}$$

The forces acting on body "b" are

external forces: $F_{eb} = F \underline{t}$

contact forces: $F_{cb} = - C_b u_2 \underline{t} - K_b (X_b - X_a) \underline{t} + F_{nb} \underline{n}$

field forces: $F_{fb} = 0.707 M_b g \underline{t} - 0.707 M_b g \underline{n}$

The resultant force acting of body "b" is

$$F_b = F \underline{t} + 0.707 M_b g \underline{t} - 0.707 M_b g \underline{n} - C_b u_2 \underline{t} - K_b (X_b - X_a) \underline{t} + F_{nb} \underline{n}$$

where F_{na} and F_{nb} are the workless contact forces between each body and the inclined plane.

step 7 - Obtain the resultant inertial forces and torques: The resultant inertial torques are zero since the system only has translational motion (angular velocities and accelerations are zero).

The resultant inertial force acting of body "a" and body "b" are

$$F^*_a = A_a M_a = \frac{du_1}{dt} M_a \underline{t} = \ddot{X}_a M_a \underline{t}$$

$$F^*_b = A_b M_b = \left(\frac{du_2}{dt} + \frac{du_1}{dt} \right) M_b \underline{t} = \ddot{X}_b M_b \underline{t}$$

step 8 – Setup the equations of motion using (1)

for the first Generalized Coordinate and second Generalized Coordinates

$$\frac{\partial \underline{V}_a}{\partial u_1}\left(\underline{F}_a - \underline{F}_a^*\right) + \frac{\partial \underline{V}_b}{\partial u_1}\left(\underline{F}_b - \underline{F}_b^*\right) = 0$$

$$\frac{\partial \underline{V}_a}{\partial u_2}\left(\underline{F}_a - \underline{F}_a^*\right) + \frac{\partial \underline{V}_b}{\partial u_2}\left(\underline{F}_b - \underline{F}_b^*\right) = 0$$

The first term of the first equation of motion can be written as

$$\frac{\partial \underline{V}_a}{\partial u_1}\left(\underline{F}_a - \underline{F}_a^*\right) = \underline{t} \cdot \left[C_b u_2 \underline{t} + K_b (X_a - X_b)\underline{t} - C_a u_1 \underline{t} - K_a X_a \underline{t} \right] +$$

$$\underline{t} \cdot \left[0.707 M_a g \underline{t} - 0.707 M_a g \underline{n} + F_{na} \underline{n} - \ddot{X}_a M_a \underline{t} \right]$$

The second term of the first equation of motion can be written as

$$\frac{\partial \underline{V}_b}{\partial u_1}\left(\underline{F}_b - \underline{F}_b^*\right) = \underline{t} \cdot \left[F \underline{t} - C_b u_2 \underline{t} - K_b (X_a - X_b)\underline{t} + F_{nb} \underline{n} \right] +$$

$$\underline{t} \cdot \left[0.707 M_b g \underline{t} - 0.707 M_b g \underline{n} - \ddot{X}_b M_b \underline{t} \right]$$

The first equation of motion is obtained by simplifying both terms and grouping

$$F = \left(\ddot{X}_b - 0.707 g \right) M_b + \left(\ddot{X}_a - 0.707 g \right) M_a + C_a u_1 + K_a X_a$$

The first term of the second equation of motion is zero since the velocity partial derivative is zero. The second term of this second equation of motion is

$$\frac{\partial \underline{V}_b}{\partial u_2}\left(\underline{F}_b - \underline{F}_b^*\right) = \underline{t} \cdot \left[F \underline{t} - C_b u_2 \underline{t} - K_b (X_a - X_b)\underline{t} + F_{nb} \underline{n} \right] +$$

$$\underline{t} \cdot \left[0.707 M_b g \underline{t} - 0.707 M_b g \underline{n} - \ddot{X}_b M_b \underline{t} \right]$$

Simplifying, the second equation of motion can be written as

$$F = \left(\ddot{X}_b - 0.707 \, g \right) M_b + C_b u_2 + K_b \left(X_a - X_b \right)$$

Note - The workless constraint forces F_{na} and F_{nb} are eliminated by the scalar product of the velocity partials. Therefore Kane's Method provides a sure way to eliminate workless constraints that other method such as Lagrange do not.

REFERENCES

[1] D. Stewart, " A platform with six degrees of freedom", Proc. of the Institute for Mechanical Engineering, London, Vol. 180, pp. 371 - 386, 1965.

[2] M. Griffis and J. Duffy, "A Foward Displacement Analysis of a Class of Stewart Platforms," Journal of Robotic Systems, Vol. 6, No. 6, pp. 703 - 720, June 1989.

[3] W. Lin, M. Griffis and J. Duffy, " Foward Displacement Analyses of the 4-4 Stewart Platforms, " Trans. ASME, Journal of Mechanical Design, Vol. 114, No. 3, pp. 444-450., September 1992.

[4] W. Lin, C. Crane and J. Duffy, "Closed-Form Foward Displacement Analysis of the 4-5 In-Parallel Platforms," Trans. ASME, Journal of Mechanical Design, Vol. 116, No. 1, pp. 47-53, March 1994.

[5] E.F. Fichter and E.D. McDowell, "A Novel Design for a Robot Arm", ASME Advances in Computer Technology, pp. 250 - 256, 1980.

[6] E.F. Fichter, "A Stewart platform-based manipulator: General theory and practical construction", International Journal of Robotics Research, Vol. 5, No. 2, pp. 165 - 190, 1986.

[7] K. Sugimoto, "Kinematic and dynamic analysis of parallel manipulators by means of motor algebra", ASME Journal of Mechanisms, Transmissions and Automation in Design, Vol. 109, pp. 1 - 5, 1987.

[8] W.Q.D. Do and D.C.H. Yang, " Inverse Dynamic Analysis and Simulation of a Platform Type of Robot", Journal of Robotic Systems, Vol 5, No. 3, pp.209 - 227, 1988.

[9] G. Lebret, K. Liu and F.L. Lewis, "Dynamic Analysis and Control of a Stewart Platform Manipulator", Journal of Robotic Systems, Vol. 10, No. 5, pp. 629 - 655, 1993.

[10] H. Pang and M. Shahinpoor, "Inverse Dynamics of a Parallel Manipulator", Journal of Robotic Systems, Vol. 11, No.8, pp. 693 - 702, 1994.

[11] G.H. Pfreundschuh, T.G. Sugar and V. Kumar, "Design and Control of a Three-Degrees-of-Freedom, in-Parallel, Actuated Manipulator", Journal of Robotic Systems, Vol. 11, No.2, pp. 103 - 115, 1994.

[12] C.C. Nguyen, S.S. Antrazi , Z. Zhou and C.E. Campbell Jr., "Adaptive Control of a Stewart Platform Base Manipulator", Journal of Robotic Systems, Vol. 10, No.2, pp. 657 - 687, 1993.

[13] H. Asada and J.J. Slotine, "Robot Analysis and Control", John Wiley & Sons, New York, 1986.

[14] H. Asada and K. Youcef-Toumi, "Direct Drive Robots: Theory and Practice", MIT Press, Cambridge, 1987.

[15] P.W. Likins, "Analytical Dynamics and Nonrigid Spacecraft Simulation", NASA Technical Report 32-1593, Jet Propulsion Laboratory, July 1974.

[16] M. Griffis and J. Duffy, "Kinestatic Control: A Novel Theory for Simultaneously Regulating Force and Displacement, " Trans. ASME, Journal of Mechanical Design, Vol. 113, No. 4, pp. 508-515., December 1991.

[17] J. Duffy and C. Crane, "Development of a Prototype Kinestatic Platform for Application to Space and Ground Servicing Tasks, Phase I: Concept Modeling", Nasa Design Report, September 1993.

[18] R. Paul, "Robot Manipulators: Mathematics, Programming and Control ", Cambridge, The MIT Press, 1981.

[19] J.M. Rico and J. Duffy, "A Simple Method for the Velocity and Acceleration Analysis of In Parallel Platforms", Proc. of the Ninth World Congress on the Theory of Machines and Mechanisms, Vol. 1, September 1995.

[20] J. Duffy and M. Griffis, "Geometry of Mechanisms and Robots II", Course notes for EML 6282 , Graduate Course, Dept. of Mechanical Engineering, University of Florida, 1994.

[21] J. Phillips, "Freedom in Machinery, Vol 1 & 2", Cambridge, Cambridge University Press, 1982.

[22] K.H. Hunt, "Kinematic Geometry of Mechanisms", Oxford, Claredon Press, 1978.

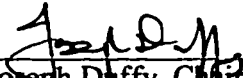[23] R.S. Ball, "A Treatise on the Theory of Screws", Cambridge, Cambridge University Press, 1900.

[24] A.G. Erdman and G.N. Sandor, "Mechanism Design: Analysis and Design", Englewood Cliffs, Prentice Hall, 1984.

[25] J. Tlusty, "Fundamentals of Production Engineering", Course notes for EML 6324 , Graduate Course, Dept. of Mechanical Engineering, University of Florida, 1994.

[26] S.D. Crandall, D.C. Karnopp, E.F. Kurtz and D.C. Pridmore-Brown, "Dynamics of Mechanical and Electromechanical Systems", New York, McGraw-Hill, 1968.

[27] T.R. Kane and D.A. Levinson, " Dynamics: Theory and Applications", New York, McGraw-Hill, 1985.

[28] W.H. Press, S.A. Teukolsky, W.T. Vetterling and B.P. Flannery, "Numerical Recipes in C: The Art of Scientific Computing", 2nd ed, Cambridge, Cambridge University Press, 1992.

[29] R.C. Dorf, "Modern Control Engineering", 5th ed, Reading, Addison-Wesley, 1989.

[30] A. Kelley and I. Pohl, "C by Dissection: The Essentials of C Programming", 2nd ed, New York, The Benjamin / Cummings Publishing Company, 1992.

[31] J. Duffy, "Kinematics and Statics with Applications in Robotics", Cambridge, Cambridge University Press, 1995.

[32] C. Ahrikencheikh and A. Seireg, "Optimized-Motion Planning", New York, John Wiley & Sons, 1994.

BIOGRAPHICAL SKETCH

Ivan J. Baiges-Valentin was born in Los Angeles, California, and raised in Ponce, Puerto Rico. He received his Bachelor of Science in Mechanical Engineering from the University of Puerto Rico at Mayagüez in May 1986. His interest in mechanical design and rehabilitation engineering lead him to the graduate program of the Massachusetts Institute of Technology. There he developed a whole-arm orthosis for tremor dissipation for Multiple Sclerosis patients as his research project under the supervision of Dr. Michael Rosen at the Neumann Laboratory for Biomechanics and Human Rehabilitation. This device was awarded a U.S. Patent in August 1993. He obtained his Master of Science in August of 1989.

After completing his M.S. he worked as an instructor for the Mechanical Engineering Department of the University of Puerto Rico at Mayagüez from August 1989 to July 1993 when he took a leave of absence. He entered the mechanical engineering graduate program of the University of Florida in August 1993. He has worked the last past two years under the supervision of Dr. Joseph Duffy in the Center of Intelligent Machines and Robotics. He will receive a Ph.D. for his research in the dynamic analysis of parallel manipulators in December 1995 and return to the Mechanical Engineering Department of the University of Puerto Rico at Mayagüez as an Associate Professor.
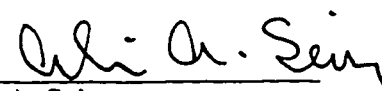
I certify that I have read this study and that in my opinion its conforms to acceptable standards of scholarly presentation and is fully adequate, in scope and quality, as a dissertation for the degree of Doctor of Philosophy.

Joseph Duffy, Chairman
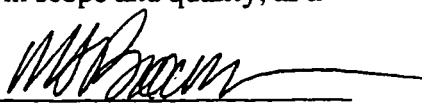Graduate Research Professor of
Mechanical Engineering

I certify that I have read this study and that in my opinion its conforms to acceptable standards of scholarly presentation and is fully adequate, in scope and quality, as a dissertation for the degree of Doctor of Philosophy.

Carl D. Crane III
Associate Professor of
Mechanical Engineering

I certify that I have read this study and that in my opinion its conforms to acceptable standards of scholarly presentation and is fully adequate, in scope and quality, as a dissertation for the degree of Doctor of Philosophy.

Gary K. Matthew
Associate Professor of
Mechanical Engineering

I certify that I have read this study and that in my opinion its conforms to acceptable standards of scholarly presentation and is fully adequate, in scope and quality, as a dissertation for the degree of Doctor of Philosophy.

Ali. A. Seireg
Ebaugh Professor of Mechanical
Engineering

I certify that I have read this study and that in my opinion its conforms to acceptable standards of scholarly presentation and is fully adequate, in scope and quality, as a dissertation for the degree of Doctor of Philosophy.
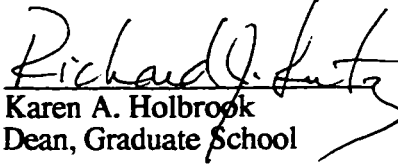
Mark T. Brown
Associate Scientist of Urban
and Regional Planning

This thesis was submitted to the Graduate Faculty of the College of Engineering and to the Graduate School and was accepted as partial fulfillment of the requirements for the degree of Doctor of Philosophy.

May 1996

Winfred M. Phillips
Dean, College of Engineering

Karen A. Holbrook
Dean, Graduate School